

PhD

3rd
CYCLE

FCUP
UA
UM
2024

U.PORTO

Higher-point Correlators and the Conformal
Bootstrap

João Vilas Boas

FC

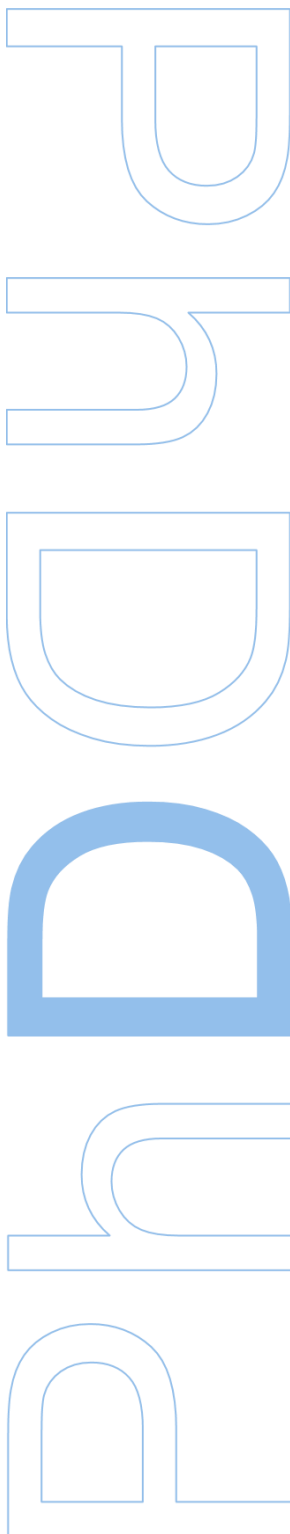
Universidade do Minho

Higher-point Correlators and the Conformal Bootstrap

João Vilas Boas

Doctor's Degree in Physics
Faculty of Sciences of the University of Porto, University of Aveiro and
University of Minho

2024



Higher-point Correlators and the Conformal Bootstrap

João Vilas Boas

Thesis carried out as part of the Doctor's Degree in Physics
Department of Physics and Astronomy
2024

Supervisor

Miguel Costa, Full Professor, FCUP

Co-supervisor

Vasco Gonçalves, Assistant Researcher, FCUP



Aos meus pais, Teresa e Rui.

To my parents, Teresa and Rui.

Acknowledgements

The following pages would not have been possible without the support, help and encouragement of many people. At the risk of not mentioning several names that deserve it, I couldn't present this thesis without recognizing a few people.

Foremost, let me thank my supervisors, Miguel and Vasco. Thank you, Miguel, for your guidance, your high scientific standards and for always believing in my abilities. Thank you also for giving me the opportunity to be part of the Simons Bootstrap Collaboration, where I learned so much from my fellow bootstrappers. Thank you, Vasco, for the countless hours you spent teaching me and helping me make progress with difficult computations. I am very much a product of those hours.

I also thank to FCT for financial support with the fellowship DFA/BD/5354/2020 with DOI 10.54499/2020.05354.BD. This fellowship was co-funded by Norte Portugal Regional Operational Program (NORTE 2020), under the PORTUGAL 2020 Partnership Agreement, through the European Social Fund (ESF).

I had the good fortune to work and collaborate with several people from whom I learned a lot. Besides my supervisors, I thank: Aaditya Salgarkar, António Antunes, Carlo Meneghelli, Raul Pereira and Xian Zhou. I also thank Filipe Serrano, Ricardo Rodrigues and José Matos for discussions and collaborations in ongoing projects.

I'm also grateful to the people I have shared an office with over the last four years. I extend my gratitude to Bruno, Henrique, João Pedro, João Pinho, Miguel Varela, Ricardo Oliveira and Simão. Thank you for all the discussions on physics and everything else. In this respect, let me also thank Professor Viana Lopes for this and for his invitations to take part in the physics summer schools as monitor and teacher.

During my PhD, I was lucky enough to be able to spend two months at EPFL in João Penedones' group. Thank you, João, for the warm welcome I had and for your inspiring and motivating insights. During those times in Lausanne, I met some wonderful people. Thanks to Adrien, Alex, Antoine, Biswajit, Jiaxin, Manuel, Veronica, Sasha, Shota and Xiang. Thank you for the great discussions and for collaborations.

My PhD wouldn't have been possible if I hadn't shared my interest in physics with many people during my bachelor's and master's degrees. Thanks to all of you that took part in that journey. I must, however, make a special mention of my friends and fellow "fadistas" Duarte and Pedro. Thank you for all the good times we had together.

I have many other friends in Porto and Barcelos to whom I owe a lot. It wouldn't be possible to mention you all in these lines, but I'll take the time to thank each of you personally. However, I cannot fail to mention Luísa, Octávio, Quesado, Vieira and Zé in Barcelos and Gabriel, Ricardo and Soraia in Porto. You are always there at every moment and make my life so much more special.

I owe all my gratitude to Inês. Thank you for all your love, for always believing in me and for your support through the highs and lows. Your intelligence, talent, fun, kindness and smile are a continuous source of inspiration and happiness.

I have to thank all my family. I'm very grateful for the fantastic family I have. Special thanks are devoted to my parents and my brother. Thank you, brother, for everything you've taught me over the years. You're always there to help me with everything and I'm very grateful to have you in my life. Finally, there are no words to express my gratitude to my parents. Thank you for all the love you've given me, for your constant support, even when you might have doubted my choices. I know that you will always be there for everything, and I know that I will always be loved by you. My life and now this thesis would not have been possible without you. This thesis is dedicated to you.

UNIVERSIDADE DO PORTO

Abstract

Faculdade de Ciências da Universidade do Porto
Departamento de Física e Astronomia

PhD Physics

Higher-point Correlators and the Conformal Bootstrap

by [João VILAS BOAS](#)

This thesis is devoted to the generalization of analytic conformal bootstrap methods to higher-point correlation functions in conformal field theories (CFTs).

We begin by reviewing the conformal bootstrap methodology and terminology starting from the basics. We proceed by revisiting the analytic lightcone bootstrap and the conformal Regge theory of four-point correlation functions as well as known results for correlators of half-BPS operators in $\mathcal{N} = 4$ SYM at strong t'hoof coupling. We further motivate the new and powerful ingredient that higher-point correlation functions can be in the conformal bootstrap program and review some of the recent results.

Following [1], we generalize the analytic lightcone bootstrap to five and six-point correlators. We rederive the lightcone conformal blocks in the snowflake channel using the lightcone limit of the operator product expansion (OPE). We then solve the crossing equation by reproducing leading-twist contributions in the direct channel with large spin contributions of double twist operators. In this way, we also fix the asymptotic large-spin behaviour of anomalous dimensions and OPE coefficients involving two and three spinning operators. We verify our results by comparing them with six-point correlators of mean-field theory and with the disconnected part of a five-point correlator in ϕ^3 theory.

We move on to generalize conformal Regge theory to five-point functions as in [2]. After reviewing some features of Regge theory for flat-space multi-point amplitudes and discussing how to find Lorentzian correlators from Euclidean ones, we propose the kinematics of Regge limit of five-point functions with two Reggeon exchanges. We analyze the analytic structure of conformal blocks both in position and Mellin space in the Regge limit and proceed to develop the conformal Regge theory of five-point correlators. As a

byproduct of our studies, we also introduce a new basis of three-point correlation functions for operators with spin and the associated Euclidean conformal blocks. Furthermore, we also write down an all-order expression for conformal blocks of scalar exchanges starting from the lightcone.

As in [3], we explore an algorithmic approach to compute five-point functions of half-BPS superprimaries in $\mathcal{N} = 4$ SYM at strong t’hooft coupling which are dual to the graviton and Kaluza-Klein modes in IIB supergravity in $\text{AdS}_5 \times S^5$. The method is entirely done in Mellin space where the analytic structure of holographic correlators is simpler and uses only factorization and a superconformal twist. Using this method, we obtain in a closed form all five-point functions with two half-BPS operators with scaling dimension $\Delta = p$ and three other with $\Delta = 2$, extending earlier results where all operators had $\Delta = 2$. As a byproduct of our analysis, we also obtain explicit results for spinning four-point functions of higher Kaluza-Klein modes.

The appendices contain several technical results and explicit computations as well as some parallel discussions to the ones in the main text.

Keywords: conformal field theory, higher-point functions, conformal bootstrap, Lorentzian CFTs, conformal Regge theory, AdS/CFT correspondence.

UNIVERSIDADE DO PORTO

Resumo

Faculdade de Ciências da Universidade do Porto

Departamento de Física e Astronomia

Doutoramento em Física

Higher-point Functions and the Conformal Bootstrap

por [João VILAS BOAS](#)

Esta tese é dedicada à generalização de métodos analíticos de *bootstrap* para funções de correlação com mais de quatro pontos em teorias de campo conformes.

Começamos por rever a metodologia e terminologia do *bootstrap* conforme desde os básicos. Prosseguimos com uma revisão sobre o *bootstrap* analítico de *lightcone*, sobre a teoria de Regge conforme para funções de correlação de quatro pontos, bem como sobre resultados conhecidos para funções correlação de operadores *half-BPS* em $\mathcal{N} = 4$ SYM no regime de forte acoplamento de *t'hooft*. Damos ainda a motivação para o novo e poderoso ingrediente que as funções de correlação de mais pontos podem ser no programa de *bootstrap* conforme e revemos alguns dos resultados recentes.

Seguindo [1], generalizamos o *bootstrap* analítico de *lightcone* para funções de correlação de cinco e seis pontos. Rederivamos os blocos conformes no limite de *lightcone* no canal *snowflake* usando o mesmo limite da *operator product expansion (OPE)*. De seguida, resolvemos as equações de *bootstrap* reproduzindo as contribuições dominantes em *twist* no canal direto com contribuições de *spin* grande de operadores do tipo *double twist*. Desta forma, fixamos também o comportamento assintótico a grande *spin* das dimensões anómalas e dos coeficientes de OPE envolvendo dois e três operadores com *spin*. Verificamos os nossos resultados comparando-os com funções correlação de seis pontos em teoria de campo médio e com a parte desconexa de uma função de cinco pontos na teoria ϕ^3 .

Prosseguimos com a generalização da teoria de Regge conforme para funções de cinco pontos como em [2]. Depois de rever algumas propriedades da teoria de Regge para amplitudes multi-ponto em espaço plano e de discutir como encontrar funções de correlação Lorentzianas a partir de correladores Euclidianos, propomos uma nova cinemática para o limite de Regge de funções de cinco pontos envolvendo duas trocas de *Reggeons*. Analisamos

a estrutura analítica dos blocos conformes, tanto em espaço de posições como em espaço de Mellin no limite de Regge e desenvolvemos a teoria de Regge conforme para funções de correlação de cinco pontos. Como bónus dos nossos estudos, introduzimos também uma nova base de funções de correlação de três pontos para operadores com spin e os blocos conformes Euclidianos associados. Além disso, escrevemos também uma expressão a partir *lightcone*, válida a todas as ordens, para blocos conformes associados a trocas de escalares.

Como em [3], exploramos uma abordagem algorítmica para calcular funções de cinco pontos de operadores *half-BPS* superprimários em $\mathcal{N} = 4$ SYM no regime de forte acoplamento de *t'hoof*t. Estes são duais ao gravitão e a outros modos *Kaluza Klein* da teoria de supergravidade IIB em $\text{AdS}_5 \times S^5$. O método é inteiramente feito em espaço de Mellin, onde a estrutura analítica das funções de correlação holográficas é mais simples, e usa apenas factorização e um *twist* superconforme. Usando este método, obtemos a forma explícita de todas as funções de cinco pontos com dois operadores *half-BPS* com dimensão $\Delta = p$ e três outros com $\Delta = 2$, estendendo resultados anteriores em que todos os operadores tinham $\Delta = 2$. Como consequência da nossa análise, obtemos também resultados explícitos para funções de quatro pontos envolvendo *spin* para modos mais altos de *Kaluza Klein*.

Os apêndices contêm vários resultados técnicos e cálculos explícitos, bem como algumas discussões paralelas às do texto principal.

Palavras-chave: teoria de campos conformes, funções de correlação de mais pontos, *Bootstrap* conforme, CFTs Lorentzianas, teoria de Regge conforme, correspondência AdS/CFT.

List of Publications

During the period of his PhD, the author contributed to several finished and ongoing projects, having at the time of writing published three works which are the focus of this thesis.

- António Antunes et al. “Lightcone bootstrap at higher points”. In: *JHEP* 03 (2022), p. 139. DOI: [10.1007/JHEP03\(2022\)139](https://doi.org/10.1007/JHEP03(2022)139). arXiv: [2111.05453 \[hep-th\]](https://arxiv.org/abs/2111.05453)
- Miguel S. Costa et al. “Conformal multi-Regge theory”. In: *JHEP* 09 (2023), p. 155. DOI: [10.1007/JHEP09\(2023\)155](https://doi.org/10.1007/JHEP09(2023)155). arXiv: [2305.10394 \[hep-th\]](https://arxiv.org/abs/2305.10394)
- Vasco Gonçalves et al. “Kaluza-Klein five-point functions from $\text{AdS}_5 \times S^5$ supergravity”. In: *JHEP* 08 (2023), p. 067. DOI: [10.1007/JHEP08\(2023\)067](https://doi.org/10.1007/JHEP08(2023)067). arXiv: [2302.01896 \[hep-th\]](https://arxiv.org/abs/2302.01896)

Contents

Acknowledgements	iii
Abstract	v
Resumo	vii
List of Publications	ix
Contents	xi
List of Figures	xv
Glossary	xix
1 Introduction	1
1.1 CFT basics	3
1.2 Higher-point functions	11
1.3 Lightcone bootstrap	14
1.4 Regge Theory	18
1.5 $\mathcal{N} = 4$ SYM and type IIB SUGRA	25
1.6 Structure of the thesis	28
2 Lightcone Bootstrap at higher points	31
2.1 Introduction	31
2.2 Kinematics and conformal blocks	32
2.2.1 Lightcone conformal blocks	34
2.3 Snowflake bootstrap	37
2.3.1 Five-point function	39
2.3.1.1 Identity in the (12) OPE	40
2.3.1.2 Identity in the (34) OPE	42

2.3.1.3	Two non-trivial exchanges	44
2.3.1.4	Stress-tensor exchange	45
2.3.2	Six-point function – snowflake	47
2.3.2.1	Exchange of three identities	48
2.3.2.2	Exchange of one identity and two leading twist operators	51
2.3.2.3	Exchange of three leading twist operators	52
2.4	Examples	55
2.4.1	Generalized free theory	56
2.4.2	ϕ^3 theory in $d = 6 - \epsilon$	56
2.4.2.1	Disconnected contribution to the five-point function	57
2.4.2.2	Comments on the six-point function	60
2.5	Discussion	60
2.A	Higher-point Conformal Blocks	63
2.A.1	Mellin amplitudes	63
2.A.2	Explicit computation of six-point blocks	66
2.A.3	Euclidean expansion of six-point conformal blocks	69
2.B	D-functions	71
2.B.1	Five Points	71
2.B.1.1	The case of D_{11112}	75
2.B.2	Six Points	77
2.B.2.1	The case of D_{111111}	78
2.C	Higher-point correlators and Harmonic Analysis	79
2.C.1	MFT six-point function from Harmonic Analysis	79
2.C.1.1	Snowflake channel	81
2.C.1.2	Comb channel	84
2.C.2	Partial wave decompositon and conformal blocks	87
2.C.3	Direct computation of spinning shadow coefficients	90
3	Conformal Multi-Regge Theory	97
3.1	Introduction	97
3.2	Scattering in flat-space and Regge theory	98
3.3	Kinematics of five-point conformal correlators	111
3.3.1	Euclidean limit	113
3.3.2	Lightcone limit	118
3.3.3	Regge limit	119
3.3.4	Conformal partial waves	121
3.4	Regge theory	122

3.4.1	Wick rotation or how to go Lorentzian	122
3.4.2	Mellin amplitudes	125
3.4.3	Comment on position space	131
3.4.4	Conformal Regge theory for five points	132
3.5	Discussion	136
3.A	Lightcone blocks	139
3.A.1	Spinning recursion relations	140
3.B	Scalar Mellin partial-wave	142
3.C	Explicit examples in position space	144
3.D	Other Regge kinematics	149
4	Kaluza-Klein Five-Point Functions from $\text{AdS}_5 \times S^5$ Supergravity	153
4.1	Introduction	153
4.2	Superconformal kinematics of five-point functions	156
4.2.1	R-symmetry	157
4.2.2	Drukker-Plefka twist and chiral algebra	159
4.3	Mellin representation	160
4.3.1	Mellin factorization	162
4.3.1.1	Exchange of scalars	163
4.3.1.2	Exchange of operators with spins 1 and 2	165
4.3.2	Drukker-Plefka twist in Mellin space	167
4.4	Bootstrapping five-point Mellin amplitudes	169
4.4.1	Strategy and ansatz	169
4.4.2	Mellin amplitude for $p = 2$	171
4.4.3	Mellin amplitudes for general p	172
4.4.4	A comment on consistency	175
4.4.5	Comments on position space	175
4.5	Discussion	178
4.A	Higher R-charge super multiplet	181
4.A.1	Conventions	182
4.A.2	Differential Operators	182
4.A.3	Four-point functions	185
	Action of $\mathcal{D}^{(J)}, \mathcal{D}^{(T)}$ on four-point functions.	186
	General structure of the correlator.	187
	The free theory check.	187
	Frame simplifications.	188
	Summary.	189

4.A.4 R- Symmetry gluing	189
Realization of $\mathfrak{su}(4)$ R-symmetry in the space of polynomials.	189
Projections and <i>gluing</i>	190
Application to five-point functions.	191
4.B Strong coupling correlators	191
4.B.1 Example of factorization	197
5 Conclusion and open directions	199
Bibliography	203

List of Figures

1.1	Radial quantization: Hilbert spaces of states live on S^{d-1} spheres and are connected by evolving them with the dilation operator.	6
1.2	The two different OPE topologies in a six-point function.	12
1.3	Contour integrals for the Sommerfeld-Watson transform for the four particle scattering in the J -complex plane. As one deforms the contour from C to C' one has to consider the contribution from dynamical singularities which here we assume to be a Regge pole.	19
1.4	Regge limit kinematics.	22
2.1	Schematic representation of the OPE channels for five- and six- point functions. In the top left we have the snowflake decomposition of the five-point function, where we emphasize the OPE coefficient involving two spinning operators. In the top right we have the snowflake decomposition of the six-point function, emphasizing the OPE coefficient of three spinning operators. In the bottom, we depict the comb-channel expansion, which may involve mixed-symmetry tensors and which we will not analyze in detail.	35
2.2	Schematic representation of the relevant lightcone limit in the z -plane. The point x_2 first approaches the lightcone of the operator at the origin, as $u \rightarrow 0$. Subsequently, it approaches the lightcone of the operator at $x_3 = (1, 0)$, which corresponds to taking $v \rightarrow 0$	38
2.3	Witten diagrams corresponding to the leading order five-point function in a large N theory. The black and red dashed lines correspond to the unitarity cuts in the direct and crossed OPE channels, allowing us to infer what the exchanged operators are.	44
2.4	A schematic form of the six-point snowflake bootstrap equation. The left hand side represents the $(12)(34)(56)$ direct-channel expansion while the right hand side represents the $(23)(45)(61)$ cross channel.	47
2.5	Witten diagrams corresponding to the leading order six-point function in a large N theory. The black and red dashed lines correspond to the unitarity cuts in the direct and crossed OPE channels, allowing us to read-off the exchanged identity and double-twist operators, respectively.	49

2.6	Schematic representation of the gravitational processes dual to the six-point comb channel on the left and to the six-point snowflake channel on the right. In the comb case, three particles come from the infinite past, interact weakly and continue towards future infinity. In the snowflake case, the blue and red particles come from the past infinity of two different time coordinates, say t_1 and t_2 , respectively. The blue one travels to future infinity along t_1 and the red one along t_2 . A third, green particle comes from past infinity in the t_1 direction and moves towards past infinity in t_2 . The process can also be interpreted in other similar ways by permuting the role of the OPEs.	55
3.1	The ten two-body Mandelstam invariants of a five-point scattering amplitude (left) and our choice of five independent ones (right).	100
3.2	Scattering process shown in the resting frame of exchanged momentum q_2 . This defines the angles θ_2 and θ_{Toller} . θ_1 is defined analogously in the rest frame of exchanged momentum q_1	101
3.3	Singularities of $A(s, t)$ in the s complex-plane at fixed t	102
3.4	Contour integrals for the Sommerfeld-Watson transform for the four particle scattering in the J -complex plane. As one deforms the contour from C to C' one has to consider the contribution from dynamical singularities which here we assume to be a Regge pole.	104
3.5	Contour deformation in $z = e^{i\theta_{\text{Toller}}}$ for doing the Froissart-Gribov continuation. The orthogonality relation holds on the black contours. We show the two different branch cuts corresponding to a_{\gtrless} discussed in (3.22).	105
3.6	Contour integrals for the Sommerfeld-Watson transform in the m -complex plane.	107
3.7	Contour of integration in J_i and m -complex planes when the respective variable is integrated first. Here, we only account for dynamical singularities given by Regge poles and ignore the existence of Regge cuts and fixed poles. Note that there are no dynamical singularities in the m -complex plane.	107
3.8	We show our proposal for the Regge limit of the five-point correlator.	112
3.9	Position of points on the Euclidean cylinder. Two points 1 and 3, are at $\tau = -\infty$ and $\tau = \infty$	113
3.10	Regge kinematics for scattering amplitudes can be defined as $s_{13}, s_{25}^2, s_{45}^2 \rightarrow \frac{1}{x^2}, x \rightarrow 0$ while keeping t_{12} and t_{34} fixed. As can be seen in Mellin space the dominant contribution to the kinematics described in figure 3.8 is the same.	127
3.11	Integration contour in spins J_1, J_2 . The blue contour can be deformed to the red contour. We assume the leading Regge pole in the J_i -plane is located at $j_i(\nu)$ and we don't draw any further dynamical singularities that might exist to the left. Red contour is understood to be deformed to the right of the other infinite series of poles depending on ℓ lying on the left in the J_i -plane.	133
3.12	Discontinuities of lightcone block under analytic continuation (3.78). In blue, the real part of the stripped-off lightcone block. In orange, the real part of the block with $\log(u_2) \rightarrow \log(u_2) + 2\pi i$. In green, the previous with $\log(u_4) \rightarrow \log(u_4) - 2\pi i$ and in red, the latter with $\log(u_5) \rightarrow \log(u_5) - 2\pi i$. On the right, a zoomed-in version of the same plot. The plots are obtained with $\delta_2 = 0.73\delta_1$	145

4.1	Inequivalent R-symmetry structures in the $\langle pp222 \rangle$ five-point function. Here (a_1, a_2) is $(1, 2)$ or $(2, 1)$ and (a_3, a_4, a_5) can be any permutation of $(3, 4, 5)$. Each thin line represents a single contraction. The thick line represents the multi-contraction t_{12}^a with the power a given by the number next to the line. The R-symmetry structures in the first row have counterparts in the $\langle 22222 \rangle$ five-point correlator. For $\langle pp222 \rangle$ they are simply obtained by multiplying the $p = 2$ structures with t_{12}^{p-2} . The R-symmetry structures in the second row are new and do not appear in $\langle 22222 \rangle$	158
4.2	Mellin amplitudes have poles correponding to the exchange of single-trace operators. The residues at the poles are associated with lower-point Mellin amplitudes. In the channel depicted in the figure, we have $n = 5$ and $q = 3$. The Mellin amplitude on the left has four points while the one on the right has only three.	162

Glossary

QFT	Quantum Field Theory
CFT	Conformal Field Theory
AdS	Anti-de Sitter
IR	Infrared
UV	Ultraviolet
SYM	Supersymmetric Yang-Mills
SUGRA	Supergravity

Chapter 1

Introduction

There is a natural human tendency to wonder and to desire to understand the fundamental elements and guiding principles of things. In the search for this ultimate *arche*, there is the need to uncover Nature’s general language. Quantum Field Theory (QFT) seems to be our best candidate for such a general framework. Indeed, QFT describes systems with infinitely many degrees of freedom in very distinct contexts. Its far reaching applicability ranging from condensed matter to high-energy collider physics, and from statistical field theory to effective theories of gravity is furthermore supported by overwhelming experimental evidence highlighting its success.

Amongst QFTs there is the special class of conformal field theories (CFTs). These theories are invariant under conformal symmetry and are therefore more constrained than generic QFTs. Moreover, from a renormalization group (RG) theory perspective, one can think of a generic QFT of an interacting system as being defined by the RG flow that is generated by a relevant deformation of a solvable theory in the ultraviolet (UV). Often the UV theory is taken to be free, which is conformally invariant. The QFT can then flow to either a nonperturbative infrared (IR) fixed point or to a gapped phase, where the interesting observables are correlation functions and the S-matrix, respectively. The former fixed points are scale-invariant theories which when unitary (reflection positive in Euclidean space) and local are expected to be enhanced to CFTs, at least in two and four (with extra technical assumptions) spacetime dimensions [4–6].¹

At long distances, many QFTs are strongly coupled. Despite the impressive development of perturbative methods to evaluate complicated Feynman diagrams, these necessarily

¹There are known examples of scale-invariant theories which are not conformal. See for instance the examples of the theory of elasticity in [7] and of dipolar ferromagnets in [8] where a shift symmetry is shown to be responsible for the breakdown of the enhancement. These known examples are non-unitary.

fail to capture the full nonperturbative character of these physical systems. The *Bootstrap* approach, which we advocate throughout this thesis, offers a new set of methods that allows us to study QFTs nonperturbatively. The philosophy goes back to finding the fundamental principles and consistency conditions that we expect to be universal and impose them at the level of the observables we are interested in. Amongst the typical constraints we impose is unitarity, the invariance under the permutation of operators and the existence of a stress tensor. Additionally, we may want to add further constraints in particular models. The philosophy is simple to explain, rigorous and can thus be applied in various contexts, such as the conformal bootstrap (see [7, 9–14]), S-matrix bootstrap (e.g., [15–18]) and more recently in quantum mechanics (e. g., [19–24]). The simplicity of these ideas contrasts with the remarkable success of its outcome. The striking example of the power of this technology is the conformal bootstrap determination of the critical exponents of the three-dimensional Ising model at the critical point which is the most precise ever [25]. These exponents describe the behaviour of physical systems close to criticality, i.e. close to continuous phase transitions. Furthermore, they do not depend on the microscopic details of systems far from criticality and are the same for systems within a given universality class. This means that knowing their exact form doesn't just teach us about the critical behaviour of a single model, but about a whole class of them.

The AdS/CFT correspondence [26–28] is another major motivation to study CFTs. The correspondence conjectures a duality between a theory in AdS spacetime and a CFT living at its boundary. In this sense, it provides a way to further understand quantum gravity in the bulk of AdS by exploring the more powerful toolkit at our disposal on the CFT side. In its strong/weak form, the duality is particularly useful for practical computations and for applications (see for instance [29]) as it offers the chance to look at the strongly-coupled behaviour of a system by solving the dual weakly-coupled theory. We will revisit this duality as part of this thesis by considering the most studied example of the correspondence: the duality between type IIB superstring theory in $AdS_5 \times S^5$ and $\mathcal{N} = 4$ SYM.

The overarching goal of this thesis is the extension of conformal bootstrap analytic results to correlation functions with more than four local operators. In doing so, we will consider both Euclidean and intrinsically Lorentzian configurations. It is therefore of primordial importance to define and review some of more standard conformal bootstrap terminology and results before we proceed to motivate and attack the set of problems we

find in the next chapters.

1.1 CFT basics

A conformal field theory is a quantum field theory whose correlations functions are covariant under conformal transformations. These are local rescalings of spacetime that preserve angles. We further require the existence of a conserved stress tensor, even in theories where there is no Lagrangian formulation available. This is a natural requirement for any local quantum field theory. Given its existence, we can define the charges

$$Q_\epsilon(\Sigma) \equiv - \int_{\Sigma} dn_\mu \epsilon_\nu T^{\mu\nu}(x) \quad (1.1)$$

where Σ is any co-dimension 1 surface surrounding the insertion of the stress tensor and n_μ is a normal vector to this surface. For these charges to be conserved, the vector fields ϵ_μ should obey the killing equations

$$\partial_\mu(\epsilon_\nu T^{\mu\nu}) = 0 \implies \partial_\mu \epsilon_\nu + \partial_\nu \epsilon_\mu = 0, \quad (1.2)$$

which in flat space has solutions

$$p_\mu = \partial_\mu, \quad m_{\mu\nu} = x_\mu \partial_\nu - x_\nu \partial_\mu. \quad (1.3)$$

These are the vector fields associated with translations and rotations, respectively.

In a CFT, besides conserved, the stress tensor is also traceless ² which allows us to relax the killing equation to its conformal version

$$\partial_\mu \epsilon_\nu + \partial_\nu \epsilon_\mu = c(x) \delta_{\mu\nu}, \quad (1.4)$$

with some scalar function $c(x)$. The conformal killing equations have two further solutions in flat space, namely

$$d = x^\mu \partial_\mu, \quad k_\mu = 2x_\mu (x^\nu \partial_\nu) - x^2 \partial_\mu, \quad (1.5)$$

which are associated with dilations (commonly referred to as dilatations) and special conformal transformations. ³ These vector fields define the conserved charges of a CFT

²This is a structural property of locally invariant conformal theories that can be tested [30].

³For completeness we should add that in curved even-dimensional spacetimes, the tracelessness of the stress tensor can be broken by a Weyl anomaly. This fact will not be important for the rest of the text of the thesis.

through (1.1), where we gave a sloppy definition of the surface Σ . This is justified since conservation of these charges is equivalent to the statement that these are topological surface operators [31].

The algebra of the quantum charges is given by

$$\begin{aligned} [D, P_\mu] &= P_\mu, & [D, K_\mu] &= -K_\mu, & [K_\mu, P_\nu] &= 2\delta_{\mu\nu}D - 2M_{\mu\nu}, \\ [M_{\mu\nu}, P_\rho] &= \delta_{\nu\rho}P_\mu - \delta_{\mu\rho}P_\nu, & [M_{\mu\nu}, K_\rho] &= \delta_{\nu\rho}K_\mu - \delta_{\mu\rho}K_\nu, \\ [M_{\mu\nu}, M_{\rho\sigma}] &= \delta_{\nu\rho}M_{\mu\sigma} - \delta_{\mu\rho}M_{\nu\sigma} + \delta_{\nu\sigma}M_{\rho\mu} - \delta_{\mu\sigma}M_{\rho\nu} \end{aligned} \quad (1.6)$$

where we use the more common notation $P_\mu = Q_{p_\mu}$, $M_{\mu\nu} = Q_{m_{\mu\nu}}$, $D = Q_d$ and $K_\mu = Q_{k_\mu}$ and all other commutators vanish. Note that this algebra is basically inherited from the algebra of the vector fields for a spacetime dimension $d \geq 3$ in which we focus on in this thesis.⁴ Moreover, the algebra presented here is the algebra of $SO(d+1, 1)$ which coincides with the Lorentz algebra in $\mathbb{R}^{d+1, 1}$.⁵ A particularly interesting feature of this algebra is found in the first line of equation (1.6). It shows that P_μ and K_μ act as raising and lowering operators for the eigenvalues of the dilation operator. It is then natural to consider local operators with fixed scaling dimension Δ at the origin such that

$$[D, \mathcal{O}(0)] = \Delta \mathcal{O}(0), \quad [M_{\mu,\nu}, \mathcal{O}^{\mathbf{a}}(0)] = (\rho_{\mu\nu})^{\mathbf{a}}_{\mathbf{b}} \mathcal{O}^{\mathbf{b}}(0), \quad (1.7)$$

where we also included the natural transformations of local operators in irreducible representations of the $SO(d)$ rotation group. Here $\rho_{\mu\nu}$ are rotation matrices and \mathbf{a} denotes the representation indices of the operator. In this thesis we will only deal with spin- J symmetric and traceless representations of $SO(d)$, but see [33, 34] for more general representations.

It follows from the conformal algebra that $P_\mu \mathcal{O}(0)$ is an operator of scaling dimension $\Delta + 1$ whereas $K_\mu \mathcal{O}(0)$ has $\Delta - 1$.⁶ Therefore, by acting successively with K_μ on an operator we can have arbitrarily low scaling dimensions. However, due to unitarity or cluster decomposition of correlation functions that we will discuss below, we require the scaling dimensions to be positive. This then imposes that there should be some local operator such that

$$[K_\mu, \mathcal{O}(0)] = 0. \quad (1.8)$$

⁴For $d = 2$, the algebra of quantum charges has a central extension compared to the one from the vector fields.

⁵This is the motivation for the "embedding space formalism" [32] where the action of the conformal group is linearized in a $d+2$ -dimensional space and then properly projected to \mathbb{R}^d .

⁶The notation $P_\mu \mathcal{O}(0)$ is shorthand for $[P_\mu, \mathcal{O}(0)]$ and similarly for K_μ . From a path integral interpretation, the commutator can be seen as surrounding $\mathcal{O}(0)$ with a topological surface operator.

These are the so-called primary operators. On the other hand, by acting with the raising operator P_μ we can build an entire family of operators with increasing scaling dimensions out of a single primary. These are the descendants of the primary operator. One can show that all local operators of a CFT are linear combinations of primaries and descendants [9]. This nontrivial fact has important consequences in the conformal block decomposition of correlation functions we will encounter later and allows us to focus on correlation functions of primary operators.

Using the conformal Ward identities in a theory with a conformal invariant vacuum, one can show that scalar one, two and three-point functions of primary operators reduce to

$$\langle \mathcal{O}(x) \rangle = \delta_{\mathcal{O},1}, \quad \langle \mathcal{O}_1(x_1) \mathcal{O}_2(x_2) \rangle = \frac{\delta_{12}}{x_{12}^{2\Delta_{\mathcal{O}}}}, \quad (1.9)$$

$$\langle \mathcal{O}_1(x_1) \mathcal{O}_2(x_2) \mathcal{O}_3(x_3) \rangle = \frac{c_{123}}{x_{12}^{\Delta_1+\Delta_2-\Delta_3} x_{13}^{\Delta_1+\Delta_3-\Delta_2} x_{23}^{\Delta_2+\Delta_3-\Delta_1}}, \quad (1.10)$$

where we use the notation $x_{ij} = |x_i - x_j|$. The generalization for operators with spin was studied in [32, 35] and will be useful in the next chapters where the explicit expressions will be shown. We see that one-point functions are identically zero except if the operator is the identity itself. On the other hand, two-point functions are power laws and depend only on a single parameter, the scaling dimension of the primary operator we consider, since they can only be nonzero if operators \mathcal{O}_1 and \mathcal{O}_2 are in fact the same. Here we chose the convention where the numerator of the two-point function is just a Kronecker delta, but other normalizations are also possible.⁷ Finally, three-point functions are also completely fixed by conformal symmetry up to overall constants c_{123} , the operator product expansion (OPE) coefficients or structure constants. These together with the spectrum of the theory, i.e. the scaling dimensions and $SO(d)$ representations of the available primary operators, are collectively known as CFT data and contain all the dynamics of a CFT. This statement stems from the OPE that we now discuss.

The OPE is better explained using the operator-state correspondence: in a CFT, every state corresponds to an operator and vice-versa. To make this correspondence more easily understandable we need to introduce the important notion of radial quantization.

To work out the quantization of a theory in QFT, we need to choose a direction in which we foliate spacetime. In standard QFT, the chosen direction is typically time and in every

⁷Even though here we are only dealing with scalars, a good example of a case where the normalization constant should not be set to 1 is the canonical normalization of correlation functions of two stress tensors where the constant of normalization is fixed from Ward identities and has physical meaning.

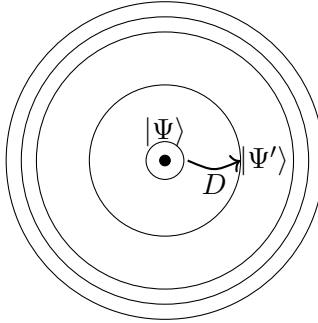


FIGURE 1.1: Radial quantization: Hilbert spaces of states live on S^{d-1} spheres and are connected by evolving them with the dilation operator.

time slice there is a corresponding Hilbert space of states. In this case, one could go from one Hilbert space to the next by evolving a state with the Hamiltonian. In a scale-invariant theory, there is another possible foliation of spacetime, where we consider Hilbert spaces to live on spheres S^{d-1} around the origin. This is the so-called radial quantization. In this quantization the natural "Hamiltonian" to evolve between Hilbert spaces is the dilation operator - see figure 1.1.

From a path-integral perspective, a local operator insertion naturally defines a state in a sphere that surrounds it. One simply integrates the path-integral over the interior of the sphere containing the operator insertion. Note that this state does not need to be an eigenstate of the dilation operator, but can nonetheless be decomposed into sums of such states.

The fact that a state living on a co-dimension 1 surface can also be interpreted by a 0-dimensional local operator seems harder to believe. It is here that scale invariance comes to play and saves the day. Since any state can be decomposed into eigenstates of the dilation operator, it is possible to use it to pull each of these eigenstates into a very small sphere around the origin and recognise the corresponding local operator. In this way, any state can be interpreted as a sum of local operators, i. e. of primaries and descendants. The reader may want to see [9, 36] for a more careful proof of the correspondence. We are then entitled to write

$$\mathcal{O}(0) \leftrightarrow \mathcal{O}(0)|0\rangle \equiv |\mathcal{O}\rangle. \quad (1.11)$$

Moreover, our primary operators correspond to primary states such that

$$D|\mathcal{O}\rangle = \Delta|\mathcal{O}\rangle, \quad K_\mu|\mathcal{O}\rangle = 0, \quad M_{\mu\nu}|\mathcal{O}\rangle = \rho_{\mu\nu}|\mathcal{O}\rangle, \quad (1.12)$$

and descendant states can be built by acting with momentum generators $P_{\mu_1} \dots P_{\mu_n}|\mathcal{O}\rangle$.

The OPE existence follows then naturally from the operator-state correspondence. Consider the insertion of two operators and the state generated at some ball that surrounds these

$$|\psi_{1,2}\rangle \equiv \mathcal{O}_1(x_1)\mathcal{O}_2(0)|0\rangle. \quad (1.13)$$

This state can be decomposed into eigenstates of the dilation operator

$$|\psi_{1,2}\rangle = \sum_k C_{12k}(x_1, \partial_{x_1}) \mathcal{O}_k(0)|0\rangle, \quad (1.14)$$

where the sum is over the primaries and the dependence on descendants is restored by the action of the derivatives in $C_{12k}(x_1, \partial_{x_1})$ on those. Using the state-operator correspondence above we can promote this equation to an operator level,

$$\mathcal{O}_1(x_1)\mathcal{O}_2(x_2) = \sum_k \frac{c_{12k}}{(x_{12}^2)^{\frac{\Delta_1+\Delta_2-\tau_k}{2}}} F_k(x_{12}, D_z, \partial_{x_1}) \mathcal{O}_k(x_2, z), \quad (1.15)$$

where we allowed the second operator to have arbitrary position now. Here we extracted c_{12k} which are the OPE coefficients that we first met in the three-point function (1.10) and therefore its name. In the context of this thesis we will always apply the OPE to scalar operators and thus the only allowed exchanges in the OPE are symmetric and traceless representations of spin J . In the equation above we are implicitly restricting our attention to that case. Moreover, to suppress the index dependence, we introduce the null polarization vectors z such that

$$\mathcal{O}(x, z) \equiv \mathcal{O}^{\mu_1 \dots \mu_n}(x) z_{\mu_1} \dots z_{\mu_n}. \quad (1.16)$$

One can recover the index dependence by acting with the Todorov operator [32]

$$D_{z^\mu} = \left(\frac{d}{2} - 1 + z \cdot \frac{\partial}{\partial z} \right) \frac{\partial}{\partial z^\mu} - \frac{1}{2} z^\mu \frac{\partial^2}{\partial z \cdot \partial z} \quad (1.17)$$

that appears in $F_k(x_{12}, D_z, \partial_{x_1})$. The exact form of the OPE can then be fixed from consistency between two-point functions and three-point functions.

The OPE is one of the most important features of a CFT as we will appreciate below. In a CFT, it has a finite radius of convergence contrarily to a generic QFT. In fact, as long as we can draw a ball separating the two operators from other operators in the theory, the OPE converges [37]. We can then use it inside a n -point correlation function to reduce it to a $n - 1$ -point function at the cost of knowing all the possibly infinite primary operators that can be exchanged in the OPE. Successive use of the OPE allows us then to reduce any n -point function to a two or three-point function, whose form is completely fixed by

conformal symmetry. This is the reason why it is valid to say that CFT data completely determines a CFT.

In this context, there are two important questions that we can raise: *What type of constraints can we impose on CFT data? What is the relevance of higher-point correlation functions?*

To answer the first question, we start by focusing on the case of unitary CFTs. This will be the case of interest for the rest of the thesis. Unitarity requires the norms of states to always be non-negative. This imposes nontrivial constraints at the level of the allowed CFT data. Concretely, the scaling dimensions of operators must obey

$$\Delta \geq \frac{d-2}{2} \quad (\text{scalars}), \quad \Delta \geq J + d - 2 \quad (\text{spinning}). \quad (1.18)$$

The clear exception is the identity operator with $\Delta = 0$. These bounds are saturated whenever there are null states in the conformal multiplet of a given operator. This is the case for free theories or conserved currents.

Furthermore, unitarity also imposes constraints at the level of the OPE coefficients. Whenever the operators involved are real (Hermitian in Lorentzian signature), the OPE coefficients are also real $c_{12k}^* = c_{12k}$.

These are the common constraints we can impose to any unitary CFT, but there is a vast space to improve on these. Here lies the connection with the second question that we now investigate.

Let us start by considering four-point functions. These are by default the observables in bootstrap studies. For this reason, from now on, when we refer to higher-point functions we mean correlation functions with five or more primary operators. Scalar four-point correlators can be written as

$$\langle \phi_1(x_1) \phi_2(x_2) \phi_3(x_3) \phi_4(x_4) \rangle = \frac{\left(\frac{x_{14}^2}{x_{24}^2} \right)^{\frac{\Delta_{21}}{2}} \left(\frac{x_{14}^2}{x_{13}^2} \right)^{\frac{\Delta_{34}}{2}}}{(x_{12}^2)^{\frac{\Delta_1 + \Delta_2}{2}} (x_{34}^2)^{\frac{\Delta_3 + \Delta_4}{2}}} g(u, v) \quad (1.19)$$

where $\Delta_{ij} = \Delta_i - \Delta_j$. The stripped-off factor in front of $g(u, v)$ takes care of the scaling of the correlation function in each operator. Hence $g(u, v)$ is just an arbitrary function of two conformally-invariant cross ratios u and v

$$u = z\bar{z} = \frac{x_{12}^2 x_{34}^2}{x_{13}^2 x_{24}^2} \quad v = (1-z)(1-\bar{z}) = \frac{x_{14}^2 x_{23}^2}{x_{13}^2 x_{24}^2}. \quad (1.20)$$

We also introduced here the very common set of cross ratios z and \bar{z} . These have a very

nice geometric interpretation. Indeed, one can use conformal transformations to take a generic four-point correlator into the configuration where $x_1 = 0$, $x_3 = (1, 0, \dots, 0)$ and x_4 is sent to infinity. The point x_2 lies then in a plane that contains all other operators. Its position in the plane is then controlled by two real numbers. In Euclidean space, we can parameterize this point with a complex variable $z = x + iy$ and $\bar{z} = z^*$. As we Wick rotate to a Lorentzian signature, z and \bar{z} become two real and independent variables.

The function $g(u, v)$ is dynamical but most of its form can be fixed from OPE machinery. If we take the OPE between operators 1-2 and 3-4 as an example, it admits the writing

$$g(u, v) = \sum_k c_{12k} c_{34k} g_{\Delta, J}^{\Delta_{12}, \Delta_{34}}(u, v) \quad (1.21)$$

where the sum is over exchanged primaries. The two OPEs reduce the four-point function to sums over two-point functions of exchanged operators. As these vanish for non-identical operators, we are left with a single sum. The kinematic functions $g_{\Delta, J}^{\Delta_{12}, \Delta_{34}}(u, v)$ are known as conformal blocks and, by construction, their form is fixed by the OPE. While this formal definition is important, in practice, their form is more easily obtained by other methods.

Conformal blocks satisfy quadratic and quartic Casimir equations [38–40]. In $d = 2$ and $d = 4$, equipped with the appropriate boundary condition resulting from the OPE, the solution is known in closed form [38, 39]. Moreover, in [39] the authors found a recursion relation relating conformal blocks in d dimensions to other in $d + 2$ dimensions. For odd spacetime dimensions no closed form is known in general. There are however other methods to compute these objects. One exploits the analytic properties of these blocks in Δ and derives recursion relations for them [41]. Another makes use of the so-called radial coordinates and computes the conformal block in a series expansion in the cross-ratios with coefficients that are rational functions of Δ [42, 43]. These methods can be combined together and applied to evaluate these conformal blocks with extreme accuracy as required for numerical studies.

Through the use of OPE, we were able to separate the dynamics of a CFT, contained in its CFT data, from the kinematics. In doing so, we have opted for some choice of pairs of operators in which we do the OPE, but there are other equivalent choices. Suppose, for simplicity, that all operators within our correlation function are equal. In our OPE expansion, we chose to pair up the operators in a 12-34 channel, which we call the direct channel. On the other hand, we could have instead performed the OPE in the pairs 14-23,

the cross channel. The equivalence of the two OPE expansions can then be written as

$$g(u, v) = \left(\frac{u}{v}\right)^{\Delta_\phi} g(v, u). \quad (1.22)$$

This equation (and the equivalent for higher-point functions) is the crux of the conformal bootstrap program. While simple at first sight, it is in fact extremely difficult to satisfy from a conformal block decomposition point of view. This happens because conformal blocks are not crossing-symmetric objects. Indeed, considering the direct-channel in the limit where $x_2 \rightarrow x_1$ with all operators in a line (i.e., $z \rightarrow 0$ and $z = \bar{z}$), the conformal block has power-law dependence in z and its leading contributions are given by operator exchanges of small scaling dimension, such as the identity itself. On the cross channel, on the other hand, the same limit leads to logarithmic behaviour in z . In fact, it can be proved that it is an infinite number of heavy operators in the cross channel that reproduces the exchange of the identity in the direct channel [37]. This is suggestive of the complicated and nontrivial constraints that this equation poses on CFT data and justifies the bootstrap program as a powerful tool.

In the region of mutual convergence of the conformal block decomposition, which turns out to be $z \in \mathbb{C} \setminus ((-\infty, 0) \cup (1, +\infty))$, the conformal bootstrap program aims to solve the crossing equation both from a rigorous numerical and analytical approaches. In this thesis, we focus on analytic methods. In this context, it is worth mentioning that different limits of the crossing equations allow us to focus on different OPE exchanges. In fact, if instead of considering the limit $x_2 \rightarrow x_1$ (which we call Euclidean OPE limit) we consider the limit where one of the operators approaches the lightcone of the other, i.e. $x_{12}^2 \rightarrow 0$ (which we call lightcone OPE limit), it follows from the form of the OPE that the leading conformal block contributions are those with lowest twist (scaling dimension minus the spin of the exchanged operator) rather than those with small scaling dimensions. Considering the lightcone limit on both sides of the crossing equation will teach us about the large spin behaviour of double twist operators that are found to be universal in every unitary CFT [44, 45]. This result will be briefly reviewed below under the name of lightcone bootstrap.

Before moving on, let us now motivate the general goal of this thesis: the extension of analytic bootstrap methods to correlation functions of more than four local primary operators.

1.2 Higher-point functions

For a long time, higher-point functions were overlooked in the conformal bootstrap program. Indeed, they admit a conformal block decomposition, but the associated conformal blocks are more complicated and functions of more cross ratios than the four-point analogues.⁸ Moreover, it is known that all CFT data can be probed already from four-point functions alone as long as all of them are considered. This provides reasonable motivation for the scarcity of studies on higher-point functions. Nevertheless, here also lies a major motivation for the increasing interest in these observables: not all four-point functions are accessible to us!

In the review we did of four-point functions, we restricted our attention to scalar correlators. The generalization to other representations can be done in principle at the cost of introducing some differential operators. As pointed out in [46], there is a set of "spinning-up" differential operators that when acting on a three-point function of the type scalar-scalar-spin produce a three-point function of three generic spin operators with shifted scaling dimensions. More recently, in [47], the authors introduced a more general class of differential operators known as weight-shifting operators. These results provide a strategy to compute general conformal blocks (with arbitrary internal and external representations) by differentiating scalar conformal blocks. The method is constructive but limited by the amount of derivatives we can take efficiently. For example, the method is not practical to access large spin operators. On the other hand, these operators appear naturally in the OPE of two scalar operators for instance.

Note that inside a scalar higher-point function, by use of the OPE, there are infinitely many four-point functions and, more importantly, infinitely more CFT data, including OPE coefficients between spinning operators. Indeed, if one is able to overcome the mathematical difficulty of dealing with the more involved structure of higher-point functions, then one is entitled to find many more OPE coefficients at a single time.

Other motivation has a more exploratory character: it is unclear what new dualities, relations or structures in the correlators might only become apparent at higher-points. In chapter 3, we will have contact with a label for different tensor structures appearing in three-point functions involving operators with spin and propose some analyticity of the OPE coefficients in it. The question about whether this analyticity exists or not appears

⁸For sufficiently large spacetime dimensions, the conformal blocks of a n -point correlator are functions of $n(n - 3)/2$ cross ratios.

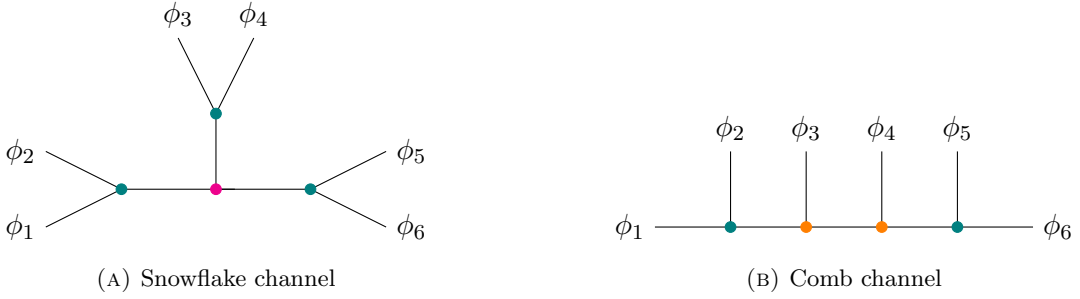


FIGURE 1.2: The two different OPE topologies in a six-point function.

quite naturally as we start considering higher-point functions. In chapter 4, we will consider correlation functions of single-trace protected operators in $\mathcal{N} = 4$ SYM at strong t'hoof coupling. In [48], it was found a hidden ten-dimensional conformal symmetry that can be used to relate correlation functions of these type of operators with different scaling dimensions. It is not clear if this symmetry survives in higher-point functions or not. If it does, it may shed light on underlying structures of these correlators that have not been appreciated so far.

In the context of the AdS/CFT correspondence, higher-point functions are also important for the so-called AdS unitarity methods [49, 50]. These relate the double discontinuity of one-loop diagrams in AdS to the square of tree-level data. The generalization for higher loops also requires the knowledge of higher-point functions.

These ideas provide a broad motivation to explore this largely uncharted territory. While the number of results available is scarce, there are valuable contributions that deserve to be mentioned. In this regard, it is important to distinguish two different topologies under OPE. The snowflake topology is the result of considering the OPE between pairs of external operators - see figure 1.2a for an example in a six-point function. On the other hand, one can instead consider the OPE of consecutive operators, both external and internal - see figure 1.2b. Note that the two topologies probe different OPE coefficients generically. In the case of the scalar six-point function we considered in figure 1.2, the snowflake channel probes OPE coefficients involving two scalars and a symmetric and traceless spin J operator as well as the coupling between three spinning operators. The comb channel configuration, on the other hand, might also depend on the OPE coefficient between an internal spin- J operator, an external scalar and a possible internal operator with mixed symmetry.

In [51], in $d = 1, 2$ dimensions, a closed-form expression for the n -point conformal

block in the comb-channel was found using shadow formalism.⁹ In more general space-time dimensions, it was also derived the five-point comb-channel conformal block with both internal and external scalar operators. This result was then generalized for any n -point correlation function in the comb-channel in [53, 54]. In this regard, [54] derived a dimensional reduction formula that relates these blocks in d dimensions to blocks in $d - 2$ dimensions. Similar studies for scalar six and seven-point functions with scalar exchanges in the (extended) snowflake channel were done in [55, 56].

While interesting and nontrivial, the results above have limited applicability. More generally, five-point conformal blocks for non-scalar OPE exchanges can be computed by considering the quadratic Casimir equations and by solving them in a series expansion [57–59].¹⁰ This method was fundamental for the first numerical studies of five-point correlation functions in the bootstrap program [58, 59]. In the same spirit as discussed for four-point functions before, [62] derived recursion relations for conformal blocks with just external scalars or with one spin 1 or 2 operator using weight-shifting operators. This relation allows us to relate arbitrary conformal blocks to blocks for scalar exchanges. The method is useful for relatively simple representations of the conformal group, but becomes very inefficient as one wants to use it for more nontrivial cases, such as the exchange of operators of large spin.

The conformal blocks are fundamental building blocks but their efficient computation for higher-point functions is still in its infancy. As pointed out in [63], the OPE simplifies in lightcone limit. In [64], this fact was used to derive integral representations for five and six-point conformal blocks. This is reviewed in chapter 2, where the explicit expressions are shown and used to set up a lightcone bootstrap program for five and six-point scalar correlators.¹¹

As we conclude this section, even though we are not focusing on numerical bootstrap methods in this thesis, we add a few remarks on notable numerical studies in higher-point functions. An important fact of the four-point numerical conformal bootstrap of unitary CFTs is the positivity of the product of OPE coefficients appearing in the crossing symmetric equation (1.22). For higher-point functions, this notion of positivity is not guaranteed generically. Therefore the uplift of numerical methods from four-point correlators to these observables is not straightforward. As mentioned above, in [58, 59] the authors overcame

⁹See also [52].

¹⁰Besides the quadratic Casimir operator, multipoint conformal blocks are also eigenfunctions of a complete set of commuting differential operators. These were discussed in [60, 61].

¹¹This work was subsequently reproduced and extended in [65, 66].

this obstacle in five-point functions by reviving a numerical method that aims to solve a truncated crossing equation [67].¹² This method however lacks the rigor of the positive semidefinite program that is used in four-point functions. Recently in [68], this program was reformulated in order to allow the numerical study of six-point functions in a comb-channel conformal block decomposition and in a line configuration in $d = 1$ dimensions. These results open up the ground for better and more rigorous numerical studies of multipoint correlators in the near future.

1.3 Lightcone bootstrap

In chapter 2, we will generalize the basic ideas of the lightcone bootstrap to five and six-point functions in a snowflake configuration. It is thus of primary importance to review and explain some basic facts of this program.

While numerical methods have attained fantastic results, a better understanding of the analytic properties of the crossing equation is a must. This is an extremely complicated problem in general but much more treatable in specific kinematics. As discussed before, in the lightcone limit, i.e. when an operator approaches the lightcone of another such that $x_{ij}^2 \rightarrow 0$, the OPE simplifies and takes the form [63]

$$\phi_1(x_1)\phi_2(x_2) = \sum_k c_{12k} \int_0^1 [dt] \frac{\mathcal{O}_{k,J}(x_1 + tx_{21}, x_{12})}{(x_{12}^2)^{\frac{2\Delta_\phi - \tau_k}{2}}} + \dots \quad (1.23)$$

where \dots represent subleading contributions and we restrict ourselves to identical scalars of scaling dimension Δ_ϕ exchanging a symmetric and traceless operator of spin J and twist τ_k . Here the form of the measure $[dt]$ is not important but will be made explicit in chapter 2 equation (2.7). It follows from this OPE limit (or, equivalently, from solving the quadratic Casimir equations in the lightcone limit) that the conformal block in the small u limit can be written as

$$g_{k,J}(u, v) = u^{\tau_k/2} (1-v)^J {}_2F_1 \left(\frac{\tau_k}{2} + J, \frac{\tau_k}{2} + J, \tau_k + 2J, 1-v \right) \equiv u^{\tau_k/2} f_{\tau_k, J}(v), \quad (1.24)$$

where we note that CFT data is organized by the twist of the exchanged operator in the OPE.

¹²This method was introduced as a possible avenue to constrain CFT data of non-unitary theories.

Considering a correlation of four identical scalar operators, we can write the crossing equation (1.22) in the small u limit as

$$\left(1 + \sum_{\tau,J} P_{\tau,J} u^{\tau/2} f_{\tau,J}(v)\right) = \left(\frac{u}{v}\right)^{\Delta_\phi} \sum_{\tau,J} P_{\tau,J} g_{\tau,J}(v, u), \quad (1.25)$$

where $P_{\tau,J}$ is the product of OPE coefficients and we isolate the contribution of the identity operator in the direct channel.

In the small u limit, the leading contribution in the direct channel is given by the identity exchange. There are no other operators of zero twist to contribute. For unitary CFTs in $d > 2$, this follows from unitarity bounds. More generically, this separation is valid whenever there is a twist gap between the identity and the next operator. In this limit, the crossing equation reduces to

$$1 \approx \left(\frac{u}{v}\right)^{\Delta_\phi} \sum_{\tau,J} P_{\tau,J} g_{\tau,J}(v, u). \quad (1.26)$$

As it was shown in [44, 45]¹³, reproducing the identity exchange by the cross channel cannot be done by a finite number of OPE exchanges. In fact, the small u limit of the conformal block in the cross channel has at most a logarithmic behaviour in u . This is insufficient to cancel the explicit u^{Δ_ϕ} in the prefactor. Indeed, the identity exchange is reproduced by large spin contributions of a family of operators known as double-twist operators. At large spin, their schematic form and twist are given by

$$[\phi\phi]_{n,J} \sim \phi(\partial^2)^n \partial_{\mu_1} \dots \partial_{\mu_J} \phi \quad \tau = 2\Delta_\phi + 2n + \gamma(n, J), \quad (1.27)$$

where n is a non-negative integer and $\gamma(n, J)$ are the anomalous dimensions that will be suppressed by spin as we will now see.

In the small u limit and at large spin, the cross-channel conformal block goes as [44]

$$g_{\tau,J}(v, u) \approx v^{\tau/2} k_{2J}(1 - z) F^{(d)}(\tau, v) \quad (1.28)$$

$$k_\beta(x) \equiv x^{\beta/2} {}_2F_1(\beta/2, \beta/2, \beta, x), \quad (1.29)$$

where $F^{(d)}(\tau, v)$ is positive, analytic near $v = 0$ and begins with a constant.¹⁴ Note that for small v this is equivalent to using a lightcone block in the cross channel. In other words,

¹³Recently the results we review next were established more rigorously in [69].

¹⁴This behaviour is easy to check in $d = 2, 4$ where the full conformal blocks are known in closed form. For general d , one can check this solution in the Casimir equation [44].

we are making the operator at position 2 approach both the lightcones of operator 1 and operator 3. This is known as the double lightcone limit.

Using equations (1.26) and (1.28) with both u and v small, we see that in order to cancel the $v^{-\Delta_\phi}$, one requires the exchange in the cross channel of operators whose twist approaches $2\Delta_\phi$ at large spin. As discussed above, the cancellation of the power in u is done by the collective contribution of these operators. The sum over spin is dominated by the region where $J^2 u$ is fixed. In this region, the hypergeometric function is well approximated by a Bessel function. Moreover, we are entitled to replace the sum over spin by an integral.¹⁵ Provided the product of OPE coefficients at large spin has an asymptotic average behaviour dictated by mean field theory OPE coefficients, this integral reproduces the exchange of the identity! There is one extra comment that must be done. We proposed the existence of double-twist operators that have an extra n dependence in their twist. This has not been explained here. In fact, their existence in the OPE of the two identical scalars follows from the corrections in v in the cross-channel block. These corrections come from $F^{(d)}(\tau, v)$ and produce higher powers of v that have to be compensated by including these operators of twist $2\Delta_\phi + 2n$. These corrections were studied in the context of the lightcone bootstrap in [70, 71]. In the rest of this brief review we will stick to the leading family with $n = 0$.

Note that these results impose already nontrivial constraints on CFT data. The existence of an operator with twist $2\Delta_\phi$ at arbitrarily high spin together with Natchmann's theorem [72, 73]¹⁶ imposes the bound $\tau_J \leq 2\Delta_\phi$ on the minimum twist per spin J .

So far, we reproduced the identity exchange in the direct channel from the cross-channel side. Naturally, we could have included subleading terms in u in the former channel. We assume that there is a single operator of nonzero minimal twist that is responsible for the first subleading contribution.¹⁷ For a unitary CFT, Natchmann's theorem guarantees that this operator is necessarily either a scalar with scaling dimension less than $d - 2$ or the stress tensor itself.¹⁸ Recall that no spin 1 operator can be exchanged in the OPE of two identical scalars.

¹⁵In doing so, one should divide the integral over spin by a factor of 2 as only even spin operators can appear in the OPE of two identical scalars.

¹⁶Natchmann's theorem states that the minimum twist allowed for each spin J exchange in the OPE is a non-decreasing function of the spin.

¹⁷A finite amount of operators with the same first nonzero minimal twist can also be studied with the same method.

¹⁸Higher spin conserved currents would also have twist $d - 2$. However, if they exist, then they would couple as if formed from free fields [74].

As long as the minimal twist $\frac{\tau_{\min}}{2} - \Delta_\phi < 0$, subleading contributions grow as $u \rightarrow 0$ and large spin contributions in the cross channel should reproduce the power-divergent behaviour in u . Including a subleading term in the direct channel, the crossing symmetric equation is given by

$$1 + P_{\tau_{\min}, J_{\min}} u^{\tau_{\min}/2} f_{\tau_{\min}, J_{\min}}(v) \approx \sum_{\tau, J} P_{\tau, J} v^{\tau/2 - \Delta_\phi} u^{\Delta_\phi} f_{\tau, J}(u). \quad (1.30)$$

In the direct channel, the small v expansion produces $\log v$ terms. From the cross-channel side, this can be reproduced by considering an anomalous dimension correction in the twist of the exchanged operators. To correctly reproduce the power $u^{\tau_{\min}/2}$, the anomalous dimensions should be of the form ¹⁹

$$\gamma(0, J) = \frac{\gamma_0}{J^{\tau_{\min}}}. \quad (1.31)$$

On top of this, the equivalence between the two channels further imposes a correction to the mean-field theory OPE coefficients at large spin of the form

$$\delta P_{2\Delta_\phi, J} = \frac{c_0}{J^{\tau_{\min}}}. \quad (1.32)$$

The coefficients γ_0 and c_0 were found explicitly in [44] and their generalization to any n in [70, 71].

In the computations presented above we have only kept the leading behaviour at large spin. By keeping subleading terms in spin in the expansion of the cross-channel conformal block, we can unveil the subleading corrections in both anomalous dimensions and corrections to OPE coefficients. This is the subject of the large spin expansion studied in [75–77].

By analysing the crossing-symmetric equation in the double lightcone limit, we are able to gain enough analytic control over it to actually bootstrap the CFT data of families of double-twist operators in a series expansion in inverse powers of spin. Quite surprisingly, in [78], building on these methods, it was shown that, in the case of the 3d Ising model, large spin expansion has an extremely good agreement with numerical data even at low spins. This happens because double-twist operators actually sit in Regge trajectories that are analytic in spin. Moreover, their OPE coefficients, that we found at large spin, are not just mere density distributions but actually correspond to a unique operator at each spin. All these results are made transparent with the Lorentzian inversion formula [79]

¹⁹In fact, the behaviour is similar for generic n .

which supersedes these lightcone bootstrap methods as a computational tool by replacing the asymptotic $1/J$ expansion by convergent sums up to spin 2.

1.4 Regge Theory

We ended the previous section by invoking the powerful result of [79] that proved analyticity of CFT data in spin. This analyticity is a natural requirement of Regge theory.

In chapter 3, we will explore the generalization of conformal Regge theory to higher-point functions and for this reason we find it useful to devote the next pages to review some basic facts about Regge theory. For a more complete review see, for instance, [80].

In flat space, Regge theory came about as a theoretical explanation of experimental observations. When plotting the squared masses and angular momenta of several mesons, they seemed to organize themselves into almost straight families. These are the famous Regge trajectories in the Chew-Frautschi plots. It was quite natural to wonder about the existence of some analyticity in spin connecting these particles. Another experimental observation is related to scattering at high centre-of-mass energy at a fixed impact parameter, known as the Regge limit. In terms of the usual Mandelstam invariants, s , t and u , it corresponds to large s , fixed t . The existence of a strong forward peak ($t < 0$ and small compared to s) in $2 \rightarrow 2$ scattering processes obeys a general rule: there is a correlation between its existence and the possibility of exchanges of resonances and particles in the t channel. However, the observed scaling of the cross sections in the centre-of-mass energy, at large values of s , cannot be explained by a finite number of resonances in the t channel and a whole family of them has to be considered. This is also naturally imposed by Regge theory.

To understand these ideas, let us start by writing down a partial-wave decomposition in the t channel of a $2 \rightarrow 2$ amplitude of identical spinless particles of mass m ,

$$A(s, t) = \sum_J^{\infty} (2J + 1) a_J(t) P_J(z), \quad (1.33)$$

where $z = \cos \theta_t = 1 + 2s/(t - 4m^2)$, $P_J(z)$ is a Legendre polynomial of first kind of degree J , θ_t denotes the t -channel scattering angle, J is the angular momentum of the exchanged particles and $a_J(t)$ are the partial-wave coefficients.

Clearly, this sum only converges in the t -channel physical region $t > 4m^2$ and $s < 0$ and therefore cannot be applied to Regge limit. Note that for large s , and consequently

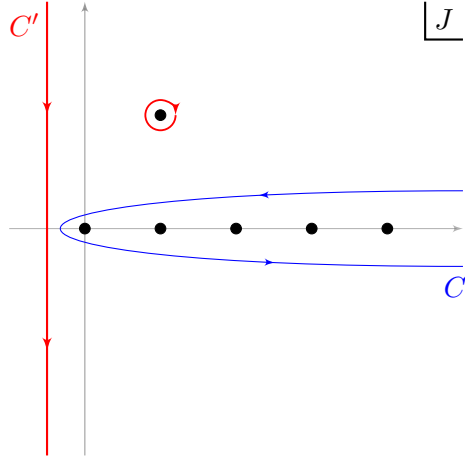


FIGURE 1.3: Contour integrals for the Sommerfeld-Watson transform for the four particle scattering in the J -complex plane. As one deforms the contour from C to C' one has to consider the contribution from dynamical singularities which here we assume to be a Regge pole.

large z , the Legendre polynomial goes as

$$P_J(z) \sim z^J. \quad (1.34)$$

Hence, we need to find a proper analytic continuation of this partial-wave decomposition in the region where it converges, before analytically continuing it to the Regge limit region, inside the s -channel physical region. This can be done by replacing the sum over spin by an integral by performing a Sommerfeld-Watson transform,

$$A(s, t) = \int_C \frac{dJ}{2\pi i} \frac{\pi}{\sin \pi J} (2J + 1) a(J, t) P_J(-z), \quad (1.35)$$

where C is the blue contour depicted in figure 1.3. We also use the fact $P_J(z) = (-1)^J P_J(-z)$. It is simple to check that by capturing the residues at the poles inside the contour one recovers the partial-wave series.

While performing the analytic continuation in spin, we assumed that the partial-wave coefficients $a_J(t)$ have a good and unique analytic continuation in angular momentum, $a(J, t)$, that matches their values at integers. This is however not true. In fact, the problem can be understood from the Froissart-Gribov formula for the partial-wave coefficients

$$a_J(t) = \frac{1}{2\pi i} \int_{z_0}^{\infty} dz \left(\text{Disc}_s A(s(t, z), t) + (-1)^J \text{Disc}_u A(u(t, -z), t) \right) Q_J(z), \quad (1.36)$$

where Q_J is a Legendre polynomial of the second kind and $\text{Disc}_{s(u)}$ denotes the discontinuity of the amplitude along the normal branch-cuts corresponding to s -channel (u -channel)

physical regions starting at z_0 .²⁰ Most importantly for our discussion here, the term $(-1)^J$ does not have a good analytic continuation in J . We are thus led to consider the contributions of odd and even J separately.²¹ We can then write

$$A^\pm(s, t) = \int_C \frac{dJ}{2\pi i} \frac{\pi}{2\pi i \sin \pi J} (2J+1) a^\pm(J, t) (P_J(-z) \pm P_J(z)) , \quad (1.37)$$

where the $+$ ($-$) sign has contributions from even (odd) angular momentum contributions.²²

The prescription above has a well-defined analytic continuation. This follows from Carlson's theorem²³ that guarantees its uniqueness given the good asymptotic behaviour of the integrand in the t -channel physical region at large J . Moreover, this further allows us to deform the contour C to C' in figure 1.3 by dropping the arcs at infinity.

As we now analytically continue the amplitude from the t -channel physical region to the Regge limit, it is possible that singularities (which are functions of t) cross our contour of integration. In this review and in the rest of the thesis, we will restrict ourselves to the first singularity that crosses the contour and assume that it is a pole. This is the so-called leading Regge pole due to the large s behaviour of the Legendre polynomial in equation (1.34). This pole is necessarily contained in the $a^\pm(J, t)$

$$a^\pm(J, t) \simeq \frac{\beta(t)}{J - \alpha(t)} , \quad (1.38)$$

where we only show the near-pole behaviour. Taking the Regge limit and picking up the residue at the leading pole we find the leading behaviour

$$A^\pm(s, t) \sim (2\alpha(t) + 1)\beta(t) \frac{\left((-s)^{\alpha(t)} \pm s^{\alpha(t)}\right)}{\sin(\pi\alpha(t))} , \quad (1.39)$$

where we absorbed nonsingular factors into $\beta(t)$. In this expression we neglect subleading contributions from the background integral and from other singularities. In fact, one could have continued pushing the contour all the way to left and capturing the subleading contributions. As one moves the contour past $\text{Re}(J) < -1/2$, the asymptotic behaviour at

²⁰In $2 \rightarrow 2$ scattering of the lightest spinless particles of a theory, one does not expect any other anomalous branch-cut singularities.

²¹For identical spinless particles, only even contributions matter. We decided to keep the two cases for completeness of the discussion.

²²Another possible decomposition of the amplitude that has good analytic continuation will be discussed in chapter 3 and related to this one.

²³Carlson theorem says that, if a function $f(z)$ is regular and diverges no faster than $e^{k|z|}$ for large z with $\text{Re}(z) \geq 0$, where $k < \pi$, and $f(z) = 0$ for $z = 0, 1, 2, 3, \dots$, then $f(z) = 0$ everywhere.

large s of the Legendre polynomials changes. In [81], Mandelstam explained how to correctly capture pole contributions past this point and ensure that the remaining background integral is indeed subleading.

The presented Regge theory explained not only the experimental observation of families of operators that seem to be analytic in angular momentum, the so-called Regge trajectories, but also used them to derive the observed behaviour of cross sections at large s .

In the context of AdS/CFT correspondence it is natural to wonder about the CFT description of a high-energy scattering in AdS. Thanks to the works of [82–85], it was understood the corresponding kinematics of Regge limit in the CFT side. Later, in [86], Regge theory was established in CFTs.

As we will see below, the Regge limit in CFTs corresponds to an intrinsically Lorentzian configuration that probes causal relations between operators. Adding causality as a new constraint in bootstrap is a major advantage of considering Lorentzian kinematics of CFTs. There are several examples of CFT results that follow from causality (in some cases exploring Regge limit)²⁴: the proof of the ANEC [89], conformal collider bounds proof [90, 91], finding Einstein gravity from large N CFTs and putting bounds on Weyl anomaly coefficients [92–96].

To consider Regge kinematics, we need to understand how to Wick rotate correlation functions from Euclidean to Lorentzian space. This was carefully studied in [97, 98]. In chapter 3, we will review some of their results. For the moment, let us just briefly give the prescription to find a given Lorentzian correlator, also called Wightman function, from an Euclidean correlator,

$$\langle \mathcal{O}(t_1, \mathbf{x}_1) \dots \mathcal{O}(t_n, \mathbf{x}_n) \rangle \equiv \lim_{\substack{\epsilon_i \rightarrow 0 \\ \epsilon_1 > \dots > \epsilon_n}} \langle \mathcal{O}(\epsilon_1 + it_1, \mathbf{x}_1) \dots \mathcal{O}(\epsilon_n + it_n, \mathbf{x}_n) \rangle^E, \quad (1.40)$$

where the superscript E corresponds to Euclidean space. Wightman functions are correlation functions of local operators that commute at spacelike separation and have an associated ordering. For four-point correlators and with the appropriate ordering of ϵ 's above, the limit defines a convergent Lorentzian correlator (at least in distributional sense) obeying Wightman axioms [97].

In a CFT, the Regge limit corresponds to the kinematics of figure 1.4 where all operators lie in a single plane. Moreover, operator 1 is in the past of 4 and operator 2 in the future of 3.

²⁴See also [87, 88]

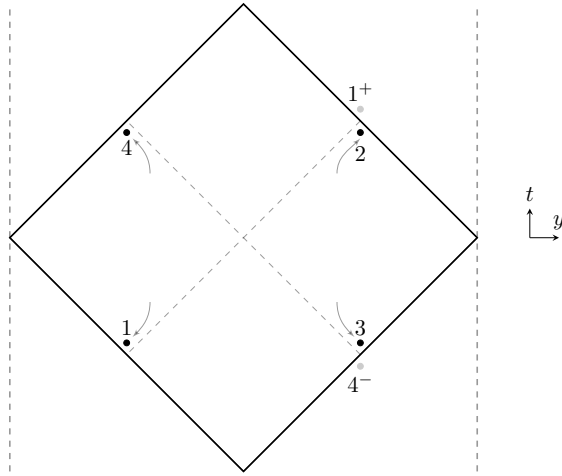


FIGURE 1.4: Regge limit kinematics.

For simplicity, let us consider that all operators are identical scalars as above. We also consider a Wightman correlator with an ordering compatible with the time ordering of figure 1.4, i.e. $\langle \phi_4 \phi_1 \phi_2 \phi_3 \rangle$. This correlation function admits a conformal block decomposition in terms of the two cross ratios z and \bar{z} presented in (1.20) which are real and independent in Lorentzian kinematics. Starting from a configuration where all points are spacelike separated from each other (which is basically equivalent to an Euclidean configuration) and boosting the operators to the configuration of figure 1.4, we can check the effect of the ϵ -prescription of (1.40) at the level of the cross-ratios. It is easy to show that \bar{z} goes through a branch-cut of the conformal block in the interval $(1, +\infty)$, before both $z, \bar{z} \rightarrow 0$ with fixed z/\bar{z} . Note that this behaviour in the cross ratios mimics the Euclidean OPE limit in the 12-34 channel, but with the important difference that for Regge limit this happens after a branch-cut has been crossed. This crossing is a clear indication that the OPE decomposition in this channel does not converge. However, similarly to the story we presented for flat space, Regge theory provides a way to resum OPE contributions in such a way as to show the dominant contribution of a Regge pole/Reggeon exchange which is an example of a light-ray operator [99].

As \bar{z} crosses the branch-cut, the conformal block develops a discontinuity that is proportional to a block where the roles of scaling dimensions and spin are permuted as $(\Delta, J) \rightarrow (1 - J, 1 - \Delta)$. In the limit where both $z, \bar{z} \rightarrow 0$, this block goes as

$$g_{1-J, 1-\Delta}(z, \bar{z}) \sim (z\bar{z})^{\frac{1-J}{2}} \quad (1.41)$$

and dominates the Regge limit. Moreover, the sum over spins for this block seems clearly divergent. However, it can be shown that the correlator is actually bounded in the Regge

limit. This can be proved by invoking a different OPE channel where no branch-cuts are crossed. Alternatively, one can use a Cauchy-Schwarz-inequality type of argument, based on a positive-definite Rindler inner product (note that the kinematics of figure 1.4 is Rindler symmetric), to bound the Regge correlator by the Euclidean one [100]. This boundedness suggests that OPE coefficients of large and low spins should talk and balance each other in order to produce a bounded behaviour of the correlator. In fact, this is indeed what follows from the Lorentzian inversion formula [79, 101].

Let us now briefly see how Regge theory can be formulated for a correlation in a CFT. Similarly to flat space, the connected part of a four-point correlator of identical scalars admits a conformal partial wave expansion. Stripping off a prefactor, we can write

$$g(u, v) = \sum_J \int_{-\infty}^{\infty} d\nu b_J(\nu) F_{\nu, J}(u, v), \quad (1.42)$$

where we use a principal series representation where the scaling dimension associated to the partial wave is given by $\Delta = d/2 + i\nu$. The function $F_{\nu, J}(u, v)$ is the so-called conformal partial wave and it is related with the conformal blocks

$$F_{\nu, J}(u, v) = \kappa_{\nu, J} g_{h+i\nu, l}(u, v) + \kappa_{-\nu, J} g_{h-i\nu, J}(u, v), \quad \kappa_{\nu, J} = \frac{i\nu}{2\pi K_{h+i\nu, J}}, \quad (1.43)$$

where $h = d/2$ and the second conformal block is known as the shadow of the first. The exact form of the coefficients $K_{\Delta, J}$ is not important for the discussion we do here - see [86].

In order to recover the conformal block decomposition for the exchange of an operator of scaling dimension Δ and spin J from (1.42), using the fact that $g_{h+i\nu, J}$ decays exponentially in $\text{Im}(\nu) \rightarrow -\infty$, one deforms the contour in ν into the lower half plane and picks the necessary poles. It is then clear that the partial amplitude $b_J(\nu)$ must have poles of the form

$$b_J(\nu) \approx \frac{r(\Delta, J)}{\nu^2 + (\Delta - h)^2}, \quad r(\Delta, l) = f_{12k} f_{34k} K_{\Delta, J}. \quad (1.44)$$

This reminds us of the discussion we had for flat-space provided that $b_J(\nu)$ can be analytically continued in spin.

To further explore the similarities with the presentation of Regge theory in flat space, we will switch from this position-space presentation to a Mellin space one. This is also the language used in [86] and the space where we will make most of the discussion in chapter 3.

The connected part of a four-point scalar correlator of identical scalars can be written in Mellin space

$$\langle \phi(x_1) \dots \phi(x_4) \rangle_c = \int [d\delta] M(\delta_{ij}) \prod_{1 \leq i < j \leq 4} \Gamma(\delta_{ij}) x_{ij}^{-2\delta_{ij}}, \quad (1.45)$$

where $M(\delta_{ij})$ is called Mellin amplitude and the δ_{ij} are jointly called Mellin variables. The integral runs parallel to the imaginary axis.

Conformal invariance imposes constraints in the Mellin variables

$$\sum_{j=1}^4 \delta_{ij} = 0, \quad \delta_{ii} = -\Delta_i, \quad (1.46)$$

in such a way that we are left with only two independent Mellin variables. For later similarity with the flat-space result, we define two independent Mellin variables s and t as

$$s = -2\delta_{13}, \quad t = 2\Delta_\phi - 2\Delta_{12}. \quad (1.47)$$

As in position space, we can also write down a conformal partial wave decomposition in Mellin space,

$$M(s, t) = \sum_J \int_{-\infty}^{+\infty} d\nu b_J(\nu) M_{\nu, J}(s, t), \quad (1.48)$$

where the partial waves $M_{\nu, J}(s, t)$ are obtained by a Mellin transform of the position space partial wave $F_{\nu, J}(u, v)$. Moreover, $M_{\nu, J}(s, t) = M_{-\nu, J}(s, t)$ can be written as

$$M_{\nu, J}(s, t) = \omega_{\nu, J}(t) P_{\nu, J}(s, t), \quad (1.49)$$

where $P_{\nu, J}(s, t)$ are the Mack polynomials of degree J in both s and t . The function $\omega_{\nu, J}(t)$ is just an overall normalization that can be extracted from the Mack polynomials such that at large s they behave as $P_{\nu, J}(s, t) \sim s^J$ and its explicit form can be found in [86].

In fact, as shown in [86], the Regge kinematics of figure 1.4 is dominated in Mellin space by the region of large s and fixed t . This resemblance with flat-space Regge limit explains the suggestive relabelling of the Mellin variables.

Just as in flat space, we can replace the sum over spin by an integral by doing an equivalent Sommerfeld-Watson transform. In doing so, we have to assume that $b_J(\nu)$ has a good analytic continuation in spin. As in flat space, however, one expects that this is not in general the case and even and odd spins have to be considered separately. This was later proved with the Lorentzian inversion formula [79]. In fact, for identical scalars only even

spin contributions can appear in the OPE and therefore we do not have to consider two separate cases. The general expectation for the need of two distinct cases in this Mellin space formulation comes from a property of Mack polynomials

$$\mathcal{P}_{\nu,J}(z, t) = P\left(\frac{(z-1)t}{2}, t\right), \quad \mathcal{P}_{\nu,J}(-z, t) = (-1)^J \mathcal{P}_{\nu,J}(z, t) \quad (1.50)$$

where $z = 1 + 2s/t$ and J is integer. Note that this is the same property of Legendre polynomials that is ultimately related to a bad analytic continuation in spin and that forced us to consider even and odd spins separately.

After performing the Sommerfeld-Watson transform and picking up the contribution from the leading Regge pole, we are left with

$$\begin{aligned} M(s, t) &\approx \int_{-\infty}^{+\infty} d\nu \frac{\pi}{2 \sin(\pi j(\nu))} \frac{j'(\nu) r(j(\nu))}{2\nu} \omega_{\nu, j(\nu)}(t) \left(\mathcal{P}_{\nu, j(\nu)}(-z, t) + \mathcal{P}_{\nu, j(\nu)}(z, t) \right) \\ &\approx \int_{-\infty}^{+\infty} d\nu \frac{\pi}{2 \sin(\pi j(\nu))} \frac{j'(\nu) r(j(\nu))}{2\nu} \omega_{\nu, j(\nu)}(t) \left(s^{j(\nu)} + (-s)^{j(\nu)} \right) \end{aligned} \quad (1.51)$$

where in the second line we took the large s limit. Here we also used the fact that after analytic continuations the pole in ν of $b_J^+(\nu)$ becomes a pole in J ,

$$b_J^+(\nu) \approx \frac{r(\Delta(J), J)}{\nu^2 + (\Delta - h)^2} \approx -\frac{j'(\nu) r(j(\nu))}{2\nu(J - j(\nu))}, \quad (1.52)$$

where $j(\nu)$ is the inverse function of $\Delta(J)$ defined by

$$\nu^2 + (\Delta(j(\nu)) - h)^2 = 0. \quad (1.53)$$

We reviewed Regge theory in the context of CFTs and in flat space. One of the great successes of conformal Regge theory is the, now proved, analyticity in spin of CFT data. In chapter 3, by exploring the generalization of conformal Regge theory to five-point functions, we will propose the existence of analyticity in a label for different tensor structures of three-point functions involving two spinning operators.

1.5 $\mathcal{N} = 4$ SYM and type IIB SUGRA

One of the most celebrated and studied examples of the AdS/CFT duality involves $\mathcal{N} = 4$ SYM. This theory is a maximally supersymmetric gauge theory in 4 dimensions with $SU(N)$ gauge group that is conformal for all values of the coupling g_{YM} . Its field content is given by the gauge bosons A_μ , six real massless scalars Φ^I with $I = 1, \dots, 6$, four chiral fermions Ψ_α^a and four anti-chiral fermions $\bar{\Psi}_{\dot{\alpha}a}$ with $a = 1, \dots, 4$. All the fields transform

in the adjoint representation of $SU(N)$. Moreover, in planar limit, i.e in the large N limit, this theory enjoys integrability properties that make it more tractable and, possibly, completely solvable [102, 103].

$\mathcal{N} = 4$ is conjectured to be dual to IIB superstring theory in $\text{AdS}_5 \times S^5$ with radius of curvature R and N units of field strength F_5 flux through S^5 [26]. Under the conjecture the couplings can be related in both sides of the duality,

$$g_{\text{YM}}^2 = 2\pi g_s, \quad 2\lambda \equiv 2g_{\text{YM}}^2 N = R^4/\alpha'^2, \quad (1.54)$$

where g_s is the string coupling constant and $\sqrt{\alpha'}$ is the string length. We have also introduced the t'Hooft coupling λ .

This duality comes as an example of the holographic principle, and if proven, shows that the two theories are actually dynamically equivalent. In other words, information of five-dimensional IIB string theory obtained from Kaluza-Klein reduction on S^5 should have a description from the four-dimensional CFT at the boundary of AdS.

In this thesis, we consider the strong coupling limit of $\mathcal{N} = 4$ SYM, i.e. both N and λ large. In this limit, the theory is dual to classical type-IIB supergravity and all massive string excitations decouple leaving behind only supergravity states: single-particle and two-body bound states. From the CFT theory, this is the same as to say that we should only consider dual operators that are protected in this limit, i.e. operators which have a scaling dimension that is fixed and does not grow with λ .

The single-particle states of the graviton and the Kaluza-Klein multiplets are dual to protected half-BPS operators. Supersymmetry allows us to organize the operators into superconformal multiplets where the bottom components, the superprimaries, generate their superdescendants by action of supercharges, see for instance [104]. We can thus consider correlation functions of the half-BPS superprimaries,

$$\mathcal{O}_p(x, t) = \text{Tr} \left(\Phi^{\{I_1} \dots \Phi^{I_p\}} \right) t_{I_1} \dots t_{I_p}, \quad I_k = 1, \dots, 6, \quad p = 2, 3, \dots, \quad (1.55)$$

that transform as a rank- p symmetric and traceless representation (denoted by the curly bracket) of the $SU(4) \simeq SO(6)$ R-symmetry group. Here Φ^I are elementary scalar fields and t_I are null polarization vectors that are introduced for a convenient index-free notation. These operators belong to short multiplets, obeying a shortening condition that fixes their scaling dimensions to be integer and $\Delta = p$.

On the other hand, two-particle bound states are dual to double-trace operators. While belonging to long multiplets, in the strict large N , their scaling dimension is fixed and protected. These operators are then degenerate and of the form

$$\mathcal{O}_{pq} = \mathcal{O}_p \partial^J \square^{\frac{1}{2}(\tau-p-q)} \mathcal{O}_q, \quad (1.56)$$

with twist τ and spin J . Considering $1/N^2$ corrections, double-trace operators acquire anomalous dimensions which have the form found in [105].

As mentioned above, we are focusing our attention on correlation functions of half-BPS superprimaries. As in the usual conformal bootstrap scenario, the study of holographic correlators is far more developed for four-point functions than for higher-point analogues, where there is still no systematic study of the superconformal ward identities implications available.

Four-point correlators, for generic values of the coupling, encode a large amount of non-protected data, while two- and three-point functions of half-BPS operators obey non-renormalization theorems that allows one to compute them from free field theory [106–114].²⁵ This makes clear the relevance of four-point correlators to access the data of the theory. The AdS/CFT dictionary defines a diagrammatic strategy to compute these correlation functions. To leading order in N , one has to consider all possible Witten diagrams at tree level with external legs given by bulk-to-boundary propagators and internal legs by bulk-to-bulk propagators. The vertices can be read off from the effective action of supergravity. This is not trivial whatsoever. In fact, the quartic scalar vertices were obtained in [120] in a herculean feat since they take 15 pages to be written. Luckily, in $AdS_5 \times S^5$, there is still some simplification in place as noted in [121]: the complicated exchange Witten diagrams can be written as finite sums over contact diagrams, the so-called D-functions. Despite this simplification, the computation by traditional methods is extremely cumbersome and therefore only produced very few explicit results. Examples are: the computation of correlators of four identical half-BPS operators with scaling dimension with $p = 2$ [122], $p = 3$ [123] and $p = 4$ [124]; the next-to-next-to-extremal correlators with two equal weights, i.e. the cases $p_1 = n + k, p_2 = n - k, p_3 = p_4 = k + 2$ [125–127].

The key simplification that the exchange Witten diagrams can be written as finite sums over D-functions led the authors of [128] to change gears and propose a bootstrap

²⁵Extremal and next-to-extremal four-point functions of half-BPS operators also obey non-renormalization theorems [115–119]. Extremality of these correlators is defined as $2E = \sum_{i=1}^3 p_i - p_4$ where we assume p_4 is the largest scaling dimension. Extremal and next-to-extremal cases correspond to $E = 0$ and $E = 1$.

philosophy instead. They proposed to write the answer as sums over D-functions with undetermined coefficients. After removing some redundancy and linear dependence of the D-functions, by reducing all of them to a seed function with known differential relations, one can use superconformal ward identities to fix the undetermined coefficients. This bootstrap eschews the complicated effective action of supergravity and is therefore more amenable to compute correlators with generic weights p . In the same paper, it was also proposed an ansatz for the generic $\langle \mathcal{O}_{p_1} \mathcal{O}_{p_2} \mathcal{O}_{p_3} \mathcal{O}_{p_4} \rangle$ in Mellin space. This ansatz was later rederived from a conjectured ten-dimensional conformal symmetry of these operators at tree-level in [48] which allowed to compute $\langle \mathcal{O}_{p_1} \mathcal{O}_{p_2} \mathcal{O}_{p_3} \mathcal{O}_{p_4} \rangle$ from differentiating the simpler and known $\langle \mathcal{O}_2 \mathcal{O}_2 \mathcal{O}_2 \mathcal{O}_2 \rangle$.

In this thesis, we propose to further extend the bootstrap approach to compute five-point correlators of these operators and we formulate it entirely in Mellin space. This will be the subject of chapter 4 where we fix the form of the correlator $\langle \mathcal{O}_p \mathcal{O}_p \mathcal{O}_2 \mathcal{O}_2 \mathcal{O}_2 \rangle$.

Recently, these ideas have received an increasing interest and various results deserve mentioning. In [57], the form of $\langle \mathcal{O}_2 \mathcal{O}_2 \mathcal{O}_2 \mathcal{O}_2 \mathcal{O}_2 \rangle$ was found using a bootstrap method that largely motivated our framework. Similar ideas were also applied to study the tree-level five-point correlator of the lowest Kaluza-Klein mode of SYM theory on $\text{AdS}_5 \times S^3$ dual to the correlator of the flavour current multiplet in the dual $\mathcal{N} = 2$ superconformal field theory [129]. In [130], it was found the extension of the previous result to six-point functions, using Mellin factorization, a key element of our chapter 4, and flat space constraints.

1.6 Structure of the thesis

Having reviewed some essential facts about CFTs, Regge theory and the strong coupling limit of the $\mathcal{N} = 4$ SYM and IIB supergravity in $\text{AdS}_5 \times S^5$, we are now in place to attack some of the open problems we address in the following chapters.

In chapter 2, we extend the analytic lightcone bootstrap to the study of five- and six-point scalar correlation functions. As mentioned before, we restrict our attention to the snowflake topology of these correlators, which corresponds to only performing OPEs between the external operators. After explaining the derivation of the higher-point conformal blocks in the lightcone limit, using the lightcone OPE limit, we proceed as in the four-point bootstrap we reviewed above: we isolate the direct-channel singularities associated with the leading twist operator exchanges and reproduce them with the large spin behaviour of

double-twist-like operators in the cross channel. This allows us to probe and fix the large-spin form of anomalous dimensions and OPE coefficients involving two spinning operators and one external scalar in the five-point case, and between three spinning operators in the six-point case. Our results are then checked by explicit results for the six-point mean-field theory correlator and for the disconnected parts of a five-point correlator in ϕ^3 theory in $d = 6 - \epsilon$. We give some extra technical details in Appendix 2.5. This includes some explicit results on higher-point blocks, an analysis of higher-point D-functions using standard techniques from AdS perturbation theory as well as some results on the conformal harmonic analysis of higher-point functions.

In chapter 3, we extend conformal Regge theory to the case of a five-point correlator of identical scalars. We start by reviewing some flat-space literature on higher-point amplitudes in the context of Regge theory. This literature, while containing important results, is largely unfamiliar to most community and was abandoned in face of the scarcity of known results about analytic properties of multi-point amplitudes. Nonetheless, it pointed out several subtleties and resolutions that guided us in our study in the context of CFTs. We proceed by studying several limits of OPE at the level of five-point functions, namely Euclidean, lightcone and Regge limits. We comment on the differences and organization of the leading operators in each case. In the Euclidean limit, we found a new basis of three-point functions with spinning operators that factorizes the conformal block in each of the five cross ratios. In the section dedicated to the lightcone limit, besides revisiting the derivation of the lightcone blocks, we write down an expression valid up to all subleading corrections, whenever the exchanged operators are scalars. We also propose for the first time the appropriate kinematics for a five-point correlation function in the Regge limit, which in terms of the cross ratios behaves similarly to the Euclidean limit but only after branch cuts have been crossed. Moreover, we show that in Mellin space this kinematics can be phrased in terms of Mellin variables in a way that resembles the flat-space multi-Regge limit. After reviewing how to define Wightman functions from Euclidean correlators, we use a conformal partial-wave writing of the correlator and describe the associated Regge theory in Mellin space. To do so we propose a well-defined analytic continuation not only in spin but also in the label of different three-point structures, which forces us to consider the contribution of (at least) 8 different signatures. While the spin of Regge trajectories are associated with poles in the partial-wave coefficients, we conjecture that there is no pole

associated with this new label and write the Sommerfeld-Watson accordingly. Some technical discussions and computations are in Appendix 3.5. In particular, we derive recursion relations obeyed by lightcone blocks and compute explicitly the scalar Mellin partial wave. We also use this appendix to study the Regge limit in position space for the special case where the lightcone blocks can be integrated explicitly. Finally, we suggest the kinematics for a single Reggeon exchange within a five-point function as well as for triple Reggeon exchanges in a snowflake six-point function.

In the penultimate chapter 4, we present a bootstrap algorithm to find the five-point correlator of half-BPS superprimaries $\langle \mathcal{O}_p \mathcal{O}_p \mathcal{O}_2 \mathcal{O}_2 \mathcal{O}_2 \rangle$. After reviewing superconformal kinematics, we discuss two choices of polarization vectors (from index-free notation) that impose nontrivial constraints from superconformal symmetry on correlators. We proceed to discuss Mellin amplitudes and their factorization properties. This is a key element to fix the singular part of our ansatz for these correlation functions, while regular terms are fixed by the constraints we just mentioned. The factorization of the Mellin result into three- and four-point functions glued together requires the knowledge of four-point correlators involving spin 1 and spin 2 operators. These can be found in analytic superspace and explicit expressions are given in Appendix 4.5, where an example of a factorization is also shown in detail.

Lastly, we conclude with a brief summary of the main results of this thesis and discuss possible open directions for the near and far future.

Chapter 2

Lightcone Bootstrap at higher points

2.1 Introduction

Analytic bootstrap methods have given a structural understanding of CFTs by leveraging the analytic structure of four-point functions [44, 45, 70, 71, 75–78, 93, 94, 96, 131]. Typically such studies consider the four-point function of scalar operators. This fact limits the data that can be accessed to scalar/scalar/symmetric traceless (of spin J) OPE coefficients. However, it is important to consider OPE coefficients between multiple spinning operators, of which an important example is the OPE coefficient of three stress tensors [90, 132]. A possibility would be to extend the analytic bootstrap to the four-point function of operators with spin, but this approach is technically challenging and works mostly in a case by case basis. An alternative is to consider higher-point functions of scalar operators, which through the OPE contains information about operators of arbitrary spin [64, 133]. In this case the technical challenge lies upon our knowledge of higher-point conformal blocks, which is still incomplete [51, 57–59, 62, 133].

For the scalar four-point function, the lightcone bootstrap predicts the universal behaviour of scalar/scalar/spin J OPE coefficients at large spin, which are of mean field type [44, 45]. Subsequent corrections, that include scaling dimensions and OPE coefficients, are determined by the leading twist operators in the theory [44, 45]. This large spin expansion is actually convergent up to a low spin value determined by the Regge behaviour of the four-point function [79, 101]. A remarkable check of the accuracy of this method was done in the 3D Ising model where the numerical bootstrap provided the data for comparison [78, 134] (see also [135] for the $O(2)$ model). Motivated by this success, our goal is to

extend the lightcone bootstrap to the case of higher-point functions and therefore access OPE data involving spinning operators.

More concretely, we bootstrap five- and six-point functions. In the five-point case there is an unique OPE topology which involves the exchange of two operators of spin J_1 and J_2 and therefore includes the scalar/spin J_1 /spin J_2 OPE coefficient, see (2.42) and (2.48). In the six-point case we consider the snowflake OPE channel which involves the exchange of three operators of spin J_1 , J_2 and J_3 and therefore includes the spin J_1 /spin J_2 /spin J_3 OPE coefficient, see (2.62), (2.70) and (2.75). This bootstrap analysis is done in section 2.3, which follows section 2.2 where we review the kinematics and derive the lightcone conformal blocks for five- and six-point functions. Our results are tested in section 2.4 for the case of generalized free theory and of theories with a cubic coupling, whose block decomposition we determine explicitly. We conclude with a discussion of open problems in section 2.5.

Additional technical details are given in the appendices: appendix 2.A gives more details on higher-point blocks, including some comments about the Euclidean expansion and the Mellin representation; appendix 2.B discusses higher-point D -functions based on AdS techniques; appendix 2.C presents new results on conformal harmonic analysis relevant for higher-point functions and can be read mostly independently from the main text.

2.2 Kinematics and conformal blocks

It is a well known property that n -point correlation functions in a conformal field theory depend nontrivially on $n(n-3)/2$ conformal invariant variables for high enough spacetime dimension¹. The choice of conformal invariant cross-ratios usually depends on the problem one is analysing. In a four-point function, that depends on two cross-ratios (say u and v), there are several choices of cross-ratios used throughout the literature, for example

$$u = z\bar{z} = \frac{x_{12}^2 x_{34}^2}{x_{13}^2 x_{24}^2}, \quad v = (1-z)(1-\bar{z}) = \frac{x_{14}^2 x_{23}^2}{x_{13}^2 x_{24}^2}, \quad (2.1)$$

or

$$s = |z|, \quad \xi = \cos \theta = \frac{z + \bar{z}}{2|z|}. \quad (2.2)$$

¹There are relations between conformal invariant cross-ratios for low dimensions ($d \leq n-2$) such that the number of independent variables is instead $nd - (d+1)(d+2)/2$.

This chapter is focused on the analytic bootstrap of five- and six-point correlation functions, and therefore we will need to use appropriate sets of cross-ratios. For the five-point function it will be convenient to work with the five variables u_1, \dots, u_5 given by

$$u_1 = \frac{x_{12}^2 x_{35}^2}{x_{13}^2 x_{25}^2}, \quad u_{i+1} = u_i|_{x_j \rightarrow x_{j+1}}, \quad (2.3)$$

where in this definition the subscript in x_j is taken modulo 5 (for example $x_6 \equiv x_1$). For the six-point function we introduce the nine cross-ratios u_1, \dots, u_6 and U_1, \dots, U_3 defined by

$$u_1 = \frac{x_{12}^2 x_{35}^2}{x_{13}^2 x_{25}^2}, \quad u_{i+1} = u_i|_{x_j \rightarrow x_{j+1}}, \quad U_1 = \frac{x_{13}^2 x_{46}^2}{x_{14}^2 x_{36}^2}, \quad U_{i+1} = U_i|_{x_j \rightarrow x_{j+1}}, \quad (2.4)$$

where the subscript in x_j is now taken modulo 6.

We will be interested in the Lorentzian lightcone expansion of correlation functions. The difference between the Lorentzian and Euclidean expansions can be easily understood from the OPE of two operators. In the Euclidean case the operators are taken to be coincident ($x_{ij} \rightarrow 0$) while in the Lorentzian case the operators approach the lightcone of each other ($x_{ij}^2 \rightarrow 0$). As is well known, the Euclidean limit is dominated by the operators with lowest scaling dimension, in contrast with the Lorentzian case that is dominated by the operator with lowest twist $\tau = \Delta - J$. This is evident from the leading term of the formula for the OPE

$$\phi(x_1) \phi(x_2) \approx \sum_k C_{12k} \frac{(x_{12} \cdot \mathcal{D}_z)^J \mathcal{O}_{k,J}(x_1, z)}{(x_{12}^2)^{\frac{2\Delta_\phi - \tau_k}{2}}} + \dots \quad \text{Euclidean} \quad (2.5)$$

$$\phi(x_1) \phi(x_2) \approx \sum_k C_{12k} \int_0^1 [dt] \frac{\mathcal{O}_{k,J}(x_1 + tx_{21}, x_{12})}{(x_{12}^2)^{\frac{2\Delta_\phi - \tau_k}{2}}} + \dots \quad \text{Lorentzian} \quad (2.6)$$

where the \dots represent subleading terms in each expansion, z is a null polarization vector,

$$[dt] = \frac{\Gamma(\Delta_k + J)}{\Gamma^2(\frac{\Delta_k + J}{2})} (t(1-t))^{\frac{\Delta_k + J}{2} - 1} dt, \quad (2.7)$$

and \mathcal{D}_z is the so-called Todorov operator [136]

$$\mathcal{D}_z = \left(\frac{d}{2} - 1 + z \cdot \frac{\partial}{\partial z} \right) \frac{\partial}{\partial z^\mu} - \frac{1}{2} z^\mu \frac{\partial^2}{\partial z \cdot \partial z}. \quad (2.8)$$

The formulae above are key in obtaining the conformal block expansion around both limits. For example, in the four-point function case it is trivial to obtain the lightcone block from

(2.6), with the result

$$\begin{aligned} \langle \phi(x_1) \dots \phi(x_4) \rangle &\approx \sum_k \frac{C_{12k}}{(x_{12}^2)^{\frac{2\Delta_\phi - \tau_k}{2}}} \int [dt] \langle \mathcal{O}_k(x_1 + tx_{21}, x_{12}) \phi(x_3) \phi(x_4) \rangle \\ &= \sum_k \frac{C_{12k}^2}{(x_{12}^2 x_{34}^2)^{\frac{2\Delta_\phi - \tau_k}{2}}} \int \frac{[dt] (x_{13}^2 x_{24}^2 - x_{14}^2 x_{23}^2)^J}{(x_{23}^2 t + (1-t)x_{13}^2)^{\frac{\Delta_k + J}{2}} (x_{24}^2 t + (1-t)x_{14}^2)^{\frac{\Delta_k + J}{2}}}, \end{aligned} \quad (2.9)$$

where we have changed variables $t \rightarrow t/(t+1)$ and $t \rightarrow tx_{24}^2/x_{14}^2$. The lightcone block for the exchange of an operator \mathcal{O}_k is defined by this leading term in the expansion

$$\langle \phi(x_1) \dots \phi(x_4) \rangle \approx \frac{1}{(x_{12}^2 x_{34}^2)^{\Delta_\phi}} \sum_k C_{12k}^2 (\mathcal{G}_k(u, v) + \dots), \quad (2.10)$$

where

$$\mathcal{G}_k(u, v) = u^{\tau_k/2} (1-v)^{J_k} {}_2F_1 \left(\frac{\Delta_k + J_k}{2}, \frac{\Delta_k + J_k}{2}, \Delta_k + J_k, 1-v \right) \equiv u^{\tau_k/2} g_k(v). \quad (2.11)$$

We defined the function $g_k(v)$ for later convenience. Note that the expansion (2.10) is merely schematic, since subleading terms in the lightcone limit of a lower twist block can dominate with respect to the lightcone limit of a higher twist block.

2.2.1 Lightcone conformal blocks

Let us start with the lightcone expansion of the five-point conformal block. Applying twice the OPE limit (2.6) we obtain

$$\langle \phi(x_1) \dots \phi(x_5) \rangle \approx \sum_{k_i} \left(\prod_{i=1}^2 C_{\phi\phi k_i} \int [dt_i] \right) \frac{\langle \mathcal{O}_{k_1}(x_1 + t_1 x_{21}, x_{12}) \mathcal{O}_{k_2}(x_3 + t_2 x_{43}, x_{34}) \phi(x_5) \rangle}{(x_{12}^2)^{\frac{2\Delta_\phi - \tau_{k_1}}{2}} (x_{34}^2)^{\frac{2\Delta_\phi - \tau_{k_2}}{2}}}. \quad (2.12)$$

The limits $x_{12}^2 \rightarrow 0$ and $x_{34}^2 \rightarrow 0$ correspond to $u_1 \rightarrow 0$ and $u_3 \rightarrow 0$, respectively. The three-point function in the integrand involves the external scalar and two symmetric traceless operators with arbitrary spin as depicted in the top-left part of figure 2.1. Our convention for three-point functions of symmetric and traceless operators is [32]

$$\langle \mathcal{O}_{k_1}(x_1, z_1) \dots \mathcal{O}_{k_3}(x_3, z_3) \rangle = \sum_{\ell_i} \frac{C_{J_1 J_2 J_3}^{\ell_1 \ell_2 \ell_3} V_{1,23}^{J_1 - \ell_2 - \ell_3} V_{2,31}^{J_2 - \ell_1 - \ell_3} V_{3,12}^{J_3 - \ell_1 - \ell_2} H_{12}^{\ell_3} H_{13}^{\ell_2} H_{23}^{\ell_1}}{(x_{12}^2)^{\frac{h_1 + h_2 - h_3}{2}} (x_{13}^2)^{\frac{h_1 + h_3 - h_2}{2}} (x_{23}^2)^{\frac{h_2 + h_3 - h_1}{2}}}, \quad (2.13)$$

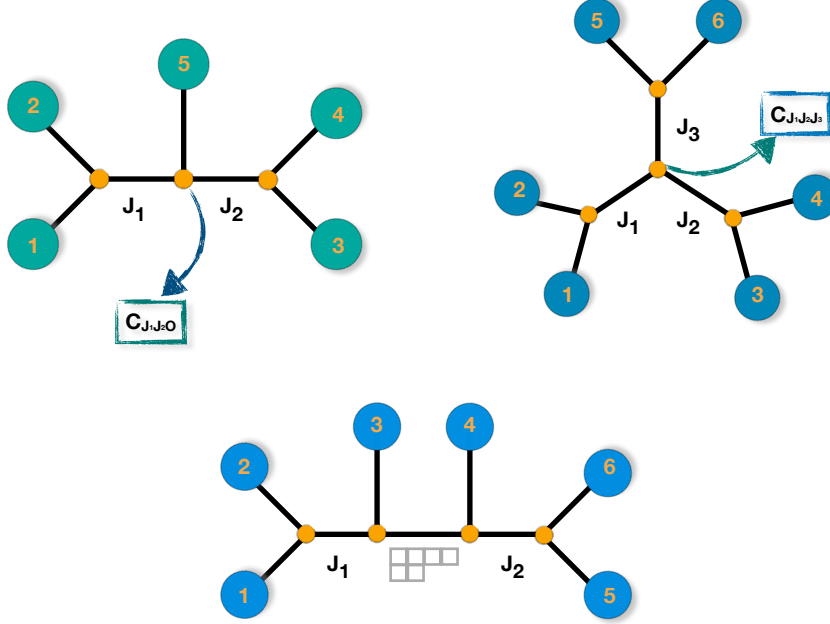


FIGURE 2.1: Schematic representation of the OPE channels for five- and six-point functions. In the top left we have the snowflake decomposition of the five-point function, where we emphasize the OPE coefficient involving two spinning operators. In the top right we have the snowflake decomposition of the six-point function, emphasizing the OPE coefficient of three spinning operators. In the bottom, we depict the comb-channel expansion, which may involve mixed-symmetry tensors and which we will not analyze in detail.

where we used a null polarization vector z_i to encode the indices of the operators, $h_i = \Delta_i + J_i$ and V and H are defined as

$$V_{i,j,k} = \frac{(z_i \cdot x_{ij})x_{ik}^2 - (z_i \cdot x_{ik})x_{ij}^2}{x_{jk}^2}, \quad H_{ij} = (z_i \cdot x_{ij})(z_j \cdot x_{ij}) - \frac{x_{ij}^2(z_i \cdot z_j)}{2}. \quad (2.14)$$

The sum in $\ell_i \in \{0, \dots, \min(J_k)\}$ counts the possible tensor structures. In the five-point case we have a three-point function of a scalar with two operators of spin J_1 and J_2 , therefore the different structures are labelled by $\ell_3 \equiv \ell$ and ℓ_1 and ℓ_2 vanish. After doing simple and straightforward manipulations we arrive at the explicit expression for the lightcone block defined by

$$\langle \phi(x_1) \dots \phi(x_5) \rangle \approx \frac{1}{(x_{12}^2 x_{34}^2)^{\Delta_\phi}} \left(\frac{x_{13}^2}{x_{15}^2 x_{35}^2} \right)^{\frac{\Delta_\phi}{2}} \sum_{k_1, k_2, \ell} P_{k_1 k_2 \ell} \mathcal{G}_{k_1 k_2 \ell}(u_i), \quad (2.15)$$

where

$$\mathcal{G}_{k_1 k_2 \ell}(u_i) = u_1^{\frac{\tau_1}{2}} u_3^{\frac{\tau_2}{2}} (1 - u_2)^\ell u_5^{\frac{\Delta_\phi}{2}} \int [dt_1] [dt_2] \frac{(1 - t_1(1 - u_2)u_4 - u_2u_4)^{J_2 - \ell} (1 - t_2(1 - u_2)u_5 - u_2u_5)^{J_1 - \ell}}{(1 - (1 - u_4)t_2)^{\frac{h_2 - \tau_1 - 2\ell + \Delta_\phi}{2}} (1 - (1 - u_5)t_1)^{\frac{h_1 - \tau_2 - 2\ell + \Delta_\phi}{2}} (1 - (1 - t_1)(1 - t_2)(1 - u_2))^{\frac{h_1 + h_2 - \Delta_\phi}{2}}} \cdot \quad (2.16)$$

The expansion (2.15) includes a product of three OPE coefficients that we denote by

$$P_{k_1 k_2 \ell} = C_{\phi \phi k_1} C_{\phi \phi k_2} C_{\phi k_1 k_2}^{(\ell)}. \quad (2.17)$$

Formula (2.16) is valid as long as one of the exchanged operators is not the identity. In such a case the OPE instead simplifies to

$$\phi(x_1)\phi(x_2) \approx \frac{C_{\phi \phi \mathcal{I}}}{(x_{12}^2)^{\Delta_\phi}} \mathcal{I}, \quad (2.18)$$

which forces the other exchanged operator to be the same as the external one. When the exchanged operator in the (12) OPE is the identity we have (in this case there is a single $\ell = 0$ structure)

$$\mathcal{G}_{\mathcal{I} \phi}(u_i) = \left(\frac{u_3 u_5}{u_4} \right)^{\frac{\Delta_\phi}{2}}, \quad (2.19)$$

on the other hand, when the identity is flowing in the (34) OPE, we have

$$\mathcal{G}_{\phi \mathcal{I}}(u_i) = u_1^{\frac{\Delta_\phi}{2}}. \quad (2.20)$$

For the lightcone expansion of the six-point conformal block we need to apply the OPE limit (2.6) three times. We will choose the snowflake channel as illustrated in the top-right of figure 2.1. In this choice the exchanged operators are always symmetric traceless tensors of spin J_i . This gives

$$\langle \phi(x_1) \dots \phi(x_6) \rangle \approx \frac{1}{(x_{12}^2 x_{34}^2 x_{56}^2)^{\Delta_\phi}} \sum_{k_i, \ell_i} P_{k_i \ell_i} \mathcal{G}_{k_i \ell_i}(u_i, U_i) = \quad (2.21)$$

$$\sum_{k_i} \left(\prod_{i=1}^3 C_{\phi \phi k_i} \int [dt_i] \right) \frac{\langle \mathcal{O}_{k_1}(x_1 + t_1 x_{21}, x_{12}) \mathcal{O}_{k_2}(x_3 + t_2 x_{43}, x_{34}) \mathcal{O}_{k_3}(x_5 + t_3 x_{65}, x_{56}) \rangle}{(x_{12}^2)^{\frac{2\Delta_\phi - \tau_1}{2}} (x_{34}^2)^{\frac{2\Delta_\phi - \tau_2}{2}} (x_{56}^2)^{\frac{2\Delta_\phi - \tau_3}{2}}}.$$

Using the three-point function conventions (2.14) and defining $\mathcal{T} = \sum_i \tau_i$, $L = \sum_i \ell_i$ and $H = \sum_i h_i$ we obtain

$$\begin{aligned} \mathcal{G}_{k_i \ell_i}(u_i, U_i) &\equiv u_1^{\frac{\tau_1}{2}} u_3^{\frac{\tau_2}{2}} u_5^{\frac{\tau_3}{2}} g_{k_i \ell_i}(u_2, u_4, u_6, U_i) \\ &= \prod_{i=1}^3 u_{2i-1}^{\frac{\tau_i}{2}} \int [dt_i] \frac{u_{2i}^{\ell_i} \chi_i^{\ell_{1-i}} (1 - \chi_i)^{\ell_{2-i} - \tau_{2-i} + \mathcal{T}/2} (1 - u_{2i})^{J_{i+1} + \ell_{i+1} - L} \mathcal{A}_i^{J_i + \ell_i - L}}{\mathcal{B}_i^{\ell_i - \Delta_i - L + H/2}}, \end{aligned} \quad (2.22)$$

where we use the notation $\ell_i \equiv \ell_{i+3}$ and²

$$\begin{aligned} \mathcal{A}_i &= \frac{1}{(1 - u_{2(i-1)})} \left[(1 - t_{i-1})(1 - \chi_{1-i}) (-1 + u_{2(i-1)} - (1 - t_{i+1})u_{2(i-1)}\chi_{2-i} + \chi_{3-i}) \right. \\ &\quad \left. + t_{i-1}u_{2(i+1)}(1 - \chi_{3-i}) (-1 + u_{2(i-1)} - (1 - t_{i+1})u_{2(i-1)}\chi_{2-i}) \right], \end{aligned} \quad (2.23)$$

$$\mathcal{B}_i = 1 - \chi_{2-i} - t_{1+i}(1 - u_{2i} - \chi_{2-i} + (1 - t_{i-1})u_{2i}\chi_{1-i}),$$

with χ_i defined as $\chi_i = \frac{U_i - u_{2(2-i)}}{U_i}$. A nice property of the χ variables is that the conformal block factorizes in products of three ${}_2F_1$ in the limit $\chi_i \rightarrow 0$. Another nice property is that ℓ_{1-i} determines the leading power of χ_i , as can easily be seen in (2.22).

When one of the exchanged operators is the identity, the remaining two are equal to each other, which leads to the simplified expression

$$\mathcal{G}_{kk\mathcal{I}}(u_i, U_i) = \left(\frac{u_1 u_3}{U_2} \right)^{\frac{\tau_k}{2}} g_k(u_2/U_1), \quad (2.24)$$

where $g_k(v)$ contains is the four-point block as defined in (2.11).

2.3 Snowflake bootstrap

Let us start by recalling the basic features of the lightcone bootstrap for four-point correlators [44, 45]. A four-point function of local operators ϕ can be decomposed in the (12) or (23) OPE channels

$$\frac{1}{(x_{12}^2 x_{34}^2)^{\Delta_\phi}} \sum_{\mathcal{O}_k} C_{\phi\phi k}^2 G_k(u, v) = \frac{1}{(x_{23}^2 x_{14}^2)^{\Delta_\phi}} \sum_k C_{\phi\phi k}^2 G_k(v, u), \quad (2.25)$$

where $G_k(u, v)$ is the full conformal block in the (12) channel. This bootstrap equation has been used to extract properties of conformal field theories following both analytic and numerical approaches.

²The reader may have realized that due to the cyclic defining property of the cross-ratios we can for example refer to the even cross-ratios u_2, u_4, u_6 in the product as $u_{2(i-1)}$.

Low twist operators dominate in the lightcone $x_{12}^2 \rightarrow 0$ limit of the left hand side of the bootstrap equation. Unitary CFTs obey the following bounds for the twist of operators

$$\tau = 0 \quad \text{identity}, \quad \tau \equiv \Delta - J \geq \begin{cases} (d-2)/2 & \text{scalar} \\ d-2 & \text{spin}, \end{cases} \quad (2.26)$$

and so the leading term on the left hand side of the bootstrap equation is given by

$$\frac{1}{(x_{12}^2 x_{34}^2)^{\Delta_\phi}} \sum_k C_{\phi\phi k}^2 G_k(u, v) = \frac{1}{(x_{12}^2 x_{34}^2)^{\Delta_\phi}} \left[1 + C_{\phi\phi k_*}^2 u^{\frac{\tau_{k_*}}{2}} g_{k_*}(v) + \dots \right], \quad (2.27)$$

where we have used that the conformal block behaves as $G_k(u, v) \rightarrow \mathcal{G}_k(u, v) = u^{\frac{\tau}{2}} g_k(v)$ in the $u \rightarrow 0$ limit. The assumption is that above the identity there is a unique operator \mathcal{O}_{k_*} with leading twist. Next we take the limit of $x_{23}^2 \rightarrow 0$, which moves the point x_2 to the corner of the square made by the lightcones of points 1 and 3, which can be taken respectively at 0 and 1 in the complex z -plane, as shown in figure 2.2. It is possible to take this second limit, which corresponds to v small, and use the right hand side of (2.25).

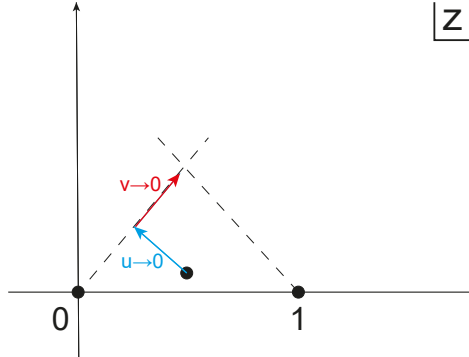


FIGURE 2.2: Schematic representation of the relevant lightcone limit in the z -plane. The point x_2 first approaches the lightcone of the operator at the origin, as $u \rightarrow 0$. Subsequently, it approaches the lightcone of the operator at $x_3 = (1, 0)$, which corresponds to taking $v \rightarrow 0$.

Each term in the $u \rightarrow 0$ limit will diverge at most logarithmically, which apparently contradicts the power law divergence of the left hand side of the equation. The emergence of the power law singularity was addressed in [44, 45] and it boils down to the contribution of double-twist operators $[\phi\phi]_{0,J} \sim \phi \square^0 \partial^J \phi$ whose twist approaches $2\Delta_\phi$ at large spin. The stronger divergence is recovered by performing the infinite sum over spin of these double-twist families. In particular, this fixes the density of OPE coefficients for this family of

operators at large spin to be³

$$C_{\phi\phi[\phi\phi]_{0,J}}^2 \sim \frac{8\sqrt{\pi}}{\Gamma(\Delta_\phi)^2 2^{2\Delta_\phi+J}} J^{2\Delta_\phi-3/2}, \quad (2.28)$$

which is the behaviour of OPE coefficients in Mean Field Theory.

Additionally, the leading twist operator above the identity in the direct channel leads to $1/J$ suppressed corrections to the OPE coefficients along with *anomalous dimension* type corrections, which means the twist of these families behaves as

$$\tau_{[\phi\phi]_{0,J}} = 2\Delta_\phi + \frac{k}{J^{\tau^*}}. \quad (2.29)$$

At this level the large spin expansion is merely asymptotic, and the OPE coefficients and anomalous dimensions cannot be assigned to a single operator of a given spin. However, the large spin expansion actually converges at least down to spin 2, and the OPE coefficients are really associated to a unique operator at each spin, which follows from the fact that the double-twist operators really sit in Regge trajectories that are analytic in spin. All these remarkable facts were established through the Lorentzian inversion formula [79]. This formula systematizes the large spin perturbation theory/lightcone-bootstrap and essentially supersedes it as a computational tool [137–139]. In this work, however, we are interested in higher-point functions which are much richer, and for which a Lorentzian inversion formula is presently unavailable. Therefore we must resort to the more pedestrian large spin perturbation theory. It would of course be interesting to develop higher-point Lorentzian inversion formulae and reproduce and extend the results we will derive below.

2.3.1 Five-point function

Let us consider the more complicated case of the five-point function. We now have an exchange of two operators, and their contribution is captured by the block expansion in a given channel. We consider the (12)(34) and (23)(45) channels for the five-point function $\langle \phi(x_1)\phi(x_2)\phi(x_3)\phi(x_4)\phi(x_5) \rangle$,

$$\frac{(x_{13}^2)^{\frac{\Delta_\phi}{2}}}{(x_{12}^2 x_{34}^2)^{\Delta_\phi}} \sum_{k_1, k_2, \ell} P_{k_1 k_2 \ell} G_{k_1 k_2 \ell}^{12,34}(u_i) = \frac{(x_{24}^2)^{\frac{\Delta_\phi}{2}}}{(x_{23}^2 x_{45}^2)^{\Delta_\phi}} \sum_{n_1, n_2, \ell} P_{n_1 n_2 \ell} G_{n_1 n_2 \ell}^{23,45}(u_i). \quad (2.30)$$

The limit $x_{12}^2, x_{34}^2 \rightarrow 0$ is dominated by low twist operators in the (12)(34) channel. The natural candidate to lead this expansion is the identity operator, however it is not possible

³This differs from some conventions in the literature by a factor of 2^J due to our conformal block normalization.

to have two identities being exchanged at the same time, since that would imply a nonzero three-point functions between two identities and the scalar operator $\phi(x_5)$. It is however possible to have one identity being exchanged in one OPE and another operator in the other OPE. In this case the conformal blocks simplify considerably and the exchanged operator must be the external one. The block simplifies to a product of a two- and three-point function, check (2.19) and (2.20). Thus, we conclude that the first terms in the lightcone limit in the channel (12)(34) are given by

$$C_{\phi\phi\phi}\mathcal{G}_{\mathcal{I}\phi}(u_i) + C_{\phi\phi\phi}\mathcal{G}_{\phi\mathcal{I}}(u_i) = C_{\phi\phi\phi} \left(\left(\frac{u_3 u_5}{u_4} \right)^{\frac{\Delta_\phi}{2}} + u_1^{\frac{\Delta_\phi}{2}} \right). \quad (2.31)$$

There is possibly another leading term from two exchanges of the leading twist operator \mathcal{O}_{k_*} . This term has a lightcone limit in the channel (12)(34) given by

$$C_{\phi\phi k_*} C_{\phi\phi k_*} C_{k_* k_* \phi} \mathcal{G}_{k_* k_* \ell}(u_i). \quad (2.32)$$

The term that dominates is determined by the rate at which u_1 and u_3 go to zero and by the twist of ϕ and \mathcal{O}_{k_*} . Below we shall address both possibilities. We may then take the other limits $x_{23}^2, x_{45}^2, x_{15}^2 \rightarrow 0$, corresponding to $u_2, u_4, u_5 \rightarrow 0$, which as we shall see, are suitable for the expansion in the (23)(45) channel. The decomposition in this channel takes the form

$$\left(\frac{u_1 u_3^2 u_5}{u_2^2 u_4^2} \right)^{\Delta_\phi/2} \sum_{n_1, n_2, \ell} P_{n_1 n_2 \ell} \mathcal{G}_{n_1 n_2 \ell}^{23,45}(u_i), \quad (2.33)$$

where we collected here the prefactors on both sides of (2.30). The powers of u_2, u_4 in the denominator of (2.33) impose constraints on the operators that need to be present in the conformal block decomposition of the channel (23)(45).

2.3.1.1 Identity in the (12) OPE

Let us understand this in more detail. First consider the term

$$C_{\phi\phi\phi}\mathcal{G}_{\mathcal{I}\phi}(u_i) = C_{\phi\phi\phi} \left(\frac{u_3 u_5}{u_4} \right)^{\frac{\Delta_\phi}{2}}, \quad (2.34)$$

where the identity is exchanged in the (12) OPE. The cross-ratios u_2 and u_4 , when taken to be small, control the twist of the exchanged operators in the cross channel. We can use this to infer what class of operators are contributing in the cross channel where the blocks

behave as

$$\mathcal{G}_{n_1 n_2 \ell}^{23,45}(u_i) = u_2^{\tau_{n_1}/2} u_4^{\tau_{n_2}/2} g_{n_1 n_2 \ell}(u_1, u_3, u_5). \quad (2.35)$$

Combining these behaviours with the prefactor in (2.33) we can conclude that the operators n_1 have a twist that approaches $2\Delta_\phi$, and therefore correspond to the usual leading double-twist operators. Moreover, in this case the operator n_2 must have twist Δ_ϕ . This corresponds to the exchange of the external operator itself. Therefore the cross-channel OPE data is given by

$$P_{[\phi\phi]_0, J, \phi} = C_{\phi\phi[\phi\phi]_0, J} C_{\phi\phi\phi} C_{\phi\phi[\phi\phi]_0, J}, \quad (2.36)$$

from which we can see that the single-trace OPE coefficient cancels on both sides of the crossing equation, and we are left with data that is known from the four-point bootstrap, namely scalar/scalar/double-twist OPE coefficients.

Actually this case reduces to the crossing of the four-point function of ϕ and its descendants. Firstly, in the direct channel, since the five-point function factorizes into a product of 2 and 3-pt functions, we can use the (45) OPE into the exchanged scalar operator ϕ , which acts on the MFT 4-pt function of ϕ at points 1235. Secondly, in the cross channel the (45) OPE reduces the five-point block into an action on the four-point block with external ϕ at points 1523 and double-twist exchange. This shows the problem reduces to that of the four-point function.

Nevertheless it is instructive to check this result explicitly using the lightcone blocks in (2.16) to describe the cross-channel contributions. In this case $J_2 = \ell = 0$ and $\Delta_2 = \Delta_\phi$. Additionally for large spin J_1 the dimension of the exchanged operator approaches the double-twist value $\Delta_1 = 2\Delta_\phi + J_1$. This significantly simplifies the expression (2.16) for the blocks. In practice, it is useful to expand the integrand using the binomial theorem and performing the t_i integrals, which leads to a representation in terms of an infinite sum of hypergeometric functions. In fact, the sum is dominated by the region $u_1 \sim J_1^{-2}$, similarly to the four-point case. This allows one to simplify the hypergeometric functions into Bessel functions, so the large spin limit of the lightcone block reads

$$\mathcal{G}_{[\phi\phi]_0, J_1 \phi}^{23,45}(u_i) \approx \sum_{n=0}^{\infty} \frac{J_1^{n+\frac{1}{2}} \Gamma\left(\frac{\Delta_\phi+1}{2}\right) \Gamma\left(\frac{2n+\Delta_\phi}{2}\right) u_1^{\frac{\Delta_\phi+n}{2}} u_2^{\Delta_\phi} (1-u_3)^n u_4^{\frac{\Delta_\phi}{2}} K_n(2J_1\sqrt{u_1})}{2^{1-3\Delta_\phi-J_1} \pi \Gamma(n+1) \Gamma(n+\Delta_\phi)}. \quad (2.37)$$

Imposing the well-known large spin asymptotics of the scalar/scalar/double-twist OPE coefficients (2.28), one can do the sum over J_1 by approximating it as an integral. This

reproduces the correct power of u_1 at fixed n . The correct power of u_3 is then recovered by doing the infinite sum over n .

We remark that one can then consider the related contribution where we swap the exchanged operators in the cross channel, meaning we have $\mathcal{O}_{n_1} = \phi$ and $\mathcal{O}_{n_2} = [\phi\phi]_{0,J_2}$. This obviously corresponds to a factorized correlator in a different channel which is subleading in the lightcone limit here considered.

2.3.1.2 Identity in the (34) OPE

On the other hand, when we exchange the identity in the (34) OPE, the direct-channel contribution is

$$C_{\phi\phi\phi} u_1^{\frac{\Delta_\phi}{2}}. \quad (2.38)$$

Thus, since the leading powers of u_2 and u_4 in the cross-channel expression (2.33) are the same, the operators that are exchanged in the cross channel will both have the double-twist value $2\Delta_\phi$. This allows us to probe the double-twist/double-twist/scalar OPE coefficient on the cross channel

$$P_{[\phi\phi]_{0,J_1}[\phi\phi]_{0,J_2}\ell} = C_{\phi\phi[\phi\phi]_{0,J_1}} C_{\phi\phi[\phi\phi]_{0,J_2}} C_{\phi[\phi\phi]_{0,J_1}[\phi\phi]_{0,J_2}}^{(\ell)}. \quad (2.39)$$

It is important to notice that the double-twist/double-twist/scalar OPE coefficient depends on the additional quantum number ℓ , which encodes the tensor structure associated to spin-spin-scalar three-point functions.

Since the scalar/scalar/double-twist coefficients are fixed from the four-point analysis, matching to the direct channel we immediately discover the remarkable non-perturbative relation

$$C_{\phi[\phi\phi]_{0,J_1}[\phi\phi]_{0,J_2}}^{(\ell)} \propto C_{\phi\phi\phi}, \quad (2.40)$$

which would be expected in a perturbative theory. With a more careful analysis, we will now fix the large spin asymptotics of this OPE coefficient, along with its ℓ dependence.

We need to reproduce the power law behaviour in the variables u_1 , u_3 and u_5 , which will emerge from the infinite sum over J_1 , J_2 and ℓ in the cross channel. More specifically, we consider the limit $J_1, J_2 \rightarrow \infty$ with $u_1 J_1^2$ and $u_5 J_2^2$ fixed. It is possible to approximate the lightcone block in this regime by approximating the integrand in (2.16), so that one

finds integral representations of two Bessel functions,⁴

$$\begin{aligned} \mathcal{G}_{[\phi\phi]_0, J_1 [\phi\phi]_0, J_2 \ell}^{23,45}(u_i) &\approx \frac{2^{4\Delta_\phi + J_1 + J_2}}{\pi} J_1^{1/2} J_2^{1/2} u_2^{\Delta_\phi} u_4^{\Delta_\phi} (1 - u_3)^\ell \\ &\quad u_1^{\frac{1}{4}(3\Delta_\phi + 2\ell)} u_5^{\frac{1}{4}(\Delta_\phi + 2\ell)} K_{\ell + \frac{\Delta_\phi}{2}} \left(2J_1 u_1^{1/2} \right) K_{\ell + \frac{\Delta_\phi}{2}} \left(2J_2 u_5^{1/2} \right). \end{aligned} \quad (2.41)$$

It is not hard to see that for consistency with the $u_3 \rightarrow 0$ limit the power law behavior in u_1, u_5 has to be reproduced term by term in the sum over ℓ . This leads to the ansatz

$$P_{[\phi\phi]_0, J_1 [\phi\phi]_0, J_2 \ell} \approx C_{\phi\phi\phi} b_\ell 2^{-J_1 - J_2} J_1^{\ell+3(\Delta_\phi-1)/2} J_2^{\ell+3(\Delta_\phi-1)/2}, \quad (2.42)$$

which, upon performing the integrals over J_1 and J_2 , reproduces the power law behavior in u_1 and u_5 . Since $\ell \in \{0, \dots, \min(J_1, J_2)\}$, this leaves us with an infinite sum over ℓ to perform, which will recover the power law behavior in u_3 . In particular, we need to zoom in on the $\ell \rightarrow \infty$ region, with u_3 approaching zero such that $u_3\ell$ is kept fixed. In this limit, we can use the approximation $(1 - u_3)^\ell \approx e^{-u_3\ell}$. Then, we can take the asymptotic large ℓ behaviour of the coefficient b_ℓ to be ⁵

$$b_\ell \approx \frac{\Delta_\phi \Gamma\left(\frac{1+\Delta_\phi}{2}\right)}{2^{3\Delta_\phi-3} \sqrt{\pi} \Gamma(\Delta_\phi)^2 \Gamma\left(1 + \frac{\Delta_\phi}{2}\right)} \ell^{-2\ell} e^{2\ell} \ell^{-\Delta_\phi}. \quad (2.43)$$

We can then approximate the sum over ℓ by an integral, which gives the correct power law behaviour in u_3 and finally reproduces the identity contribution in the direct channel.

Both leading terms with an identity exchange are understood as a five-point function which factorizes into a product of a two- and three-point functions. A simple example of CFTs expected to present this behaviour are holographic theories with cubic couplings. We can draw bulk Witten diagrams and look at their unitarity cuts to infer the exchanged operators in the corresponding channel. This is presented in figure 2.3. Clearly, this picture is consistent with the results obtained from the lightcone limit analysis.

⁴This procedure deserves a word of caution. Strictly speaking we should first take the limit of $u_1, u_3 \rightarrow 0$, keeping large spin contributions, and only then take $u_2, u_4 \rightarrow 0$. In practice, since we use the lightcone block expansion (2.16) in the cross channel, we are swapping the order of limits. This is justified a posteriori since the asymptotics of OPE coefficients at large spin that we obtain match the examples studied in section 2.4.

⁵The same result could be obtained by explicitly performing the sum over ℓ assuming $b_\ell \propto \frac{1}{\ell! \Gamma(\ell + \Delta_\phi)}$. However, this cannot be used to determine the form of the coefficients at finite ℓ since the leading singularity in $u_3 \rightarrow 0$ only determines the asymptotic behaviour at $\ell \rightarrow \infty$. Remarkably this turns out to be the exact form of the coefficients in the disconnected correlator in section 2.4.2.1. A similar situation also occurs for the six-point case.

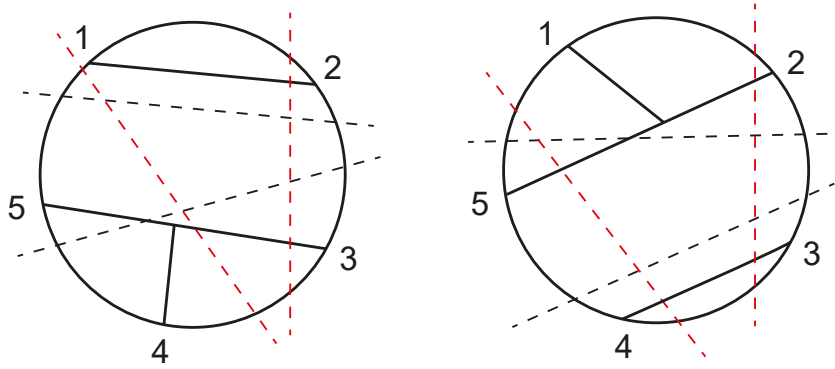


FIGURE 2.3: Witten diagrams corresponding to the leading order five-point function in a large N theory. The black and red dashed lines correspond to the unitarity cuts in the direct and crossed OPE channels, allowing us to infer what the exchanged operators are.

2.3.1.3 Two non-trivial exchanges

The case of two non-trivial exchanges is more subtle. When the exchanged operators are identical to the external ones, the lightcone limit of the block in the channel $(12)(34)$ is given by

$$C_{\phi\phi\phi}^3(u_1u_3u_5)^{\frac{\Delta_\phi}{2}} \frac{\Gamma(\Delta_\phi)^2}{\Gamma(\frac{\Delta_\phi}{2})^4} \left(\zeta_2 + \ln u_4 \ln u_5 + 2S_{\frac{\Delta_\phi-2}{2}}(\ln u_4 + \ln u_5) + 4S_{\frac{\Delta_\phi-2}{2}}^2 - S_{\frac{\Delta_\phi-2}{2}}^{(2)} + \dots \right), \quad (2.44)$$

where $S_\alpha^{(n)}$ denotes the degree- n harmonic number and the dots represent subleading terms in u_2 , u_4 and u_5 . The powers of u_2 and u_4 indicate that the exchanged operators in the cross channel should once again be of double-twist type. However, since the powers of u_5 are the same for both block expansions in the small u_5 limit, one cannot employ the usual argument which ensures that operators with large spin J_2 dominate the cross channel. This means that the information in this OPE is not universal. The leading power of u is a constant, which can be achieved block by block in the cross channel, and therefore the usual argument for the necessity of large spin double-twist operators is not valid.

One can instead study the case where the two exchanged scalar operators \mathcal{O}_{k_*} are different from the external one, but identical among themselves.

$$\mathcal{G}_{k_*k_*}^{12,34}(u_i) \approx a_{\Delta_*\Delta_\phi} (u_1u_3u_5)^{\Delta_*/2} u_4^{\frac{\Delta_*-\Delta_\phi}{2}}, \quad (2.45)$$

with

$$a_{\Delta_*\Delta_\phi} = \frac{\pi 4^{\Delta^*-1} \Gamma(\frac{\Delta_*+1}{2})^2 \csc^2(\pi(\frac{\Delta_*-\Delta_\phi}{2}))}{\Gamma(\frac{\Delta_*-\Delta_\phi}{2}+1)^2 \Gamma(\frac{\Delta_\phi}{2})^2}. \quad (2.46)$$

When $\Delta_* < \Delta_\phi$ this is the leading term. On the other hand, for $\Delta_* \geq \Delta_\phi$ the leading

powers are instead integers and lead to the same limitation discussed above. Nevertheless, the term (2.45) is still present and can also be bootstrapped.

Notably, the power of u_4 will change the nature of the exchanged operators in the (45) OPE. In particular, we now have that the operator must have dimension asymptoting to $\Delta_* + \Delta_\phi + J_2$. Thus we prove the existence of the double-twist operators $[\phi\mathcal{O}_*]_{0,J_2}$ built out of the external ϕ and the internal \mathcal{O}_* . We see an asymmetry between the exchanges in the cross channel, since the operators in the (23) channel are still the double-twist composites $[\phi\phi]_{0,J_1}$. This is similar to the case of identity exchange in the (12) channel which also leads to an asymmetry in the cross-channel exchanges. In particular, swapping the cross-channel exchanges in the (23) and (45) OPEs leads to a subleading contribution in the direct channel.

The calculation in the cross channel is similar to that of the previous subsection. Both families of double-twist operators must be in the large spin regime, which gives the following approximation for the cross-channel conformal block

$$\mathcal{G}_{[\phi\phi]_{0,J_1}[\phi\mathcal{O}_*]_{0,J_2}\ell}^{23,45}(u_i) \approx \frac{2^{3\Delta_\phi + \Delta_* + J_1 + J_2}}{\pi} J_1^{1/2} J_2^{1/2} u_2^{\Delta_\phi} u_4^{(\Delta_\phi + \Delta_*)/2} (1 - u_3)^\ell u_1^{\frac{1}{4}(2\Delta_\phi + \Delta_* + 2\ell)} u_5^{\frac{1}{4}(\Delta_\phi + 2\ell)} K_{\ell + \frac{\Delta_*}{2}} \left(2J_1 u_1^{1/2} \right) K_{\ell + \frac{\Delta_\phi}{2}} \left(2J_2 u_5^{1/2} \right). \quad (2.47)$$

Once again the sum over large spins J_1 and J_2 must be done for fixed ℓ and we then sum over ℓ . The correct asymptotics for the OPE coefficients in this case is given by

$$P_{[\phi\phi]_{0,J_1}[\phi\mathcal{O}_*]_{0,J_2}\ell} \approx q_{\Delta_*\Delta_\phi} 2^{-J_1 - J_2} J_1^{\frac{4\Delta_\phi - 3 + 2\ell - \Delta_*}{2}} J_2^{\frac{3\Delta_\phi - 3 + 2\ell - 2\Delta_*}{2}} \ell^{-2\ell} e^{2\ell} \ell^{-\Delta_\phi}, \quad (2.48)$$

where

$$q_{\Delta_*\Delta_\phi} = P_{\mathcal{O}_*\mathcal{O}_*} a_{\Delta_*,\Delta_\phi} \frac{2^{5-3\Delta_\phi-\Delta_*}}{\Gamma(\frac{\Delta_\phi-\Delta_*}{2})\Gamma(\Delta_\phi-\frac{\Delta_*}{2})^2}. \quad (2.49)$$

The factor of $P_{\mathcal{O}_*\mathcal{O}_*} = C_{\phi\phi\mathcal{O}_*}^2 C_{\phi\mathcal{O}_*\mathcal{O}_*}$ is needed to match the direct channel.

2.3.1.4 Stress-tensor exchange

In a general CFT, the leading twist operators are usually scalars of scaling dimension less than $d - 2$ or the stress tensor which has dimension d and spin 2, and therefore twist $d - 2$. A spin 1 conserved current also has twist $d - 2$ but, since we are studying the OPE of identical scalars, only even spin operators can be exchanged. Thus, we are only left to consider the case of the stress tensor⁶.

⁶Higher spin conserved currents also have twist $d - 2$ but they only exist in free theories and we therefore ignore them.

In this case, the direct-channel contribution has three terms associated to the tensor structures with $\ell = 0, 1, 2$. In the cyclic lightcone limit, it turns out that the powerlaw behavior in $u_4 \rightarrow 0$ is suppressed by ℓ and therefore the tensor structure with $\ell = 0$ dominates. The block behaves very similarly to the scalar case, with the role of Δ_* being played by the twist of the stress tensor $d - 2$, up to some extra prefactors. Concretely, the direct-channel block contains the following term in the lightcone expansion

$$\mathcal{G}_{TT\ell=0} \approx a_{T,\Delta_\phi} (u_1 u_3 u_5)^{(d-2)/2} u_4^{\frac{d-2-\Delta_\phi}{2}}, \quad (2.50)$$

with

$$a_{T,\Delta_\phi} = \frac{\pi 4^{d-1} \Gamma\left(\frac{d+3}{2}\right)^2 \sec^2\left(\pi \frac{\Delta_\phi+3-d}{2}\right)}{\Gamma^2\left(\frac{\Delta_\phi+4}{2}\right) \Gamma^2\left(\frac{d-\Delta_\phi}{2}\right)}. \quad (2.51)$$

In the block expansion this term will come multiplied by the product of OPE coefficients $P_{TT\ell=0}$. Once again there are terms where the powers of u_4 and u_5 are constant and cannot be reproduced by large spin double twist families in the cross channel. The term in (2.50) is the leading one for $d - 2 - \Delta_\phi < 0$, but it remains in the expansion otherwise, so it can be bootstrapped. The physics in the cross channel is very similar to the scalar case as well. The small u_2 and u_4 behavior is matched by operators of the form $[\phi\phi]_{0,J_1}$ in the (23) OPE and $[\phi T]_{0,J_2}$ in the (45) OPE, with twists asymptoting to $2\Delta_\phi$ and $d - 2 + \Delta_\phi$ at large J_1 and J_2 , respectively. The large spin limit is needed to obtain the right power law behavior in u_1 and u_5 , and finally the large ℓ limit reproduces the small u_3 behavior. The cross-channel blocks and OPE coefficients are the same as in the scalar case with the replacement $\Delta_* \rightarrow d - 2$, up to the different prefactor which is fixed by the direct-channel block. More concretely, the cross-channel block in the large spin limit becomes

$$\begin{aligned} \mathcal{G}_{[\phi\phi]_{0,J_1} [\phi T]_{0,J_2} \ell}^{23,45} &\approx \frac{2^{3\Delta_\phi+d-2+J_1+J_2}}{\pi} J_1^{1/2} J_2^{1/2} u_2^{\Delta_\phi} u_4^{(\Delta_\phi+d-2)/2} (1-u_3)^\ell \\ &\quad u_1^{\frac{1}{4}(2\Delta_\phi+d-2+2\ell)} u_5^{\frac{1}{4}(\Delta_\phi+2\ell)} K_{\ell+\frac{d-2}{2}}\left(2J_1 u_1^{1/2}\right) K_{\ell+\frac{\Delta_\phi}{2}}\left(2J_2 u_5^{1/2}\right), \end{aligned} \quad (2.52)$$

and the OPE coefficients

$$P_{[\phi\phi]_{0,J_1} [\phi T]_{0,J_2} \ell} \approx q_{T\Delta_\phi} 2^{-J_1-J_2} J_1^{\frac{1}{2}(-1+2\ell-d+4\Delta_\phi)} J_2^{\frac{1}{2}(1+2\ell-2d+3\Delta_\phi)} \ell^{-2\ell} e^{2\ell} \ell^{-\Delta_\phi}, \quad (2.53)$$

where

$$q_{T\Delta_\phi} = P_{TT\ell=0} a_{T\Delta_\phi} \frac{2^{7-3\Delta_\phi-d}}{\Gamma\left(\frac{\Delta_\phi-d+2}{2}\right) \Gamma\left(\Delta_\phi - \frac{d-2}{2}\right)^2}. \quad (2.54)$$

2.3.2 Six-point function – snowflake

The six-point function is a richer object as it admits two very different OPE decompositions that are usually denoted by snowflake and comb. One distinction between them is that in the snowflake decomposition we do three OPEs in nonconsecutive pairs of points and therefore all OPEs involve two external scalars. Therefore there will be an OPE coefficient between three symmetric traceless operators of arbitrary spin, as can be seen in the top-right of figure 2.1. On the other hand, in the comb channel the OPE involves consecutive pairs of operators. Thus, after performing the OPE between two external scalars, the resulting symmetric traceless operator will be fused with another external scalar and can produce a mixed symmetry tensor operator, which in the mean field theory limit should correspond to a triple-twist operator. The bottom part of figure 2.1 illustrates this structure. In this chapter we use the lightcone OPE between scalars (2.6) and therefore limit our analysis to the snowflake channel, whose bootstrap equation we depict in figure 2.4.

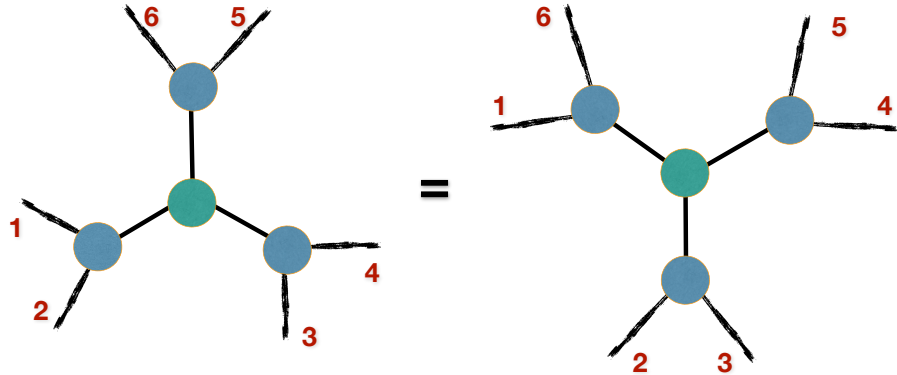


FIGURE 2.4: A schematic form of the six-point snowflake bootstrap equation. The left hand side represents the $(12)(34)(56)$ direct-channel expansion while the right hand side represents the $(23)(45)(61)$ cross channel.

We start by considering the block expansion in the direct $(12)(34)(56)$ channel

$$\langle \phi(x_1) \dots \phi(x_6) \rangle = \frac{1}{(x_{12}^2 x_{34}^2 x_{56}^2)^{\Delta_\phi}} \sum_{k_i, \ell_i} P_{k_i \ell_i} G_{k_i \ell_i}^{12, 34, 56}(u_i, U_i). \quad (2.55)$$

and take the lightcone limits $x_{12}^2 \rightarrow 0$, $x_{34}^2 \rightarrow 0$, $x_{56}^2 \rightarrow 0$, which correspond to $u_1 \rightarrow 0$, $u_3 \rightarrow 0$, $u_5 \rightarrow 0$. The leading contributions in this limit come from the exchange of three identities, one identity and two leading twists or three leading twists. For now we take the

leading twist to be a scalar, so that

$$\begin{aligned}
\langle \mathcal{O}(x_1) \dots \mathcal{O}(x_6) \rangle &\approx \frac{1}{(x_{12}^2 x_{34}^2 x_{56}^2)^{\Delta_\phi}} \left[P_{\mathcal{I}\mathcal{I}\mathcal{I}} \mathcal{G}_{\mathcal{I}\mathcal{I}\mathcal{I}}(u_i, U_i) + \left(P_{\mathcal{I}k_*k_*} \mathcal{G}_{\mathcal{I}k_*k_*}(u_i, U_i) + \text{perm} \right) \right. \\
&\quad \left. + P_{k_*k_*k_*} \mathcal{G}_{k_*k_*k_*}(u_i, U_i) \right] = \\
&= \frac{1}{(x_{12}^2 x_{34}^2 x_{56}^2)^{\Delta_\phi}} \left[1 + \left(C_{\phi\phi k_*}^2 \left(\frac{u_1 u_3}{U_2} \right)^{\frac{\tau_{k_*}}{2}} g_{k_*}(u_2/U_1) + \text{perm} \right) \right. \\
&\quad \left. + C_{\phi\phi k_*}^3 C_{k_*k_*k_*}(u_1 u_3 u_5)^{\frac{\tau_{k_*}}{2}} g_{k_*k_*k_*}(u_{2i}, U_i) \right], \tag{2.56}
\end{aligned}$$

where Δ_* is the dimension of the leading twist operator \mathcal{O}_{k_*} and the functions g_{k_*} and $g_{k_*k_*k_*}$ are defined from the four- and six-point lightcone blocks in (2.11) and (2.22), respectively. Then we take the three distances x_{23}^2 , x_{45}^2 and x_{16}^2 to zero, or in cross-ratios $u_{2i} \rightarrow 0$, which will be appropriate to study the OPE decomposition in the cross channel (23)(45)(16) in the lightcone limit. The four-point conformal block g_{k_*} simplifies considerably in this limit

$$g_{k_*}(u_i/U_j) \approx -\frac{\Gamma(\Delta_* + J_*)}{\Gamma^2(\frac{\Delta_* + J_*}{2})} \left(S_{\frac{\Delta_* + J_* - 2}{2}} + \ln(u_i/U_j) \right) + \dots, \tag{2.57}$$

where the \dots represent subleading terms in u_i/U_j . However, after taking $u_{2i} \rightarrow 0$ the function $g_{k_*k_*k_*}(u_{2i}, U_i)$ of the six-point conformal lightcone block is still a nontrivial function of the cross-ratios U_i , so we take one further limit $x_{24}^2, x_{26}^2, x_{46}^2 \rightarrow 0$, or equivalently $U_i \rightarrow 0$, which we refer to as the origin limit [133]. Let us remark that we do this just to make the problem technically simpler. With this extra limit one gets

$$\begin{aligned}
g_{k_*k_*k_*}(u_{2i}, U_i) &\approx -\frac{\Gamma^3(\Delta_*)}{\Gamma^6(\frac{\Delta_*}{2})} \left[\frac{\prod_i \ln U_i}{3} + 2S_{\frac{\Delta_* - 2}{2}} \ln U_1 \ln U_2 + \left(4S_{\frac{\Delta_* - 2}{2}}^2 - S_{\frac{\Delta_* - 2}{2}}^{(2)} + \zeta_2 \right) \ln U_1 \right. \\
&\quad \left. + \frac{2}{3} S_{\frac{\Delta_* - 2}{2}} \left(4S_{\frac{\Delta_* - 2}{2}}^2 - 3S_{\frac{\Delta_* - 2}{2}}^{(2)} + 3\zeta_2 \right) + \dots \right] + \text{perm}, \tag{2.58}
\end{aligned}$$

where the \dots represent subleading terms. We give the derivation of this result in appendix 2.A. Notice that up to this order the correlator is polynomial of degree three in the logarithm of the cross-ratios, which contrasts with the behavior in a planar gauge theory[64].

2.3.2.1 Exchange of three identities

Given the crossing equation

$$\sum_{k_i, \ell_i} P_{k_i \ell_i} G_{k_i \ell_i}^{12, 34, 56}(u_i, U_i) = \prod_{i=1}^3 \left(\frac{u_{2i-1}}{u_{2i}} \right)^{\Delta_\phi} \sum_{k_i, \ell_i} P_{k_i \ell_i} G_{k_i \ell_i}^{23, 45, 16}(u_i, U_i), \tag{2.59}$$

the limit taken above should be compatible with the cross-channel decompositions in the channel (23)(45)(16). As we just described, the left hand side of this equation starts with a one and then has subleading corrections in the cross-ratios $u_{\text{odd}} \rightarrow 0$, while on the right hand side there is an apparent power law divergence in u_{even} in the prefactor. This implies that the cross-channel decomposition involves operators with dimension approximately equal to $2\Delta_\phi + J$ that cancel the prefactor $u_{2i}^{\Delta_\phi}$ in the denominator. Each individual conformal block in the (23)(45)(16) channel is regular in the cross-ratios u_{odd} as they approach zero, which is not enough to cancel the prefactor $u_{2i-1}^{\Delta_\phi}$ and recover the identity contribution of the direct channel.⁷ The solution is similar to that of the four- and five-point correlators in the sense that the identity is recovered from the infinite sum of double-twist operators with large spin. This can also be intuitively understood by looking at the "unitarity cuts" of a disconnected Witten diagram as in figure 2.5.

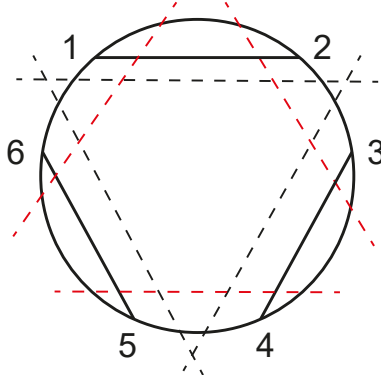


FIGURE 2.5: Witten diagrams corresponding to the leading order six-point function in a large N theory. The black and red dashed lines correspond to the unitarity cuts in the direct and crossed OPE channels, allowing us to read-off the exchanged identity and double-twist operators, respectively.

We will now choose the kinematics where both u_{odd} and U_i are sent to zero with the same rate J^{-2} , with ℓ_i fixed. This is not the choice we did in the direct channel above, but we will recover its kinematics by sending $u_{\text{odd}}/U_i \rightarrow 0$ afterwards. The conformal block simplifies considerably in this limit and is given by a product of three Bessel functions

$$\mathcal{G}_{k_i \ell_i}^{23,45,16} \approx \prod_{i=1}^3 \frac{2^{J_i + \tau_i} J_i^{\frac{1}{2}}}{\pi^{\frac{1}{2}}} u_{2i}^{\frac{\tau_i}{2}} \chi_i^{\ell_i} K_{\frac{2\ell_{i-1} - 2\ell_{i+1} + \tau_{i+1} - \tau_{i-1}}{2}} \left(2J_i \sqrt{U_{2i-1}} \right) U_{2i-1}^{\frac{2\ell_{i-1} + 2\ell_{i+1} + \tau_{i-1} - \tau_{i+1}}{2}}, \quad (2.60)$$

⁷This behavior is similar to that of scalar exchange in the direct channel (2.58) and is given in appendix 2.A for general spin.

where we can see that the parameter ℓ_i controls the cross-ratio $\chi_i = 1 - u_{2i+3}/U_{2i-1}$. The direct-channel limit that we took above can be recovered in the cross channel by studying the limit where χ_i approaches 1, which in turn is controlled by the large ℓ_i region.⁸ We can now use (2.60) in the crossing equation (2.59) to reproduce the identity exchange of the direct channel

$$1 \approx \frac{1}{8} \left(\prod_{n=1}^3 \left(\frac{u_{2n-1}}{u_{2n}} \right)^{\Delta_\phi} \int dJ_n d\ell_n \right) P_{k_i \ell_i} \mathcal{G}_{k_i \ell_i}^{23,45,16}(u_i, U_i), \quad (2.61)$$

where we transformed the sums in k_i, ℓ_i in the crossing equation to integrals in J_n, ℓ_n (including a factor of 1/2 because we are only summing over even spins). We can assume that the product of OPE coefficients $P_{k_i \ell_i}$ has the large J_i power law behavior

$$P_{k_i \ell_i} \approx C \prod_{n=1}^3 2^{-J_n} J_n^{a_n} f_n(\ell_n). \quad (2.62)$$

Integrating over J_i we obtain

$$1 \approx \prod_{i=1}^3 \prod_{\epsilon=\pm} \int d\ell_i f(\ell_i) \frac{2^{2\Delta_\phi} u_{2i-1}^{\Delta_\phi} \chi_i^{\ell_i}}{\pi^{\frac{1}{2}}} \Gamma\left(\frac{3+2a_i+2\epsilon(\ell_{i+1}-\ell_{i-1})}{4}\right) U_{2i-1}^{\frac{2(\ell_{i-1}+\ell_{i+1})-2a_i-3}{4}}, \quad (2.63)$$

where we used that $\tau_i = 2\Delta_\phi$ to leading order in large J_i . Then we consider the limit where $u_{\text{odd}}/U_i \rightarrow 0$. Remember that we need a power law divergence in u_{odd} to kill the prefactor in (2.61) and, as expected, this is generated by the tail of the sum in ℓ_i . In this regime we can replace $\chi_i^{\ell_i}$ by $\exp(-\ell_i u_{2i-3}/U_{2i-3})$, where we are keeping fixed the argument of the exponential in the limit. The powers of U_i cannot depend on ℓ_i otherwise this would give rise to a non-trivial in behavior U_i , which is not consistent with the left-hand side of (2.61), so we conclude that

$$a_i = r + \left(\sum_j \ell_j \right) - \ell_i, \quad (2.64)$$

with r a constant that does not depend on ℓ_i . We can, at this point, take the large ℓ_i behavior of the Γ functions in (2.63). The ℓ_i behavior of the expression suggests that for

⁸We stress that we made the choice of considering the limit $U_i \rightarrow 0$ to simplify the expression for the block. Alternatively, one could mimic the approach of [133] and keep these cross-ratios finite. We emphasize however that our choice of taking the origin limit respects an order: $U_i \rightarrow 0$ only after $u_i \rightarrow 0$. The latter limit is dominated by large J_i and large ℓ_i , whereas the subsequent $U_i \rightarrow 0$ imposes $J_i \gg \ell_i \gg 1$.

large ℓ_i the function $f(\ell_i)$ has the following form

$$f_i(\ell_i) \approx e^{2\ell_i} \ell_i^{g-2\ell_i}, \quad (2.65)$$

with g and c constants. Putting everything together and after doing the ℓ_i integration we obtain

$$1 \approx C 2^{6\Delta_\phi} \Gamma^2 \left(\frac{3}{2} + g + r \right) \prod_{i=1}^3 u_{2i-1}^{\Delta_\phi - \frac{3}{2} - g - r} U_i^{\frac{3}{4} + g + \frac{r}{2}}, \quad (2.66)$$

which fixes both r, g and c to be

$$r = \frac{4\Delta_\phi - 3}{2}, \quad g = -\Delta_\phi, \quad C = \frac{1}{2^{6\Delta_\phi} \Gamma^3(\Delta_\phi)}. \quad (2.67)$$

This fixes the asymptotic form of $P_{k_i \ell_i}$ proposed in (2.62).

2.3.2.2 Exchange of one identity and two leading twist operators

So far we have only reproduced the contribution of the identity in the direct-channel OPE decomposition (2.56). As we have seen subleading contributions depend non trivially on the cross-ratios, even in the limit where all u_i approach zero, cf. (2.57) and (2.58). One key difference is that we will have to generate logs of the cross-ratios from the cross-channel OPE decomposition. Some of these logs are generated by allowing a correction to the dimension of the double-twist operators of the form

$$\tau_i = 2\Delta_\phi + \frac{k}{J_i^a}. \quad (2.68)$$

The conformal block, in the large spin limit, depends on the twist of the exchanged operator in an explicit way as can be seen in (2.60). It is easy to perturb the previous computation, done to reproduce the contribution of the identity with the cross-channel double-twist exchange, and include the correction to the dimension of these operators. First we expand (2.60) at large J_i and keep the first subleading term in the series. Then, performing the integrals in J_i and ℓ_i we obtain the following correction to the contribution of the leading twist operators exchange

$$k \frac{\Gamma^2\left(\frac{2\Delta_\phi - \tau_*}{2}\right)}{\Gamma^2(\Delta_\phi)} \sum_j \left[\ln \frac{u_{2j} u_{2j+3} U_{2j+1}^{\frac{1}{2}}}{(u_{2j-1} u_{2j+1} U_{2j-1}^3)^{\frac{1}{2}}} - (S_{\Delta_\phi} - S_{\Delta_{\frac{2\phi-a}{2}}}) \right] \left(\frac{u_{2j-1} u_{2j+1}}{U_{2j+1}} \right)^{\frac{a}{2}}. \quad (2.69)$$

This term has the correct power law behavior coming from the direct-channel contribution of the identity and two leading twist operators, cf. (2.56) or (2.24). This fixes $a = \tau_*$, in

agreement with the four-point function calculation. Moreover, it contains some of the logs coming from the four-point block function g_{k*} , but it also has some unexpected log terms. It is precisely these terms that will allow us to fix the correction to the OPE coefficient between three double-twist operators

$$P_{k_i \ell_i} = P_{k_i \ell_i}^{MFT} \left(1 + \sum_j \frac{\sum_k (c_{j,k} \ln J_k + b_{j,k} \ln \ell_k) + v_j}{J_j^{\tau_*}} + \dots \right), \quad (2.70)$$

where $c_{i,j}$, $b_{i,j}$ and v_i are coefficients that we will fix. Upon inserting this in the cross-channel conformal block decomposition, and integrating over J_i and ℓ_i , we obtain

$$\sum_j \left[\ln \left(\prod_i u_{2i-1}^{-b_{j,i+1} - \frac{c_{j,i} + c_{j,i-1}}{2}} U_{2i-1}^{b_{j,i+1} + \frac{c_{j,i-1}}{2}} \right) - \frac{2v_j}{k} - \left(S_{\Delta_\phi} - S_{\Delta_{\frac{2\phi - \tau_*}{2}}} \right) \right] \left(\frac{u_{2j-1} u_{2j+1}}{\tilde{U}_{j+1}} \right)^{\frac{\tau_*}{2}}. \quad (2.71)$$

The correct log behavior imposes that

$$\begin{aligned} b_{i,i} = 0, \quad b_{i,i+1} = b_{i,i+2} = \frac{k}{2}, \quad c_{i,i} = 0, \quad c_{i,i+1} = c_{i,i+2} = -\frac{k}{2}, \quad v_1 = k S_{\frac{\tau+2J}{2}} \\ k = -\frac{C_{\phi\phi\tau*}^2 \Gamma^2(\Delta_\phi) \Gamma(2J + \tau*)}{2^{2J*-1} \Gamma^2(\frac{2\Delta_\phi - \tau*}{2}) \Gamma^2(\frac{2J + \tau*}{2})}. \end{aligned} \quad (2.72)$$

Thus, we see that we can reproduce exchanges in the direct channel that include at least one identity by taking into account the contribution of large spin double-twist operators in the cross channel. Moreover this procedure fixes the dimension and OPE coefficients of these operators at large spin. The formula for the OPE coefficients is one of the main results of this chapter.

2.3.2.3 Exchange of three leading twist operators

Before analysing the contribution of the exchange of three leading twist operators in the direct channel, let us see what is the effect of dressing the large spin double-twist contribution in the cross channel by a term of the form $\prod_{i=1}^3 J_i^{q_i} \ell_i^{r_i}$. This can be used, for example, to check what is the cross-ratio dependence of the corrections to the double-twist exchange in the cross channel at large spin

$$\prod_{i=1}^3 \left(\frac{u_{2i-1}}{u_{2i}} \right)^{\Delta_\phi} \int dJ_i d\ell_i P_{J_i, \ell_i}^{\text{tree}} \left[\prod_{j=1}^3 J_j^{q_j} \ell_i^{r_j} \right] G_{k_i \ell_i}^{23,45,16}(u_i, U_i) \propto \prod_{j=1}^3 \frac{U_{2j-1}^{\frac{q_{j-1}+2r_{j+1}}{2}}}{u_{2j-1}^{\frac{q_j+q_{j-1}}{2} + r_{j+1}}}. \quad (2.73)$$

It follows that multiple corrections to the dimension of operators exchanged in the OPEs (23)(45) and (23)(45)(16), where $r_i = 0$ and two or three nonvanishing exponents q_i equal $-\tau_*$, have, respectively, terms of the form

$$\left(\frac{u_1 u_5}{U_2 U_3}\right)^{\frac{\tau_*}{2}} u_3^{\tau_*} \left[\ln u_2 \ln u_4 + \dots \right], \quad \frac{(u_1 u_3 u_5)^{\tau_*}}{(U_1 U_2 U_3)^{\frac{\tau_*}{2}}} \left[\ln u_2 \ln u_4 \ln u_6 + \dots \right], \quad (2.74)$$

where the \dots stand for the contribution of log terms in other cross-ratios that are not important for the present discussion. One important feature of these two results is that at least one power of u_{odd} is given by τ_* . This can be thought as coming from the direct-channel contribution of a family of operators whose twist asymptotes to $2\tau_*$. Another curious feature is that there is necessarily a dependence on $\ln u_{\text{even}}$ that cannot be generated by the contribution of a single conformal block, as we can see from (2.58). This suggests that this term comes from the contribution in the direct channel of an infinite family of operators with twist $2\tau_*$. This behavior was already observed in [78] for the case of the four-point function from the existence of $\log^2 v$ terms.

Now we are ready to reproduce the last term in (2.56) from the cross-channel decomposition. Since the direct-channel contribution (2.58) does not have any $\ln u_{\text{even}}$ we conclude from the analysis of the previous paragraph that this term does not come from the correction of the dimension of double-twist operators. Therefore it must come solely from the correction to the OPE coefficient, which we propose to have the form

$$P_{J_i, \ell_i} = P_{J_i, \ell_i}^{\text{tree}} \left(1 + \sum_j \frac{\sum_k (c_{j,k} \ln J_k + b_{j,k} \ln \ell_k) + v_j}{J_j^{\tau_*}} + \frac{p(\ln J_j, \ln \ell_j)}{\prod_j J_j^{\tau_*} \ell_j^{\frac{\tau_*}{2}}} + \dots \right). \quad (2.75)$$

where the $c_{i,j}$, $b_{i,j}$ and v_i were already fixed in the previous section and $p(\ln J_j, \ln \ell_j)$ is a polynomial function of the third degree⁹

$$\begin{aligned} p(\ln J_j, \ln \ell_j) = & c_1 - c_2 \ln \frac{J_3^2}{\ell_1 \ell_2} \ln \frac{J_2^2}{\ell_1 \ell_3} \ln \frac{J_1^2}{\ell_2 \ell_3} + c_3 \ln \frac{J_1 J_2 J_3}{\ell_1 \ell_2 \ell_3} + 2c_4 \left[\ln J_1 \ln \left(\frac{J_2 J_3}{\ell_1} \right)^2 \frac{1}{\ell_2 \ell_3} \right. \\ & \left. + \ln J_2 \ln \frac{J_3^2}{\ell_2^2 \ell_1 \ell_3} - \ln J_3 \ln \ell_3^2 \ell_2 \ell_1 + \frac{3(\ln \ell_1 \ln \ell_2 \ell_3 + \ln \ell_2 \ln \ell_3)}{2} + \frac{\ln^2 \ell_1 + \ln^2 \ell_2 + \ln^2 \ell_3}{2} \right]. \end{aligned} \quad (2.76)$$

⁹This ansatz is justified because the scalar conformal block is a polynomial of degree 3 in log of cross-ratios

This polynomial generates the terms

$$\frac{(\prod_i u_i)^{\frac{\tau_*}{2}} \Gamma^3\left(\frac{2\Delta_\phi - \tau_*}{2}\right)}{\Gamma^3(\Delta_\phi)} \left[8c_1 + c_2 \ln U_1 \ln U_2 \ln U_3 - 4c_3 \ln U_1 U_2 U_3 + 2c_4 \sum_{i < j} \ln U_i \ln U_j \right], \quad (2.77)$$

upon integration in J_i and ℓ_i . A simple comparison with (2.58) fixes the values of c_i to be

$$\begin{aligned} c_2 &= P_{k_* k_* k_*} \frac{\Gamma(\Delta_*) \Gamma^3(\Delta_\phi)}{\Gamma^2(\frac{\Delta_*}{2}) \Gamma^3(\frac{2\Delta_\phi - \Delta_*}{2})}, & c_3 &= \frac{1}{4} \left(S_{\frac{\Delta_* - 2}{2}}^{(2)} - 4S_{\frac{\Delta_* - 2}{2}}^2 - \zeta_2 \right) c_2, \\ c_1 &= \frac{1}{4} S_{\frac{\Delta_* - 2}{2}} \left(4S_{\frac{\Delta_* - 2}{2}}^2 - 3S_{\frac{\Delta_* - 2}{2}}^{(2)} + 3\zeta_2 \right) c_2, & c_4 &= S_{\frac{\Delta_* - 2}{2}} c_2. \end{aligned} \quad (2.78)$$

for a scalar leading twist operator and

$$\begin{aligned} c_1 &= \Gamma^3(\Delta_\phi) \frac{P_{000} \mathbb{B}_{000}^{(0)} + 3P_{001} \mathbb{B}_{001}^{(0)} + 3P_{002} \mathbb{B}_{002}^{(0)}}{\Gamma^3(\frac{2\Delta_\phi - \tau_*}{2})}, & c_2 &= \Gamma^3(\Delta_\phi) \frac{P_{000} \mathbb{B}_{000}^{(3)}}{\Gamma^3(\frac{2\Delta_\phi - \tau_*}{2})}, \\ c_3 &= 2\Gamma^3(\Delta_\phi) \frac{P_{000} \mathbb{B}_{000}^{(1)} + P_{001} \mathbb{B}_{001}^{(1)} + P_{002} \mathbb{B}_{002}^{(1)}}{\Gamma^3(\frac{2\Delta_\phi - \tau_*}{2})}, & c_4 &= \Gamma^3(\Delta_\phi) \frac{P_{000} \mathbb{B}_{000}^{(2)}}{\Gamma^3(\frac{2\Delta_\phi - \tau_*}{2})} \end{aligned} \quad (2.79)$$

for the exchange a stress tensor, where we used the block for stress-tensor exchange derived in appendix 2.A.2 and wrote $P_{\ell_1 \ell_2 \ell_3} \equiv P_{TTT \ell_1 \ell_2 \ell_3}$. We emphasize the absence of the OPE coefficients associated with the structures where two or three of the ℓ_i 's are equal to 1. This happens since such structures are subleading in the $U_i \rightarrow 0$ limit. The constants $\mathbb{B}_{\ell_1 \ell_2 \ell_3}^{(m)}$ are the coefficients multiplying the degree- m polynomial of $\ln U_i$ in the block associated to the tensor structure labeled by ℓ_1 , ℓ_2 and ℓ_3 . These coefficients can be read off from equation (2.114) in appendix 2.A.2. We remark that, as is well known, the OPE coefficients of the stress tensor are not all independent and in fact satisfy

$$\begin{aligned} P_{011} &= -2 \frac{8(P_{000} + P_{001}) + d(d+2)P_{002}}{(d+4)(d-2)}, \\ P_{111} &= \frac{32(2+d)P_{000} + 8d(6+d)P_{001} - 4d(d^2 - 20)P_{002}}{(d-2)^2(d+2)(d+4)}, \end{aligned} \quad (2.80)$$

since its correlation functions satisfy conservation equations [32]. This means that the different OPE coefficients associated to the ℓ_i tensor structures are related to a set of three independent numbers.

We end this section with a speculative holographic interpretation of our bootstrap results which can be skipped by the more orthodox readers. In a four-point function, radial quantization allows us to visualize a weak gravitational process in AdS where two particles with large relative angular momentum come from the infinite past, interact, and

continue towards the infinite future. This picture can be generalized for the six-point function in the comb channel, which instead corresponds to a three-body gravitational interaction. However, in the snowflake OPE that we analyzed, one cannot assign a single time coordinate which leads to the cylinder picture. Instead, this channel corresponds to a gravitational process where the asymptotic states are defined with respect to distinct time coordinates¹⁰, where the underlying geometry is instead a "pair of pants". The physical process is more easily understood by inspecting figure 2.6.

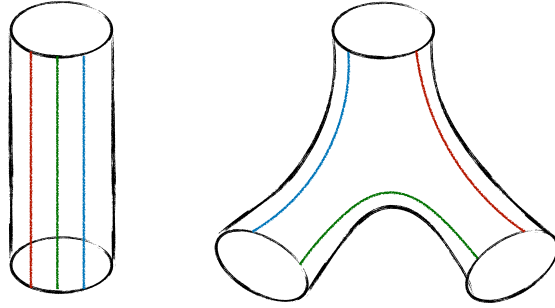


FIGURE 2.6: Schematic representation of the gravitational processes dual to the six-point comb channel on the left and to the six-point snowflake channel on the right. In the comb case, three particles come from the infinite past, interact weakly and continue towards future infinity. In the snowflake case, the blue and red particles come from the past infinity of two different time coordinates, say t_1 and t_2 , respectively. The blue one travels to future infinity along t_1 and the red one along t_2 . A third, green particle comes from past infinity in the t_1 direction and moves towards past infinity in t_2 . The process can also be interpreted in other similar ways by permuting the role of the OPEs.

2.4 Examples

Consistency conditions of the bootstrap equations for higher-point functions impose constraints on the behaviour of three point functions of spinning operators as we have seen in the previous sections. The goal of this section is to extract OPE coefficients of spinning operators by performing an explicit conformal block decomposition of the generalized free field theory correlator, as well as theories with cubic couplings, and confirm some of our previous results.

¹⁰We thank Pedro Vieira for discussions on this point.

2.4.1 Generalized free theory

The six-point function of operators ϕ in a generalized free field theory is given by

$$\langle \prod_{i=1}^6 \phi(x_i) \rangle_{\text{MFT}} = \sum_{\text{perm}} \langle \phi(x_1)\phi(x_2) \rangle \langle \phi(x_3)\phi(x_4) \rangle \langle \phi(x_5)\phi(x_6) \rangle = \sum_{\text{perm}} \frac{1}{(x_{12}^2 x_{34}^2 x_{56}^2)^{\Delta_\phi}}, \quad (2.81)$$

where we should sum over all permutations of operator positions. We can extract a prefactor $(x_{12}^2 x_{34}^2 x_{56}^2)^{\Delta_\phi}$ to write everything just in terms of cross-ratios,

$$\begin{aligned} (x_{12}^2 x_{34}^2 x_{56}^2)^{\Delta_\phi} \langle \prod_{i=1}^6 \phi(x_i) \rangle_{\text{MFT}} &= 1 + (u_1 u_3 u_5)^{\Delta_\phi} \left(1 + (u_2 u_4 u_6)^{-\Delta_\phi} + \sum_{i=1}^3 U_i^{-\Delta_\phi} \right) \\ &+ \sum_{i=1}^3 \left[\left(\frac{u_{2i+1} u_{2i+3}}{U_{2i-1}} \right)^{\Delta_\phi} + \left(\frac{u_{2i-1} u_{2i+1} u_{2i+3}}{u_{2i+2} U_{2i-1}} \right)^{\Delta_\phi} + \left(\frac{u_{2i+1} u_{2i+3} U_{2i+1}}{u_{2i+2} U_{2i-1}} \right)^{\Delta_\phi} \right]. \end{aligned} \quad (2.82)$$

The prefactor we have extracted is appropriate to analyze the OPE limit in the channel (12)(34)(56). The first term in (2.82) corresponds to the exchange of three identity operators and the others can contain one identity and two double-twist operators, or three double-twist operators. A systematic analysis of the operators that are exchanged in the OPE in these three channels can be done using the six-point conformal blocks [64] or the Casimir differential operator together with the boundary condition of the block in the lightcone limit [133]. We obtained for the OPE of three leading double-twist operators, which can not be extracted from the four-point function of ϕ , the result

$$P_{J_i \ell_i} = \prod_{i=1}^3 \frac{\left(J_i + \ell_i - \sum_j \ell_j + 1 \right)_{(\sum_j \ell_j) - \ell_i} (\Delta_\phi)_{\frac{J_i}{2}} (\Delta_\phi)_{J_i}}{2^{\ell_i - 1} J_i! \ell_i! (\Delta_\phi)_{\ell_i} \left(\frac{J_i + 2\Delta_\phi - 1}{2} \right)_{\frac{J_i}{2}}}. \quad (2.83)$$

By taking first the large J_i and then the large ℓ_i limit we recover the asymptotic behavior (2.62) derived from the lightcone bootstrap in the previous section.

Note that for a free theory with $\Delta_\phi = (d - 2)/2$ this is the full set of OPE data that can be extracted from this correlator. In a generalized free theory there are subleading double-twist operators $\phi \square^n \partial^J \phi$ whose OPE coefficients could be extracted.

2.4.2 ϕ^3 theory in $d = 6 - \epsilon$

We now consider turning on a cubic coupling which will allow us to further test our predictions involving, for example, the five-point function which vanishes for mean field theory.

The five-point function in ϕ^3 theory is given by¹¹

$$\left\langle \prod_{i=1}^5 \phi(x_i) \right\rangle = \sum_{perm} \langle \phi(x_1)\phi(x_2) \rangle \langle \phi(x_3)\phi(x_4)\phi(x_5) \rangle + \left. \left\langle \prod_{i=1}^5 \phi(x_i) \right\rangle \right|_{\text{conn}}. \quad (2.84)$$

This correlation function only has odd powers of ϵ as can be seen by drawing a few Feynman diagrams or from the structure of perturbation theory around the \mathbb{Z}_2 symmetric free theory. The leading term is a factorized correlator given by a product of a two-point function and a three-point function. The two-point function starts at the free theory order, but the three-point functions starts at order ϵ , with a tree level contact diagram. The connected contribution starts at order ϵ^3 and coexists with corrections to the factorized correlator. To leading order in the ϵ expansion the connected contribution is given by

$$\left. \langle \phi(x_1) \dots \phi(x_5) \rangle \right|_{\text{conn}} = \sum_{perm} \frac{(C_{\phi\phi\phi}^{(1)})^3}{x_{12}^2 x_{34}^2} \int \frac{d^6 x_0}{x_{10}^2 x_{20}^2 x_{30}^2 x_{40}^2 (x_{50}^2)^2}. \quad (2.85)$$

This six-dimensional integral is proportional to a D -function D_{11112} which we analyze in Appendix 2.B.

2.4.2.1 Disconnected contribution to the five-point function

Let us write the block decomposition as

$$\langle \phi(x_1) \dots \phi(x_5) \rangle^{(1)} = \frac{x_{13}^2}{x_{12}^4 x_{34}^4 x_{15}^2 x_{35}^2} \sum_{k_1, k_2, \ell} P_{k_1 k_2 \ell}^{(1)} G_{k_1 k_2 \ell}^{(12)(34)}(u_i), \quad (2.86)$$

where the superscript (1) indicates the order in the ϵ expansion. We used that $\Delta_\phi = 2 + O(\epsilon)$ and that $P_{k_1 k_2 \ell}$ starts at order ϵ . Our goal is to derive the spectrum and OPE coefficients of the operators exchanged in the (12)(34) channel for the leading disconnected contribution that is given by

$$\begin{aligned} \left. \langle \prod_{i=1}^5 \phi(x_i) \rangle \right|_{\text{conn}}^{(1)} &= \frac{C_{\phi\phi\phi}^{(1)} x_{13}^2}{x_{12}^4 x_{34}^4 x_{15}^2 x_{35}^2} \left(u_1^{\frac{\Delta_\phi}{2}} + \left(\frac{u_3 u_5}{u_4} \right)^{\frac{\Delta_\phi}{2}} + \left(\frac{u_1 u_3}{u_2 u_4^2 u_5} \right)^{\frac{\Delta_\phi}{2}} \left[(u_1 u_4^2)^{\frac{\Delta_\phi}{2}} + (u_3 u_5^2)^{\frac{\Delta_\phi}{2}} + \right. \right. \\ &\quad \left. \left. (u_2 u_4^2 u_5^2)^{\frac{\Delta_\phi}{2}} \left(u_1^{\frac{\Delta_\phi}{2}} + u_3^{\frac{\Delta_\phi}{2}} \right) \right] + \left(\frac{u_1^2 u_3^2}{u_2^2 u_4} \right)^{\frac{\Delta_\phi}{2}} \left[1 + (u_2 u_4 u_5)^{\frac{\Delta_\phi}{2}} + u_2^{\Delta_\phi} \left(u_4^{\frac{\Delta_\phi}{2}} + u_5^{\frac{\Delta_\phi}{2}} \right) \right] \right) \end{aligned} \quad (2.87)$$

¹¹This result can be obtained easily with the method of skeleton expansions as presented in [140]. It would be interesting to do conformal block decomposition for five- and six-point correlators in ϕ^3 and see how the respective spinning OPE coefficients compare with the ones in $\mathcal{N} = 4$ SYM [133].

To obtain the block decomposition we use two independent methods which serves as a cross-check of the calculation. Firstly we consider the Euclidean expansion of the five-point block discussed in Appendix E of [57], and match it to the small u_1 and u_3 expansion of the correlator. Using this we can obtain as many OPE coefficients as we desire. We can then conjecture a general form for arbitrary J_1, J_2 and ℓ , which we subsequently test by comparing to the explicit higher order results. Alternatively, we can use a generalization of the technique of [141] to higher-point correlators [133]. We act with the Casimir differential operators on the correlator in terms of its small u_1, u_3 expansion. Since the conformal blocks are eigenfunctions of the Casimir operator, we can fix the OPE coefficients order by order in u_1, u_3 by acting recursively with the differential operators. Again, we can do this to arbitrarily high order, guess the general form of the coefficients and check it to even higher order.

We find that depending on which pair of operators form the two-point function we have different sets of operators being exchanged. When the two-point function is between points x_1 and x_2 , we have the identity in the (12) OPE and ϕ in the (34) OPE. The product of OPE coefficients is simply given by $P_{\mathcal{I}\phi}^{(1)} = C_{\phi\phi\phi}^{(1)}$. Similarly, when the two-point function is between points x_3 and x_4 , we have $P_{\phi\mathcal{I}}^{(1)} = C_{\phi\phi\phi}^{(1)}$. When the two-point function is between points x_1 and x_5 , or between x_2 and x_5 , the result is less trivial since it leads to an expansion with an infinite number of operators. Adding up these two contributions, we find in the (12) OPE the double-twist operators $[\phi\phi]_{0,J}$, with dimension $4+J$ and (even) spin J , along with the operator ϕ in the (34) OPE. In this case we obtain $P_{[\phi\phi]_{0,J}\phi}^{(1)} = C_{\phi\phi\phi}^{(1)} C_{\phi\phi[\phi\phi]_{0,J}}^2$, where

$$C_{\phi\phi[\phi\phi]_{0,J}}^2 = \frac{2^{J+1}\Gamma(J+2)^2\Gamma(J+3)}{\Gamma(J+1)\Gamma(2J+3)}, \quad (2.88)$$

which is the usual formula for the OPE coefficients of two scalar operators and a leading double-twist operator, which holds in MFT with $\Delta_\phi = 2$. We may also consider the factorised correlator with generic Δ_ϕ .¹² In this case we have several infinite towers of subleading twist operators with dimension $2\Delta_\phi + 2n + J$ and spin J . We checked that the OPE coefficients are again given by the four-point MFT result. This can be easily understood by using the convergent OPE in the (34) channel, as discussed in section 2.3.1.1. A similar story holds when the two-point function is between points x_3 and x_5 , or between x_4 and x_5 ,

¹²For example studying ϕ^3 theory in AdS with a massive scalar such that $m^2 = \Delta_\phi(\Delta_\phi - d)$.

Finally we can have a two-point function between x_1 and x_3 , x_1 and x_4 , x_2 and x_3 , and x_2 and x_4 , which are the most non-trivial and interesting cases. Together they admit an expansion in terms of blocks where the exchanged operators are $[\phi\phi]_{0,J_1}$ in the (12) OPE and $[\phi\phi]_{0,J_2}$ in the (34) OPE. Thus we access OPE coefficients with one scalar and two spinning operators, which have the extra quantum number ℓ . It is not hard to propose the formula for the OPE coefficients in the case $\ell = 0$, where the dependence in J_1 and J_2 turns out to factorize due to the nature of the tensor structure of $\ell = 0$. We find, for generic Δ_ϕ ,

$$P_{[\phi\phi]_{0,J_1}[\phi\phi]_{0,J_2}\ell=0}^{(1)} = \pi 2^{6-4\Delta_\phi} \prod_{i=1}^2 \frac{2^{-J_i} \Gamma\left(J_i + \frac{\Delta_\phi}{2}\right) \Gamma(J_i + 2\Delta_\phi - 1)}{\Gamma(J_i + 1) \Gamma\left(\frac{\Delta_\phi}{2}\right) \Gamma(\Delta_\phi) \Gamma\left(J_i + \Delta_\phi - \frac{1}{2}\right)}, \quad (2.89)$$

which for the $\Delta_\phi = 2$ case drastically simplifies to

$$P_{[\phi\phi]_{0,J_1}[\phi\phi]_{0,J_2}\ell=0}^{(1)} = \frac{\pi 2^{-J_1-J_2-2} \Gamma(J_1 + 3) \Gamma(J_2 + 3)}{\Gamma(J_1 + \frac{3}{2}) \Gamma(J_2 + \frac{3}{2})}. \quad (2.90)$$

For higher ℓ we find that the J_1 and J_2 dependence no longer factorizes. Instead, for $\Delta_\phi = 2$ we find that the ratio $P_{[\phi\phi]_{0,J_1}[\phi\phi]_{0,J_2}\ell}^{(1)}/P_{[\phi\phi]_{0,J_1}[\phi\phi]_{0,J_2}\ell=0}^{(1)}$ is given by a symmetric polynomial in J_1 and J_2 , with maximum degree 2ℓ in both variables combined and maximum degree ℓ in each variable separately. For example, the first few polynomials are given by

$$\begin{aligned} \frac{P_{\ell=1}}{P_{\ell=0}} &= \frac{1}{2} \left(3 + (J_1 + J_2) + J_1 J_2 \right), \\ \frac{P_{\ell=2}}{P_{\ell=0}} &= \frac{1}{12} \left(J_2^2 J_1^2 + J_2 J_1^2 + J_2^2 J_1 + 7 J_2 J_1 + 6(J_1 + J_2) + 18 \right), \\ \frac{P_{\ell=3}}{P_{\ell=0}} &= \frac{1}{144} \left(J_2^3 J_1^3 - (J_2 J_1^3 + J_2^3 J_1) + 12 J_2^2 J_1^2 \right. \\ &\quad \left. + 12(J_2 J_1^2 + J_2^2 J_1) + 85 J_2 J_1 + 72(J_1 + J_2) + 216 \right), \end{aligned} \quad (2.91)$$

where here we used the shorthand notation $P_{\ell=i} \equiv P_{[\phi\phi]_{0,J_1}[\phi\phi]_{0,J_2}\ell=i}^{(1)}$. We can easily write down these polynomials to a very high order.¹³ Unfortunately we did not find a closed form at arbitrary ℓ . Nevertheless, we could perform the simpler task of finding the large J_1, J_2 at fixed ℓ behavior, which in fact we were able to do for generic Δ_ϕ . We found that

$$\frac{P_{[\phi\phi]_{0,J_1}[\phi\phi]_{0,J_2}\ell}^{(1)}}{P_{[\phi\phi]_{0,J_1}[\phi\phi]_{0,J_2}\ell=0}^{(1)}} \approx \frac{(J_1 J_2)^\ell}{\Gamma(\ell + 1) (\Delta_\phi)_\ell}, \quad (2.92)$$

¹³We can also write down a few of them for general Δ_ϕ . In this case there is also a simple additional denominator.

Combining this result with the large spin behavior of the $\ell = 0$ OPE coefficient, and then taking the large ℓ limit, we find a perfect match with formula (2.42) obtained using the lightcone bootstrap!

2.4.2.2 Comments on the six-point function

The six-point function of a scalar ϕ in the ϵ expansion is given by

$$\begin{aligned} \langle \prod_{i=1}^6 \phi(x_i) \rangle &= \sum_{perm} \langle \phi(x_1)\phi(x_2) \rangle \langle \phi(x_3)\phi(x_4) \rangle \langle \phi(x_5)\phi(x_6) \rangle + \sum_{perm} \langle \phi(x_1)\phi(x_2) \rangle \langle \prod_{i=3}^6 \phi(x_i) \rangle \Big|_{conn} \\ &+ \sum_{perm} \langle \phi(x_1)\phi(x_2)\phi(x_3) \rangle \langle \phi(x_4)\phi(x_5)\phi(x_6) \rangle + \langle \prod_{i=1}^6 \phi(x_i) \rangle \Big|_{conn}. \end{aligned} \quad (2.93)$$

The leading term is given by the mean field theory discussed above (with $\Delta_\phi = 2 + O(\epsilon)$) and is of order ϵ^0 . The partially factorized terms (two-point function times four-point function and three-point function times another three-point function) begin at order ϵ^2 . These have subsequent corrections of order ϵ^4 , which is the order at which the connected contributions begin. At leading order the latter is given by

$$\langle \prod_{i=1}^6 \phi(x_i) \rangle \Big|_{conn} = C_{\phi\phi\phi}^4 \left(\int \frac{d^6 x_0}{x_{12}^2 x_{34}^2 x_{56}^2 \prod_{i=1}^6 x_{i0}^2} + \int \frac{d^6 x_7 d^6 x_8}{x_{12}^2 x_{17}^2 x_{27}^2 (x_{37}^2)^2 x_{47}^2 x_{48}^2 (x_{58}^2)^2 (x_{68}^2)^2 x_{78}^2} \right) + \text{perm},$$

where the first integral is the same as the six-point D -function D_{111111} , which we analyze in Appendix 2.B. It would be nice to systematically study all these corrections and to match the asymptotics of the OPE coefficients with the lightcone bootstrap results presented in section (2.3.2).

2.5 Discussion

We have shown how to use the lightcone bootstrap for five- and six-point functions to determine the large spin behaviour of some new OPE coefficients. For the five-point function, in the case of a direct-channel identity exchange we determined the large J_1, J_2 and ℓ behaviour of the OPE coefficient $C_{\phi[\phi\phi]_{0,J_1}[\phi\phi]_{0,J_2}}^{(\ell)}$ in the cross channel. For the case of a leading twist exchange in the direct channel, including the possibility of the stress tensor exchange, we determined the asymptotic behaviour of $C_{\phi[\phi\phi]_{0,J_1}[\phi\mathcal{O}_*]_{0,J_2}}^{(\ell)}$. For the six-point function, in the case of a direct-channel identity exchange, we determined the large J_i and ℓ_i behaviour of $C_{[\phi\phi]_{0,J_1}[\phi\phi]_{0,J_2}[\phi\phi]_{0,J_3}}^{(\ell_i)}$. Subleading corrections to this OPE coefficient due

to the direct-channel leading twist exchange were also bootstrapped. An interesting interpretation of these results emerges in connection to the origin limit $U_i \rightarrow 0$. In this limit we observed that the correlation function diverges at most as $\log U_i^3$ in contrast with the planar gauge theory case where the divergences can be an arbitrary power of $\log U_i$ [64, 133]. The difference between these results follows from the existence or not of a twist gap in a CFT correlator.

Our knowledge of higher-point conformal blocks is still in its infancy. In particular, our work was limited to the leading order expansion of the blocks in the lightcone limit. In our notation this corresponds to the leading term in the limit $u_{\text{odd}} \rightarrow 0$ that defines the lightcone blocks. It would be very interesting to study subleading corrections to the blocks in this limit, which would allow us to bootstrap OPE coefficients with subleading double-twist operators of the form $[\phi\phi]_{n,J}$ and $[\phi\mathcal{O}_*]_{n,J}$. Additionally, to simplify our analysis, we often took the origin limit $U_i \rightarrow 0$. It would also be interesting to compute subleading terms in this expansion, which can be done using only the available lightcone blocks.

In this chapter, we only considered the lightcone blocks in the snowflake channel. For the six-point function, the comb-channel block would lead to a different expansion involving the exchange of mixed symmetry operators, which should be of triple-twist type. Such operators are expected to be degenerate at large spin, but this degeneracy should be lifted at finite spin. It is a very interesting question whether the bootstrap would be able to address this question in the large spin expansion. First results in this direction were obtained in [66]. This could be a sign of analyticity in spin for each triple-twist family.

Analyticity is also an open question regarding the new OPE coefficients whose large spin behaviour we determined here. In this case, since there is a unique operator at each spin and analyticity has been proven in the simpler case of the OPE coefficient $C_{\phi\phi[\phi\phi]_{0,J}}$, we could also expect analyticity to hold. However, the situation here is more subtle because in this case we also have the label ℓ_i that parametrizes tensor structures and is basis dependent. This is an interesting question since in the case of $C_{[\phi\phi]_{0,J_1}[\phi\phi]_{0,J_2}[\phi\phi]_{0,J_3}}^{(\ell_i)}$ it would connect to the OPE coefficients of the low spin contributions of this family of operators. In particular, for an appropriate choice of the external scalar operators, this will connect to the OPE coefficient between three energy-momentum tensors $C_{TTT}^{(\ell_i)}$. In this case one would hope to derive reliable predictions by including the contributions from the first terms in the large J expansion.

Analyticity in spin is also important for Regge theory of higher-point functions which

we will discuss in the next chapter. This is clear since Conformal Regge Theory relies on the analytic continuation in spin [86]. In the four-point case the Lorentzian inversion formula established such analyticity [79]. Thus, deriving a Lorentzian inversion formula for higher-point functions would shed light in this problem and, most likely, systematize the calculations reported in this chapter.

A more ambitious problem is to set up the Euclidean numerical bootstrap for higher-point functions, with obvious gains in the available CFT data. As it is well known, positivity is a key ingredient in the numerical bootstrap of four-point functions. In the case of the six-point function it is possible to choose reflection positive kinematics, however such positivity is not guaranteed term by term in the block expansion. The situation looks even worse in the case of the five-point function, since this correlator can not be seen as a positive norm of a state. One possibility would be to consider a positive semi-definite matrix whose matrix elements would involve the four-, five- and six-point functions. We hope to return to these questions in the future.

Appendices for chapter 2

2.A Higher-point Conformal Blocks

2.A.1 Mellin amplitudes

The Mellin amplitude of a connected n -point function of scalar conformal correlators can be defined as [142, 143]

$$\langle \mathcal{O}_1(x_1) \dots \mathcal{O}_n(x_n) \rangle = \int [d\gamma] M(\gamma_{ij}) \prod_{1 \leq i < j \leq n} \Gamma(\gamma_{ij}) (x_{ij}^2)^{-\gamma_{ij}} , \quad (2.94)$$

where $[d\gamma]$ denotes an integration with the constraints

$$\sum_{i=1}^n \gamma_{ij} = 0 , \quad \gamma_{ij} = \gamma_{ji} , \quad \gamma_{ii} = -\Delta_i . \quad (2.95)$$

It is a well known fact by now that the OPE implies that the Mellin amplitude is a meromorphic function of the Mellin variables γ_{ij} . For each exchange of a primary operator with dimension Δ and spin J there is an infinite set of poles in the Mellin amplitude,

$$M \approx \frac{\mathcal{Q}_m}{\gamma_{LR} - (\Delta - J + 2m)} , \quad m = 0, 1, 2, \dots , \quad (2.96)$$

where

$$\gamma_{LR} = - \left(\sum_{i=1}^k p_i \right)^2 = \sum_{a=1}^k \sum_{i=k+1}^n \gamma_{ai} , \quad (2.97)$$

with the p_i defined such that $p_i \cdot p_j = \gamma_{ij}$. The residue \mathcal{Q}_m is related to lower point functions and conformal blocks [144]. The label m is associated to the contribution of higher twist descendant operators.

In particular, the equivalence between (2.94) and conformal block decompositions (2.15) and (2.21) imposes that the Mellin amplitude for the five and six-point correlator needs to

have the following poles

$$M_5 \approx \frac{\sum_l C_{12J_1} C_{34J_2} C_{5J_1J_2}^{(l)} F_l(\gamma)}{\left(\gamma_{12} - \frac{J_1 - \Delta_{J_1} + 2\Delta_\phi}{2}\right) \left(\gamma_{34} - \frac{J_2 - \Delta_{J_2} + 2\Delta_\phi}{2}\right)}, \quad (2.98)$$

$$M_6 \approx \frac{\sum_{l_i} C_{12J_1} C_{34J_2} C_{56J_3} C_{J_1J_2J_3}^{(l_i)} F_{l_1l_2l_3}(\gamma)}{\left(\gamma_{12} - \frac{J_1 - \Delta_{J_1} + 2\Delta_\phi}{2}\right) \left(\gamma_{34} - \frac{J_2 - \Delta_{J_2} + 2\Delta_\phi}{2}\right) \left(\gamma_{56} - \frac{J_3 - \Delta_{J_3} + 2\Delta_\phi}{2}\right)}, \quad (2.99)$$

where the functions F_l and $F_{l_1l_2l_3}$ are computed by Mellin transforming the lightcone blocks used in this chapter and C_{XYZ} are OPE coefficients. In the following we will determine the form of F_l and $F_{l_1l_2l_3}$ for some specific cases¹⁴.

Let us start with the five-point lightcone conformal block (2.16) with identical scalar operators $\mathcal{O}_i = \phi$, and write the numerator using the binomial formula

$$\begin{aligned} & \sum_{i_1, i_2, j_1, j_2} \binom{J_1 - l}{i_1} \binom{i_1}{j_1} \binom{J_2 - l}{i_2} \binom{i_2}{j_2} \int \frac{[dt_1][dt_2] t_1^{i_2 - j_2} (1 - t_1)^{j_2} t_2^{i_1 - j_1} (1 - t_2)^{j_1}}{(1 - (1 - t_2)u_4)^{\frac{\Delta_2 - \Delta_1 + J_1 + J_2 - 2l + \Delta_\phi}{2}}} \quad (2.100) \\ & \times \frac{u_1^{\frac{\Delta_1 - J_1}{2}} u_3^{\frac{\Delta_2 - J_2}{2}} (1 - u_2)^l u_2^{j_1 + j_2} u_5^{i_1} u_4^{i_2}}{(1 - (1 - t_1)(1 - t_2)(1 - u_2))^{\frac{\Delta_1 + \Delta_2 + J_1 + J_2 - \Delta_\phi}{2}} (1 - (1 - t_1)u_5)^{\frac{\Delta_1 - \Delta_2 + J_1 + J_2 - 2l + \Delta_\phi}{2}}}. \end{aligned}$$

Next we introduce three Mellin variables s_1, s_2, s_3 with respect to the cross-ratios u_2, u_4 and u_5 ,

$$\begin{aligned} & \sum_{i_1, i_2, j_1, j_2} \binom{J_1 - l}{i_1} \binom{i_1}{j_1} \binom{J_2 - l}{i_2} \binom{i_2}{j_2} u_1^{\frac{\Delta_1 - J_1}{2}} u_3^{\frac{\Delta_2 - J_2}{2}} (1 - u_2)^l \int ds_1 ds_2 ds_3 \Gamma(s_1) \Gamma(s_2) \Gamma(s_3) \\ & u_2^{-s_1 + j_1 + j_2} u_4^{-s_2 + i_2} u_5^{-s_3 + i_1 + \frac{\Delta_\phi}{2}} \left(\frac{\Delta_1 + J_1 + \Delta_2 + J_2 - \Delta_\phi}{2} \right)_{-s_1} \\ & \left(\frac{\Delta_2 - \Delta_1 - 2l + J_1 + J_2 + \Delta_\phi}{2} \right)_{-s_2} \left(\frac{\Delta_1 - \Delta_2 - 2l + J_1 + J_2 + \Delta_\phi}{2} \right)_{-s_3} \mathcal{B}_{s_1, s_2, s_3}, \quad (2.101) \end{aligned}$$

with the function $\mathcal{B}_{s_1, s_2, s_3}$ given by

$$\mathcal{B}_{s_1, s_2, s_3} = \int [dt_1][dt_2] (1 - t_1)^{i_2 - j_2 - s_3} t_1^{\frac{\Delta_2 - \Delta_1 - J_1 - J_2 + 2(s_3 - s_1) + 2l - \Delta_\phi + 2j_2}{2}} t_2^{i_1 - j_1 - s_2} (1 - t_2)^{\frac{\Delta_1 - \Delta_2 - J_1 - J_2 + 2l + 2(s_2 - s_1) + 2j_1 - \Delta_\phi}{2}} (1 - t_1(1 - t_2))^{\frac{2s_1 - J_1 - J_2 - \Delta_1 - \Delta_2 + \Delta_\phi}{2}}. \quad (2.102)$$

For $J_1 = J_2 = 0$ the function $\mathcal{B}_{s_1, s_2, s_3}$ can be integrated to

$$\mathcal{B}_{s_1, s_2, s_3} = \frac{\Gamma(\Delta_1) \Gamma(\Delta_2) \Gamma\left(\frac{\Delta_1 - \Delta_\phi + 2(s_2 - s_1)}{2}\right) \Gamma\left(\frac{\Delta_2 - \Delta_\phi + 2(s_3 - s_1)}{2}\right) \Gamma\left(\frac{2(s_1 - s_2 - s_3) + \Delta_\phi}{2}\right)}{\Gamma^2\left(\frac{\Delta_1}{2}\right) \Gamma^2\left(\frac{\Delta_2}{2}\right) \Gamma\left(\frac{\Delta_1 + \Delta_2 - 2s_1 - \Delta_\phi}{2}\right)}. \quad (2.103)$$

¹⁴It would be interesting to repeat the analysis of appendix A.1 of [86] for higher-point functions.

One of the advantages of this Mellin representation for the conformal block is that it makes it easier to study certain limits. For example, to get the leading term in the $u_2, u_4, u_5 \rightarrow 0$ limit we just have to close each contour s_1, s_2, s_3 to the left picking all the poles along the way. Notice that $\mathcal{B}_{s_1, s_2, s_3}$ for generic spin can be written as a ${}_3F_2$ hypergeometric series

$$\begin{aligned} \mathcal{B}_{s_1, s_2, s_3} = & \frac{\Gamma\left(\frac{J_1+\Delta_1+1}{2}\right) \Gamma\left(\frac{J_2+\Delta_2+1}{2}\right) \Gamma\left(i_2 - j_2 + \frac{J_1}{2} - s_3 + \frac{\Delta_1}{2}\right) \Gamma\left(i_1 - j_1 + \frac{J_2}{2} - s_2 + \frac{\Delta_2}{2}\right)}{2^{2-\Delta_1-\Delta_2-J_1-J_2} \pi \Gamma\left(\frac{J_1}{2} + \frac{\Delta_1}{2}\right) \Gamma\left(\frac{J_2}{2} + \frac{\Delta_2}{2}\right)} \\ & \frac{\Gamma\left(\ell + j_1 - \frac{J_1}{2} - s_1 + s_2 + \frac{\Delta_1}{2} - \frac{\Delta_\phi}{2}\right) \Gamma\left(\ell + j_2 - \frac{J_2}{2} - s_1 + s_3 + \frac{\Delta_2}{2} - \frac{\Delta_\phi}{2}\right)}{\Gamma\left(\ell + i_1 - \frac{J_1}{2} + \frac{J_2}{2} - s_1 + \frac{\Delta_1+\Delta_2-\Delta_\phi}{2}\right) \Gamma\left(\ell + i_2 + \frac{J_1}{2} - \frac{J_2}{2} - s_1 + \frac{\Delta_1+\Delta_2-\Delta_\phi}{2}\right)} \quad (2.104) \\ & {}_3F_2\left(\begin{array}{c} -\frac{\Delta_\phi}{2} + \frac{\tau_1}{2} + j_1 - s_1 + s_2 + \ell, -\frac{\Delta_\phi}{2} + \frac{\tau_2}{2} + j_2 - s_1 + s_3 + \ell, -\frac{\Delta_\phi}{2} + \frac{h_1}{2} + \frac{h_2}{2} - s_1 \\ -\frac{\Delta_\phi}{2} + \frac{\Delta_1}{2} + \frac{\Delta_2}{2} + i_2 + \frac{J_1}{2} - \frac{J_2}{2} - s_1 + \ell, -\frac{\Delta_\phi}{2} + \frac{\Delta_1}{2} + \frac{\Delta_2}{2} + i_1 - \frac{J_1}{2} + \frac{J_2}{2} - s_1 + \ell \end{array}; 1\right). \end{aligned}$$

To find F_l one needs to relate the Mellin transform we have computed to the Mellin amplitude definition in (2.94). We use the conditions (2.95) to write the Mellin amplitude in terms of five independent Mellin variables, namely: $\gamma_{12}, \gamma_{34}, \gamma_{13}, \gamma_{15}, \gamma_{35}$. After computing the integral in γ_{12} and γ_{34} , we can relate the two sets of Mellin variables, s_i 's and γ_{ij} , by demanding the exponents of the cross-ratios to be the same on both expressions. To do so, we first expand $(1 - u_2)^l = \sum_k \binom{l}{k} (-u_2)^k$. We find then the relation

$$\begin{aligned} s_1 &= \frac{2j_1 + 2j_2 + 2k - J_2 + \Delta_{J_2} - 2\gamma_{13} - 2\gamma_{35}}{2}, \quad s_3 = \gamma_{15} + i_1, \\ s_2 &= \frac{2i_2 + J_1 - J_2 - \Delta_{J_1} + \Delta_{J_2} + \Delta_\phi - 2\gamma_{35}}{2}. \end{aligned} \quad (2.105)$$

This relation depends on indices that are summed over. Thus, performing the change of variables in (2.101) leads us to finite sums of contour integrals. We would like to swap the order of sums and integrals to be able to write F_l from those finite sums. This can be done if we are allowed to move, without crossing any poles, all the contours to the same region. Assuming this can be done ¹⁵, to find F_l is just simple algebra. For specific values of spin and scaling dimension of the exchanged operators, it is easy to see that F_l defined in this way is, as expected, a polynomial in the Mellin variables $\gamma_{13}, \gamma_{15}, \gamma_{35}$ whose degree depends on J_1, J_2, l .

It is possible to repeat the same analysis for the six-point conformal block in the light-cone. Since the method is essentially the same we will just quote here the Mellin transform

¹⁵To be rigorous one needs to study in detail the very complicated pole structure of the integrand. This is particularly challenging due to the possible presence of fake poles. As discussed in [145], gamma functions that depend on more than a single Mellin variable can naively suggest the presence of families of poles that differ depending on the order of integration of the Mellin variables. These poles are fake.

of the block for the exchange of scalar operators

$$\prod_{i=1}^3 \frac{u_{2i-1}^{\frac{\Delta_i}{2}} \Gamma(\Delta_i)}{\Gamma(\frac{\sum_j \Delta_j - 2\Delta_i}{2}) \Gamma^2(\frac{\Delta_i}{2})} \int \prod_{i=1}^6 ds_i \Gamma(s_i) \prod_{i=1}^3 \frac{U_{2i-1}^{s_i}}{u_{2i} U_{-i}} U_i^{-s_{3+i}} \Gamma\left(\frac{\Delta_i - 2(s_i + \bar{s}_i)}{2}\right) \Gamma\left(\frac{\Delta_{21} - 2(s_3 + s_6 - s_2)}{2}\right) \Gamma\left(\frac{\Delta_{13} - 2(s_2 + s_4 - s_1)}{2}\right) \Gamma\left(\frac{\Delta_{32} - 2(s_1 + s_5 - s_3)}{2}\right), \quad (2.106)$$

where $\bar{s}_1 = s_5 + s_6$, $\bar{s}_2 = s_4 + s_5$, $\bar{s}_3 = s_4 + s_6$ and $\Delta_{ij} = \Delta_i - \Delta_j$. To relate this to F_{000} we repeat the analysis above. We write the usual Mellin amplitude definition (2.94) in terms of 9 independent Mellin variables γ_{ij} . After integrating in γ_{12} , γ_{34} and γ_{56} , it is easy to relate the remaining γ_{ij} to s_i 's by imposing the same power behaviour of the cross-ratios on both Mellin representations. We find:

$$s_1 = \gamma_{23}, \quad s_2 = \gamma_{45}, \quad s_3 = \gamma_{16}, \quad s_4 = \gamma_{46}, \quad s_5 = \gamma_{24}, \quad s_6 = \gamma_{26}. \quad (2.107)$$

A simple computation shows that F_{000} is independent of γ_{ij} as one would expect for scalar exchanges.

2.A.2 Explicit computation of six-point blocks

In the following we compute the leading lightcone limit contribution for the exchange of three minimal-twist operators in the snowflake channel of the six-point function. For simplicity, let us first consider that the corresponding operators are scalars. It will be useful to recall the definition of the block $g_{k*k*k*}(u_{2i}, U_i)$ given in (2.22). This is a complicated three-dimensional integral even in the simpler scalar case. One can show, however, that no divergences appear from the limit $u_{2i} \rightarrow 0$ ¹⁶, since the U_i 's act as regulators of those possible divergences. This substantially simplifies our analysis. The situation for the spinning operators is technically more involved but it is still free of divergences in the limit of $u_{2i} \rightarrow 0$.

As an example, consider the exchange of three leading-twist scalar operators with dimension 2 in terms of the cross-ratios y_u, y_v, y_w ¹⁷ defined as

$$U_1 = \frac{y_u(1-y_v)(1-y_w)}{(1-y_uy_v)(1-y_uy_w)}, \quad U_2 = \frac{y_v(1-y_u)(1-y_w)}{(1-y_vy_u)(1-y_vy_w)}, \quad U_3 = \frac{y_w(1-y_u)(1-y_v)}{(1-y_wy_u)(1-y_wy_v)}. \quad (2.108)$$

¹⁶This can be checked for example with the HyperInt package [146]. We find only logarithmic divergences in U_i whenever $U_i \rightarrow 0$.

¹⁷The appearance of these cross-ratios is not surprising given the duality between null polygon Wilson loops and correlation functions, see [133] for recent development in this topic. In fact these cross-ratios have appeared before in the study of WL/scattering amplitudes in $\mathcal{N} = 4$ SYM [147].

In these cross-ratios, the block becomes

$$g_{222}(0, U_i) = \prod_{i=0}^3 \int_0^\infty \frac{dt_i (y_i y_{i+1} - 1)^2}{y_i(y_{i+1} - 1)(y_{i-1} - 1) + t_i(1 + t_{i+1})(y_i y_{i+1} - 1)(y_i y_{i-1} - 1)}, \quad (2.109)$$

where we have changed variables $t_i \rightarrow t_i/(t_i + 1)$ and identified $y_1 = y_v$, $y_2 = y_u$ and $y_3 = y_w$. The subscripts should be understood $\bmod 3$. These cross-ratios appear to be a more natural choice to compute these integrals, as the integrand factorizes into simpler pieces. The integration can be done exactly and written in terms of hyperlogarithmic functions as

$$\begin{aligned} g_{222}(0, U_i) = & \frac{(1 - y_u y_w)(1 - y_v y_w)(1 - y_u y_v)}{(1 - y_w)(1 - y_u)(1 - y_v)(y_u y_v y_w - 1)} \left(H_0(y_u) \left(H_{0,1}(y_w) + H_{0,1}(y_v) - H_{0,y_w^{-1}}(y_v) \right) \right. \\ & - H_0(y_v) \left(H_{0,y_w^{-1}}(y_u) + H_{0,(y_v y_w)^{-1}}(y_u) - H_{0,1}(y_w) - H_{0,y_v^{-1}}(y_u) - H_{0,1}(y_u) \right) + 2H_{0,(y_v y_w)^{-1},y_v^{-1}}(y_u) \\ & + H_0(y_w) \left(H_{0,y_w^{-1}}(y_v) + H_{0,1}(y_v) + H_{0,y_w^{-1}}(y_u) - H_{0,y_v^{-1}}(y_u) + H_{0,1}(y_u) - H_{0,(y_v y_w)^{-1}}(y_u) \right) \\ & + 2H_1(y_v) \left(H_{0,y_w^{-1}}(y_u) - H_{0,(y_v y_w)^{-1}}(y_u) \right) - 2H_{0,y_w^{-1},y_v^{-1}}(y_v) + H_{0,y_v^{-1},0}(y_u) - H_{0,(y_v y_w)^{-1},0}(y_u) \\ & + H_{0,y_w^{-1},0}(y_v) + 2 \left(H_{0,1,1}(y_u) + H_{0,1,1}(y_v) + H_{0,1,1}(y_w) \right) - 2H_{0,(y_v y_w)^{-1},1}(y_u) - 2H_{0,y_v^{-1},y_v^{-1}}(y_u) \\ & - (H_{0,1,0}(y_u) + H_{0,1,0}(y_v) + H_{0,1,0}(y_w)) + 2H_{y_w^{-1}}(y_v) \left(H_{0,(y_v y_w)^{-1}}(y_u) - H_{0,1}(y_u) \right) \\ & + 2H_1(y_w) \left(H_{0,y_v^{-1}}(y_u) - H_{0,(y_v y_w)^{-1}}(y_u) \right) + 2H_{0,(y_v y_w)^{-1},y_w^{-1}}(y_u) - 2H_{0,y_w^{-1},y_w^{-1}}(y_u) \\ & \left. + H_0(y_u)H_0(y_v)H_0(y_w) + H_{0,y_w^{-1},0}(y_u) + \zeta_2(H_0(y_w) + H_0(y_u) + H_0(y_v)) \right). \end{aligned} \quad (2.110)$$

The hyperlogarithm functions H are defined recursively via the integral [146]

$$H_{\omega_1, \omega_2, \dots, \omega_n}(z) = \int_0^z \frac{dt}{t - \omega_1} H_{\omega_2, \dots, \omega_n}(z), \quad H_{0,0,\dots,0}(z) = \frac{\ln^n z}{n!}, \quad H(z) = 1. \quad (2.111)$$

One can then check that in the limit where all $y_i \rightarrow 0$ (which corresponds to $U_i \rightarrow 0$), the integral (2.109) is given by

$$\lim_{y_i \rightarrow 0} (2.109) \approx -\ln(y_u) \ln(y_v) \ln(y_w) - \zeta_2 \ln(y_w) - \zeta_2 \ln(y_u) - \zeta_2 \ln(y_v), \quad (2.112)$$

which is consistent with the behaviour in (2.58). In fact, one can repeat this computation for several even integer values of the dimension of the exchanged scalar operators. In this class of examples, the integral can be performed with the HyperInt package. We use several parameterizations of the block and guess its general form in the kinematic limit we consider in this chapter, namely $u_{2i-1} \rightarrow 0$, followed by $u_{2i} \rightarrow 0$ and in last place $U_i \rightarrow 0$. This is (2.58). We will later confirm these results by using a Mellin representation which we will

define below.

For a stress tensor exchange, the form of the integrand is more complicated. Even for specific values of the ℓ_i 's and of the space-time dimension d , we find that these computations extend in time and therefore this procedure becomes less useful. It is however worth stating that if we restrict ourselves to the case where $y_u = y_v = y_w$ these computations can be performed very quickly in HyperInt. We use these results as a sanity check for the Mellin method we now present.

In the kinematics relevant for the bootstrap calculation of section 2.3 we need to take $u_{2i} \rightarrow 0$, in which case we can derive a simplified Mellin representation. For that we consider the lightcone block (2.22), set $u_{2i} \rightarrow 0$ in the integrand¹⁸ and then we Mellin transform with respect to the cross-ratios U_i . After some massaging we obtain

$$g_{k*k*k*}^{\ell_1 \ell_2 \ell_3} = \prod_i^3 \int [ds_i] \Gamma(s_i) \frac{\Gamma(2J + \tau)}{2^J \Gamma\left(\frac{2J+\tau}{2}\right)^2} \sum_{n_i, m_i} (-1)^{m_i} U_i^{m_i + n_i - s_i + \ell_{2-i}} \frac{\binom{J - \ell_{2-i} - \ell_{3-i}}{n_i} \binom{J - n_{i+1} - \ell_{1-i} - \ell_{2-i}}{m_i} \Gamma(s_i - n_i - \ell_{2-i} + \ell_{1-i})}{(2J - s_i - \ell_{1-i} - \ell_{3-i} + \frac{\tau}{2})_{s_i} (J + m_{i+1} + n_i - s_i - s_{i+1} + \frac{\tau}{2})_{s_i - n_i - \ell_{2-i} + \ell_{1-i}}}, \quad (2.113)$$

in the case where all the operators have the same twist and spin. The sums over n_i and m_i were introduced to reduce the binomials that appeared in the numerator into monomials of U_i .

We would like to make an expansion in the limit $U_i \rightarrow 0$. In Mellin language this is simply done by closing the s_i contours to the left and picking the corresponding poles. At leading order only some poles contribute. We will call these the leading poles. The leading poles will only come from the gamma functions explicitly written above and which only depend on one of the Mellin variables.

We observe that the position of the leading poles does not depend on the value of m_i . Therefore in the limit $U_i \rightarrow 0$, the leading contributions have to come from the terms with $m_i = 0$. For fixed values of spin, twist and ℓ_i , we perform the sum over n_i and pick the residues of leading poles. These leading contributions are located at values of s_i such that the exponent of the corresponding U_i becomes 0, which leads to the expected logarithmic behaviour when there is a double pole¹⁹. If we use this mechanism in the case of scalar

¹⁸This does not lead to any divergences as discussed above.

¹⁹Other poles of the family will always contribute at subleading orders. In fact, if we have s_i smaller than the required value, there will be a non-vanishing power U_i which leads to a subleading contribution. On the other hand, if s_i is instead larger, there is no corresponding pole and the residue is 0. In other words, leading poles are the rightmost poles of the family prescribed by the explicit gamma functions we wrote above.

minimal-twist exchange, we immediately reproduce the result of (2.58)! Moreover, we can also check that this procedure for the leading poles nicely matches the results of direct integration using HyperInt in the limit $y_u = y_v = y_w$.

For a stress tensor exchange, we have three possible values of ℓ_i 's, namely 0,1 and 2. If two or three ℓ_i 's take value 1, those contributions will be subleading by powers of U_i . We thus list the results for the remaining cases

$$\begin{aligned}
g_{TTT}^{000} &= -\frac{\Gamma(\tau+4)^3}{64\Gamma\left(\frac{\tau+4}{2}\right)^6} \left[\prod_i^3 \frac{\ln U_i}{3} + \left(4 \left(S_{\frac{\tau}{2}+1} \right)^2 - S_{\frac{\tau}{2}+1}^{(2)} + \frac{8(\tau(\tau+6)+2)}{\tau(\tau+2)(\tau+4)(\tau+6)} + \zeta_2 \right) \ln U_1 \right. \\
&\quad \left. + 2S_{\frac{\tau}{2}+1} \ln U_1 \ln U_2 - \frac{S_{\frac{\tau}{2}+1}}{3} \left(8 \left(S_{\frac{\tau}{2}+1} \right)^2 - 6S_{\frac{\tau}{2}+1}^{(2)} \right) - \frac{S_{\frac{\tau}{2}+1} \left(8(\tau(\tau+6)+2) + \zeta_2 \right)}{2\tau(\tau+2)(\tau+4)(\tau+6)} + \text{perm} \right], \\
g_{TTT}^{100} &= -\frac{\Gamma(\tau+4)^3(\tau(\tau+6)+4)}{16\Gamma\left(\frac{\tau+4}{2}\right)^6 \tau(\tau+2)(\tau+4)(\tau+6)} \left[2S_{\frac{\tau}{2}+1} + \ln U_2 \right] \tag{2.114} \\
g_{TTT}^{200} &= -\frac{\Gamma(\tau+4)^3}{4\Gamma\left(\frac{\tau+4}{2}\right)^6 \tau(\tau+2)(\tau+4)(\tau+6)} \left[2S_{\frac{\tau}{2}+1} + \ln U_2 \right],
\end{aligned}$$

where $\tau = d - 2$ is the twist of the stress-tensor. Notice the result diverges for $\tau = 0$. This is not a problem since we are considering the case where there is a twist gap which happens for $d > 2$. For other non-vanishing ℓ_i , the result is obtained by permuting the cross-ratios.

2.A.3 Euclidean expansion of six-point conformal blocks

The results of the main part of the chapter were derived using the leading term of the conformal blocks expanded around the lightcone. We will shift gears in this section and analyze the conformal blocks expanded around the Euclidean OPE limit in a similar approach to the one done for four- and five-point function conformal blocks [39, 42, 57].

The two key ingredients in the derivation of the blocks are that they satisfy the Casimir differential equation

$$\left[\frac{1}{2} \left(L_{AB}^{(i_1)} + L_{AB}^{(i_2)} \right)^2 - C_{\Delta,J} \right] f_{\Delta,J}(x_i) = 0, \tag{2.115}$$

with

$$C_{\Delta,J} = \Delta(\Delta - d) + J(J + d - 2), \tag{2.116}$$

where L_{AB} are the generators of the conformal group and their boundary condition coming from the OPE

$$\mathcal{O}(x_{i_1})\mathcal{O}(x_{i_2}) = \sum_k C_{i_1 i_2 k} \frac{x_{i_1 i_2}^{\mu_1} \cdots x_{i_1 i_2}^{\mu_J}}{(x_{i_1 i_2}^2)^{\frac{\Delta_{i_1} + \Delta_{i_2} - \Delta_k + J_k}{2}}} \mathcal{O}_{k, \mu_1 \dots \mu_J}(x_{i_2}). \quad (2.117)$$

In the Euclidean OPE limit there are three cross-ratios that approach zero

$$s_1^2 = u_1, \quad s_2^2 = u_3, \quad s_3^2 = u_5, \quad (2.118)$$

and six others that remain fixed

$$\begin{aligned} \xi_1 &= \frac{U_1 - u_2 U_2}{s_1 U_1}, & \xi_2 &= \frac{U_3 - u_4 U_1}{s_2 U_3}, & \xi_3 &= \frac{U_2 - u_6 U_3}{s_3 U_2}, \\ \xi_4 &= \frac{(u_2 - U_1) U_2}{s_1 s_2 U_1}, & \xi_5 &= \frac{(u_6 - U_2) U_3}{s_1 s_3 U_2}, & \xi_6 &= \frac{(u_4 - U_3) U_1}{s_2 s_3 U_3}, \end{aligned} \quad (2.119)$$

in a six-point correlation function and are analogous to the four-point cross-ratios written in equation (2.2). The cross-ratios that remain fixed can be interpreted as measuring the angles that the points 2, 4, 6 approach 1, 3, 5. It follows from the OPE (2.117) that the conformal block should behave as

$$G_{\Delta_i, J_i}(s_i, \xi_i) = \prod_{j=1}^3 s_j^{\Delta_j} g_{J_i}(\xi_i), \quad s_i \rightarrow 0, \quad (2.120)$$

where $g_{J_i}(\xi_i)$ ²⁰ is a polynomial function of the cross-ratios ξ_i that satisfies three differential equations coming from the Casimir of the channel (12) in the limit $s_i \rightarrow 0$,

$$\begin{aligned} & \left[(4 - \xi_1^2) \partial_{\xi_1}^2 + (4 - \xi_4^2) \partial_{\xi_4}^2 + (4 - \xi_5^2) \partial_{\xi_5}^2 - 2(2\xi_2 + \xi_1 \xi_4) \partial_{\xi_1} \partial_{\xi_4} \right. \\ & - 2(2\xi_2 + \xi_1 \xi_4) \partial_{\xi_1} \partial_{\xi_4} - 2(2\xi_3 + \xi_1 \xi_5) \partial_{\xi_1} \partial_{\xi_5} + (1 - d)(\xi_1 \partial_{\xi_1} + \xi_4 \partial_{\xi_4} + \xi_5 \partial_{\xi_5}) \\ & \left. + 2(2\xi_2 \xi_3 - \xi_4 \xi_5 - 2\xi_6) \partial_{\xi_4} \partial_{\xi_5} + J_1(J_1 + d - 2) \right] g_{J_i}(\xi_i) = 0, \end{aligned} \quad (2.121)$$

with similar equations for the channels (34) and (56). These three differential equations, together with the boundary condition for $\lambda \rightarrow 0$,

$$g_{J_i}(\xi_i) \rightarrow \xi_1^{J_1 - \ell_2 - \ell_3} \xi_2^{J_2 - \ell_1 - \ell_3} \xi_3^{J_3 - \ell_1 - \ell_2} \xi_4^{\ell_3} \xi_5^{\ell_2} \xi_6^{\ell_1}, \quad \xi_{1,2,3} \rightarrow \frac{\xi_{1,2,3}}{\lambda}, \quad \xi_{4,5,6} \rightarrow \frac{\xi_{4,5,6}}{\lambda^2}, \quad (2.122)$$

²⁰This is the analogue of the Gegenbauer polynomial that appears in the leading term of the OPE of a four-point function conformal block. Let us also remark that this function appears in the definition of the conformal block using the shadow formalism.

fix completely the form of the function. It is possible (and easy) to get subleading corrections of $g_{J_i}(\xi_i)$ for any value of J_i and ℓ_i from the differential equations. By analyzing these corrections we were able to check that the function $g_{J_i}(\xi_i)$ satisfies relations of the type

$$\xi_k g_{J_i, \ell_i}(\xi_i) = \sum_{i=-1}^1 c_{i_1 \dots i_6}^{(k)} g_{J_1+i_1, J_2+i_2, \dots, \ell_3+i_4, \dots, \ell_1+i_6}(\xi_i), \quad (2.123)$$

that can be used to define it recursively. One example of these relations is²¹

$$\begin{aligned} c_{-100000}^{(1)} &= \frac{4(J_1 - \ell_2 - \ell_3)(J_1 + \ell_2 + \ell_3)}{(2J_1 + d - 4)(2J_1 + d - 2)}, & c_{100000}^{(1)} &= 1, \\ c_{-100-100}^{(1)} &= -\frac{2\ell_3(d + 2(\ell_2 + \ell_3 - 2))}{(2J_1 + d - 4)(2J_1 + d - 2)}, & c_{-1000-10}^{(1)} &= -\frac{2\ell_2(d + 2(\ell_2 + \ell_3 - 2))}{(2J_1 + d - 4)(2J_1 + d - 2)}, \\ c_{-100-1-10}^{(1)} &= -\frac{4\ell_2\ell_3}{(2J_1 + d - 4)(2J_1 + d - 2)}, & c_{-100-1-11}^{(1)} &= \frac{4\ell_2\ell_3}{(2J_1 + d - 4)(2J_1 + d - 2)}. \end{aligned} \quad (2.124)$$

Let us remark that there are similar relations for the Gegenbauer polynomial and for the five-point analogue[57].

It is an interesting open problem to obtain a representation of the conformal block as a series expansion in s_i , as was done for four and five points[42, 57]²².

2.B D-functions

In this appendix we analyze five- and six-point D-functions using standard technology from perturbation theory in AdS [49, 148].

2.B.1 Five Points

We start from a five-point contact Witten diagram with a non-derivative interaction

$$W_{\Delta_1, \dots, \Delta_5}^{\text{ctc}}(x_1, \dots, x_5) = \int_{AdS_{d+1}} d^{d+1}y K_{\Delta_1}(x_1, y) \dots K_{\Delta_5}(x_5, y) = D_{\Delta_1, \dots, \Delta_5}, \quad (2.125)$$

where the bulk-boundary propagator is defined as

$$K_{\Delta}(x_i, y) = \left(\frac{z}{(\vec{x}_i - \vec{y})^2 + z^2} \right)^{\Delta}. \quad (2.126)$$

²¹The other relations as well as the definition of $g_{J_i, \ell_i}(\xi_i)$ in terms of a recurrence relation is provided in a auxiliary file.

²²It would also be interesting to see how the recent and new approaches to the conformal blocks[60–62] can help in this problem.

We can expand this in five-point conformal blocks without knowing their explicit form, using Harmonic analysis and the conformal partial waves. We will do this in the (12)(34) channel, but other channels can be obtained with the same method. Start by introducing auxiliary $1 = \int_{AdS} dy' \delta(y' - y)$ and attach the bulk to boundary propagators to the auxiliary points in the desired (12)(34) structure, i.e.

$$W^{\text{ctc}} = \int dy dy' dy'' K_{\Delta_1}(x_1, y') K_{\Delta_2}(x_2, y') K_{\Delta_3}(x_3, y'') K_{\Delta_4}(x_4, y'') K_{\Delta_5}(x_5, y) \delta(y' - y) \delta(y'' - y). \quad (2.127)$$

Next, we use the spectral representation of the AdS delta function and the split representation of the harmonic function to obtain

$$\delta(y_1 - y_2) = \int dx' \int_{-i\infty}^{+i\infty} \frac{dc}{2\pi i} \rho_\delta(c) K_{h+c}(x', y_1) K_{h-c}(x', y_2), \quad (2.128)$$

where c is the imaginary spectral parameter, $h = d/2$ and the spectral function for the Dirac delta is

$$\rho_\delta(c) = \frac{\Gamma\left(\frac{d}{2} + c\right) \Gamma\left(\frac{d}{2} - c\right)}{2\pi^d \Gamma(-c) \Gamma(c)}. \quad (2.129)$$

Now, all three bulk integrals can be performed, since they are of the AdS three-point function type

$$\int dy K_{\Delta_1}(x_1, y) K_{\Delta_2}(x_2, y) K_{\Delta_3}(x_3, y) = a_{\Delta_1, \Delta_2, \Delta_3} \langle \mathcal{O}_1(x_1) \mathcal{O}_2(x_2) \mathcal{O}_3(x_3) \rangle, \quad (2.130)$$

where

$$\langle \mathcal{O}_1(x_1) \mathcal{O}_2(x_2) \mathcal{O}_3(x_3) \rangle = \frac{1}{x_{12}^{\Delta_{12,3}} x_{23}^{\Delta_{23,1}} x_{13}^{\Delta_{13,2}}} \quad (2.131)$$

is the kinematical three-point function without OPE coefficient, and

$$a_{\Delta_1, \Delta_2, \Delta_3} = \frac{\pi^{\frac{d}{2}} \Gamma\left(\frac{\Delta_1 + \Delta_2 - \Delta_3}{2}\right) \Gamma\left(\frac{\Delta_1 + \Delta_3 - \Delta_2}{2}\right) \Gamma\left(\frac{\Delta_2 + \Delta_3 - \Delta_1}{2}\right)}{2\Gamma(\Delta_1) \Gamma(\Delta_2) \Gamma(\Delta_3)} \Gamma\left(\frac{\Delta_1 + \Delta_2 + \Delta_3 - d}{2}\right). \quad (2.132)$$

We are then left with two spectral integrals and two boundary integrals

$$W^{\text{ctc}} = \int [dc'] [dc''] dx' dx'' \rho_\delta(c') \rho_\delta(c'') a_{\Delta_1, \Delta_2, h+c'} a_{h-c', \Delta_5, h-c''} a_{h+c'', \Delta_3, \Delta_4} \quad (2.133)$$

$$\langle \mathcal{O}_1(x_1) \mathcal{O}_2(x_2) \mathcal{O}_{h+c'}(x') \rangle \langle \mathcal{O}_{h-c'}(x') \mathcal{O}_5(x_5) \mathcal{O}_{h-c''}(x'') \rangle \langle \mathcal{O}_{h+c''}(x'') \mathcal{O}_3(x_3) \mathcal{O}_4(x_4) \rangle,$$

where $[dc] = dc/2\pi i$. The position space integrals precisely coincide with the definition of the five-point conformal partial wave for the exchange of two scalar operators of dimension

$h + c'$ and $h + c''$

$$\Psi_{h+c',h+c''}^{\Delta_1 \dots \Delta_5}(x_i) = \int dx dx' \langle \mathcal{O}_1 \mathcal{O}_2 \mathcal{O}_{h+c'}(x') \rangle \langle \mathcal{O}_{h-c'}(x') \mathcal{O}_5 \mathcal{O}_{h-c''}(x'') \rangle \langle \mathcal{O}_{h+c''}(x'') \mathcal{O}_3 \mathcal{O}_4 \rangle. \quad (2.134)$$

Thus, we find the partial have expansion for the five-point contact Witten diagram

$$W^{ctc} = \int [dc'][dc''] \tilde{\rho}_5(c', c'') \Psi_{h+c',h+c''}^{\Delta_1 \dots \Delta_5}(x_i), \quad (2.135)$$

with

$$\tilde{\rho}_5(c', c'') = \rho_\delta(c') \rho_\delta(c'') a_{\Delta_1, \Delta_2, h+c'} a_{h-c', \Delta_5, h-c''} a_{h+c'', \Delta_3, \Delta_4}. \quad (2.136)$$

To obtain the conformal block expansion we deform the contours towards the real axis and pick up the physical poles. To do this we need the relation between the conformal partial waves and the conformal blocks. Since they solve the same Casimir equations, the conformal partial waves must be a linear combination of the blocks for the exchanged operators and their shadows. We provide a detailed analysis of this relation in Appendix 2.C. The coefficients can be obtained in the OPE limits and are given in terms of shadow factors K ($h - c$ appears since it is the shadow of $h + c$)

$$\Psi_{h+c',h+c''}^{\Delta_1 \dots \Delta_5}(x_i) = K_{h-c'}^{\Delta_5, h-c''} K_{h-c''}^{\Delta_5, h+c'} G_{h+c',h+c''}^{\Delta_1 \dots \Delta_5}(x_i) + 3 \text{ shadow terms} \quad (2.137)$$

With

$$K_{\Delta, J}^{\Delta_1, \Delta_2} = \left(-\frac{1}{2} \right)^J \frac{\pi^{\frac{d}{2}} \Gamma(\Delta - \frac{d}{2}) \Gamma(\Delta + J - 1) \Gamma(\frac{\tilde{\Delta} + \Delta_1 - \Delta_2 + J}{2}) \Gamma(\frac{\tilde{\Delta} + \Delta_2 - \Delta_1 + J}{2})}{\Gamma(\Delta - 1) \Gamma(d - \Delta + J) \Gamma(\frac{\Delta + \Delta_1 - \Delta_2 + J}{2}) \Gamma(\frac{\Delta + \Delta_2 - \Delta_1 + J}{2})}, \quad (2.138)$$

which are related to the shadow factors S we will compute below by $K_{\Delta, J}^{\Delta_1, \Delta_2} = (-\frac{1}{2})^J S_{\Delta, J}^{\Delta_1, \Delta_2}$.

We will carefully describe these factors in Appendix 2.C. Note that since we only exchange scalar operators we always have $J = 0$ so we suppress that label. We now have the block expansion in contour integral form

$$W^{ctc} = \int [dc'][dc''] \rho_5(c', c'') G_{h+c',h+c''}^{\Delta_1 \dots \Delta_5}(x_i), \quad (2.139)$$

where

$$\rho_5(c', c'') = 4 K_{h-c'}^{\Delta_5, h-c''} K_{h-c''}^{\Delta_5, h+c'} \tilde{\rho}_5(c', c'') \quad (2.140)$$

and the factor of 4 comes from the shadow combinations. The function ρ_5 contains three families of poles corresponding to the exchanged operators. Introducing the notation $\Delta' =$

$h + c'$, we have

$$\text{Family 1: } \Delta' = \Delta_1 + \Delta_2 + 2n_1, \quad \Delta'' = \Delta_3 + \Delta_4 + 2m_1, \quad (2.141)$$

$$\text{Family 2: } \Delta' = \Delta_1 + \Delta_2 + 2n_2, \quad \Delta'' = \Delta_1 + \Delta_2 + \Delta_5 + 2n_2 + 2m_2, \quad (2.142)$$

$$\text{Family 3: } \Delta' = \Delta_3 + \Delta_4 + \Delta_5 + 2n_3 + 2m_3, \quad \Delta'' = \Delta_3 + \Delta_4 + 2m_3. \quad (2.143)$$

Thus we can write the block expansion as

$$\begin{aligned} W^{\text{ctc}} = & \sum_{n_1, m_1=0}^{\infty} P_{[12]_{n_1}[34]_{m_1}} G_{[12]_{n_1}, [34]_{m_1}}^{\Delta_1 \dots \Delta_5} + \sum_{n_2, m_2=0}^{\infty} P_{[12]_{n_2}[125]_{n_2+m_2}} G_{[12]_{n_2}, [125]_{n_2+m_2}}^{\Delta_1 \dots \Delta_5} \\ & + \sum_{n_3, m_3=0}^{\infty} P_{[345]_{n_3+m_3}[34]_{m_3}} G_{[345]_{n_3+m_3}, [34]_{m_3}}^{\Delta_1 \dots \Delta_5}, \end{aligned} \quad (2.144)$$

where $[ij]_n$ denotes the scalar double-twist $[\mathcal{O}_i \mathcal{O}_j]_n$ with n laplacians, and similarly for the triple-twists $[ijk]_{n+m}$. The P_{ab} are related to the OPE coefficients through (2.17) with $\ell = 0$. Finally, we specify how to obtain the P_{ab} from the residues of ρ_5

$$\begin{aligned} P_{[12]_{n_1}[34]_{m_1}} &= \text{Res}_{\Delta'' = \Delta_3 + \Delta_4 + 2m_1} \text{Res}_{\Delta' = \Delta_1 + \Delta_2 + 2n_1} \rho_5(\Delta', \Delta''), \\ P_{[12]_{n_2}[125]_{n_2+m_2}} &= \text{Res}_{\Delta'' = \Delta_1 + \Delta_2 + \Delta_5 + 2n_2 + 2m_2} \text{Res}_{\Delta' = \Delta_1 + \Delta_2 + 2n_2} \rho_5(\Delta', \Delta''), \\ P_{[345]_{n_3+m_3}[34]_{m_3}} &= \text{Res}_{\Delta'' = \Delta_3 + \Delta_4 + 2m_3} \text{Res}_{\Delta' = \Delta'' + \Delta_5 + 2n_3} \rho_5(\Delta', \Delta''). \end{aligned} \quad (2.145)$$

Some comments on this block expansion are in order:

- We have exchange of both double-twist and triple-twist operators. Unlike the double-twist operators, of which there is only one of a given dimension, triple-twist operators are degenerate at leading order in $1/N$. Since we have operators of dimension $\Delta_1 + \Delta_2 + \Delta_5 + 2(n + m)$, and we sum over both n and m this means that there are $p + 1$ triple-twist operators of dimension $\Delta_1 + \Delta_2 + \Delta_5 + 2p$.
- Large N counting determines that a connected five-point function has a leading behaviour $\sim 1/N^3$. (One can have factorized three-point \times two-point functions at order $1/N$ but let's ignore those). We can check this large N behaviour in the OPE coefficients. For family 1 we have

$$P_{[12]_{n_1}[34]_{m_1}} = C_{12[12]_{n_1}} C_{[12]_{n_1} 5[34]_{m_1}} C_{[34]_{m_1} 34} \quad (2.146)$$

where the first and last OPE coefficient are the MFT ones, so we are accessing the $1/N^3$ information in $C_{[12]_{n_1} 5[34]_{m_1}}$. For the second family we have

$$P_{[12]_{n_2} [125]_{n_2+m_2}} = C_{12[12]_{n_2}} C_{[12]_{n_2} 5[125]_{n_2+m_2}} C_{[125]_{n_2+m_2} 34}, \quad (2.147)$$

where now the first two OPE coefficients are MFT (although the second one is single-twist/double-twist/triple-twist), and the $1/N^3$ data we are probing is $C_{[125]_{n_2+m_2} 34}$. The third family is similar to the second one.

- For generic dimensions we have an expansion in terms of blocks, however when the exchanged operators in different families have dimensions that differ by an even integer, we find that the OPE coefficients naively diverge. This happens when

$$\Delta_1 + \Delta_2 + \Delta_5 - \Delta_3 - \Delta_4 = 2p \quad \text{or} \quad \Delta_1 + \Delta_2 - \Delta_5 - \Delta_3 - \Delta_4 = 2q \quad (2.148)$$

for some $p, q \in \mathbb{Z}$. By carefully regulating the external dimensions and taking the limit, one finds that the divergences in OPE coefficients cancel, and we get instead derivatives of the blocks with respect to the exchanged dimension. This is the tell-tale sign of anomalous dimensions for the exchanged operators. We will see this explicitly in the D_{11112} example that we will analyze below. Equivalently, we can take the integer separated dimensions at the level of the spectral function, which will then have double poles. Picking their residues also leads to the derivatives of the blocks. In particular, recall that the D functions which admit a closed form expression are the ones where the total dimension is an even integer. This means that either $\Delta_1 + \Delta_2 + \Delta_5$ and $\Delta_3 + \Delta_4$ are both odd or both even. In any case, their difference is an even number, and will therefore satisfy the above condition. Therefore, we learn that explicitly computable D-functions must always contain derivatives of blocks.

2.B.1.1 The case of D_{11112}

The simplest computable (in terms of ladder integrals) five-point D-function is D_{11112} . As argued above, this D-function contains blocks and derivatives of blocks corresponding to anomalous dimensions in its expansion. Following the limiting procedure described in the previous section, the coefficients in the expansion can be read off. We can organize the sum into two integers corresponding to the two exchanged operators. It is actually more convenient to pick the two integers to parametrize the dimension of one of the operators and the difference between the two. We separate the cases with same dimension and positive

difference, since they are qualitatively different. Therefore we write

$$\begin{aligned}
W^{\text{ctc}} = & \sum_{n_1=0}^{\infty} \frac{\Gamma_{2n_1+1} \Gamma_{n_1+1}^2 \Gamma_{-\frac{d}{2}+n_1+2}^2 \Gamma_{-\frac{d}{2}+2n_1+3} \left(1 - \frac{3\delta_{0,n_1}}{4}\right)}{2\pi^{-d/2} \Gamma_{2n_1+2}^2 \Gamma_{-\frac{d}{2}+2n_1+2}^2} G_{2+2n_1, 2+2n_1} \\
& + \sum_{n_1=0, \delta=1}^{\infty} \left(\frac{\pi^{d/2} \delta \Gamma_{n_1+1} \Gamma_{\delta+n_1+1} \Gamma_{\delta+2n_1+1} \Gamma_{-\frac{d}{2}+n_1+2} \Gamma_{-\frac{d}{2}+\delta+n_1+2}}{\Gamma_{-\frac{d}{2}+\delta+2n_1+3}^{-1} \Gamma_{2n_1+2} \Gamma_{-\frac{d}{2}+2n_1+2} \Gamma_{2(\delta+n_1+1)} \Gamma_{2(\delta+n_1+1)-\frac{d}{2}}} \partial_{\Delta_1} G_{2+2(n_1+\delta), 2+2n_1} \right. \\
& \left. + \left[\frac{\delta \left(S_{-\frac{d}{2}+\delta+n_1+1} + S_{-\frac{d}{2}+\delta+2n_1+2} - 2 \left(S_{-\frac{d}{2}+2\delta+2n_1+1} + S_{2\delta+2n_1+1} \right) + S_{\delta+n_1} + S_{\delta+2n_1} \right) + 1}{2\pi^{-d/2} \Gamma_{2n_1+2} \Gamma_{-\frac{d}{2}+2n_1+2} \Gamma_{2(\delta+n_1+1)} \Gamma_{2(\delta+n_1+1)-\frac{d}{2}}} \right. \right. \\
& \left. \left. \Gamma_{n_1+1} \Gamma_{-\frac{d}{2}+n_1+2} \Gamma_{\delta+n_1+1} \Gamma_{\delta+2n_1+1} \Gamma_{-\frac{d}{2}+\delta+n_1+2} \Gamma_{-\frac{d}{2}+\delta+2n_1+3} G_{2+2(n_1+\delta), 2+2n_1} \right] + (\Delta_1 \leftrightarrow \Delta_2) \right),
\end{aligned} \tag{2.149}$$

where we introduced the shorthand notation $\Gamma_a \equiv \Gamma(a)$. Specializing for concreteness to the case $d = 4$ and explicitly writing the block expansion for the first few operators, we have

$$\begin{aligned}
8W^{\text{ctc}} = & 4\pi^2 G_{2,2} - \frac{10}{9}\pi^2 G_{2,4} - \frac{134}{675}\pi^2 G_{2,6} - \frac{10}{9}\pi^2 G_{4,2} + \frac{4}{9}\pi^2 G_{4,4} - \frac{16}{225}\pi^2 G_{4,6} - \frac{134}{675}\pi^2 G_{6,2} \\
& - \frac{16}{225}\pi^2 G_{6,4} + \frac{4}{225}\pi^2 G_{6,6} + \frac{4}{3}\pi^2 G_{2,4}^{(0,1)} + \frac{8}{45}\pi^2 G_{2,6}^{(0,1)} + \frac{2}{15}\pi^2 G_{4,6}^{(0,1)} \\
& + \frac{4}{3}\pi^2 G_{4,2}^{(1,0)} + \frac{8}{45}\pi^2 G_{6,2}^{(1,0)} + \frac{2}{15}\pi^2 G_{6,4}^{(1,0)} + \text{higher dimension operators},
\end{aligned} \tag{2.150}$$

which has the expected left-right symmetry. On the other hand, D_{11112} admits an explicit position space expression in terms of a linear combination of products of rational functions of the five cross-ratios and one-loop ladder functions $\Phi(z, \bar{z})$ with the arguments being all possible five-point cross-ratios. In practice, we have to invert to the variables u, v and use

$$\begin{aligned}
\Phi(u, v) = & \frac{2\text{Li}_2(1-v) + \log(u) \log(v)}{1-v} + \\
& \frac{u(2(v+1)\text{Li}_2(1-v) + \log(u)(-2v + v \log(v) + \log(v) + 2) + 2(v + v \log(v) - 1))}{(1-v)^3} + O(u^2).
\end{aligned} \tag{2.151}$$

Using the radial expansion for the five-point blocks described in [57]

$$G_{\Delta', \Delta''} = \sum_{n', n''} a_{n', n''} s_1^{\Delta'+n'} s_2^{\Delta''+n''} \mathcal{H}_{n', n''}(\chi_1, \chi_2, \chi_3), \tag{2.152}$$

Where $a_{n', n''}$ are kinematically fixed coefficients, s_1, s_2 are radial variables which are small in the double (12)(34) OPE limit and \mathcal{H} is a polynomial in the χ_1, χ_2, χ_3 angular variables,²³

²³We have $2\chi_1 = \xi_1, 2\chi_2 = \xi_3$ and $-2\chi_3 = \xi_1$ in terms of the ξ_i variables introduced in [57].

which are fixed in this limit. As an example we have:

$$G_{2,2} = s_2^2 s_1^2 + s_2^2 s_1^3 \chi_1 - s_2^3 s_1^2 \chi_2 + \frac{1}{3} s_2^2 s_1^4 (4\chi_1^2 - 1) + \frac{1}{2} s_2^3 s_1^3 (\chi_3 - 2\chi_1 \chi_2) + \frac{1}{3} s_2^4 s_1^2 (4\chi_2^2 - 1) + O(s^7). \quad (2.153)$$

Using the explicit blocks and the expression in terms of ladder functions, we can form an expansion in the small s_1, s_2 limit, and we precisely reproduce the block expansion derived through harmonic analysis in the previous section.

2.B.2 Six Points

It is not hard to generalize the previous analysis to the six-point D-function. We will consider the expansion in terms of the snowflake partial wave

$$\Psi_{A,B,C}^{\text{sf}} = \int dx_{7,8,9} \langle \mathcal{O}_1 \mathcal{O}_2 \mathcal{O}_A(x_7) \rangle \langle \mathcal{O}_3 \mathcal{O}_4 \mathcal{O}_B(x_8) \rangle \langle \mathcal{O}_5 \mathcal{O}_6 \mathcal{O}_C(x_9) \rangle \langle \tilde{\mathcal{O}}_A^\dagger(x_7) \tilde{\mathcal{O}}_B^\dagger(x_8) \tilde{\mathcal{O}}_C^\dagger(x_9) \rangle, \quad (2.154)$$

A similar analysis to the five-point case leads to the spectral function

$$\tilde{\rho}_6(c_1, c_2, c_3) = \rho_\delta(c_1) \rho_\delta(c_2) \rho_\delta(c_3) a_{\Delta_1, \Delta_2, h+c_1} a_{\Delta_3, \Delta_4, h+c_2} a_{\Delta_5, \Delta_6, h+c_3} a_{h-c_1, h-c_2, h-c_3}. \quad (2.155)$$

Using the OPE limits discussed in Appendix 2.C, we can then determine the proportionality factor between the partial wave and the block

$$\Psi_{h+c_1, h+c_2, h+c_3}(x_i) = K_{h-c_1}^{h-c_2, h-c_3} K_{h-c_2}^{h+c_1, h-c_3} K_{h-c_3}^{h+c_1, h+c_2} G_{h+c_1, h+c_2, h+c_3}(x_i) + 7 \text{ shadow terms} \quad (2.156)$$

Such that we can represent the six-point function by

$$W^{ctc} = \int [dc_{1,2,3}] \rho_6(c_{1,2,3}) G_{h+c_1, h+c_2, h+c_3}(x_i), \quad (2.157)$$

with

$$\rho_6(c_{1,2,3}) = 8 K_{h-c_1}^{h-c_2, h-c_3} K_{h-c_2}^{h+c_1, h-c_3} K_{h-c_3}^{h+c_1, h+c_2} \tilde{\rho}_6(c_{1,2,3}). \quad (2.158)$$

This spectral function leads to the following families of exchanged operators

- 1: $\Delta_A = \Delta_1 + \Delta_2 + 2n_1, \Delta_B = \Delta_3 + \Delta_4 + 2n_2, \Delta_C = \Delta_5 + \Delta_6 + 2n_3,$ (2.159)
- 2: $\Delta_A = \Delta_3 + \Delta_4 + \Delta_5 + \Delta_6 + 2m_t, \Delta_B = \Delta_3 + \Delta_4 + 2m_2, \Delta_C = \Delta_5 + \Delta_6 + 2m_3,$
- 3: $\Delta_A = \Delta_1 + \Delta_2 + 2p_1, \Delta_B = \Delta_1 + \Delta_2 + \Delta_5 + \Delta_6 + 2p_t, \Delta_C = \Delta_5 + \Delta_6 + 2p_3,$
- 4: $\Delta_A = \Delta_1 + \Delta_2 + 2q_1, \Delta_B = \Delta_3 + \Delta_4 + 2q_2, \Delta_C = \Delta_1 + \Delta_2 + \Delta_3 + \Delta_4 + 2q_t,$

where $m_t = m_1 + m_2 + m_3$ and similarly for the other indices. Note that we identify double- and quadruple-twist operator families in the spectrum.

2.B.2.1 The case of D_{111111}

Once again we consider integer valued D-functions, the simplest of which has all dimensions equal to 1. They are particularly useful in the study of ϕ^3 theory in $6 - \epsilon$ dimensions. On the lightcone (12)(34)(56), the D -function D_{111111} has been computed in [149]. The fact that all dimensions are identical and furthermore integer, leads to the usual degeneracies, and pole collisions, which are responsible for generating derivatives of blocks, and therefore tree level anomalous dimensions.

Note that for poles to collide, we must have that some double-twist operators in family 1 have the same dimension as a quadruple trace operator in families 2,3 or 4. Therefore, the sum of operators naturally organizes in terms of a triangle function. If the three dimensions satisfy the triangle inequality, then there are no pole collisions, and the contributions can only come from family 1. If the triangle inequality is violated by some exchanged operator (and of course this can only happen to one operator at a time), then we must consider the poles in family 1 along with the family who has that operator as a quadruple trace (e.g. if

$\Delta_A \geq \Delta_B + \Delta_C$ then we take family 2). We write

$$\begin{aligned}
W^{\text{ctc}} = & \sum_{n_1, n_2, n_3=0}^{\infty} \frac{\pi^{d/2}}{2} \Gamma_{3-\frac{d}{2}+n_1+n_2+n_3} \prod_{i=1}^3 \frac{\Gamma_{n_i+1} \Gamma_{2-\frac{d}{2}+n_1} \Gamma_{1-n_i+n_j+n_k}}{\Gamma_{2+2n_i} \Gamma_{2-\frac{d}{2}+2n_i}} G_{2+2n_1, 2+2n_2, 2+2n_3} + \\
& + \left(\sum_{n_1, n_2, \delta}^{\infty} \frac{\Gamma_{n_1+1} \Gamma_{n_2+1} \Gamma_{-\frac{d}{2}+n_1+2} \Gamma_{-\frac{d}{2}+n_2+2} \Gamma_{\delta+2n_1+1} \Gamma_{\delta+2n_2+1}}{\Gamma_{2n_1+2} \Gamma_{2n_2+2} \Gamma_{-\frac{d}{2}+2n_1+2} \Gamma_{-\frac{d}{2}+2n_2+2}} \right. \\
& \times \frac{\pi^{d/2} \Gamma_{-\frac{d}{2}+n_t+2} \Gamma_{n_t+1} \Gamma_{-\frac{d}{2}+\delta+2n_1+2n_2+3}}{\Gamma_{\delta} \Gamma_{2(n_t+1)} \Gamma_{-\frac{d}{2}+2n_t+2}} \partial_{\Delta_3} G_{2+2n_1, 2+2n_2, 2+2n_t} + \\
& \sum_{n_1, n_2, \delta}^{\infty} \frac{-\psi_{-\frac{d}{2}-\delta+2n_t+3} - \psi_{-\frac{d}{2}+n_t+2} + 2\psi_{-\frac{d}{2}+2n_t+2} + \psi_{\delta} - \psi_{\delta+2n_1+1} + 2\psi_{2n_t} - \psi_{\delta+2n_2+1} - \psi_{n_t+1}}{\Gamma_{n_2+1}^{-1} \Gamma_{-\frac{d}{2}+n_1+2}^{-1} \Gamma_{-\frac{d}{2}+n_2+2}^{-1} \Gamma_{\delta+2n_1+1}^{-1} \Gamma_{\delta} \Gamma_{2n_1+2} \Gamma_{2n_2+2} \Gamma_{-\frac{d}{2}+2n_1+2} \Gamma_{-\frac{d}{2}+2n_2+2} \Gamma_{2(n_t+1)}} \\
& \times \frac{-\pi^{d/2} \Gamma_{n_1+1} \Gamma_{n_t+1} \Gamma_{-\frac{d}{2}-\delta+2n_t+3}}{2\Gamma_{-\frac{d}{2}+2n_t+2} \Gamma_{\delta+2n_2+1}^{-1} \Gamma_{-\frac{d}{2}+n_t+2}^{-1}} G_{2+2n_1, 2+2n_2, 2+2n_t} + (\Delta_3 \leftrightarrow \Delta_1) + (\Delta_3 \leftrightarrow \Delta_2) \Big) , \\
\end{aligned} \tag{2.160}$$

where $n_t = n_1 + n_2 + \delta$ and $\psi_a = S_a - a^{-1} - \gamma_E$.

2.C Higher-point correlators and Harmonic Analysis

Harmonic analysis of the conformal group leads to the Euclidean inversion formula, which extracts the CFT data from the full correlator. This tool is available even for higher-point functions, but is generically not a useful apparatus for computations. A notable exception is the case of MFT correlators where the inversion can be performed rather explicitly in the case of four-pt functions [150]. In this appendix we derive some of the results needed to generalize this procedure to higher-point functions.

2.C.1 MFT six-point function from Harmonic Analysis

We will study the six-point function of identical real scalar operators ϕ of dimension Δ_ϕ presented previously in (2.81). Before moving on, it is important to point out that depending on the OPE channel (snowflake vs comb), we can have different amounts of identity operator exchanges which must be accounted separately in the conformal partial wave expansion, since they are non-normalizable with respect to the Euclidean inversion formula. To analyze this we recall the definition of the six-point partial waves. The snowflake partial

wave is

$$\Psi_{A,B,C}^{\text{sf},1\dots6,abcd} = \int_{7,8,9} \langle \mathcal{O}_1 \mathcal{O}_2 \mathcal{O}_A(x_7) \rangle^a \langle \mathcal{O}_3 \mathcal{O}_4 \mathcal{O}_B(x_8) \rangle^b \langle \mathcal{O}_5 \mathcal{O}_6 \mathcal{O}_C(x_9) \rangle^c \langle \tilde{\mathcal{O}}_A^\dagger(x_7) \tilde{\mathcal{O}}_B^\dagger(x_8) \tilde{\mathcal{O}}_C^\dagger(x_9) \rangle^d, \quad (2.161)$$

where we introduced the notation $\int_{i,j,\dots} = \int dx_i dx_j \dots$ to make the equations more compact, a, b, c, d are tensor structure labels and the daggers denote the dual representation, meaning the indices of the A, B, C exchanged operators are contracted. We can now identify the problematic identity exchanges. The $12 - 34 - 56$ contraction corresponds to the exchange of three identity operators, which is non-normalizable but can trivially be written as the conventional prefactor times 1. We can also have the exchange of one identity operator and two non-trivial double-twists. This will be the case, for example in the Wick contraction $12 - 35 - 46$. Pulling out the prefactor, we will be able to expand this in a factorized form, as a two-point function times a four-point function, and of course the block expansion of the four-pt function will be the non-trivial, but well-known MFT one. In total, we have one wick contraction with three identities and six with one identity. Below, we will therefore focus on the eight remaining non-trivial ones. On the other hand, we have the comb-channel partial wave:

$$\Psi_{A,B,C}^{c,1\dots6,abcd} = \int_{7,8,9} \langle \mathcal{O}_1 \mathcal{O}_2 \mathcal{O}_A(x_7) \rangle^a \langle \tilde{\mathcal{O}}_A^\dagger(x_7) \mathcal{O}_3 \mathcal{O}_B(x_8) \rangle^b \langle \tilde{\mathcal{O}}_B^\dagger(x_8) \mathcal{O}_4 \mathcal{O}_C(x_9) \rangle^c \langle \tilde{\mathcal{O}}_C^\dagger(x_9) \mathcal{O}_5 \mathcal{O}_6 \rangle^d. \quad (2.162)$$

We can now have two identity exchanges (which is again a factor of 1 with the conventional prefactor choice), or one identity exchange (four choices). We must account for $15 - 34 - 26$ and $16 - 34 - 25$ Wick contractions which exchanged an identity in the snowflake channel, but do not do so in the comb channel. The remaining eight non-trivial contractions are the same as before.

To obtain the OPE coefficients, we will be using the euclidean inversion formula, which amounts to integrating the euclidean correlator multiplied by an appropriate conformal partial wave. This works because of the orthogonality property of partial waves. The appropriate inner product is given by

$$\left(\langle O_1 \dots O_n \rangle, \langle \tilde{O}_1^\dagger \dots \tilde{O}_n^\dagger \rangle \right) = \int \frac{d^d x_1 \dots d^d x_n}{\text{vol SO}(d+1, 1)} \langle O_1 \dots O_n \rangle \langle \tilde{O}_1^\dagger \dots \tilde{O}_n^\dagger \rangle. \quad (2.163)$$

2.C.1.1 Snowflake channel

For the snowflake partial waves we find the orthogonality property

$$\left(\Psi_{ABC}^{\text{sf},1\dots6,abcd}, \Psi_{\tilde{A}'^{\dagger}\tilde{B}'^{\dagger}\tilde{C}'^{\dagger}}^{\text{sf},\tilde{1}^{\dagger}\dots\tilde{6}^{\dagger},efgh} \right) = \frac{\delta_{A,A'}\delta_{B,B'}\delta_{C,C'}}{\mu(\Delta_A, J_A)\mu(\Delta_B, J_B)\mu(\Delta_C, J_C)} \times \\ \left(\langle 12A \rangle^a, \langle \tilde{1}^{\dagger}\tilde{2}^{\dagger}\tilde{A}^{\dagger} \rangle^e \right) \left(\langle 34B \rangle^b, \langle \tilde{3}^{\dagger}\tilde{4}^{\dagger}\tilde{B}^{\dagger} \rangle^f \right) \left(\langle 56C \rangle^c, \langle \tilde{5}^{\dagger}\tilde{6}^{\dagger}\tilde{C}^{\dagger} \rangle^g \right) \left(\langle \tilde{A}^{\dagger}\tilde{B}^{\dagger}\tilde{C}^{\dagger} \rangle^d, \langle ABC \rangle^h \right), \quad (2.164)$$

where $\delta_{X,X'} = 2\pi\delta(\nu_X - \nu_{X'})\delta_{J_X, J_{X'}}$ and we adopted the shorthand notation $X \equiv \mathcal{O}_X$.

The snowflake partial wave expansion is given by

$$\langle \mathcal{O}_1 \dots \mathcal{O}_6 \rangle = \sum_{J_A, J_B, J_C} \int d\nu_A d\nu_B d\nu_C I_{abcd}^{\text{sf}}(\nu_A, J_A, \nu_B, J_B, \nu_C, J_C) \Psi_{A,B,C}^{\text{sf},1\dots6}(x_i), \quad (2.165)$$

and we invert this with the orthogonality relation

$$I^{efgh} \equiv \left(\langle \mathcal{O}_1 \dots \mathcal{O}_6 \rangle, \Psi_{\tilde{A}'^{\dagger}\tilde{B}'^{\dagger}\tilde{C}'^{\dagger}}^{\text{sf},\tilde{1}^{\dagger}\dots\tilde{6}^{\dagger},efgh} \right) = \frac{I_{abcd}^{\text{sf}}(\nu_A, J_A, \nu_B, J_B, \nu_C, J_C)}{\mu(\Delta_A, J_A)\mu(\Delta_B, J_B)\mu(\Delta_C, J_C)} \times \\ \left(\langle 12A \rangle^a, \langle \tilde{1}^{\dagger}\tilde{2}^{\dagger}\tilde{A}^{\dagger} \rangle^e \right) \left(\langle 34B \rangle^b, \langle \tilde{3}^{\dagger}\tilde{4}^{\dagger}\tilde{B}^{\dagger} \rangle^f \right) \left(\langle 56C \rangle^c, \langle \tilde{5}^{\dagger}\tilde{6}^{\dagger}\tilde{C}^{\dagger} \rangle^g \right) \left(\langle \tilde{A}^{\dagger}\tilde{B}^{\dagger}\tilde{C}^{\dagger} \rangle^d, \langle ABC \rangle^h \right) \quad (2.166)$$

Taking identical real scalars $\mathcal{O}_i = \mathcal{O} = \mathcal{O}^{\dagger}$, this reduces the calculation of the spectral function to the calculation of the integral on the left hand side of the above equation, which is given by

$$I^a = \int \frac{dx_{1,\dots,9}}{\text{Vol}} \langle \tilde{\mathcal{O}}(x_1)\tilde{\mathcal{O}}(x_2)\tilde{\mathcal{O}}_A^{\dagger}(x_7) \rangle \langle \tilde{\mathcal{O}}(x_3)\tilde{\mathcal{O}}(x_4)\tilde{\mathcal{O}}_B^{\dagger}(x_8) \rangle \langle \tilde{\mathcal{O}}(x_5)\tilde{\mathcal{O}}(x_6)\tilde{\mathcal{O}}_C^{\dagger}(x_9) \rangle \times \\ \langle \mathcal{O}_A(x_7)\mathcal{O}_B(x_8)\mathcal{O}_C(x_9) \rangle^a \langle \mathcal{O}(x_1) \dots \mathcal{O}(x_6) \rangle_{\text{MFT}}. \quad (2.167)$$

As discussed above, the MFT correlator consists of fifteen triplets of Wick contractions. Clearly, when either of the pairs are 12, 34 or 56, we can integrate one of the variables, and this will shadow transform one of the three-point functions. However, we will then have a three-point function with two coincident points, integrated over this point, which is badly divergent. This is the reason why such contributions are non-normalizable and need to be accounted for separately. Therefore, we henceforth focus on a representative contribution, and the remaining ones can be obtained in an identical manner (in fact some of them give a manifestly equal result). Let us take for concreteness

$\langle \mathcal{O}(x_1)\mathcal{O}(x_3) \rangle \langle \mathcal{O}(x_2)\mathcal{O}(x_5) \rangle \langle \mathcal{O}(x_4)\mathcal{O}(x_6) \rangle \subset \langle \mathcal{O}(x_1) \dots \mathcal{O}(x_6) \rangle_{\text{MFT}}$ Performing the integration over $x_{3,5,6}$ applies shadow transforms on the 3-pt functions:

$$I^a = \int \frac{dx_{1,2,4,7,8,9}}{\text{Vol}} \langle \tilde{\mathcal{O}}(x_1)\tilde{\mathcal{O}}(x_2)\tilde{\mathcal{O}}_A^\dagger(x_7) \rangle \langle S[\tilde{\mathcal{O}}](x_1)\tilde{\mathcal{O}}(x_4)\tilde{\mathcal{O}}_B^\dagger(x_8) \rangle \langle S[\tilde{\mathcal{O}}](x_2)S[\tilde{\mathcal{O}}](x_4)\tilde{\mathcal{O}}_C^\dagger(x_9) \rangle \times \langle \mathcal{O}_A(x_7)\mathcal{O}_B(x_8)\mathcal{O}_C(x_9) \rangle^a, \quad (2.168)$$

with the shadow transform for the scalar defined as

$$\langle S[\mathcal{O}](x) \dots \rangle = \int dy \langle \tilde{\mathcal{O}}(x)\tilde{\mathcal{O}}(y) \rangle \langle \mathcal{O}(y) \dots \rangle. \quad (2.169)$$

We also define the shadow factor for the three-point functions, which is the fundamental building block for the following calculations

$$\langle S[\mathcal{O}]\mathcal{O}_I\mathcal{O}_J \rangle^a = S([\mathcal{O}]\mathcal{O}_I\mathcal{O}_J)_b^a \langle \tilde{\mathcal{O}}\mathcal{O}_I\mathcal{O}_J \rangle^b. \quad (2.170)$$

We can now write the spectral function as

$$I^a = \int \frac{dx_{1,2,4,7,8,9}}{\text{Vol}} \langle \tilde{\mathcal{O}}(x_1)\tilde{\mathcal{O}}(x_2)\tilde{\mathcal{O}}_A^\dagger(x_7) \rangle \langle \mathcal{O}(x_1)\tilde{\mathcal{O}}(x_4)\tilde{\mathcal{O}}_B^\dagger(x_8) \rangle \langle \mathcal{O}(x_2)\mathcal{O}(x_4)\tilde{\mathcal{O}}_C^\dagger(x_9) \rangle \times S([\tilde{\mathcal{O}}]\tilde{\mathcal{O}}\tilde{\mathcal{O}}_C^\dagger)S(\mathcal{O}[\tilde{\mathcal{O}}]\tilde{\mathcal{O}}_C^\dagger)S([\tilde{\mathcal{O}}]\tilde{\mathcal{O}}\tilde{\mathcal{O}}_B^\dagger) \langle \mathcal{O}_A(x_7)\mathcal{O}_B(x_8)\mathcal{O}_C(x_9) \rangle^a. \quad (2.171)$$

Let us make a few comments. First note that there is some freedom in choosing what operators we actually shadow transform, and in the case where we transform two in the same three-point function, we can also choose the order. This leads to apparently different expressions, which presumably give the same result in the end. We should also point out that independently of these choices, the shadow factors only include one spinning operator and are therefore known in closed form for any J and d . Additionally, it is clear that each three-point function has exactly one point in common with the other ones, and therefore the position space integrals remain non-trivial.

To address this, we note that an integral of two three-point functions integrated by a common point is just a four-point partial wave, which admits well-known crossing relations, whose kernel are the $6j$ symbols of the conformal group. There is now some freedom in choosing over what integration point to perform crossing. Crossing over the scalar corresponds to a $6j$ symbol with three spinning operators. Crossing over a spinning one

will lead to a similar result. Let us first define the $6j$ symbol²⁴ through the crossing relation

$$\Psi_{\Delta', J'}^{3214, ab}(x_3, x_2, x_1, x_4) = \sum_J \int [d\Delta] \left\{ \begin{array}{ccc} [\Delta_1, J_1] & [\Delta_2, J_2] & [\Delta', J'] \\ [\Delta_3, J_3] & [\Delta_4, J_4] & [\Delta, J] \end{array} \right\}^{abcd} \Psi_{\Delta, J}^{1234, cd}(x_1, x_2, x_3, x_4). \quad (2.172)$$

Let us cross through the scalar at x_4 using

$$\int dx_4 \langle \tilde{\mathcal{O}}_C^\dagger(x_9) \mathcal{O}(x_2) \mathcal{O}(x_4) \rangle \langle \tilde{\mathcal{O}}(x_4) \mathcal{O}(x_1) \tilde{\mathcal{O}}_B^\dagger(x_8) \rangle = \sum_{J'} \int [d\Delta'] \left\{ \begin{array}{ccc} \Delta & \Delta & \Delta \\ [\tilde{\Delta}_C, J_C] & [\tilde{\Delta}_B, J_B] & [\Delta', J'] \end{array} \right\}^b \int dx_4 \langle \mathcal{O}(x_1) \mathcal{O}(x_2) \mathcal{O}'(x_4) \rangle \langle \tilde{\mathcal{O}}'^\dagger(x_4) \tilde{\mathcal{O}}_C^\dagger(x_9) \tilde{\mathcal{O}}_B^\dagger(x_8) \rangle^b. \quad (2.173)$$

With this, we can easily perform the x_1, x_2 integrals using the bubble integral formula

$$\int dx_{1,2} \langle \tilde{\mathcal{O}}(x_1) \tilde{\mathcal{O}}(x_2) \tilde{\mathcal{O}}_A^\dagger(x_7) \rangle \langle \mathcal{O}(x_1) \mathcal{O}(x_2) \mathcal{O}'(x_4) \rangle = \frac{\delta_{A, \mathcal{O}'}}{\mu(\Delta_A, J_A)} \delta(x_{74}) \left(\langle \tilde{\mathcal{O}} \tilde{\mathcal{O}} \tilde{\mathcal{O}}_A^\dagger \rangle, \langle \mathcal{O} \mathcal{O} \mathcal{O}_A \rangle \right). \quad (2.174)$$

The delta function between operators \mathcal{O}_A and \mathcal{O}' removes the auxiliary spectral integral, and the position space delta function gives a final pairing between A, B, C three-point functions. Collecting everything, we obtain

$$I^a = S([\tilde{\mathcal{O}}] \tilde{\mathcal{O}} \tilde{\mathcal{O}}_C^\dagger) S(\mathcal{O} [\tilde{\mathcal{O}}] \tilde{\mathcal{O}}_C^\dagger) S([\tilde{\mathcal{O}}] \tilde{\mathcal{O}} \tilde{\mathcal{O}}_B^\dagger) \left\{ \begin{array}{ccc} \Delta & \Delta & \Delta \\ [\tilde{\Delta}_C, J_C] & [\tilde{\Delta}_B, J_B] & [\Delta_A, J_A] \end{array} \right\}^b \times \frac{\left(\langle \tilde{\mathcal{O}} \tilde{\mathcal{O}} \tilde{\mathcal{O}}_A^\dagger \rangle, \langle \mathcal{O} \mathcal{O} \mathcal{O}_A \rangle \right)}{\mu(\Delta_A, J_A)} \left(\langle \tilde{\mathcal{O}}_A^\dagger \tilde{\mathcal{O}}_B^\dagger \tilde{\mathcal{O}}_C^\dagger \rangle^b, \langle \mathcal{O}_A \mathcal{O}_B \mathcal{O}_C \rangle^a \right). \quad (2.175)$$

Note that we have a $6j$ symbol with three spinning operators. When one or two of these operators are scalars, this should be related to well-known $6j$ symbols through the tetrahedral S_4 symmetry. Otherwise, this is a non-trivial object to be obtained either through weight-shifting operators, or more directly from the Euclidean inversion formula applied to the cross-channel partial wave with the appropriate tensor structures.

²⁴Our convention for the $6j$ symbol differs from others in the literature by a normalization factor.

2.C.1.2 Comb channel

In the comb channel we have slight modifications to the orthogonality properties. The orthogonality relation now reads

$$\begin{aligned} \left(\Psi_{ABC}^{c,1\dots 6,abcd}, \Psi_{\tilde{A}'^\dagger \tilde{B}'^\dagger \tilde{C}'^\dagger}^{c,\tilde{1}^\dagger\dots \tilde{6}^\dagger,efgh} \right) &= \frac{\delta_{A,A'}\delta_{B,B'}\delta_{C,C'}}{\mu(\Delta_A, J_A)\mu(\Delta_B, J_B)\mu(\Delta_C, J_C)} \times \\ &\left(\langle 12A \rangle^a, \langle \tilde{1}^\dagger \tilde{2}^\dagger \tilde{A}^\dagger \rangle^e \right) \left(\langle \tilde{A}^\dagger 3B \rangle^b, \langle A \tilde{3}^\dagger \tilde{B}^\dagger \rangle^f \right) \left(\langle \tilde{B}^\dagger 4C \rangle^c, \langle B \tilde{4}^\dagger \tilde{C}^\dagger \rangle^g \right) \left(\langle \tilde{C}^\dagger 56 \rangle^d, \langle C \tilde{5}^\dagger \tilde{6}^\dagger \rangle^h \right), \end{aligned} \quad (2.176)$$

from which the spectral function now follows from the Euclidean inversion integral

$$\begin{aligned} I^{efgh} \equiv \left(\langle \mathcal{O}_1 \dots \mathcal{O}_6 \rangle, \Psi_{\tilde{A}'^\dagger \tilde{B}'^\dagger \tilde{C}'^\dagger}^{c,\tilde{1}^\dagger\dots \tilde{6}^\dagger,efgh} \right) &= \frac{I_{abcd}^c(\nu_A, J_A, \nu_B, J_B, \nu_C, J_C)}{\mu(\Delta_A, J_A)\mu(\Delta_B, J_B)\mu(\Delta_C, J_C)} \times \\ &\left(\langle 12A \rangle^a, \langle \tilde{1}^\dagger \tilde{2}^\dagger \tilde{A}^\dagger \rangle^e \right) \left(\langle \tilde{A}^\dagger 3B \rangle^b, \langle A \tilde{3}^\dagger \tilde{B}^\dagger \rangle^f \right) \left(\langle \tilde{B}^\dagger 4C \rangle^c, \langle B \tilde{4}^\dagger \tilde{C}^\dagger \rangle^g \right) \left(\langle \tilde{C}^\dagger 56 \rangle^d, \langle C \tilde{5}^\dagger \tilde{6}^\dagger \rangle^h \right), \end{aligned} \quad (2.177)$$

Once again, we specialize to the case of identical external scalars \mathcal{O} , such that the spectral function can be obtained from the integral

$$\begin{aligned} I^{ab} = \int \frac{dx_{1,\dots,9}}{\text{Vol}} \langle \tilde{\mathcal{O}}(x_1) \tilde{\mathcal{O}}(x_2) \tilde{\mathcal{O}}_A^\dagger(x_7) \rangle \langle \mathcal{O}_A(x_7) \tilde{\mathcal{O}}(x_3) \tilde{\mathcal{O}}_B^\dagger(x_8) \rangle^a \langle \mathcal{O}_B(x_8) \tilde{\mathcal{O}}(x_4) \tilde{\mathcal{O}}_C^\dagger(x_9) \rangle^b \times \\ \langle \mathcal{O}_C(x_9) \tilde{\mathcal{O}}(x_5) \tilde{\mathcal{O}}(x_6) \rangle \langle \mathcal{O}(x_1) \dots \mathcal{O}(x_6) \rangle_{\text{MFT}}. \end{aligned} \quad (2.178)$$

34 Identity

As discussed above, in the Comb channel there are two qualitatively different types of terms without an identity exchange. The non-trivial contractions in the snowflake channel are also non-trivial in the comb channel. However, the $\langle \mathcal{O}(x_3) \mathcal{O}(x_4) \rangle$ Wick contraction, which is an identity exchange in the snowflake OPE, now becomes a non-trivial contribution. Let us take the $15 - 34 - 26$ contraction. This gives a contribution

$$\begin{aligned} I^{ab} \supset \int \frac{dx_{1,2,3,7,8,9}}{\text{Vol}} \langle \tilde{\mathcal{O}}(x_1) \tilde{\mathcal{O}}(x_2) \tilde{\mathcal{O}}_A^\dagger(x_7) \rangle \langle \mathcal{O}_A(x_7) \tilde{\mathcal{O}}(x_3) \tilde{\mathcal{O}}_B^\dagger(x_8) \rangle^a \langle \mathcal{O}_B(x_8) S[\tilde{\mathcal{O}}](x_3) \tilde{\mathcal{O}}_C^\dagger(x_9) \rangle^b \times \\ \langle \mathcal{O}_C(x_9) S[\tilde{\mathcal{O}}](x_1) S[\tilde{\mathcal{O}}](x_2) \rangle. \end{aligned} \quad (2.179)$$

Note that there is again a lot of freedom in what operator to take the shadow transform, and in the subsequent steps. However, it is unavoidable to obtain a shadow transform on a three-point function with two spinning operators, which gives a complicated (matrix)

shadow factor

$$I^{ab} \supset \int \frac{dx_{1,2,3,7,8,9}}{\text{Vol}} \langle \tilde{\mathcal{O}}(x_1) \tilde{\mathcal{O}}(x_2) \tilde{\mathcal{O}}_A^\dagger(x_7) \rangle \langle \mathcal{O}_A(x_7) \tilde{\mathcal{O}}(x_3) \tilde{\mathcal{O}}_B^\dagger(x_8) \rangle^a \langle \mathcal{O}_B(x_8) \mathcal{O}(x_3) \tilde{\mathcal{O}}_C^\dagger(x_9) \rangle^c \times \\ S(\mathcal{O}_C[\tilde{\mathcal{O}}] \tilde{\mathcal{O}}) S(\mathcal{O}_C \mathcal{O}[\tilde{\mathcal{O}}]) S(\mathcal{O}_B[\tilde{\mathcal{O}}] \tilde{\mathcal{O}}_C)^b{}_c \langle \mathcal{O}_C(x_9) \mathcal{O}(x_1) \mathcal{O}(x_2) \rangle. \quad (2.180)$$

We can now apply the bubble integral formula for the $x_{1,2}$ integrals. This imposes a delta function between operators A and C , and also on their positions, $x_7 - x_9$. In the end, we obtain

$$I^{ab} \supset \frac{\delta_{A,C}}{\mu(\Delta_A, J_A)} S(\mathcal{O}_C[\tilde{\mathcal{O}}] \tilde{\mathcal{O}}) S(\mathcal{O}_C \mathcal{O}[\tilde{\mathcal{O}}]) S(\mathcal{O}_B[\tilde{\mathcal{O}}] \tilde{\mathcal{O}}_C)^b{}_c \left(\langle \tilde{\mathcal{O}} \tilde{\mathcal{O}} \tilde{\mathcal{O}}_A \rangle, \langle \mathcal{O}_A \mathcal{O} \mathcal{O} \rangle \right) \times \\ \left(\langle \mathcal{O}_A \tilde{\mathcal{O}} \tilde{\mathcal{O}}_B \rangle^a, \langle \mathcal{O}_B \mathcal{O} \tilde{\mathcal{O}}_A \rangle^c \right). \quad (2.181)$$

We again emphasize that this depends on a non-trivial shadow factor.

Non-trivial contractions: one point in common

Now, we have to consider again the eight non-trivial Wick contractions, which contain no identity operators in any channel. There are two further classes of Wick contractions, ones which will induce two common points between two pairs of three-point functions, and ones where all three-point functions will have one point in common with each other. A representative example of the second type is the Wick contraction 14 – 25 – 36. Its contribution to the spectral function is given by

$$I^{ab} \supset \int \frac{dx_{1,\dots,9}}{\text{Vol}} \langle \tilde{\mathcal{O}}(x_1) \tilde{\mathcal{O}}(x_2) \tilde{\mathcal{O}}_A^\dagger(x_7) \rangle \langle \mathcal{O}_A(x_7) \tilde{\mathcal{O}}(x_3) \tilde{\mathcal{O}}_B^\dagger(x_8) \rangle^a \langle \mathcal{O}_B(x_8) \tilde{\mathcal{O}}(x_4) \tilde{\mathcal{O}}_C^\dagger(x_9) \rangle^b \times \\ \langle \mathcal{O}_C(x_9) \tilde{\mathcal{O}}(x_5) \tilde{\mathcal{O}}(x_6) \rangle \langle \mathcal{O}(x_1) \mathcal{O}(x_4) \rangle \langle \mathcal{O}(x_2) \mathcal{O}(x_5) \rangle \langle \mathcal{O}(x_3) \mathcal{O}(x_6) \rangle. \quad (2.182)$$

As usual we have some freedom in what operators to shadow transform. In this case, this is particularly relevant, since out of the three shadow factors, we can have either zero, one or two "difficult" shadow factors, depending on what operators we transform. Sticking to the easiest possibility, we inevitably get only one common point per three-point function, which means that once again we need to use crossing relations or $6j$ symbols to proceed with the position space integrals. It is convenient to cross through $\mathcal{O}_A(x_7)$ and then do

the $x_{2,3}$ integrals using the bubble formula. In the end we get

$$I^{ab} \supset \left\{ \begin{array}{ccc} \Delta & [\tilde{\Delta}_B, J_B] & [\Delta_A, J_A] \\ \tilde{\Delta} & \tilde{\Delta} & [\Delta_C, J_C] \end{array} \right\}^{ac} S([\tilde{\mathcal{O}}]\tilde{\mathcal{O}}\tilde{\mathcal{O}}_A)S(\mathcal{O}_C[\tilde{\mathcal{O}}]\tilde{\mathcal{O}})S(\mathcal{O}_C\mathcal{O}[\tilde{\mathcal{O}}]) \times \frac{(\langle \tilde{\mathcal{O}}\tilde{\mathcal{O}}\tilde{\mathcal{O}}_C^\dagger \rangle, \langle \mathcal{O}\mathcal{O}\mathcal{O}_C \rangle)}{\mu(\Delta_C, J_C)} \left(\langle \mathcal{O}\tilde{\mathcal{O}}_B^\dagger \mathcal{O}_C \rangle^c, \langle \tilde{\mathcal{O}}\mathcal{O}_B \tilde{\mathcal{O}}_C^\dagger \rangle^b \right) \quad (2.183)$$

There is just one more class of Wick contractions to analyze.

Non-trivial contractions: two points in common

We can also have two-point functions connecting the adjacent three-point functions of the partial wave. A representative example for this case is the Wick contraction 16 – 23 – 45. The contribution to the spectral function is given by

$$I^{ab} \supset \int \frac{dx_{1,\dots,9}}{\text{Vol}} \langle \tilde{\mathcal{O}}(x_1)\tilde{\mathcal{O}}(x_2)\tilde{\mathcal{O}}_A^\dagger(x_7) \rangle \langle \mathcal{O}_A(x_7)\tilde{\mathcal{O}}(x_3)\tilde{\mathcal{O}}_B^\dagger(x_8) \rangle^a \langle \mathcal{O}_B(x_8)\tilde{\mathcal{O}}(x_4)\tilde{\mathcal{O}}_C^\dagger(x_9) \rangle^b \times \langle \mathcal{O}_C(x_9)\tilde{\mathcal{O}}(x_5)\tilde{\mathcal{O}}(x_6) \rangle \langle \mathcal{O}(x_1)\mathcal{O}(x_6) \rangle \langle \mathcal{O}(x_2)\mathcal{O}(x_3) \rangle \langle \mathcal{O}(x_4)\mathcal{O}(x_5) \rangle. \quad (2.184)$$

Once again, we have the freedom to perform the shadow transforms, and we can get either zero, one or two hard factors. Let us get all simple factors by making the choice

$$I^{ab} \supset \int \frac{dx_{1,\dots,9}}{\text{Vol}} \langle \tilde{\mathcal{O}}(x_1)\mathcal{O}(x_3)\tilde{\mathcal{O}}_A^\dagger(x_7) \rangle \langle \mathcal{O}_A(x_7)\tilde{\mathcal{O}}(x_3)\tilde{\mathcal{O}}_B^\dagger(x_8) \rangle^a \langle \mathcal{O}_B(x_8)\tilde{\mathcal{O}}(x_4)\tilde{\mathcal{O}}_C^\dagger(x_9) \rangle^b \times S(\mathcal{O}_C[\tilde{\mathcal{O}}])S(\mathcal{O}_C\mathcal{O}[\tilde{\mathcal{O}}])S(\tilde{\mathcal{O}}[\tilde{\mathcal{O}}]\tilde{\mathcal{O}}_A) \langle \mathcal{O}_C(x_9)\mathcal{O}(x_4)\mathcal{O}(x_1) \rangle. \quad (2.185)$$

There are now two possible approaches. We can try to do, for example the x_3, x_7 integrals, which would involve a bubble integral with a spinning operator integrated over

$$\int_{3,7} \langle \tilde{\mathcal{O}}(x_1)\mathcal{O}(x_3)\tilde{\mathcal{O}}_A^\dagger(x_7) \rangle \langle \mathcal{O}_A(x_7)\tilde{\mathcal{O}}(x_3)\tilde{\mathcal{O}}_B^\dagger(x_8) \rangle^a = \frac{\delta_{\tilde{\mathcal{O}}_B, \mathcal{O}} \delta(x_1 - x_8)}{\mu(\Delta, 0)} \left(\langle \tilde{\mathcal{O}}\mathcal{O}\tilde{\mathcal{O}}_A \rangle, \langle \mathcal{O}\tilde{\mathcal{O}}\mathcal{O}_A \rangle \right). \quad (2.186)$$

This would mean that the operator exchanged at $\mathcal{O}_B(x_8)$ would need to be the same as the external operator. It is not hard to argue that this is possible in MFT. We are then able to do the final three-point pairing and obtain

$$I \supset S(\mathcal{O}_C[\tilde{\mathcal{O}}])S(\mathcal{O}_C\mathcal{O}[\tilde{\mathcal{O}}])S(\tilde{\mathcal{O}}[\tilde{\mathcal{O}}]\tilde{\mathcal{O}}_A) \frac{(\langle \tilde{\mathcal{O}}\mathcal{O}\tilde{\mathcal{O}}_A \rangle, \langle \mathcal{O}\tilde{\mathcal{O}}\mathcal{O}_A \rangle)}{\mu(\Delta, 0)} \left(\langle \tilde{\mathcal{O}}\tilde{\mathcal{O}}\tilde{\mathcal{O}}_C \rangle, \langle \mathcal{O}\mathcal{O}\mathcal{O}_C \rangle \right). \quad (2.187)$$

Note that the tensor structure indices went away, since \mathcal{O}_B became a scalar operator, and therefore all tensor structures became unique.

2.C.2 Partial wave decompositon and conformal blocks

In the previous section we formally derived the partial wave decomposition of MFT six-point functions. However, to obtain the actual CFT data, we need to write down the conformal block decomposition and read-off the OPE coefficients. In this subsection, we establish a relation between the partial wave decomposition and the conformal block expansion. We quickly review the case of the four-point function which can be expanded in partial waves as

$$\langle \mathcal{O}_1 \mathcal{O}_2 \mathcal{O}_3 \mathcal{O}_4 \rangle = \sum_{\rho} \int_{\frac{d}{2}}^{\frac{d}{2}+i\infty} \frac{d\Delta}{2\pi i} I_{ab}(\Delta, \rho) \Psi_{\mathcal{O}}^{\mathcal{O}_i(ab)}(x_i) + \text{discrete}. \quad (2.188)$$

Here discrete is associated with possible additional isolated contributions, notably including the identity. The partial wave is defined in terms of a conformally-invariant integral involving two three-point structures

$$\Psi_{\mathcal{O}}^{\mathcal{O}_i(ab)}(x_i) = \int d^d x \langle \mathcal{O}_1 \mathcal{O}_2 \mathcal{O}(x) \rangle^{(a)} \langle \mathcal{O}_3 \mathcal{O}_4 \tilde{\mathcal{O}}^\dagger(x) \rangle^{(b)}. \quad (2.189)$$

In order to relate the partial wave decomposition to conformal blocks we follow the strategy of [150]. The partial wave in (2.189) is a solution of the Casimir equation and therefore one can establish its relation to conformal blocks by uniquely estimating its form in the OPE limit $x_1 \rightarrow x_2$. Obviously the Euclidean OPE limit cannot be taken simply inside the integral as the integrand probes regions where the OPE in the pair (12) is no longer valid. However, understanding the leading behaviour outside this region is enough to match those contributions to a given conformal block. For concreteness, consider the replacement

$$\langle \mathcal{O}_1 \mathcal{O}_2 \mathcal{O}(x) \rangle^{(a)} \rightarrow C_{12\mathcal{O}}^{(a)} \langle \mathcal{O}^\dagger(x_2) \mathcal{O}(x) \rangle, \quad (2.190)$$

where $C_{12\mathcal{O}}^{(a)}$ encodes leading terms in the OPE $\mathcal{O}_1 \times \mathcal{O}_2$. With this replacement the integral in (2.189) becomes a shadow transform of $\tilde{\mathcal{O}}^\dagger$,

$$\Psi_{\mathcal{O}}^{\mathcal{O}_i(ab)} \sim C_{12\mathcal{O}}^{(a)} \langle \mathcal{O}_3 \mathcal{O}_4 \mathbf{S}[\tilde{\mathcal{O}}^\dagger] \rangle^{(b)} = S(\mathcal{O}_3 \mathcal{O}_4 [\tilde{\mathcal{O}}^\dagger])_c^b C_{12\mathcal{O}}^{(a)} \langle \mathcal{O}_3 \mathcal{O}_4 \mathcal{O}^\dagger \rangle^{(c)}. \quad (2.191)$$

On the other hand, the conformal block $G_{\mathcal{O}}^{(ab)}$ is a solution of the Casimir equation, which in the OPE limit of $\mathcal{O}_1 \times \mathcal{O}_2$ behaves as

$$G_{\mathcal{O}}^{(ab)} \sim C_{12\mathcal{O}}^{(a)} \langle \mathcal{O}_3 \mathcal{O}_4 \mathcal{O}^\dagger \rangle^{(b)}, \quad (x_1 \rightarrow x_2). \quad (2.192)$$

It is thus clear that the partial wave must contain a term

$$\Psi_{\mathcal{O}}^{\mathcal{O}_i(ab)} \supset S(\mathcal{O}_3 \mathcal{O}_4 [\tilde{\mathcal{O}}^\dagger])_c^b G_{\mathcal{O}}^{(ac)}. \quad (2.193)$$

Similarly, if one performs an OPE on $\mathcal{O}_3 \times \mathcal{O}_4$ instead, it is straightforward to show that the partial wave contains a term

$$\Psi_{\mathcal{O}}^{\mathcal{O}_i(ab)} \supset S(\mathcal{O}_1 \mathcal{O}_2 [\mathcal{O}])_c^a G_{\tilde{\mathcal{O}}}^{(cb)}. \quad (2.194)$$

Putting everything together we conclude that

$$\Psi_{\mathcal{O}}^{\mathcal{O}_i(ab)} = S(\mathcal{O}_3 \mathcal{O}_4 [\tilde{\mathcal{O}}^\dagger])_c^b G_{\mathcal{O}}^{(ac)} + S(\mathcal{O}_1 \mathcal{O}_2 [\mathcal{O}])_c^a G_{\tilde{\mathcal{O}}}^{(cb)}, \quad (2.195)$$

which reflects the fact that the Casimir equation is invariant under $\Delta \rightarrow d - \Delta$. Inserting this relation on (2.188), extending the integration region along the entire imaginary axis and using shadow symmetry, allows us to write

$$\langle \mathcal{O}_1 \dots \mathcal{O}_4 \rangle = \sum_{\rho} \int_{\frac{d}{2}-i\infty}^{\frac{d}{2}+i\infty} \frac{d\Delta}{2\pi i} C_{ac}(\Delta, \rho) G_{\mathcal{O}}^{(ac)}, \quad (2.196)$$

where $C_{ac}(\Delta, \rho) \equiv I_{ab}(\Delta, \rho) S(\mathcal{O}_3 \mathcal{O}_4 [\tilde{\mathcal{O}}^\dagger])_c^b$. As usual we can then deform the contour integration away from the principal series and pick up poles of $C_{ac}(\Delta, \rho)$ on the real line, which have residues that encode CFT data. For a particular exchanged operator \mathcal{O}_* , we have

$$C_{12*} C_{34*} = -\text{Res}_{\Delta=\Delta_*} C(\Delta, \rho_*). \quad (2.197)$$

This formalism can straightforwardly be adapted to the case of higher-point functions. For five-point functions, the discussion has already been presented in [49], but we also review it here. We consider the partial wave

$$\Psi_{A,B}^{\mathcal{O}_i(abc)}(x_i) = \int d^d x_A d^d x_B \langle \mathcal{O}_1 \mathcal{O}_2 \mathcal{O}_A \rangle^{(a)} \langle \tilde{\mathcal{O}}_A^\dagger \mathcal{O}_5 \tilde{\mathcal{O}}_B^\dagger \rangle^{(b)} \langle \mathcal{O}_B \mathcal{O}_3 \mathcal{O}_4 \rangle^{(c)} \quad (2.198)$$

where $\mathcal{O}_{A,B}$ are exchanged operators. A five-point function can be decomposed in terms of this partial wave

$$\langle \mathcal{O}_1 \dots \mathcal{O}_5 \rangle = \sum_{\rho_A, \rho_B} \int_{\frac{d}{2}}^{\frac{d}{2}+i\infty} \frac{d\Delta_A}{2\pi i} \int_{\frac{d}{2}}^{\frac{d}{2}+i\infty} \frac{d\Delta_B}{2\pi i} I_{abc}(\Delta_A, \rho_A; \Delta_B, \rho_B) \Psi_{A,B}^{\mathcal{O}_i(abc)}(x_i). \quad (2.199)$$

To expand this partial wave in terms of conformal blocks we again consider OPE limits. In particular, we take $x_1 \rightarrow x_2$ and $x_3 \rightarrow x_4$ at the level of the integrand and we observe

that the partial wave must contain the term

$$\Psi_{A,B}^{\mathcal{O}_i(abc)}(x_i) \supset C_{12A}^{(a)} C_{34B}^{(c)} \langle \mathbf{S}[\tilde{\mathcal{O}}_A^\dagger] \mathcal{O}_5 \mathbf{S}[\tilde{\mathcal{O}}_B^\dagger] \rangle^{(b)} = (S_A^{5\tilde{B}})_d^b (S_{\tilde{B}}^{A5})_e^d \underbrace{C_{12A}^{(a)} C_{34B}^{(c)} \langle \mathcal{O}_A^\dagger \mathcal{O}_5 \mathcal{O}_B^\dagger \rangle^{(e)}}_{\propto G_{AB}^{(aec)}}, \quad (2.200)$$

where we have used the shorthand notation $S_A^{BC} = S([\mathcal{O}_A] \mathcal{O}_B \mathcal{O}_C)$ and recognized the leading behaviour of the conformal block $G_{AB}^{(aec)}$ in the OPE limits $x_1 \rightarrow x_2$ and $x_3 \rightarrow x_4$. As above, we notice that the partial wave $\Psi_{A,B}^{\mathcal{O}_i(abc)}(x_i)$ is a solution of the Casimir equations, one for each OPE exchange, and therefore it enjoys the invariance $\Delta \leftrightarrow d - \Delta$. We can then propose the decomposition

$$\Psi_{A,B}^{\mathcal{O}_i}(x_i) = R_1 G_{AB}(x_i) + R_2 G_{\tilde{A}\tilde{B}}(x_i) + R_3 G_{A\tilde{B}}(x_i) + R_4 G_{\tilde{A}B}(x_i), \quad (2.201)$$

where, as we have seen, $R_1^a = (S_A^{5\tilde{B}})_c^a (S_{\tilde{B}}^{A5})_b^c$. In order to find the remaining R_i 's we explore the symmetry of the partial wave:

$$\begin{aligned} \Psi_{A,B}^{\mathcal{O}_i(abc)}(x_i) &= \int d^d x_A d^d x_B \langle \mathcal{O}_1 \mathcal{O}_2 \mathcal{O}_A \rangle^{(a)} \langle \tilde{\mathcal{O}}_A^\dagger \mathcal{O}_5 \tilde{\mathcal{O}}_B^\dagger \rangle^{(b)} \langle \mathcal{O}_B \mathcal{O}_3 \mathcal{O}_4 \rangle^{(c)} \\ &= \int d^d x_A d^d x'_A d^d x_B ((S_A^{5\tilde{B}})^{-1})_d^b \langle \mathcal{O}_1 \mathcal{O}_2 \mathcal{O}_A \rangle^{(a)} \langle \tilde{\mathcal{O}}_A^\dagger \tilde{\mathcal{O}}_{A'} \rangle \langle \mathcal{O}_{A'}^\dagger \mathcal{O}_5 \tilde{\mathcal{O}}_B^\dagger \rangle^{(d)} \langle \mathcal{O}_B \mathcal{O}_3 \mathcal{O}_4 \rangle^{(c)} \\ &= \int d^d x_A d^d x_B (S_A^{12})_d^a ((S_A^{5\tilde{B}})^{-1})_e^b \langle \mathcal{O}_1 \mathcal{O}_2 \tilde{\mathcal{O}}_A \rangle^{(d)} \langle \mathcal{O}_A^\dagger \mathcal{O}_5 \tilde{\mathcal{O}}_B^\dagger \rangle^{(e)} \langle \mathcal{O}_B \mathcal{O}_3 \mathcal{O}_4 \rangle^{(c)} \\ &= (S_A^{12})_d^a ((S_A^{5\tilde{B}})^{-1})_e^b \Psi_{\tilde{A},B}^{\mathcal{O}_i(dec)}(x_i). \end{aligned} \quad (2.202)$$

Performing an OPE expansion on the $\Psi_{\tilde{A},B}^{\mathcal{O}_i(abc)}(x_i)$, we observe

$$\Psi_{\tilde{A},B}^{\mathcal{O}_i(abc)}(x_i) \supset (S_A^{5\tilde{B}})_d^b (S_{\tilde{B}}^{A5})_e^d G_{\tilde{A}B}^{(aec)}(x_i), \quad (2.203)$$

from which follows that

$$R_2^{ab} = (S_A^{12})_d^a (S_{\tilde{B}}^{A5})_e^b. \quad (2.204)$$

Similarly, one can show that

$$R_3 = S_{\tilde{A}}^{5\tilde{B}} S_B^{34}, \quad R_4 = S_A^{12} S_B^{34}. \quad (2.205)$$

Just as we have shown in the 4-point case, one can use the shadow symmetry of I_{abc} to extend the region of integration such that

$$\langle \mathcal{O}_1 \dots \mathcal{O}_5 \rangle = \sum_{\rho_A, \rho_B} \int_{\frac{d}{2}-i\infty}^{\frac{d}{2}+i\infty} \frac{d\Delta_A}{2\pi i} \int_{\frac{d}{2}-i\infty}^{\frac{d}{2}+i\infty} \frac{d\Delta_B}{2\pi i} I_{abc}(\Delta_A, \rho_A; \Delta_B, \rho_B) (S_A^{5\tilde{B}})_d^b (S_{\tilde{B}}^{A5})_e^d G_{AB}^{aec}. \quad (2.206)$$

The exact same techniques can be applied to six-point functions. Here, we focus on the snowflake decomposition which admits the partial wave expansion (2.165), where the snowflake partial wave is defined in (2.161). In a completely analogous procedure as discussed above, we can relate this partial wave to conformal blocks. In particular, from the shadow invariance of the Casimir equations it is natural to expand the partial wave as

$$\begin{aligned} \Psi_{A,B,C}^{\mathcal{O}_i}(x_i) = & R_1 G_{ABC} + R_2 G_{\tilde{A}BC} + R_3 G_{A\tilde{B}C} + R_4 G_{AB\tilde{C}} \\ & + R_5 G_{\tilde{A}\tilde{B}C} + R_6 G_{A\tilde{B}\tilde{C}} + R_7 G_{\tilde{A}B\tilde{C}} + R_8 G_{\tilde{A}\tilde{B}\tilde{C}}, \end{aligned} \quad (2.207)$$

where

$$\begin{aligned} R_1 &= S_A^{\tilde{B}\tilde{C}} S_B^{A\tilde{C}} S_C^{AB}, \quad R_2 = S_A^{12} S_B^{\tilde{A}\tilde{C}} S_C^{\tilde{A}B}, \quad R_3 = S_B^{34} S_A^{\tilde{B}\tilde{C}} S_C^{A\tilde{B}}, \quad R_4 = S_C^{56} S_A^{\tilde{B}\tilde{C}} S_B^{A\tilde{C}}, \\ R_5 &= S_A^{12} S_B^{34} S_C^{\tilde{A}\tilde{B}}, \quad R_6 = S_B^{34} S_C^{56} S_A^{\tilde{B}\tilde{C}}, \quad R_7 = S_A^{12} S_C^{56} S_B^{\tilde{A}\tilde{C}}, \quad R_8 = S_A^{12} S_B^{34} S_C^{56}. \end{aligned} \quad (2.208)$$

The computation of these coefficients exactly mimics the computations in (2.202) and below. One can now insert (2.207) on the partial wave expansion and extend the region of integration to the whole imaginary axis, keeping only one term which reads

$$\begin{aligned} \langle \mathcal{O}_1 \dots \mathcal{O}_6 \rangle = & \sum_{\rho_A, \rho_B, \rho_C} \int_{\frac{d}{2}-i\infty}^{\frac{d}{2}+i\infty} \frac{d\Delta_A}{2\pi i} \frac{d\Delta_B}{2\pi i} \frac{d\Delta_C}{2\pi i} I_{abcd}(\Delta_A, \rho_A; \Delta_B, \rho_B; \Delta_C, \rho_C) \times \\ & S_{\tilde{A}}^{\tilde{B}\tilde{C}}{}^d{}_e S_{\tilde{B}}^{A\tilde{C}}{}^e{}_f S_{\tilde{C}}^{AB}{}^f{}_g G_{ABC}^{(abcg)}. \end{aligned} \quad (2.209)$$

2.C.3 Direct computation of spinning shadow coefficients

In the previous subsections, we have repeatedly come across shadow coefficients involving multiple spinning operators but the computation of these shadow coefficients is an important question on its own. In this subsection, we will derive some of them using the shadow formalism. In [150] some of these coefficients were computed using weight-shifting operators from which recursion relations were derived [47]. Here, we extend these results and compute directly the explicit integration involved in the definition of these coefficients. We can write the shadow transform of an operator in a three-point structure as

$$\langle \mathcal{O}_1 \mathcal{O}_2 \mathcal{S}[\mathcal{O}_3] \rangle^{(a)} = \int d^d x_0 \langle \tilde{\mathcal{O}}_3 \tilde{\mathcal{O}}_0^\dagger \rangle \langle \mathcal{O}_1 \mathcal{O}_2 \mathcal{O}_0 \rangle^{(a)}, \quad (2.210)$$

where we have an implicit contraction of indices. Here we only consider symmetric and traceless representations of the conformal group and so the two- and three-point structures can be written in terms of the two fundamental building blocks [32] that appeared in (2.14).

In particular we choose the normalization of the two-point structure to take the form

$$\langle \mathcal{O}(x_1, z_1) \mathcal{O}(x_2, z_2) \rangle = \frac{H_{12}^J}{x_{12}^{\Delta+J}}. \quad (2.211)$$

On the other hand, the three-point structure is given by (2.13) once we omit the OPE coefficients. As in the main text, we use here the index-free notation of [32, 46]. In particular, in what follows we will use the formula

$$(a \cdot \mathcal{D}_z)^J (b \cdot z)^J = \frac{(J!)^2}{2^J} (a^2 b^2)^{\frac{J}{2}} C_J^{h-1} \left(\frac{a \cdot b}{(a^2 b^2)^{\frac{1}{2}}} \right), \quad (2.212)$$

where C_J^{h-1} is a Gegenbauer polynomial and $h = d/2$.

Before moving on to more complicated examples, let us, as a warm-up, compute the shadow integral for three scalar operators. In this case, we can use the well-known star-triangle formula [151]

$$\int d^d x_0 \frac{1}{(x_{10}^2)^a (x_{20}^2)^b (x_{30}^2)^c} = \underbrace{\frac{\pi^h \Gamma(h-a) \Gamma(h-b) \Gamma(h-c)}{\Gamma(a) \Gamma(b) \Gamma(c)}}_{\equiv G(a, b, c)} \frac{1}{(x_{12}^2)^{h-c} (x_{13}^2)^{h-b} (x_{23}^2)^{h-a}}, \quad (2.213)$$

with $a + b + c = 2h$ to get

$$\begin{aligned} \langle \phi_{\Delta_1} \phi_{\Delta_2} \mathcal{S}[\phi_{\Delta_3}] \rangle &= \int d^d x_0 \frac{1}{x_{30}^{2(d-\Delta_3)}} \frac{1}{(x_{12}^2)^{\frac{\Delta_1+\Delta_2-\Delta_3}{2}} (x_{10}^2)^{\frac{\Delta_1-\Delta_2+\Delta_3}{2}} (x_{20}^2)^{\frac{-\Delta_1+\Delta_2+\Delta_3}{2}}} \\ &= \frac{\pi^h \Gamma(\Delta_3 - h) \Gamma(\frac{\tilde{\Delta}_3 + \Delta_1 - \Delta_2}{2}) \Gamma(\frac{\tilde{\Delta}_3 + \Delta_2 - \Delta_1}{2})}{\Gamma(2h - \Delta_3) \Gamma(\frac{\Delta_3 + \Delta_1 - \Delta_2}{2}) \Gamma(\frac{\Delta_3 + \Delta_2 - \Delta_1}{2})} \langle \phi_{\Delta_1} \phi_{\Delta_2} \phi_{\tilde{\Delta}_3} \rangle, \end{aligned} \quad (2.214)$$

from which we can easily read the shadow coefficient $S(\phi_{\Delta_1} \phi_{\Delta_2} [\phi_{\Delta_3}])$.

In [150] the authors computed the shadow coefficients for the case where two of the operators were scalars and one of them had spin J . Here we compute the coefficients corresponding to two spinning operators and a scalar and we shall recover their results as a restriction. Let us take the operators at x_1 and x_3 to be spinning operators whereas the operator at x_2 is a scalar. In this case the three-point structure simplifies and we are left just with the label $\ell_2 = \ell$. We first do a shadow transform of the operator at x_3

$$\begin{aligned} \langle \mathcal{O}_{\Delta_1, J_1} \phi_{\Delta_2} \mathcal{S}[\mathcal{O}_{\Delta_3, J_3}] \rangle^{(\ell)} &= \\ &= \int d^d x_0 \langle \tilde{\mathcal{O}}_{\Delta_3, J_3}(x_3, z_3) \tilde{\mathcal{O}}_{\Delta_3, \mu_1 \dots \mu_{J_3}}^\dagger(x_0) \rangle \langle \mathcal{O}_{\Delta_1, J_1}(x_1, z_1) \phi_{\Delta_2}(x_2) \mathcal{O}_{\Delta_3}^{\mu_1 \dots \mu_{J_3}}(x_0) \rangle^{(\ell)}, \end{aligned} \quad (2.215)$$

where the indices to be contracted are explicitly shown. In light of the results of [32], this contraction can be simply done in terms of encoding polynomials that depend on

the building blocks H_{ij} and $V_{i,jk}$. By doing so, one immediately recognizes that the term associated with the two-point function is already of the desired form $(a \cdot \mathcal{D}_{z_0})^{J_3}$ with $a^\mu = (x_{03} \cdot z_3)x_{03}^\mu - \frac{1}{2}x_{03}^2 z_3^\mu$.²⁵ The terms in the three-point structure require some additional care. It is easy to see however that the z_0 -dependent terms can be completed to a binomial of degree J_3 of form $(b \cdot z_0)^{J_3}$, as appears in (2.212). After using this equation, one then needs to expand back the binomial and collect only the term we have started with. The computation is straightforward and leads to the following expression for our integral

$$\int d^d x_0 \frac{(x_{12}^2)^{-\frac{1}{2}(\Delta_1+J_1+\Delta_2-\Delta_3+J_3-2\ell)}}{2^{J_3}(x_{01}^2)^{\frac{1}{2}(\Delta_1+J_1-\Delta_2+\Delta_3-J_3)}(x_{02}^2)^{\frac{1}{2}(-\Delta_1-J_1+\Delta_2+\Delta_3-J_3+2\ell)}(x_{03}^2)^{\tilde{\Delta}_3+J_3}} \times \\ \times V_{1,20}^{J_1-\ell} (V_{3,01} + V_{3,20})^{J_3-\ell} (V_{3,01}(x_{01} \cdot z_1) - \mathcal{H}_{0,3,1})^\ell, \quad (2.216)$$

where for compactness we defined $\mathcal{H}_{i,j,k} = (x_{ij} \cdot z_j)(x_{kj} \cdot z_k) - \frac{1}{2}(z_j \cdot z_k)x_{ij}^2$.

After performing the expansion of the integrand, one observes that all the terms to be integrated take the simple form

$$\frac{(x_{01} \cdot z_1)^\alpha (x_{03} \cdot z_3)^\beta}{(x_{01}^2)^a (x_{02}^2)^b (x_{03}^2)^c}. \quad (2.217)$$

The terms in the numerator can be found from taking derivatives of the denominator as

$$(z_j \cdot \partial_{x_j})^\alpha (x_{ij}^2)^{-a} = 2^\alpha \frac{\Gamma(a+\alpha)}{\Gamma(a)} \frac{(x_{ij} \cdot z_j)^\alpha}{(x_{ij}^2)^{a+\alpha}}. \quad (2.218)$$

It is then easy to integrate the terms in (2.217) by swapping the order of integration and differentiation

$$\int d^d x_0 \frac{(x_{01} \cdot z_1)^\alpha (x_{03} \cdot z_3)^\beta}{(x_{01}^2)^a (x_{02}^2)^b (x_{03}^2)^c} = \frac{\Gamma(a-\alpha)}{2^\alpha \Gamma(a)} \frac{\Gamma(c-\beta)}{2^\beta \Gamma(c)} G(a-\alpha, b, c-\beta) \times \\ \times (z_1 \cdot \partial_{x_1})^\alpha (z_3 \cdot \partial_{x_3})^\beta (x_{12}^2)^{c-h-\beta} (x_{13}^2)^{b-h} (x_{23}^2)^{a-h-\alpha}, \quad (2.219)$$

where $a+b+c = 2h+\alpha+\beta$ and $G(a, b, c)$ was defined in (2.213).

We can use a conformal transformation to fix the position of the scalar operator x_2 at infinity. For a scalar, this can be safely done without loss of information. Indeed, there is only one nonzero ℓ_i which controls both z_1 and z_3 and there is no z_2 -dependence. If one does so, the integrand simplifies and the x_{i2}^2 drop out. The action of the derivatives can

²⁵Notice that $a^2 = 0$. We may then just keep the term $k = 0$ in the series definition of the Gegenbauer polynomial, $C_J^\lambda(z) = \sum_{k=0}^{\lfloor \frac{J}{2} \rfloor} \frac{(-1)^k (\lambda)_{J-k} (2z)^{J-2k}}{k!(J-k)!}$.

then be given in terms of known functions,

$$\begin{aligned}
 (z_1 \cdot \partial_{x_1})^\alpha (z_3 \cdot \partial_{x_3})^\beta (x_{13}^2)^{b-h} &= 2^\alpha 2^\beta \frac{\Gamma(h + \alpha + \beta - b)}{\Gamma(h - b)} (x_{31} \cdot z_1)^\alpha (x_{13} \cdot z_3)^\beta (x_{13}^2)^{b-h-\alpha-\beta} \times \\
 &\quad \times {}_2F_1\left(-\alpha, -\beta, b + 1 - h - \alpha - \beta; \frac{z_1 \cdot z_3 x_{13}^2}{2x_{13} \cdot z_3 x_{13} \cdot z_1}\right). \tag{2.220}
 \end{aligned}$$

Putting everything together, we find

$$\begin{aligned}
 &\langle \mathcal{O}_{\Delta_1, J_1} \phi_{\Delta_2} \mathcal{S}[\mathcal{O}_{\Delta_3, J_3}] \rangle^{(\ell)} = \\
 &= \sum_{p=0}^{J_3-\ell} \sum_{q=0}^{\ell} \sum_{s=0}^{\ell-q} \sum_{t=0}^p \sum_{r=0}^q \sum_{w=0}^{\infty} \sum_{m=0}^{s+w} \binom{J_3-\ell}{p} \binom{\ell}{q} \binom{\ell-q}{s} \binom{p}{t} \binom{q}{r} \binom{s+w}{m} \times \\
 &\quad (-1)^{J_3+r+s+t+2w-m} 2^{-J_3} \frac{\pi^h \Gamma\left(\frac{J_1+J_3+2r-2s+2t+\Delta_1-\Delta_2+\tilde{\Delta}_3}{2}\right) \Gamma\left(\frac{J_1-J_3+2p-2t-\Delta_1+\Delta_2+\tilde{\Delta}_3}{2}\right)}{\Gamma\left(\frac{J_1+J_3-2p-2q+2r-2s+2t+\Delta_1-\Delta_2+\Delta_3}{2}\right) \Gamma\left(\frac{J_1-J_3+2p-2t-\Delta_1+\Delta_2+\Delta_3}{2}\right)} \times \\
 &\quad \frac{\Gamma(\Delta_3 - h)}{\Gamma(1+w) \Gamma(p+q+\tilde{\Delta}_3)} \frac{(-p-q)_w (-J_1 + q - r + s)_w}{\left(\frac{2-J_1-J_3-2r+2s-2t-\Delta_1+\Delta_2-\tilde{\Delta}_3}{2}\right)_w} \underbrace{\frac{H_{13}^m V_{1,23}^{J_1-m} V_{3,12}^{J_3-m}}{(x_{13}^2)^{\frac{\Delta_1+J_1-\Delta_2+\tilde{\Delta}_3+J_3}{2}}}}_{\langle \mathcal{O}_{\Delta_1, J_1} \phi_{\Delta_2} \mathcal{O}_{\tilde{\Delta}_3, J_3} \rangle^{(m)}} \tag{2.221}
 \end{aligned}$$

from which we can easily read the shadow coefficients associated with each possible three-point structure. One can check that this expression reproduces the results of [150] as a special case.²⁶ It is worth stating that all the sums here have indeed a finite number of terms. This can be seen from the expression above by noticing that for sufficiently large w the Pochhammer symbols in the numerator will vanish.

One could have wanted to do instead the shadow transform of the scalar operator. That case is simpler as there is no need to deal with the contractions of indices as we did in the beginning of this subsection. Keeping x_2 at infinity, we have the following integral to do

$$\int d^d x_0 \frac{(x_{13}^2)^{\frac{-\Delta_1-J_1+\Delta_2-\Delta_3-J_3}{2}}}{(x_{01}^2)^{\frac{\Delta_1+J_1+\Delta_2-\Delta_3-J_3}{2}} (x_{03}^2)^{\frac{-\Delta_1-J_1+\Delta_2+\Delta_3+J_3}{2}}} V_{1,03}^{J_1-\ell} V_{3,10}^{J_3-\ell} H_{13}^\ell, \tag{2.222}$$

²⁶Strictly speaking there is a 2^{-J_3} difference which follows from a different normalization of the two-point function.

which can be integrated in the exact same way as before. This is a straightforward computation and we find

$$\begin{aligned}
& \langle \mathcal{O}_{\Delta_1, J_1} \mathcal{S}[\phi_{\Delta_2}] \mathcal{O}_{\Delta_3, J_3} \rangle^{(\ell)} = \\
& \sum_{p=0}^{J_1-\ell} \sum_{q=0}^{J_3-\ell} \sum_{r=0}^{\ell} \sum_{s=0}^{\infty} \sum_{m=0}^{\ell+s-r} \binom{J_1-\ell}{p} \binom{J_3-\ell}{q} \binom{\ell}{r} \binom{\ell+s-r}{m} (-1)^{J_1+J_3-p+q-r+2s+\ell-m} \times \\
& \frac{\pi^h \Gamma(J_1 + J_3 - p - q - 2\ell + \Delta_2 - h) \Gamma\left(\frac{-J_1+J_3+\Delta_1+\tilde{\Delta}_2-\Delta_3}{2}\right) \Gamma\left(\frac{J_1-J_3-\Delta_1+\tilde{\Delta}_2+\Delta_3}{2}\right)}{\Gamma(1+s) \Gamma(\tilde{\Delta}_2) \Gamma\left(\frac{J_1+J_3-2p-2\ell+\Delta_1+\Delta_2-\Delta_3}{2}\right) \Gamma\left(\frac{J_1+J_3-2q-2\ell-\Delta_1+\Delta_2+\Delta_3}{2}\right)} \times \\
& \frac{(-J_1+p+\ell)_s (-J_3+q+\ell)_s}{(1+h+p+q+2\ell-J_1-J_3-\Delta_2)_s} \underbrace{\frac{H_{13}^m V_{1,23}^{J_1-m} V_{3,12}^{J_3-m}}{(x_{13}^2)^{\frac{\Delta_1+J_1-\tilde{\Delta}_2+\Delta_3+J_3}{2}}}}_{\langle \mathcal{O}_{\Delta_1, J_1} \phi_{\tilde{\Delta}_2} \mathcal{O}_{\Delta_3, J_3} \rangle^{(m)}}. \tag{2.223}
\end{aligned}$$

The shadow coefficients computed in this way also reproduce the known results of [150] in the appropriate restriction.

Lastly, let us comment on the more generic situation where all operators have spin, which is, of course, more complicated. Note that we were only able to write the action of the derivatives in such a compact form because we fixed x_2 to infinity. In the more general case, we are no longer able to naively set x_2 to infinity since we would lose control of ℓ_1 and ℓ_3 . On the other hand, we can still successfully integrate the shadow transform in a case-by-case basis, but this becomes cumbersome for large values of spin. For completeness, let us write down the integral that remains after having dealt with the contraction of indices

$$\begin{aligned}
& \int d^d x_0 \frac{(-1)^{\ell_1+\ell_2} (x_{12}^2)^{\frac{-\Delta_1-J_1-\Delta_2-J_2+\Delta_3-J_3+2\ell_2}{2}}}{2^{J_3} (x_{01}^2)^{\frac{\Delta_1+J_1-\Delta_2-J_2+\Delta_3+J_3}{2}} (x_{02}^2)^{\frac{-\Delta_1-J_1+\Delta_2+J_2+\Delta_3-J_3+2\ell_2}{2}} (x_{03}^2)^{\tilde{\Delta}_3+J_3-\ell_2} (x_{13}^2)^{\ell_2} (x_{23}^2)^{J_3-\ell_1}} \times \\
& \times H_{12}^{\ell_3} V_{1,20}^{J_1-\ell_2-\ell_3} V_{2,01}^{J_2-\ell_1-\ell_3} \left(V_{3,02} \left(V_{2,01} x_{01}^2 - x_{12} \cdot z_2 x_{02}^2 \right) + \mathcal{H}_{0,3,2} x_{12}^2 \right)^{\ell_1} \times \\
& \times \left(V_{1,03} \left(V_{3,02} x_{02}^2 x_{13}^2 + V_{3,21} x_{03}^2 x_{12}^2 - x_{13} \cdot z_3 x_{03}^2 x_{23}^2 \right) + \mathcal{H}_{0,1,3} x_{13}^2 x_{23}^2 \right)^{\ell_2} \times \\
& \times \left(V_{3,21} x_{03}^2 x_{12}^2 + V_{3,02} \left(x_{02}^2 x_{13}^2 - x_{01}^2 x_{23}^2 \right) \right)^{J_3-\ell_1-\ell_2}, \tag{2.224}
\end{aligned}$$

where we assume that the shadow transform is done in the operator at x_3 . One can easily see that all the terms can be integrated in the same way as before

$$\int d^d x_0 \frac{(x_{01} \cdot z_1)^\alpha (x_{02} \cdot z_2)^\beta (x_{03} \cdot z_3)^\gamma}{(x_{01}^2)^a (x_{02}^2)^b (x_{03}^2)^c} = \frac{\Gamma(a - \alpha)}{2^\alpha \Gamma(a)} \frac{\Gamma(b - \beta)}{2^\beta \Gamma(b)} \frac{\Gamma(c - \gamma)}{2^\gamma \Gamma(c)} G(a - \alpha, b - \beta, c - \gamma) \\ \times (z_1 \cdot \partial_{x_1})^\alpha (z_2 \cdot \partial_{x_2})^\beta (z_3 \cdot \partial_{x_3})^\gamma (x_{12}^2)^{c-h-\gamma} (x_{13}^2)^{b-h-\beta} (x_{23}^2)^{a-h-\alpha}, \quad (2.225)$$

where $a + b + c = 2h + \alpha + \beta + \gamma$.

This is all we need to successfully compute any shadow coefficient of a three-point function of three operators in spin J_i representation, but we did not manage to find a simple and compact formula for the action of derivatives in the above expression. While one can use this formalism to compute the shadow coefficients of three spinning operators, in practice the procedure becomes too computationally expensive at large spin. It would be interesting to investigate if the weight-shifting formalism of [150] offers a more efficient alternative.

Chapter 3

Conformal Multi-Regge Theory

3.1 Introduction

The vast majority of results of conformal bootstrap rely on the study of correlation functions of four primary operators. While the full set of these contain all the dynamical data of a theory, it is true that as the spin of these operators is increased the task of finding these data becomes more and more challenging. This is the reasoning why most conformal bootstrap works focus on correlation functions of scalar operators. In recent years, on the other hand, it has become more and more appreciated the fact that consistency conditions at the level of scalar higher-point functions can be the appropriate setting to deal with this problem. Indeed, higher-point correlators give us access to more data than their lower-point counterparts and in particular can probe many spinning data. Due to the central role of conformal blocks in the conformal bootstrap, these have been considered for higher-point functions in [51, 57–62, 152, 153]. Although their structure is generically intricate, it simplifies drastically in the lightcone limit where bootstrap studies have been performed in [1, 64–66]. Higher-point correlation functions have also been considered in multiple contexts, for instance in holographic theories [3, 57, 129, 130] and more recently in numerical bootstrap [58, 59, 68].

An important tool in the analytical conformal bootstrap is the Regge limit [83, 84, 86]. The Regge limit of four-point correlation functions in CFTs is the conformal analogue of the limit of high centre-of-mass energy at fixed impact parameter of scattering amplitudes in quantum field theory. Through AdS/CFT, it is thus relevant to study high-energy scattering in the bulk. In terms of cross ratios, Regge limit resembles the behavior of Euclidean OPE. However, in Regge limit this happens after a branch-cut of the conformal

block decomposition is crossed. Conformal Regge theory provides a resummation of the OPE in terms of families of operators called *Regge trajectories* [86]. In doing so, one needed to assume a well-defined analytic continuation of OPE data to complex spin, which was later established by the inversion formula [79]. This also puts the analytical conformal bootstrap using the lightcone limit on a firm footing, by showing that the large spin expansion is not asymptotic, but convergent. Regge limit has also been studied in the context of holography [83, 84, 154]. Recently, these ideas have been tested on several physical models, with great success [78, 155]. Regge limit and Regge behavior of correlation functions have also played an important role in imposing causality constraints [92–94, 96, 156, 157].

This success in CFTs and the natural interest for multi-particle high-energy scattering calls for a deeper analysis of Regge limit. In this chapter we start the discussion of the generalization of the Regge limit to higher-point functions, mostly focusing on the case of five-point functions. In the process we will also briefly review flat-space literature about Regge theory for higher-point amplitudes that has not been object of attention for a long time.

The outline of the chapter is as follows. In section 3.2, we review the literature on the multi-Regge limit for S-matrix. In section 3.3, we discuss the setup of five-point correlation functions in conformal field theories. We review the Euclidean OPE limit and the lightcone limit and contrast it with our proposal for Regge limit. In section 3.4, we discuss analytic properties of the correlator as it is continued to Regge limit. Here we also consider the corresponding Mellin amplitude and Mellin partial wave and show that they produce the expected Regge behavior in position space. In subsection 3.4.4, we consider the analytic continuation of the Mellin amplitude in three quantum numbers by means of Sommerfeld-Watson transforms and resum the contribution of two leading Regge trajectories. Finally, we conclude with some open directions in section 3.5.

3.2 Scattering in flat-space and Regge theory

In this section, we review Regge theory for scattering amplitudes in flat space. We begin by reviewing the key ingredients in the case of $2 \rightarrow 2$ scattering process in four-dimensional Lorentzian spacetime. Then, we review the generalization to the case of higher-point scattering amplitudes. It will serve as the main inspiration for the conformal Regge theory that we will consider later.

Let us restrict to the more familiar case of $2 \rightarrow 2$ scattering, where we define the Mandelstam invariants as

$$s = -(k_1 + k_3)^2, \quad t = -(k_1 + k_2)^2, \quad u = -(k_1 + k_4)^2, \quad (3.1)$$

with k_i the external incoming momenta. The Regge limit corresponds to the high-energy limit of an amplitude, where $s \rightarrow \infty$ with fixed t . Regge theory, on the other hand, comes in play to address the experimental observation that s -channel processes exhibit a small t peak whenever there are exchanges of particles or resonances in the t -channel. One would like to understand this behavior by considering a partial wave decomposition of the amplitude. Consider the scattering amplitude of four spinless particles with equal mass m in the t -channel decomposition

$$A(s, t) = \sum_{J=0}^{\infty} (2J+1) a_J(t) P_J(z), \quad (3.2)$$

where $z = \cos \theta = 1 + 2s/(t - 4m^2)$ and $P_J(z)$ is a Legendre polynomial of first kind of degree J . θ denotes the t -channel scattering angle and J is the angular momentum of the exchanged particles. This series converges in the t -channel physical region, namely the region $t > 4m^2$ and $s < 0$, and therefore is not reliable to study the large s limit. Note that the large s limit of a spin J partial wave behaves as s^J . The infinite sum over J gets more and more contributions from the higher J partial waves, in this limit. Regge theory provides a rewriting of (3.2) in a form that can be analytically continued to this large s region. This is done by complexifying angular momentum, extending Regge's idea [158], and allows to resum the contribution of a family of particles that correctly predict the observed large s behavior.

Naturally, one would like to extend Regge theory to multi-particle exchange amplitudes. The analytic structure of these amplitudes is less well understood than the four-point analogue. The increasing number of Mandelstam invariants turns this into a more technically-challenging goal, but there have been important contributions in the 70's that we now briefly review for the case of five-point amplitudes (see [159–169] for more details).

As represented in figure 3.1 (left), one can define ten two-body Mandelstam invariants for a five-point function, in an analogous way to the $2 \rightarrow 2$ scattering definition (3.1), i.e.

$$s_{ij} = -(k_i + k_j)^2, \quad (3.3)$$

where k_i are again external incoming momenta. Similarly, we define t_{ij} - and u_{ij} -type

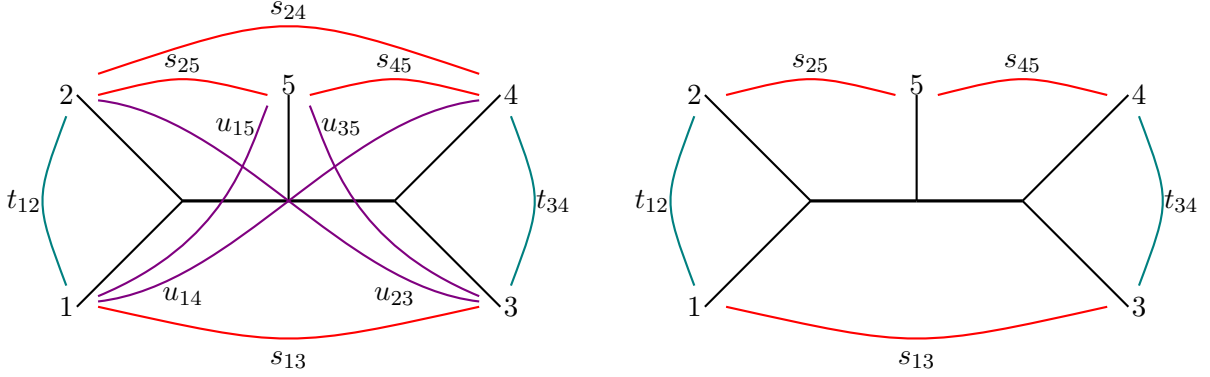


FIGURE 3.1: The ten two-body Mandelstam invariants of a five-point scattering amplitude (left) and our choice of five independent ones (right).

invariants. Since not all the invariants are independent, we shall choose the following five as independent, $s_{13}, s_{25}, s_{45}, t_{12}, t_{34}$, as shown in figure 3.1 (right). We will be focusing on the double Regge limit where $s_{25}, s_{45} \rightarrow \infty$, and necessarily $s_{13} \rightarrow \infty$, while t_{12} and t_{34} are held fixed. It is also possible to define a single Regge limit by considering either $s_{25} \rightarrow \infty$ with s_{13}/s_{25} also fixed, or $s_{45} \rightarrow \infty$ with s_{13}/s_{45} fixed.¹

Let us consider the partial-wave decomposition of an amplitude $A = A(s_{25}, s_{45}, \eta; t_{12}, t_{34})$ of five identical massive particles in the t_{12}, t_{34} channels,

$$A = \sum_{m=-\infty}^{\infty} \sum_{J_{1,2}=|m|}^{\infty} \prod_{i=1}^2 (2J_i + 1) a_{J_1, J_2, m}(t_{12}, t_{34}) z^m d_{0m}^{J_1}(\cos \theta_1) d_{m0}^{J_2}(\cos \theta_2), \quad (3.4)$$

where $\eta \equiv s_{13}/(s_{25}s_{45})$ and $z \equiv e^{i\theta_{\text{Toller}}}$, as defined below. Here m denotes the allowed helicities of exchanged particles. We also use Wigner- d functions which can be written in terms of Jacobi polynomials $\mathcal{P}_J^{\alpha, \beta}$ as

$$d_{m'm}^J(\cos \theta) = \left(\frac{(J+m)!(J-m)!}{(J+m')!(J-m')!} \right)^{\frac{1}{2}} \left(\sin \frac{\theta}{2} \right)^{m-m'} \left(\cos \frac{\theta}{2} \right)^{m+m'} \mathcal{P}_{J-m}^{m-m', m+m'}(\cos \theta), \quad (3.5)$$

with

$$\mathcal{P}_J^{\alpha, \beta}(z) = \sum_{n=0}^J \frac{(-1)^n}{n!} \frac{J!}{(J-n)!} \frac{\Gamma(n+\alpha+1)\Gamma(J-n+\beta+1)}{\Gamma(J+\alpha+\beta+2)} z^{n+\alpha} (1-z)^{J-n+\beta}. \quad (3.6)$$

The scattering angles θ_1, θ_2 and θ_{Toller} have a clear physical meaning - see e.g. [164]. Consider the scattering process shown in the figure 3.1 with the exchanged momenta $q_1^2 = t_{12}$

¹Another interesting limit to consider is the helicity-pole limit where $s_{25} \rightarrow \infty$ with $s_{13}/s_{25} \rightarrow \infty$ while t_{12}, t_{34} and s_{45} are fixed (or the one where the roles of s_{25} and s_{45} are swapped). This limit is experimentally accessible in inclusive cross-sections [170]. It is also possible to consider the limit $s_{13} \rightarrow \infty$ with all the other Mandelstam invariants kept fixed.

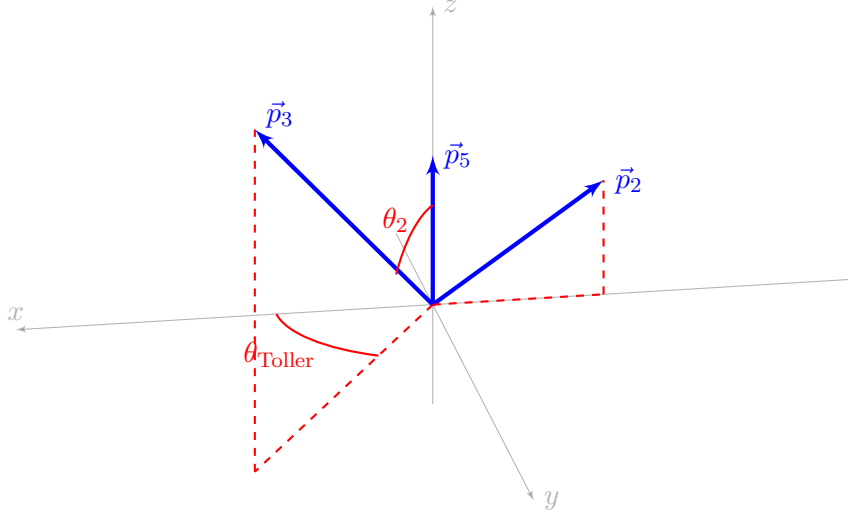
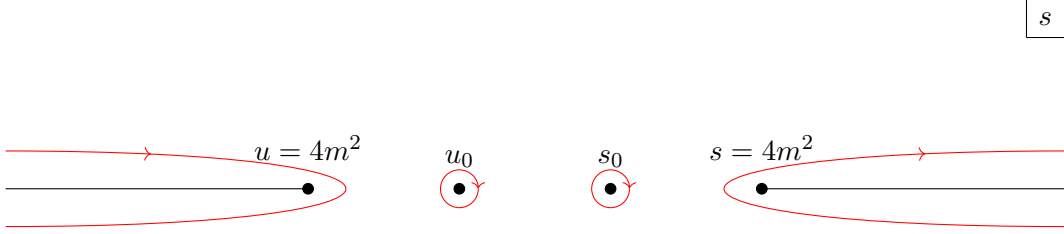


FIGURE 3.2: Scattering process shown in the resting frame of exchanged momentum q_2 . This defines the angles θ_2 and θ_{Toller} . θ_1 is defined analogously in the rest frame of exchanged momentum q_1 .

and $q_2^2 = t_{34}$. Firstly, we lump together particles 3, 4 and treat them as a single particle of momentum q_2 . The angle θ_1 is defined as the scattering angle of the process $12 \rightarrow 5(34)$ which happens in a single plane in the center of mass frame. Secondly, we consider the rest frame of the exchanged momentum q_2 . We denote the three momentum of particle- i by \vec{p}_i . As depicted in figure 3.2, we can choose a coordinate system where \vec{p}_5 is aligned with the z -axis and \vec{p}_2 lies somewhere in xz -plane. We define θ_2 as the zenith-angle of \vec{p}_3 , whereas θ_{Toller} is the azimuth angle. Alternatively, the Toller angle can be thought of as the angle between the two scattering planes corresponding to the q_1 and q_2 rest frames, respectively.

The scattering angles are related to the Mandelstam invariants in a nontrivial way - see e.g. [162, 165],

$$\begin{aligned}
 s_{25} &= 2m^2 + \frac{1}{2} (t_{34} - m^2 - t_{12}) + \frac{1}{2} \left(\frac{(t_{12} - 4m^2)\lambda(t_{12}, t_{34}, m^2)}{t_{12}} \right)^{1/2} \cos \theta_1, \\
 s_{45} &= 2m^2 + \frac{1}{2} (t_{12} - m^2 - t_{34}) + \frac{1}{2} \left(\frac{(t_{34} - 4m^2)\lambda(t_{12}, t_{34}, m^2)}{t_{34}} \right)^{1/2} \cos \theta_2, \\
 s_{13} &= 2m^2 + \frac{1}{4} (m^2 - t_{12} - t_{34}) + \frac{1}{4} \left(\frac{(t_{12} - 4m^2)\lambda(t_{12}, t_{34}, m^2)}{t_{12}} \right)^{1/2} \cos \theta_1 \\
 &\quad + \frac{1}{4} \left(\frac{(t_{34} - 4m^2)\lambda(t_{12}, t_{34}, m^2)}{t_{34}} \right)^{1/2} \cos \theta_2 + \frac{1}{4} \left(\frac{(t_{12} - 4m^2)(t_{34} - 4m^2)}{t_{12}t_{34}} \right)^{1/2} \times \\
 &\quad \left(m^2 - t_{12} - t_{34} \right) \cos \theta_1 \cos \theta_2 - \frac{1}{2} \left((t_{12} - 4m^2)(t_{34} - 4m^2) \right)^{1/2} \sin \theta_1 \sin \theta_2 \cos \theta_{\text{Toller}}, \tag{3.7}
 \end{aligned}$$

FIGURE 3.3: Singularities of $A(s, t)$ in the s complex-plane at fixed t .

where we use $\lambda(a, b, c) = a^2 + b^2 + c^2 - 2ab - 2bc - 2ca$. Note that here m corresponds to the mass of the exchanged particles and should not be confused with helicity. We believe the context makes clear which one we refer to. We emphasize that only s_{13} depends on θ_{Toller} . Moreover, in the double Regge limit,

$$\eta \sim \frac{2(t_{12}t_{34})^{1/2} \cos \theta_{\text{Toller}} + m^2 - t_{12} - t_{34}}{\lambda(t_{12}, t_{34}, m^2)}, \quad (3.8)$$

independently of θ_1 and θ_2 . This map suffers from some kinematical singularities in terms of the variables t_{12}, t_{34} . These will be extracted from the possible types of singularities that we study below and we focus only on dynamical singularities.

To explore the double Regge region from the partial wave decomposition (3.4), we need a well-defined analytic continuation of the amplitude. In contrast to the $2 \rightarrow 2$ scattering, for multiparticle scattering besides considering complex angular momentum, one also needs to account for helicity dependence. As stressed in [159–162], the analytic continuation of the amplitude to complex helicity values is also required. The proper procedure for analytic continuation and its uniqueness deserve some comments. Let us first review some concepts in the four-point case that will straightforwardly generalize to the five-point case we wish to analyze in more detail.

We assume that a $2 \rightarrow 2$ scattering amplitude has only singularities with dynamical origin. Namely, we only consider poles associated with bound states and branch-cuts starting at physical thresholds for particle production.²

In figure 3.3 we depict these singularities at fixed t in the complex s plane. We assume the following dispersion relation at fixed t

$$A(s, t) = \frac{1}{2\pi i} \left(\int_0^{+\infty} ds' \frac{\text{Disc}_s(s', t, u')}{s' - s} + \int_0^{+\infty} du' \frac{\text{Disc}_u(s', t, u')}{u' - u} \right) = A_R(s, t) + A_L(u, t). \quad (3.9)$$

²In particular we ignore the possible existence of anomalous thresholds. However, as long as these lie on the real axis and the analytic structure resembles figure 3.3 with a different branch point for some fixed t , the discussion that follows remains valid.

Here, we have extended the notion of discontinuities Disc_s and Disc_u to include the contributions of bound-state poles.³ We have also defined A_R and A_L with respect to each of the terms. As it is clear from the definition, each of the terms has only cut contributions along one of the directions in the s complex plane. This fact is crucial in performing the analytic continuation of the amplitude with good large J behavior which happens to be unique as guaranteed by Carlson's theorem. It is also useful to define the *signatured amplitude*⁴

$$A^\delta(s, t) = \frac{1}{2}(A_R(s, t) + \delta A_L(s, t)), \quad (3.10)$$

where $\delta = \pm 1$. Note that we replace u by s in A_L ensuring that there are only cuts in a single direction. The full amplitude can be easily reconstructed from the signatured amplitudes as

$$A(s, t) = \sum_{\delta=\pm 1} (A^\delta(s, t) + \delta A^\delta(u, t)). \quad (3.11)$$

In what follows, we assume that the signatured amplitudes have the same analytic structure as the full amplitude. This assumption greatly simplifies the discussion of dynamical singularities of partial-wave amplitudes. We are entitled to consider the partial wave expansion of the signatured amplitude

$$A^\delta(s, t) = \sum_{J=0}^{\infty} (2J+1) a_J^\delta(t) P_J(z). \quad (3.12)$$

Using the orthogonality of Legendre polynomials P_J and (3.10), we can write

$$a_J^\delta(t) = \frac{1}{4\pi i} \int_{z_0}^{+\infty} dz' \left(\text{Disc}_s A_R(s', t) + \delta \text{Disc}_s A_L(s', t) \right) Q_J(z'), \quad (3.13)$$

where z_0 is the branch point of the discontinuity and Q_J is the Legendre polynomial of the second kind given by

$$Q_J(z) = \int_{-1}^1 d\zeta \frac{P_J(\zeta)}{z - \zeta}. \quad (3.14)$$

³We assumed that no subtractions were needed in order to neglect contributions from arcs at infinity from the Cauchy integral that gives rise to the dispersion relation. If this is not the case, one should proceed considering instead a subtracted amplitude.

⁴The reader might be familiar with an equivalent decomposition of the full amplitude in terms of even and odd angular momentum contributions. These are composed of signatured amplitudes. Indeed we have $A^{\text{even}} = A^+(s, t) + A^+(-s, t)$ and $A^{\text{odd}} = A^-(s, t) - A^-(-s, t)$, where we use $u \sim -s$ in Regge limit.

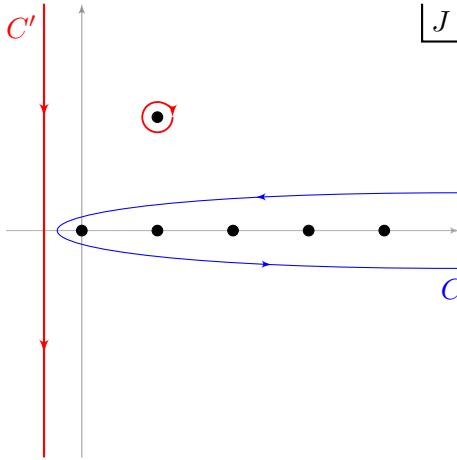


FIGURE 3.4: Contour integrals for the Sommerfeld-Watson transform for the four particle scattering in the J -complex plane. As one deforms the contour from C to C' one has to consider the contribution from dynamical singularities which here we assume to be a Regge pole.

Using the symmetry $P_J(z) = (-1)^J P_J(-z)$, we perform a Sommerfeld-Watson transform of (3.12)

$$A^\delta(s, t) = \int_C \frac{dJ}{2\pi i} \frac{\pi}{\sin \pi J} (2J+1) a^\delta(J, t) P_J(-z), \quad (3.15)$$

where C is the closed contour depicted in figure 3.4. Due to the good large J behavior of the partial-wave P_J , one can continuously deform the contour from C to C' , as shown in the same figure. We should account for all the possible singularities that may be encountered during this deformation. In this chapter, we always assume that these are pole-type singularities ⁵

$$a^\delta(J, t) \simeq \frac{\beta(t)}{J - \alpha(t)}, \quad (3.16)$$

where $\alpha(t)$ is a Regge trajectory and $\beta(t)$ is regular in t . Regularity follows from the assumption that $A^\delta(s, t)$ has the same analytic structure of the full amplitude $A(s, t)$. We also use the fact that Steinmann relations [171] impose the latter to have no double discontinuity in s and t . At large s , we keep the rightmost pole as it gives the leading contribution and write

$$A^\delta(s, t) \sim \frac{1}{2\pi i} (-s)^{\alpha(t)} \Gamma(-\alpha(t)) \beta(t), \quad (3.17)$$

where we absorbed nonsingular factors into the definition of $\beta(t)$.

⁵Other type of singularities like Regge cuts and nonsense-wrong-signature-fixed poles also exist. Moreover, singularities can also appear in a multiplicative manner but we neglect this scenario here for simplicity. The interested reader can find a discussion on those in [165] and references thereafter.

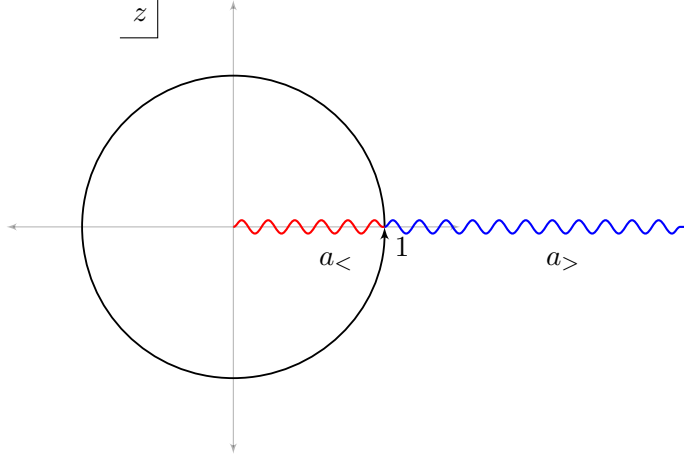


FIGURE 3.5: Contour deformation in $z = e^{i\theta_{\text{to1er}}}$ for doing the Froissart-Gribov continuation. The orthogonality relation holds on the black contours. We show the two different branch cuts corresponding to a_{\gtrless} discussed in (3.22).

For the five-particle case we consider a similar analytic structure of the amplitude in the s_{25}, s_{45} and s_{13} complex planes as in the four-particle case.⁶ We would like to decompose the full amplitude in terms of signatured amplitudes with only right-hand or left-hand cuts for each s -type invariant. We immediately see that we have to consider $2^3 = 8$ possible signatures. Indeed, one writes

$$A(s_{ij}, t_{ij}) = \sum_{\delta_{ij}=\pm 1} \left\{ \left(A^{\delta_{25}\delta_{45}\delta_{13}}(s_{25}, s_{45}, \eta, t_{12}, t_{34}) + \delta_{25} A^{\delta_{25}\delta_{45}\delta_{13}}(-s_{25}, s_{45}, \eta, t_{12}, t_{34}) + \delta_{45} A^{\delta_{25}\delta_{45}\delta_{13}}(s_{25}, -s_{45}, \eta, t_{12}, t_{34}) + \delta_{25}\delta_{45} A^{\delta_{25}\delta_{45}\delta_{13}}(-s_{25}, -s_{45}, \eta, t_{12}, t_{34}) \right) + \delta_{13}(\eta \rightarrow -\eta) \right\}, \quad (3.18)$$

where we make a slight abuse of notation by writing $u_{ij} \sim -s_{ij}$ as dictated by the double-Regge limit we are exploring. Indeed, note that each of the signatured amplitudes $A^{\delta_{25}\delta_{45}\delta_{13}}$ is a function with only right-hand cuts in each of the invariants s_{25}, s_{45} and s_{13} . While δ_{25}, δ_{45} are the already familiar signatures associated with angular momenta in the t_{12} and t_{34} channels, δ_{13} is a new signature related to the helicity at the central vertex.

⁶Generically one expects anomalous thresholds to exist in multipoint amplitudes. Here, however, we consider the simpler case where they don't appear. The same is done in the literature we are briefly reviewing (see for instance, [159–162] and section 1.4 of [164] where there is brief discussion about anomalous thresholds) and the counting of necessary signatured amplitudes follows from this assumption. It would be interesting to understand how this counting is (or not) affected by the existence of anomalous thresholds and how the partial-wave coefficients can be written as analytic functions of spin and helicity in that case. Moreover, it would be relevant to understand if the existence of anomalous thresholds indeed alters the asymptotic behaviour of the amplitude in the multi-Regge limit we describe here. Note, however, that similarly to the four-point case we commented in footnote 2, if the anomalous thresholds lie on the real line and the analytic structure still resembles that of figure 3.3, we do expect the counting and the discussion of signatured amplitudes we review here to remain valid.

Following [159], we first analyze the analytic continuation of helicity m to complex values. Inspired by the form of the partial-wave decomposition (3.4), one expects the following dispersion relation to hold in the z -complex plane,

$$A(s_{ij}, \eta, t_{ij}) = \frac{1}{2\pi i} \left(\int_{-\infty}^{-1-\epsilon} + \int_{-1+\epsilon}^{1-\epsilon} + \int_{1+\epsilon}^{+\infty} \right) \frac{\text{Disc}_z A(s_{ij}, \eta', t_{ij})}{z' - z} dz'. \quad (3.19)$$

To have a well-defined analytic continuation, we need to consider amplitudes with cuts either only on the right or only on the left half plane in the respective Mandelstam variable. Thus, we consider signatured amplitudes as introduced in (3.18). We can write

$$A^{\delta_{13}}(z) = \sum_{m=-\infty}^{+\infty} a_m^{\delta_{13}} z^m, \quad (3.20)$$

where we suppress the dependence on labels or parameters that are irrelevant for this discussion. Using the fact that signatured amplitudes are functions with only right-hand cuts,⁷ we have

$$a_m^{\delta_{13}} = \left(\frac{1}{2\pi i} \right)^2 \left(\int_0^{1-\epsilon} + \int_{1+\epsilon}^{+\infty} \right) \int_{|z|=1} \frac{\text{Disc}_z A^{\delta_{13}}(z')}{z' - z} z^{-m-1} dz' dz. \quad (3.21)$$

For $z' > 1$ and $m < 0$ the z -integral gives 0, while for $m \geq 0$, it gives z'^{-m-1} . On the other hand, if $0 < z' < 1$ and $m \geq 0$, the residues at the two poles cancel and the integral yields 0, whereas for $m < 0$ we find $-z'^{-m-1}$. We can then define, as shown in figure 3.5,

$$a_>^{\delta_{13}}(m) = \frac{1}{2\pi i} \int_{1+\epsilon}^{\infty} (z')^{-m-1} \text{Disc}_z A^{\delta_{13}}(z') dz', \quad (3.22)$$

$$a_<^{\delta_{13}}(m) = \frac{1}{2\pi i} \int_0^{1-\epsilon} (z')^{-m-1} \text{Disc}_z A^{\delta_{13}}(z') dz', \quad (3.23)$$

where it is clear that $a_>^{\delta_{13}}$ has a good asymptotic behavior in the right half-plane in the complex m variable, whereas $a_<^{\delta_{13}}$ does so on the left-half plane. We can thus perform a Sommerfeld-Watson transform in m and write

$$\begin{aligned} A^{\delta_{13}}(z) &= \sum_{m=0}^{\infty} a_>^{\delta_{13}}(m) z^m - \sum_{m=-\infty}^{-1} a_<^{\delta_{13}}(m) z^m \\ &= \frac{1}{2\pi i} \int_{C_R} dm \frac{\pi a_>^{\delta_{13}}(m) (-z)^m}{\sin \pi m} - \frac{1}{2\pi i} \int_{C_L} dm \frac{\pi a_<^{\delta_{13}}(m) (-z)^m}{\sin \pi m} \\ &= \frac{1}{2\pi i} \int_C dm \frac{\pi (a_>^{\delta_{13}}(m) + a_<^{\delta_{13}}(m))}{\sin \pi m} (-z)^m, \end{aligned} \quad (3.24)$$

⁷Note that taking $z \rightarrow -z$ is related with $\eta \rightarrow -\eta$ as one can see from (3.8).

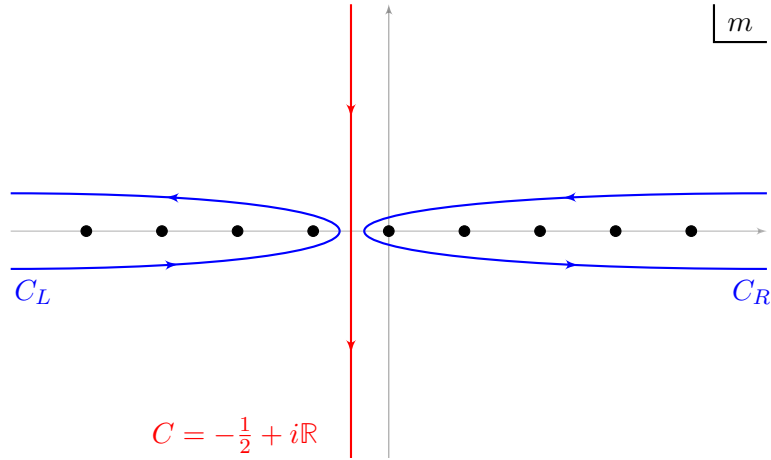


FIGURE 3.6: Contour integrals for the Sommerfeld-Watson transform in the m -complex plane.

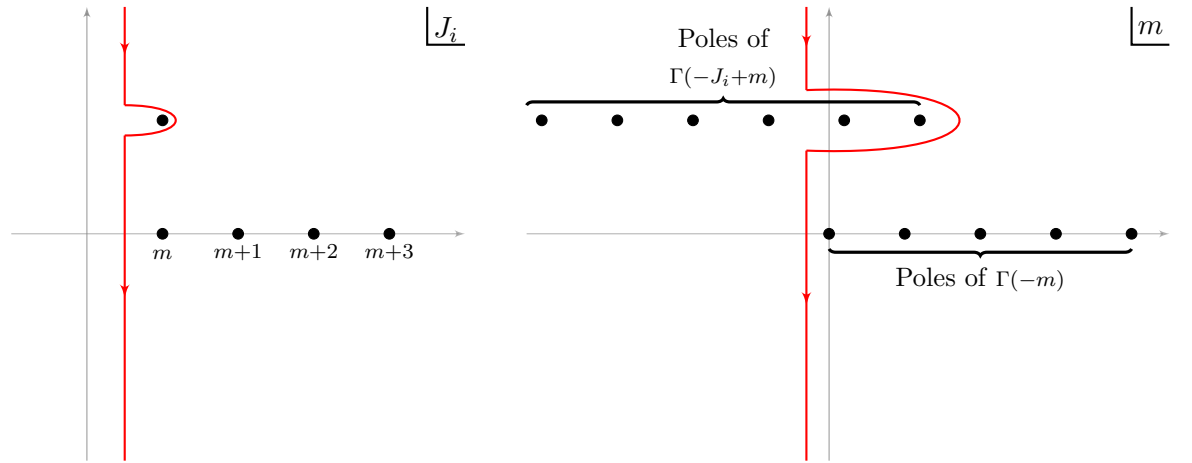


FIGURE 3.7: Contour of integration in J_i and m -complex planes when the respective variable is integrated first. Here, we only account for dynamical singularities given by Regge poles and ignore the existence of Regge cuts and fixed poles. Note that there are no dynamical singularities in the m -complex plane.

where the contours C_R, C_L and C are shown in figure 3.6. Recovering the previously suppressed dependence and parameters, we have

$$a_{\gtrless}^{\delta_{13}}(m) = \sum_{J_1, J_2=m}^{\infty} \left(\prod_{i=1}^2 (2J_i + 1) \right) a_{\gtrless, J_1, J_2, m}^{\delta_{25} \delta_{45} \delta_{13}}(t_{12}, t_{34}) d_{0m}^{J_1}(\cos \theta_1) d_{m0}^{J_2}(\cos \theta_2), \quad (3.25)$$

which only makes sense if we also analytically continue in the two angular momenta,

$$a_{\gtrless}^{\delta_{13}}(m) = \left(\prod_{i=1}^2 \int_{C_i} \frac{dJ_i}{2\pi i} \frac{\pi(2J_i + 1)}{\sin \pi(J_i - m)} \right) a_{\gtrless}^{\delta_{25} \delta_{45} \delta_{13}}(J_1, J_2, m, t_{12}, t_{34}) d_{0m}^{J_1}(-z_1) d_{m0}^{J_2}(-z_2), \quad (3.26)$$

with contours C_i as shown in figure 3.7 (left) and where $z_i = \cos \theta_i$. This is a reasonable

but non-trivial claim. In fact, [160, 161] was only able to check a well-defined analytic continuation for a single angular momentum and helicity, but not the three simultaneously. To the best of our knowledge, there is no derivation of the latter. In the following, we assume that this defines a satisfactory analytic continuation of the signatured amplitude in terms of the scattering angles and of t_{12} and t_{34} . However, we would like to rewrite it in terms of the Mandelstam invariants alone. This can be done by using the map (3.7). To find the dependence on s_{25} and s_{45} , we mimic the analysis of the four-particle case. On the other hand, the η dependence requires one more comment. We assume that $A^{\delta_{13}}$ is an even function of the Toller angle and, in particular, a function of $\cos \theta_{\text{Toller}}$ (and thus invariant under $z \rightarrow 1/z$)⁸. This requirement follows from the realization that η is an even function of θ_{Toller} and therefore only even functions of θ_{Toller} can be rewritten in terms of η . This ends up imposing $a_{>}^{\delta_{13}}(m) = -a_{<}^{\delta_{13}}(-m)$ and justifies dropping the subscripts when we write

$$A^{\delta_{13}}(\eta) = \frac{1}{2\pi i} \int_C dm \frac{\pi a^{\delta_{13}}(m)}{\sin \pi m} (-\eta)^m. \quad (3.27)$$

Note that, as we write z in terms of η , we redefine what we mean by $a^{\delta_{13}}$.⁹ We can summarize the discussion on analytic continuations of five-particle amplitudes by writing

$$\begin{aligned} A^{\delta_{25}\delta_{45}\delta_{13}}(s_{25}, s_{45}, \eta, t_{12}, t_{34}) &= \left(\frac{1}{2\pi i} \right)^3 \int_C dm \left(\prod_{i=1}^2 \int_{C_i} dJ_i (2J_i + 1) \right) \\ &\quad \frac{\pi^3 d_{0m}^{J_1}(-\cos \theta_1) d_{m0}^{J_2}(-\cos \theta_2) (-\eta)^m}{\sin \pi m \sin \pi(J_1 - m) \sin \pi(J_2 - m)} a^{\delta_{25}\delta_{45}\delta_{13}}(J_1, J_2, m, t_{12}, t_{34}) \\ &= \left(\frac{1}{2\pi i} \right)^3 \int_C dm \Gamma(-m) \left(\prod_{i=1}^2 \int_{C_i} dJ_i (2J_i + 1) \Gamma(-J_i + m) \right) \\ &\quad (-s_{25})^{J_1 - m} (-s_{45})^{J_2 - m} (-s_{13})^m a^{\delta_{25}\delta_{45}\delta_{13}}(J_1, J_2, m, t_{12}, t_{34}), \end{aligned} \quad (3.28)$$

where we used $\eta = s_{13}/(s_{25}s_{45})$ and in the second equality $a^{\delta_{25}\delta_{45}\delta_{13}}(J_1, J_2, m, t_{12}, t_{34})$ was redefined.

Under the assumption that the analytic continuation of the signatured amplitude has a good asymptotic behavior in J_1, J_2 and m such that we can ignore arcs at infinity, we focus on possible singularities that one might encounter as we move the contours to the left. In figure 3.7, we draw both m and J_i complex planes when the respective variable is

⁸See [165] for whenever this is not the case.

⁹In particular, as commented before, there are kinematical singularities in the map that we shall ignore when we discuss dynamical singularities in $a^{\delta_{13}}(m)$.

integrated first. In particular, we show the possible singularities. As before, we restrict our analysis to Regge-pole-type of singularities and we refer interested readers to [164, 165] for more details on other type of singularities. One expects the singularities in m to the left of contour and that determine the asymptotic behavior of the amplitude to be completely determined by the dynamical singularities in angular momenta. The reason for that is bi-folded. First, note that the amplitude has the asymptotic behavior

$$(-s_{25})^{J_1-m}(-s_{45})^{J_2-m}(-s_{13})^m. \quad (3.29)$$

Generically, this expression has a nonzero double discontinuity in the partially-overlapping channel invariants, namely s_{25} and s_{45} . However, this is forbidden by Steinmann relations [171]. Therefore, it must be that either $J_1 - m$ or $J_2 - m$ is a non-negative integer after the capture of poles. It then follows that, in this limit, helicity singularities are fully determined by angular momentum ones as

$$m = \alpha - N, \quad (3.30)$$

where α is the location of a dynamical singularity in J_1 or J_2 and N is a non-negative integer. In the above argument, we naturally assume that the asymptotic behavior is attained within a physical region for the amplitude. It is conceivable, however, that such asymptotics do not correspond to a physical behavior and thus the argument would require an extension of validity of Steinmann relations for those configurations. The second reason concerns the special nature of the helicity quantum number. The physical interpretation of dynamical singularities are associated with the existence of particles. As helicity is not a good Lorentz invariant and does not classify particles, as mass and spin do, we do not expect dynamical singularities in m [164, 166]. Besides, these assumptions seem to work well with specific models [164, 172] as we will see below.

We now focus on our particular case of interest, the contribution of two Regge poles $\alpha_1(t)$ and $\alpha_2(t)$ in the double Regge limit with

$$a^{\delta_{25}\delta_{45}\delta_{13}}(J_1, J_2, m, t_{12}, t_{34}) \approx \frac{\beta(m, t_{12}, t_{34})}{(J_1 - \alpha_1(t_{12}))(J_2 - \alpha_2(t_{34}))}. \quad (3.31)$$

In the Regge limit we move the C_1 and C_2 contours to the left in (3.28) and capture the poles in complex angular momentum. The leading contributions come from the rightmost

poles. We find

$$\begin{aligned}
A^{\delta_{25}\delta_{45}\delta_{13}}(s_{25}, s_{45}, \eta, t_{12}, t_{34}) &\sim \frac{1}{2\pi i} \int_C dm (2\alpha_1 + 1)(2\alpha_2 + 1)\Gamma(-m)\Gamma(-\alpha_1 + m)\Gamma(-\alpha_2 + m) \\
&\quad \times (-s_{25})^{\alpha_1 - m}(-s_{45})^{\alpha_2 - m}(-s_{13})^m \beta(m, t_{12}, t_{34}) \\
&\sim (-s_{25})^{\alpha_1}(-s_{45})^{\alpha_2} \left((-\eta)^{\alpha_1} \sum_i \Gamma(-\alpha_1 + i)\Gamma(\alpha_1 - \alpha_2 - i)\beta(\alpha_1 - i, t_{12}, t_{34}) \frac{\eta^{-i}}{i!} \right. \quad (3.32) \\
&\quad \left. + (-\eta)^{\alpha_2} \sum_i \Gamma(-\alpha_2 + i)\Gamma(\alpha_2 - \alpha_1 - i)\beta(\alpha_2 - i, t_{12}, t_{34}) \frac{\eta^{-i}}{i!} \right).
\end{aligned}$$

From the first to second line we closed the C contour to the left, capturing all the α_i -dependent poles, and absorbed overall constants into β . In particular, if we consider the limit $\eta = s_{13}/(s_{25}s_{45}) \rightarrow \infty$, we can just keep the leading contribution

$$\begin{aligned}
A^{\delta_{25}\delta_{45}\delta_{13}}(s_{25}, s_{45}, \eta, t_{12}, t_{34}) &\sim (-s_{13})^{\alpha_1}(-s_{45})^{\alpha_2 - \alpha_1}\Gamma(-\alpha_1)\Gamma(\alpha_1 - \alpha_2)\beta(\alpha_1, t_{12}, t_{34}) \\
&\quad + (-s_{13})^{\alpha_2}(-s_{25})^{\alpha_1 - \alpha_2}\Gamma(-\alpha_2)\Gamma(\alpha_2 - \alpha_1)\beta(\alpha_2, t_{12}, t_{34}),
\end{aligned} \quad (3.33)$$

which clearly does not have double discontinuities in s_{25} and s_{45} , as follows from our construction. Note that the apparent singularities in $\alpha_1 = \alpha_2$ are just spurious, as they cancel each other.

There are many subtleties and unproven statements in deriving the Regge theory result (3.32), but the final form seems very reasonable in physical terms. We can analyze these claims in specific models. We consider a dual resonance model of a five-particle amplitude in the so-called Bardakci-Ruegg representation [173]

$$\begin{aligned}
B_5 = \int \frac{dx_1}{x_1} \frac{dx_2}{x_2} x_1^{-\alpha(t_{12})} (1 - x_1)^{-1 - \alpha(s_{25})} x_2^{-\alpha(t_{34})} (1 - x_2)^{-1 - \alpha(s_{45})} \\
\times (1 - x_1 x_2)^{-\alpha(s_{13}) + \alpha(s_{25}) + \alpha(s_{45})},
\end{aligned} \quad (3.34)$$

where the integral ranges from 0 to 1 in x_1 and x_2 . We defined $\alpha(x) = \alpha_0 + x$ with α_0 the intercept of the Regge trajectory. As stated above, a single Regge limit happens when s_{25} (or s_{45}), $s_{13} \rightarrow \infty$ with their ratio fixed. In this limit, it can be shown [164] that the region $x_1 \approx 0$ dominates in the integral (3.34). For the values $0 < s_{25}/s_{13} < 1$, it can be

shown that

$$B_5 = (-s_{13})^{\alpha(t_{12})} \sum_{n=0}^{\infty} p_n \left(-\frac{s_{25}}{s_{13}} \right)^n + (-s_{13})^{\alpha(t_{34})} (-s_{25})^{\alpha(t_{12}) - \alpha(t_{34})} \sum_{n=0}^{\infty} q_n \left(-\frac{s_{25}}{s_{13}} \right)^n, \quad (3.35)$$

where

$$p_n(t_{12}, t_{34}, s_{45}) = \frac{\Gamma(n - \alpha(t_{12})) \Gamma(-n + t_{12} - t_{34}) \Gamma(n - \alpha(s_{45}))}{\Gamma(t_{12} - t_{34} - \alpha(s_{45})) n!}, \quad (3.36)$$

$$q_n(t_{12}, t_{34}, s_{45}) = \frac{\Gamma(n - \alpha(t_{34})) \Gamma(-n + t_{34} - t_{12}) \Gamma(n + t_{12} - t_{34} - \alpha(s_{45}))}{\Gamma(t_{12} - t_{34} - \alpha(s_{45})) n!}. \quad (3.37)$$

Note that there are no simultaneous singularities in the overlapping Mandelstam invariants. This follows from the explicit expressions of p_n and q_n . The first term has power-law behavior in s_{13} and poles in s_{45} , while having no singularities in s_{25} . The second term, on the other hand, has power-law behavior in both s_{25} and s_{13} times a function without any singularities in s_{45} . This is an instance of the Steinmann relations, which hold for the full amplitude. The double Regge limit corresponds to taking a further limit $s_{45} \rightarrow \infty$ with the ratio $\eta = s_{13}/(s_{25}s_{45})$ fixed. It leads to [164]

$$B_5 = (-s_{25})^{\alpha(t_{12})} (-s_{45})^{\alpha(t_{34})} \int_{-i\infty}^{i\infty} \frac{dm}{2\pi i} \Gamma(m - \alpha(t_{12})) \Gamma(m - \alpha(t_{34})) \Gamma(-m) (-\eta)^m, \quad (3.38)$$

which is of the same form as (3.32).

With the knowledge of the multi-Regge limit in S matrix theory, we are now in a position to study the multi-Regge limit in conformal field theories.

3.3 Kinematics of five-point conformal correlators

Correlation functions of local primary operators in any conformal field theory can be written in terms of a simple prefactor, that absorbs the weight of external operators, and a non-trivial function that depends on conformal invariant variables, usually called cross ratios, that contains all the dynamics of the correlator. In this chapter, we will be mostly focused

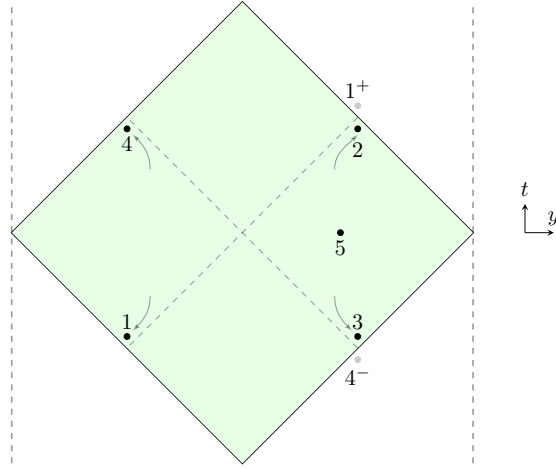


FIGURE 3.8: We show our proposal for the Regge limit of the five-point correlator.

in correlators involving five operators. These depend on five different cross ratios through¹⁰

$$\langle \mathcal{O}(x_1)\mathcal{O}(x_2)\mathcal{O}(x_3)\mathcal{O}(x_4)\mathcal{O}(x_5) \rangle = \frac{\left(\frac{x_{23}^2}{x_{13}^2}\right)^{\frac{\Delta_{12}}{2}} \left(\frac{x_{14}^2}{x_{13}^2}\right)^{\frac{\Delta_{34}}{2}}}{(x_{12}^2)^{\frac{\Delta_{1+}\Delta_2}{2}} (x_{34}^2)^{\frac{\Delta_{3+}\Delta_4}{2}}} \left(\frac{x_{13}^2}{x_{15}^2 x_{35}^2}\right)^{\frac{\Delta_5}{2}} \mathcal{G}(u_1 \dots u_5), \quad (3.39)$$

where $x_{ij}^2 = (x_i - x_j)^2$, we used the shorthand notation $\Delta_{ij} \equiv \Delta_i - \Delta_j$ and the cross ratios are defined as

$$u_1 = \frac{x_{12}^2 x_{35}^2}{x_{13}^2 x_{25}^2}, \quad u_{i+1} = u_i|_{x_i \rightarrow x_{i+1}}. \quad (3.40)$$

It is worth emphasizing that this is just a particular choice of cross ratios which is obviously not unique. For instance, $\tilde{u}_3 \equiv u_3 u_2$ would be as valid a choice as u_3 . The choice (3.40) has the nice feature that the cross ratios can be defined by transforming the x_i cyclically, *i.e.* $x_i \rightarrow x_{i+1}$. This is particularly interesting when studying observables that are cyclically symmetric [1, 64, 133].

In general, $\mathcal{G}(u_i)$ is an intricate function of the cross ratios with a complex analytic structure. One interesting question is, *what are the allowed singularities of a correlation function of five local operators and what is their physical meaning?* This is a hard question that we will not try to answer here in full generality (see [174] for progress in this direction). Instead, we shall focus on a particular singularity that is associated with the limit described in figure 3.8 and that is similar to the Regge limit of scattering amplitudes

¹⁰This is the same number as independent Mandelstam invariants in flat space scattering amplitudes as reviewed in the previous section. The connection between correlation functions in conformal field theories and scattering amplitudes is more clear in Mellin space, as we shall see in the next section.

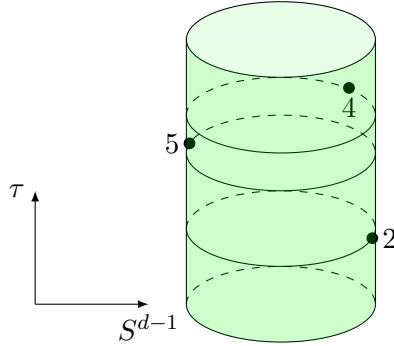


FIGURE 3.9: Position of points on the Euclidean cylinder. Two points 1 and 3, are at $\tau = -\infty$ and $\tau = \infty$.

reviewed in the previous section. There are two other more common (and simpler) singularities, the Euclidean and lightcone OPE limits which will be relevant for the Regge limit analysis. Indeed, it is possible to extract some information about these singularities from the conformal block decomposition of five points

$$\mathcal{G}(u_i) = \sum_{k_1 k_2, \ell} P_{k_1 k_2}^\ell G_{k_1 k_2}^\ell(u_1, \dots, u_5), \quad (3.41)$$

where $G_{k_1 k_2}^\ell(u_1, \dots, u_5)$ are conformal blocks in the channel (12) and (34), $P_{k_1 k_2}^\ell$ are products of three-point coefficients (to be described in more detail in the following subsection) and the sum is over all primary operators.

In the following subsections, we will review and explore the Euclidean and lightcone singularities and introduce the Regge limit for five-point correlation functions.

3.3.1 Euclidean limit

The simplest limit in a CFT is when two operators are brought close to each other. In this setup, the operator product expansion (OPE) is convergent and can be used safely. The OPE is perhaps one of the most important properties of a CFT. This feature tells that the product of two operators at distinct points can be replaced by a linear combination of operators

$$\mathcal{O}(x_1)\mathcal{O}(x_2) \approx \sum_k \frac{C_{12k}}{(x_{12}^2)^{\frac{\Delta_1 + \Delta_2 - (\Delta_k - J_k)}{2}}} F_k(x_{12}, D_z, \partial_{x_1}) \mathcal{O}_k(x_1, z), \quad (3.42)$$

where the sum runs over all primary operators, C_{12k} are the OPE coefficients and F_k is a differential operator that takes into account the contribution of descendants. The auxiliary null variable z is used to encode the open indices of a symmetric and traceless

spin J operator as

$$\mathcal{O}(x, z) \equiv z^{\mu_1} \dots z^{\mu_J} \mathcal{O}^{\mu_1 \dots \mu_J}(x), \quad (3.43)$$

while

$$D_{z^\mu} = \left(\frac{d}{2} - 1 + z \cdot \frac{\partial}{\partial z} \right) \frac{\partial}{\partial z^\mu} - \frac{1}{2} z^\mu \frac{\partial^2}{\partial z \cdot \partial z} \quad (3.44)$$

is used to recover the information about the indices. The exact form of F_k can be determined from consistency of two- and three-point correlation functions of local operators. It follows from a simple computation that, at the leading order and in the limit $x_2 \rightarrow x_1$, the function F_k is given by

$$F_k(x_{12}, D_z, \partial_{x_1}) = \frac{(x_{12} \cdot D_z)^{J_k}}{J_k! \left(\frac{d}{2} - 1 \right)_{J_k}} + \dots, \quad (3.45)$$

where \dots represent subleading terms. One feature of this simple result is that it is evident that the limit is dominated by operators with lowest dimension Δ_k . In particular, this determines the dominant contribution of a five-point conformal block in the limits $x_2 \rightarrow x_1$ and $x_4 \rightarrow x_3$

$$\sum_\ell P_{k_1 k_2}^\ell G_{k_1 k_2}^\ell(u_1, \dots, u_5) \approx \frac{C_{12k_1} C_{34k_2} (x_{12} \cdot D_z)^{J_1} (x_{34} \cdot D_{z'})^{J_2}}{(x_{12}^2)^{\frac{J_1 - \Delta_{k_1}}{2}} (x_{34}^2)^{\frac{J_2 - \Delta_{k_2}}{2}}} \langle \mathcal{O}_{k_1}(x_1, z) \mathcal{O}_{k_2}(x_3, z') \mathcal{O}(x_5) \rangle. \quad (3.46)$$

Note that the double limit in the pair of points (12) and (34) was taken to reduce the correlator to a three-point function which is fixed by symmetry as

$$\langle \mathcal{O}_{k_1}(x_1, z_1) \mathcal{O}_{k_2}(x_2, z_2) \mathcal{O}(x_3) \rangle = \sum_{\ell=0}^{\min(J_1, J_2)} \frac{C_{123}^\ell V_{123}^{J_1 - \ell} V_{213}^{J_2 - \ell} H_{12}^\ell}{(x_{12}^2)^{\frac{h_1 + h_2 - h_3}{2}} (x_{13}^2)^{\frac{h_1 + h_3 - h_2}{2}} (x_{23}^2)^{\frac{h_2 + h_3 - h_1}{2}}}, \quad (3.47)$$

where $h_i \equiv \Delta_i + J_i$ and

$$H_{12} = (z_1 \cdot x_{12})(z_2 \cdot x_{12}) - \frac{x_{12}^2 (z_1 \cdot z_2)}{2}, \quad V_{123} = \frac{(z_1 \cdot x_{12}) x_{13}^2 - (z_1 \cdot x_{13}) x_{12}^2}{x_{23}^2}. \quad (3.48)$$

It follows from (3.46) that the constants $P_{k_1 k_2}^\ell$ are given by

$$P_{k_1 k_2}^\ell = C_{12k_1} C_{34k_2} C_{k_1 k_2 5}^\ell. \quad (3.49)$$

Conformal blocks are complicated functions which are not known in closed form for general dimensions. However, it is possible to compute them as an expansion around some

limits. One method to obtain them takes advantage of the fact that they are eigenfunctions of the conformal Casimir differential equation

$$\left(\mathcal{D}_{12} - c_{\Delta_{k_1}, J_1} \right) G_{k_1 k_2}^\ell = 0, \quad (3.50)$$

with

$$c_{\Delta, J} = \Delta(\Delta - d) + J(d + J - 2), \quad \mathcal{D}_{12} = 2u_1^2 \partial_{u_1}^2 + \dots, \quad (3.51)$$

where \dots represent other subleading terms. We omitted an analogous equation in the (34) channel that can be obtained using symmetry.

The cross ratios (3.40) are not appropriate for all situations. For instance, in the limit considered above where $x_2 \rightarrow x_1$ and $x_4 \rightarrow x_3$, one has

$$u_1, u_3 \rightarrow 0, \quad u_i \rightarrow 1 \quad (i = 2, 4, 5), \quad (3.52)$$

which is insensitive to the angle at which the operators approach each other. For this limit, it is preferable to use instead another set of cross ratios¹¹[57]

$$\xi_1 = \frac{1 - u_5}{2\sqrt{u_1}}, \quad \xi_2 = \frac{1 - u_4}{2\sqrt{u_3}}, \quad \xi_3 = \frac{u_2 - 1}{2\sqrt{u_1}\sqrt{u_3}}, \quad (3.53)$$

which remain finite. These are related to the angles just mentioned above. The leading behavior, in the Euclidean OPE limit, of the five-point conformal block can be written in terms of these new cross ratios as

$$G_{k_1 k_2}^\ell = u_1^{\frac{\Delta_{k_1}}{2}} u_3^{\frac{\Delta_{k_2}}{2}} \mathcal{H}_\ell(\xi_i), \quad (3.54)$$

with

$$\mathcal{H}_\ell(\xi_i) = \prod_{i=1}^2 \frac{1}{J_i! \left(\frac{d}{2} - 1 \right)_{J_i}} \frac{(x_{12} \cdot D_z)^{J_1} (x_{34} \cdot D_{z'})^{J_2}}{(x_{12}^2)^{\frac{J_{k_1}}{2}} (x_{34}^2)^{\frac{J_{k_2}}{2}}} \frac{V_{135}^{J_1 - \ell} V_{315}^{J_2 - \ell} H_{13}^\ell}{(x_{13}^2)^{\frac{J_1 + J_3}{2}} (x_{15}^2)^{\frac{J_1 - J_2}{2}} (x_{35}^2)^{\frac{J_2 - J_1}{2}}}. \quad (3.55)$$

A brute force implementation of the action of the operators D_z and $D_{z'}$ on the previous expression for the function \mathcal{H}_ℓ will lead to a rather complicated sum [57] that we do not show since it will not be important in the discussion. A simple analysis reveals that the leading term of \mathcal{H}_ℓ in the limit $\xi_{1,2} \rightarrow \lambda \xi_{1,2}$, $\xi_3 \rightarrow \xi_3 \lambda^2$ for large λ , which corresponds to

¹¹We have decided to use slightly different angles as compared with [57] to make it appear more symmetric in the variables u_i .

considering lightcone limits¹² $x_{12}^2, x_{34}^2 \rightarrow 0$, is of the form

$$\mathcal{H}_\ell \approx \xi_1^{J_1-\ell} \xi_2^{J_2-\ell} \xi_3^\ell + \dots, \quad (3.56)$$

where the \dots represent subleading terms. Alternatively we can use the Casimir differential equation, in the Euclidean limit, to obtain subleading terms in (3.56)

$$[(1 - \xi_1^2) \partial_{\xi_1}^2 + (1 - \xi_3^2) \partial_{\xi_3}^2 - (d - 1)(\xi_1 \partial_{\xi_1} + \xi_3 \partial_{\xi_3}) - 2(\xi_1 \xi_3 + \xi_2) \partial_{\xi_1} \partial_{\xi_3} + C_{J_1}] \mathcal{H}_\ell = 0, \quad (3.57)$$

$$[(1 - \xi_2^2) \partial_{\xi_2}^2 + (1 - \xi_3^2) \partial_{\xi_3}^2 - (d - 1)(\xi_2 \partial_{\xi_2} + \xi_3 \partial_{\xi_3}) - 2(\xi_2 \xi_3 + \xi_1) \partial_{\xi_2} \partial_{\xi_3} + C_{J_2}] \mathcal{H}_\ell = 0,$$

with $C_J = J(J + 2h - 2)$. It is essential in extracting the dots in (3.56) from the Casimir equation to assume that \mathcal{H}_ℓ is polynomial in the variables ξ_i . However, this follows from the definition (3.55).

It turns out that, after changing the cross ratio ξ_3 to ζ defined by¹³

$$\xi_3 = -\xi_1 \xi_2 + \zeta \sqrt{(1 - \xi_1^2)(1 - \xi_2^2)}, \quad (3.58)$$

the Casimir differential equation becomes much simpler

$$\left[J_1 (d + J_1 - 2) + \frac{(d - 2)\zeta \partial_\zeta + (\zeta^2 - 1)\partial_\zeta^2}{\xi_1^2 - 1} + (1 - d)\xi_1 \partial_{\xi_1} + (1 - \xi_1^2)\partial_{\xi_1}^2 \right] \mathcal{H}_\ell = 0 \quad (3.59)$$

with an analogous equation for J_2 . This form of the differential equation allows to look for solutions with a factorized form

$$\tilde{\mathcal{H}} = f_1(\xi_1) f_2(\xi_2) g(\zeta), \quad (3.60)$$

where we have used tilde to emphasize that the solution is factorized and possibly different from (3.55). The function $g(\zeta)$ satisfies a differential equation that can be read from (3.59)

$$[(\zeta^2 - 1)\partial_\zeta^2 + (d - 2)\zeta \partial_\zeta + \ell'(\ell' + d - 3)] g_{\ell'} = 0, \quad (3.61)$$

where the separation constant $\ell'(\ell' + d - 3)$ was chosen for convenience. One solution to this differential equation that is polynomial in ζ is given by

$$g_{\ell'} = {}_2F_1\left(-\ell', \ell' + d - 3, \frac{d - 2}{2}, \frac{1 - \zeta}{2}\right) = \frac{\ell'! \Gamma(2h - 3)}{\Gamma(2h + \ell' - 3)} C_{\ell'}^{\frac{d-3}{2}}(\zeta). \quad (3.62)$$

¹²In this limit we can discard the second term in the differential operator D_z which in turn makes its action easier to implement. This just corresponds to throwing away the contribution of terms associated with traces.

¹³These cross ratios were introduced in the context of conformal field theories in [152].

This is clearly a polynomial of degree ℓ' . It is also simple to check that

$$f_1(\xi_1) = (1 - \xi_1^2)^{\frac{\ell'}{2}} C_{J_1 - \ell'}^{\frac{d-2}{2} + \ell'}(\xi_1), \quad (3.63)$$

is a solution to the differential equation arising from (3.59). The solution f_2 can be obtained analogously. It can also be checked that this new solution $\tilde{\mathcal{H}}_{\ell'}$ is consistent with the non-factorized \mathcal{H}_{ℓ} in (3.55). Let us see how in more detail.

Both \mathcal{H}_{ℓ} and $\tilde{\mathcal{H}}_{\ell'}$ satisfy the same differential equation, however they are not the same function. Nevertheless it is possible to express \mathcal{H}_{ℓ} in terms of $\tilde{\mathcal{H}}$ and vice-versa, that is

$$\tilde{\mathcal{H}}_{\ell'} = \sum_{\ell=0}^{\ell'} C_{\ell\ell'} \mathcal{H}_{\ell}, \quad (3.64)$$

The coefficients $C_{\ell\ell'}$ can be thought as a change of basis of three-point functions. To determine them it is useful to take the limit $\xi_{1,2} \rightarrow \lambda \xi_{1,2}$ and $\xi_3 = \xi_3 \lambda^2$, with λ large. In this limit the functions \mathcal{H}_{ℓ} and $\tilde{\mathcal{H}}_{\ell}$ behave as

$$\mathcal{H}_{\ell} \approx \xi_1^{J_1 - \ell} \xi_2^{J_2 - \ell} \xi_3^{\ell} + \dots, \quad \tilde{\mathcal{H}}_{\ell'} \approx \tilde{c} \xi_1^{J_1} \xi_2^{J_2} g_{\ell'}(\zeta) + \dots, \quad (3.65)$$

$$\tilde{c} = \frac{\Gamma(h + J_1 - 1) \Gamma(h + J_2 - 1) 2^{J_1 + J_2 - 2\ell'}}{\Gamma(h + \ell' - 1)^2 \Gamma(J_1 - \ell' + 1) \Gamma(J_2 - \ell' + 1)}, \quad (3.66)$$

where $\zeta \rightarrow (\xi_1 \xi_2 + \xi_3)/(\xi_1 \xi_2)$ and the \dots represent subleading terms. Using the previous equation and (3.64) we can find the coefficients. Let us start by $C_{\ell\ell'}$,

$$\xi_1^{J_1} \xi_2^{J_2} \sum_{\ell=0}^{\ell'} C_{\ell\ell'} \left(\frac{\xi_3}{\xi_1 \xi_2} \right)^{\ell} = \xi_1^{J_1} \xi_2^{J_2} g_{\ell'}(\zeta) = \xi_1^{J_1} \xi_2^{J_2} \sum_{k=0}^{\ell'} \frac{(-\ell')_k (\ell' + d - 3)_k}{k! \left(\frac{d-2}{2} \right)_k} \left(\frac{1 - \zeta}{2} \right)^k, \quad (3.67)$$

where $\xi_3/(\xi_1 \xi_2) = \zeta - 1$. The coefficients $C_{\ell\ell'}$ can be obtained straightaway leading to

$$C_{\ell\ell'} = \tilde{c} (-1)^{\ell} \frac{(-\ell')_{\ell} (\ell' + d - 3)_{\ell}}{\ell! \left(\frac{d-2}{2} \right)_{\ell} 2^{\ell}}. \quad (3.68)$$

To find the inverse relation we make use of the identity

$$\sum_{\ell'=0}^{\ell} \frac{(c)_{\ell} (\ell')_{\ell} (b + 2\ell') (-1)^{\ell'}}{(b + 1 + \ell')_{\ell} (b + \ell')} {}_2F_1 \left(-\ell', b + \ell', c, \frac{x}{2} \right) = \left(\frac{x}{2} \right)^{\ell}, \quad (3.69)$$

for any variable x and constants b and c . Using this equation the inverse matrix $\tilde{C}_{\ell'\ell}$ follows immediately

$$\tilde{C}_{\ell'\ell} = \frac{1}{\tilde{c}} \frac{(-1)^{\ell'}(d+2\ell'-3)\binom{\ell}{\ell'} \binom{d-2}{2}_{\ell}}{(d+\ell'-3)(d+\ell'-2)_{\ell}}. \quad (3.70)$$

This concludes the change of basis from (3.47) to the one that leads to (3.60), which we call factorized basis. In this basis, the three-point function can be written as ¹⁴

$$\langle \mathcal{O}_{k_1}(x_1, z_1) \dots \mathcal{O}(x_3) \rangle = \frac{V_{123}^{J_1} V_{213}^{J_2} \sum_{\ell=0}^{\min(J_1, J_2)} \tilde{C}_{\ell} {}_2F_1 \left(-\ell, \ell+d-3, \frac{d-2}{2}, \frac{H_{12}}{2V_{123}V_{213}} \right)}{(x_{12}^2)^{\frac{h_1+h_2-h_3}{2}} (x_{13}^2)^{\frac{h_1+h_3-h_2}{2}} (x_{23}^2)^{\frac{h_2+h_3-h_1}{2}}}, \quad (3.71)$$

where \tilde{C}_{ℓ} are the OPE coefficients in the new basis. Let us remark that this is still polynomial in the structures V and H , as it should. The factorized basis for the leading behavior of the block in the Euclidean OPE limit is a new result. It would be interesting to construct conformal blocks in a radial expansion[42, 57, 59] using this new basis.

3.3.2 Lightcone limit

The distance between two operators, in Lorentzian kinematics, can be small when one of them approaches the lightcone of the other. This is in contrast with what has been analyzed in the previous subsection where the operators were actually close in the Euclidean sense. The OPE and more generally correlation functions are naturally organized, in this limit, in terms of distances between the almost null related operators. For example, the leading term in F_k of (3.42), in the limit $x_{12}^2 \rightarrow 0$, is given by

$$F_k = (x_{12} \cdot \partial_{z_1})^{J_k} \int_0^1 [dt] e^{tx_{12} \cdot \partial_{x_1}}, \quad (3.72)$$

where

$$[dt] \equiv \frac{\Gamma(\Delta_k + J_k)}{\Gamma^2(\frac{\Delta_k + J_k}{2})} (t(1-t))^{\frac{\Delta_k + J_k}{2} - 1} dt \quad (3.73)$$

¹⁴Note that, for integer ℓ , the hypergeometric reduces to a polynomial,

$${}_2F_1 \left(-\ell, \ell+d-3, \frac{d-2}{2}, \frac{H_{12}}{2V_{123}V_{213}} \right) = \sum_{\ell'=0}^{\ell} \frac{(-\ell)_{\ell'} (\ell+d-3)_{\ell'}}{\ell'! \binom{d-2}{2}_{\ell'} 2^{\ell'}} \left(\frac{H_{12}}{2V_{123}V_{213}} \right)^{\ell'} = \sum_{\ell'=0}^{\ell} C_{\ell'\ell} \left(\frac{H_{12}}{2V_{123}V_{213}} \right)^{\ell'}. \quad (3.74)$$

for spin J_k operators. For exchanged scalar operators, it is also easy to write down the formula for F_k , including all subleading corrections,

$$F_k = \sum_{n=0}^{\infty} \frac{(-x_{12}^2)^n \left(\frac{\Delta-a}{2}\right)_n \left(\frac{\Delta+a}{2}\right)_n}{2^{2n}(\Delta)_{2n} \left(\frac{2\Delta-d}{2}\right)_n n!} {}_1F_1\left(\frac{2n+\Delta+a}{2}, 2n+\Delta, x_{21} \cdot \partial_{x_1}\right) (\partial_{x_1}^2)^n, \quad (3.74)$$

with $a = \Delta_{12}$ and ${}_1F_1(a, b, x) = \int_0^1 dt \frac{t^{a-1}(1-t)^{b-a-1}\Gamma(b)}{\Gamma(a)\Gamma(b-a)} e^{tx}$. In turn, these two formulae can be used to derive the five-point conformal blocks in the lightcone limit by just applying the OPE formula to a five-point correlator. For the leading term of spinning lightcone conformal blocks we have

$$G_{k_1 k_2, J_1, J_2}^{\ell} = u_1^{\frac{\Delta_{J_1}-J_1}{2}} u_3^{\frac{\Delta_{J_2}-J_2}{2}} (1-u_2)^{\ell} u_5^{\frac{\Delta_{\phi}}{2}} \int_0^1 [dt_1][dt_2] \mathcal{I} \quad (3.75)$$

with

$$\mathcal{I} = \frac{\left(1-t_1(1-u_2)u_4-u_2u_4\right)^{J_2-\ell} \left(1-t_2(1-u_2)u_5-u_2u_5\right)^{J_1-\ell}}{\left(1-(1-u_4)t_2\right)^{\frac{h_2-\tau_1-2\ell+\Delta_{\phi}}{2}} \left(1-(1-u_5)t_1\right)^{\frac{h_1-\tau_2-2\ell+\Delta_{\phi}}{2}} \left(1-(1-t_1)(1-t_2)(1-u_2)\right)^{\frac{h_1+h_2-\Delta_{\phi}}{2}}}. \quad (3.76)$$

For the scalar blocks in the lightcone we can write

$$G_{k_1 k_2 00}^0 = \sum_{n_1, n_2=0}^{\infty} u_1^{\frac{\Delta_{k_1}+2n_1}{2}} u_3^{\frac{\Delta_{k_2}+2n_2}{2}} u_2^{\frac{\Delta_{21}}{2}} u_4^{\frac{2n_1+\Delta_{34}-\Delta_5+\Delta_{k_1}}{2}} u_5^{\frac{2n_2+\Delta_{21}+\Delta_{k_2}}{2}} \int_0^1 dt_1 dt_2 \tilde{\mathcal{I}}_{n_1, n_2}, \quad (3.77)$$

where the formula for $\tilde{\mathcal{I}}_{n_1, n_2}$ is shown in appendix 3.A. The cross ratios u_i are appropriate to describe the lightcone limit $x_{12}^2, x_{34}^2 \rightarrow 0$, as only two of them go to zero while the others remain fixed.

One feature that is evident from the formulae above is that this limit is dominated by operators that have lowest twist, defined by $\Delta - J$. Hints of this property are already present in (3.42) and (3.45).

Another interesting attribute of the lightcone block is that it allows to probe Lorentzian regimes, this in sharp contrast with the Euclidean expansion (3.60) that is only valid when the point x_2 is in the vicinity of x_1 . In particular, the integral formulation of both (3.72) and (3.74) is specially suitable to study monodromies of the block.

3.3.3 Regge limit

The limits described in the previous section shared a common feature as they could be taken in a kinematics where all points are still spacelike separated from each other. This is a significant restriction on the positions of operators and the physics that one is probing

with a given correlation function. The goal of this subsection is to introduce and describe another limit, the Regge limit, as depicted in figure 3.8. The main novelty is that some points are timelike related, while others are still spacelike separated, more concretely the pairs of points $(1, 4), (2, 3), (3, 5), (2, 5)$ are timelike, while the other pairs remain spacelike. The configuration represented in figure 3.8 can be parametrized by the following variables

$$x_1 = -r (\sinh \delta_1, \cosh \delta_1, \mathbf{0}_{d-2}), \quad x_2 = r (\sinh \delta_2, \cosh \delta_2, \mathbf{0}_{d-2}), \quad (3.78)$$

$$x_3 = (-\sinh \delta_2, \cosh \delta_2, \mathbf{0}_{d-2}), \quad x_4 = (\sinh \delta_1, -\cosh \delta_1, \mathbf{0}_{d-2}), \quad x_5 = (0, h_1, h_2, \mathbf{0}_{d-3}).$$

where δ_i are being taken to infinity and r and h_i can assume generic values. Here we also use a d -dimensional vector of zeros denoted by $\mathbf{0}_d$. This configuration can also be written in terms of the cross ratios u_i as

$$\begin{aligned} u_1 &= \frac{4r^2 (x_5^2 + 1 - 2h_1 \cosh \delta_2)}{(1 + r^2 + 2r \cosh \delta) (x_5^2 + r^2 - 2h_1 r \cosh \delta_1)}, & u_2 &= \left(\frac{1 + r^2 - 2r \cosh \delta}{1 + r^2 + 2r \cosh \delta} \right)^2, \\ u_3 &= \frac{4 (x_5^2 + r^2 - 2h_1 r \cosh \delta_1)}{(1 + r^2 + 2r \cosh \delta) (x_5^2 + 1 - 2h_1 \cosh \delta_2)}, & (3.79) \\ u_4 &= \frac{1}{\sqrt{u_2}} \frac{x_5^2 + 1 + 2h_1 \cosh \delta_2}{x_5^2 + 1 - 2h_1 \cosh \delta_2}, & u_5 &= \frac{1}{\sqrt{u_2}} \frac{x_5^2 + r^2 + 2h_1 r \cosh \delta_1}{x_5^2 + r^2 - 2h_1 r \cosh \delta_1}, \end{aligned}$$

where $\delta = \delta_1 + \delta_2$ and $x_5^2 = h_1^2 + h_2^2$. It is simple to see that both u_1 and u_3 approach zero as the δ_i are sent to infinity and that the remaining u_i go to 1 (note that u_2 approaches 1 faster than the other two cross ratios). This limit, in terms of cross ratios, is the same as the Euclidean OPE limit discussed in section 3.3.1. The main distinction between these two limits resides in the different causal ordering of the operators. The similarity to the Euclidean OPE limit should come as no surprise to the reader that is familiar with Regge limit for four points. In reality there is a simple reason for this to be the case as one can also interpret this configuration as an OPE limit between 1^+ and 2 , as well as 3 and 4^- , where 1^+ and 4^- are defined respectively as the image of the points 1 and 4 on the next and previous Poincaré patch on the Lorentzian cylinder. This is shown in figure 3.8.

The fifth point is kind of a spectator in this limit. Nonetheless, it is important as it allows to introduce other parameters to differentiate the gaps δ_1 and δ_2 . This is essentially the same as we already see in the Regge limit of five-point scattering amplitudes.

Note that in this section we made a choice of analytic continuation but there are other possible ways to attain Regge kinematics. Indeed, with some care, one can even move the fifth point in other directions and even boost it and find similar OPE behavior after lightcones are crossed. The latter can be used as a guiding principle when we look

for Regge kinematics. In Appendix 3.D, we present some additional kinematics and path continuations that might be useful in understanding single-Reggeon exchanges or the Regge limit six-point functions in CFTs .

As mentioned before, the different causal relations between the points have important consequences. The analysis of the correlator in this setting is more elaborate and for this reason we devote the next section to it.

3.3.4 Conformal partial waves

The conformal block decomposition (3.41) is not the most appropriate option to analyze the Regge limit of correlation functions. A better alternative is to do the so-called conformal partial wave decomposition

$$\mathcal{G}(u_i) = \sum_{J_i=0}^{\infty} \sum_{\ell=0}^{\min(J_1, J_2)} \int_{-\infty}^{\infty} \frac{d\nu_1}{2\pi i} \frac{d\nu_2}{2\pi i} b_{J_1 J_2}^{\ell}(\nu_1, \nu_2) F_{\nu_1, \nu_2, J_1, J_2, \ell}(u_i), \quad (3.80)$$

where the conformal partial wave coefficient $b_{J_1 J_2}^{\ell}(\nu_1, \nu_2)$ contains all the dynamical information of the correlation function, *i.e.* dimensions and OPE coefficients. The function $F_{\nu_1, \nu_2, J_1, J_2, \ell}(u_i)$ is the conformal partial wave defined by the integral

$$F_{\nu_1, \nu_2, J_1, J_2, \ell}(u_i) = \frac{(x_{12}^2 x_{34}^2)^{\Delta_\phi} (x_{15}^2 x_{35}^2)^{\frac{\Delta_\phi}{2}}}{(x_{13}^2)^{\frac{\Delta_\phi}{2}}} \int d^d x_6 d^d x_7 \langle \mathcal{O}_{\frac{d}{2}-i\nu_1}(x_6, D_{z_1}) \mathcal{O}_{\frac{d}{2}-i\nu_2}(x_7, D_{z_2}) \mathcal{O}(x_5) \rangle^{(\ell)} \\ \times \langle \mathcal{O}(x_1) \mathcal{O}(x_2) \mathcal{O}_{\frac{d}{2}+i\nu_1}(x_6, z_1) \rangle \langle \mathcal{O}(x_3) \mathcal{O}(x_4) \mathcal{O}_{\frac{d}{2}+i\nu_2}(x_7, z_2) \rangle, \quad (3.81)$$

where the $\langle \rangle^{(\ell)}$ should be understood as the term proportional to C_{123}^{ℓ} in (3.47) (in other words, it is just the space dependence of the three-point function) and D_z is the differential operator defined in (3.44). It is simple to see that both integrals in x_6 and x_7 are conformal and that $F_{\nu_i, J_i, \ell}$ should satisfy the conformal Casimir equation in the channels (12) and (34) with eigenvalue $C_{\frac{d}{2}+i\nu_1, J}$ and $C_{\frac{d}{2}+i\nu_2, J_2}$, respectively. In particular, this implies that the conformal partial wave can be written as a linear combination of conformal blocks which solve the same equation

$$F_{\nu_1, \nu_2, J_i, \ell} = \sum_{\tilde{\ell}} \sum_{\alpha_1, \alpha_2 = \pm} A_{\alpha_1, \alpha_2}^{\ell\tilde{\ell}} G_{\frac{d}{2}+i\alpha_1\nu_1, \frac{d}{2}+i\alpha_2\nu_2, J_i}^{\tilde{\ell}}(u_i), \quad (3.82)$$

where we used the symmetry of the eigenvalue $C_{\frac{d}{2}+i\nu_i, J_i} = C_{\frac{d}{2}-i\nu_i, J_i}$. The sum over $\tilde{\ell}$ appears because the Casimir equation is not able to fix it, and so in principle we can have a sum over this number. The coefficients $A^{\ell\tilde{\ell}}$ were determined in [1] and are expressed in

terms of several sums. It would be interesting to see if the coefficients in the new basis introduced in 3.3.1 are simpler and, more importantly for this work, analytic in spin. The conformal partial waves have the advantage that are Euclidean single valued¹⁵. Recall that the correlator also enjoys this property in contrast with a single conformal block.

3.4 Regge theory

3.4.1 Wick rotation or how to go Lorentzian

The Regge limit of a correlation function is an intrinsically Lorentzian limit that explores a specific causal configuration of the operators. On the other hand, CFTs have been better understood in Euclidean space. It is thus important to understand how to analytically continue from Euclidean to Lorentzian space and what can we say about convergence and other properties of the Lorentzian correlator from CFT axioms. These questions have only very recently been discussed in firmer grounds in [97, 176], extending the works of Lüscher and Mack [177, 178]. However, there the analysis focuses only on correlation functions of $n \leq 4$ points and no systematic study for higher-point functions exists to date.¹⁶

We want to consider Lorentzian invariant correlation functions of local operators that commute at spacelike separated points,

$$\mathcal{W}(x_1, x_2, \dots, x_n) = \langle \mathcal{O}(x_1) \mathcal{O}(x_2) \dots \mathcal{O}(x_n) \rangle. \quad (3.83)$$

These are called Wightman functions (or distributions). In particular, note that up to spacelike separated points, different orders of local operators give rise to different Wightman functions. We stress that these are not the standard time-ordered correlation functions one encounters in QFT textbooks. In fact, one can decompose time-ordered correlation

¹⁵Conformal partial waves are single valued for integer J . It should be possible to add a term to them to make them single valued for positive real J as was done in [175] for four points. We hope to return to this point in the future.

¹⁶This seems to be technically challenging (see discussion of Appendix B of [97]) but we hope that our results may also increase the motivation of community to tackle these questions on higher-point functions.

functions in terms of Wightman functions¹⁷

$$\begin{aligned} \langle \Omega | T\{\mathcal{O}(x_1)\mathcal{O}(x_2) \dots \mathcal{O}(x_n)\} | \Omega \rangle &= \\ &= \langle \Omega | \mathcal{O}(t_1, \mathbf{x}_1)\mathcal{O}(t_2, \mathbf{x}_2) \dots \mathcal{O}(t_n, \mathbf{x}_n) | \Omega \rangle \theta(t_1 > t_2 > \dots > t_n) + \text{permutations} \\ &= \mathcal{W}(x_1, x_2, \dots, x_n) \theta(t_1 > t_2 > \dots > t_n) + \text{permutations}. \end{aligned} \quad (3.84)$$

One Wightman axiom states that Wightman functions are indeed tempered distributions even at coincident points. This means that when integrated against test functions belonging to Schwartz class $f(x_i) \in \mathcal{S}$, the following integral is finite

$$\int d^d x_1 \dots d^d x_n \mathcal{W}(x_1, \dots, x_n) f(x_1) \dots f(x_n) < \infty. \quad (3.85)$$

Our goal is to reach a Wightman correlation function with a given order starting from a translational- and rotational-invariant Euclidean one. The basic idea is that there should be some holomorphic function $G(x_1, \dots, x_n)$ that reduces to a Lorentzian correlator in a given limit and to a Euclidean one in another. Let us then consider a real-analytic (away from coincident points) Euclidean correlator, with operators at $x_i = (\tau_i, \mathbf{x}_i)$,

$$\langle \mathcal{O}(\tau_1, \mathbf{x}_1)\mathcal{O}(\tau_2, \mathbf{x}_2) \dots \mathcal{O}(\tau_n, \mathbf{x}_n) \rangle^E, \quad (3.86)$$

where Euclidean times τ_i are ordered $\tau_1 > \tau_2 > \dots > \tau_n$. Recall that this ordering is necessary. If we assume the existence of a Hilbert space and a Hamiltonian that is bounded from below, we get that our Euclidean correlator can be rewritten as

$$\langle \Omega | \mathcal{O}(0, \mathbf{x}_1) e^{-H(\tau_1 - \tau_2)} \mathcal{O}(0, \mathbf{x}_2) e^{-H(\tau_2 - \tau_3)} \dots \mathcal{O}(\tau_n, \mathbf{x}_n) | \Omega \rangle^E, \quad (3.87)$$

where we use the Heisenberg representation of the field operators \mathcal{O} . To avoid high-energy states being exponentially enhanced, we immediately recognize that the Euclidean correlator needs to be “time-ordered”.

To move towards a Lorentzian configuration, we want to consider an analytic continuation of the Euclidean correlator. This is achieved by taking $\tau_i \rightarrow \epsilon_i + it_i$. Heuristically, adding the imaginary parts does not harm the convergence, as long as we keep $\epsilon_1 > \dots > \epsilon_n$. This analytic continuation defines our function $G(x_1, \dots, x_n)$ that is holomorphic in $\tau_i = \epsilon_i + it_i$ and real-analytic in \mathbf{x}_i . We can then find a Lorentzian correlator

¹⁷We assume the existence of a Hilbert space with a unique vacuum Ω under the unitary action of the Poincaré group. We can however talk about Wightman distributions without making any such assumption since Wightman’s reconstruction theorem guarantees that we would find a Hilbert space once we assumed spectral and positivity properties of the distributions - see [97, 179].

by sending $\epsilon_i \rightarrow 0$ while keeping the order of limits,

$$\langle \Omega | \mathcal{O}(t_1, \mathbf{x}_1) \dots \mathcal{O}(t_n, \mathbf{x}_n) | \Omega \rangle \equiv \lim_{\substack{\epsilon_i \rightarrow 0 \\ \epsilon_1 > \dots > \epsilon_n}} \langle \Omega | \mathcal{O}(\epsilon_1 + it_1, \mathbf{x}_1) \dots \mathcal{O}(\epsilon_n + it_n, \mathbf{x}_n) | \Omega \rangle^E. \quad (3.88)$$

This formally defines our Wightman function $\mathcal{W}(x_1, \dots, x_n)$. Note that to achieve different orderings we should start from an Euclidean correlator in a different ordering. Holomorphicity may however be lost as we take $\epsilon_i \rightarrow 0$. We expect nonetheless the correlator to converge at least in a distributional sense. For CFT Wightman functions, the authors in [97] found power law bounds and used Vladimirov's theorem to assure that indeed this limit converges at least in the distributional sense (even at coincident points) for $n \leq 4$ -point functions in Minkowski space.¹⁸

We want to consider the Regge limit of CFT five-point functions of identical scalars. In this context, we are interested in correlation functions where the operator ordering is consistent with time ordering. Using the causal relations of figure 3.8, we take

$$\langle \phi(x_4) \phi(x_1) \phi(x_2) \phi(x_5) \phi(x_3) \rangle, \quad (3.89)$$

where permutations between spacelike separated operators are equivalent. As we approach the Regge kinematics, starting from a configuration where all operators are spacelike separated (essentially equivalent to a Euclidean configuration), we find branch-cut singularities whenever an operator crosses the lightcone of another. The way we deal with branch-cuts depends on the $i\epsilon$ prescription we adopted to reach this ordering of the Wightman function. In particular, as we move from fully spacelike separated points to the Regge kinematics we have $\{x_{14}^2, x_{23}^2, x_{25}^2, x_{35}^2\} \rightarrow \{|x_{14}^2|, |x_{23}^2|, |x_{25}^2|, |x_{35}^2|\} \times \exp(\pi i)$ which implies that the cross-ratios u_2, u_4 and u_5 go around 0 with the first going anticlockwise and the last two in clockwise direction. At the branch-cuts, OPEs $\phi_1 \times \phi_2$ and $\phi_3 \times \phi_4$, in which we block decompose our correlation function, are no longer convergent. We should then worry about boundedness in Regge limit. For a four-point function in the Regge limit and with operator ordering consistent with time ordering one can prove its boundedness. The general proof uses Rindler positivity [79, 180–182] and bounds the latter Wightman function with another correlator of different ordering where the OPE does converge. This proof does not work however with five-point functions. Nonetheless, we expect to be possible to find these type of bounds between different ordered Wightman functions or different channel

¹⁸All the remaining Wightman axioms were also proved from standard axioms of translational- and rotational- invariant Euclidean correlators.

decompositions but we will not make these considerations any more precise here. Conformal Regge theory, on the other hand, provides a method to resum divergent OPEs and exhibit the dominant Reggeon-exchange contributions. This resummation invokes an analytic continuation of OPE data in spin for which, in the case of four-point functions, the justification follows from the Lorentzian inversion formula [79, 101]. For higher-point functions, there are additional representation labels associated with the possible three-point structures between spinning operators.

In what follows we focus on double Reggeon-exchanges but similar analysis can be performed at the level of the single Reggeon exchanges, that we briefly discuss in Appendix 3.D. The proper $i\epsilon$ prescription for these cases follows straightforwardly from the corresponding kinematics since we want to consider the operator orderings consistent with time ordering.

3.4.2 Mellin amplitudes

The similarities of Mellin and flat space scattering amplitudes make the former a suitable tool to build intuition. The goal of this section is to analyze the Regge limit for Mellin amplitudes [86]. We shall see that the Regge limit for five operators, as defined in the previous section, is dominated by the same kinematics of flat space scattering amplitudes reviewed in section 3.2. In the following, we will review the definition of Mellin amplitudes, some of its properties and then analyze the Regge limit in this language. The definition of a Mellin amplitude, $\mathcal{M}(\delta_{ij})$, is given by¹⁹

$$\langle \mathcal{O}(x_1) \dots \mathcal{O}(x_n) \rangle = \int [d\delta_{ij}] \mathcal{M}(\delta_{ij}) \prod_{1 \leq i < j \leq n} \frac{\Gamma(\delta_{ij})}{(x_{ij}^2)^{\delta_{ij}}} , \quad (3.90)$$

where we decided to extract a standard prefactor containing Γ functions and the integration variables δ_{ij} run parallel to the imaginary axis. Since the Mellin variables are restricted by the condition $\sum_j \delta_{ij} = 0$, with $\delta_{ii} = -\Delta_i$, we shall use the following set of independent Mellin variables

$$\begin{aligned} t_{12} &= 2\Delta_\phi - 2\delta_{12} , & t_{34} &= 2\Delta_\phi - 2\delta_{34} , \\ s_{13} &= \Delta_\phi + 2\delta_{13} , & s_{25} &= -2\delta_{25} , & s_{45} &= -2\delta_{45} , \end{aligned} \quad (3.91)$$

¹⁹Here we are assuming that there exists a Mellin amplitude. This might only be true if one performs some subtractions of the correlator, such as the contribution of the identity.

which is the same number as conformal cross ratios - see figure 3.10. One advantage of Mellin amplitudes is that it is easy to analytically continue from the Euclidean configuration to Lorentzian, as the space-time dependence is simple [142]. For example, the configuration of figure 3.8 can be obtained just by adding a phase to the integrand [86]

$$G^\circlearrowleft(u_i) = \int [dt_{ij} ds_{ij}] u_4^{\frac{s_{45}}{2}} u_1^{\frac{t_{12}}{2}} u_3^{\frac{t_{34}}{2}} u_2^{\frac{s_{13}+s_{45}-t_{12}}{2}} u_5^{\frac{t_{34}-s_{25}-t_{12}}{2}} \mathcal{M}(s_{ij}, t_{ij}) e^{-i\pi \frac{2(s_{13}+s_{25}+s_{45})+\Delta_\phi}{2}} \Gamma\left(-\frac{s_{25}}{2}\right) \Gamma\left(-\frac{s_{45}}{2}\right) \Gamma\left(\frac{s_{13}+s_{25}+s_{45}}{2}\right) \Gamma\left(\frac{s_{13}-\Delta_\phi}{2}\right) \Gamma\left(\frac{t_{12}-s_{13}-s_{45}}{2}\right) \Gamma\left(\frac{t_{34}-s_{13}-s_{25}}{2}\right) \Gamma\left(\frac{2\Delta_\phi-t_{12}}{2}\right) \Gamma\left(\frac{2\Delta_\phi-t_{34}}{2}\right) \Gamma\left(\frac{\Delta_\phi+s_{25}+t_{12}-t_{34}}{2}\right) \Gamma\left(\frac{\Delta_\phi+s_{45}-t_{12}+t_{34}}{2}\right) \quad (3.92)$$

where G^\circlearrowleft is the correlator analytically continued to the Regge kinematics. This particular phase seems to make the integrand divergent for large imaginary values of s_{ij} . However, the Γ functions in the definition of the Mellin amplitude cancel this apparent divergence. To see this in more detail we just have to use the identity

$$\Gamma\left(a + i\frac{x_i}{2}\right) \Gamma\left(b - i\frac{x_i}{2}\right) \approx 2\pi e^{i\frac{\pi}{2}(a-b)} \left(\frac{x_i}{2}\right)^{a+b-1} e^{-\frac{\pi}{2}x_i}, \quad (3.93)$$

in a regime where s_{13} goes faster to infinity than s_{45} and s_{25} . In the Regge limit, as defined in section 3.3.3, we have that the cross ratios $u_2 \rightarrow 1 + \sigma_1 \sigma_2 \xi_3$, $u_4 \rightarrow 1 - \sigma_2 \xi_2$, $u_5 \rightarrow 1 - \sigma_1 \xi_1$, with $u_1 = \sigma_1^2$, $u_3 = \sigma_2^2$ going to zero while ξ_i are left fixed. This simplifies the dependence of the Mellin amplitude on the cross ratios

$$u_4^{\frac{s_{45}}{2}} u_1^{\frac{t_{12}}{2}} u_3^{\frac{t_{34}}{2}} u_2^{\frac{s_{13}+s_{45}-t_{12}}{2}} u_5^{\frac{t_{34}-s_{25}-t_{12}}{2}} \rightarrow u_1^{\frac{t_{12}}{2}} u_3^{\frac{t_{34}}{2}} e^{\frac{i(y_{25}\sigma_1\xi_1+y_{45}\sigma_2\cosh\xi_2-y_{13}\sigma_1\sigma_2\xi_3)}{2}}, \quad (3.94)$$

where we made the change $s_{ij} = iy_{ij}$. Note that the exponent is not small provided σ_i and y_{ij} scale appropriately. By putting every piece together we obtain that in the Regge limit

$$G^\circlearrowleft(u_i) = \pi^4 \int [dt_{ij}] \Gamma\left(\frac{2\Delta_\phi-t_{12}}{2}\right) \Gamma\left(\frac{2\Delta_\phi-t_{34}}{2}\right) \frac{\sigma_1^{t_{12}} \sigma_2^{t_{34}}}{2^{\frac{t_{12}+t_{34}+\Delta_\phi-16}{2}} e^{\frac{i\pi(\Delta_\phi+3t_{12}-t_{34})}{4}}} \int [dy_{ij}] y_{13}^{\frac{t_{12}+t_{34}-4-\Delta_\phi}{2}} y_{25}^{\frac{t_{12}+\Delta_\phi-t_{34}-2}{2}} y_{45}^{\frac{t_{34}+\Delta_\phi-t_{12}-2}{2}} e^{\frac{i(y_{25}\sigma_1\xi_1+y_{45}\sigma_2\cosh\xi_2-y_{13}\sigma_1\sigma_2\xi_3)}{2}} \mathcal{M}(t_{ij}, y_{ij}), \quad (3.95)$$

where we have defined $u_1 = \sigma_1^2$, $u_3 = \sigma_2^2$ and we should take the leading behavior in $\mathcal{M}(t_{ij}, y_{ij})$ when $y_{ij} \rightarrow \infty$ with $y_{13}/y_{25}y_{45}$ fixed. Thus, in the remaining part of the section we shall analyze the Mellin amplitude in this limit. Let us just remark that the region of integration that dominates in the Regge limit is the same as for flat space scattering amplitudes.

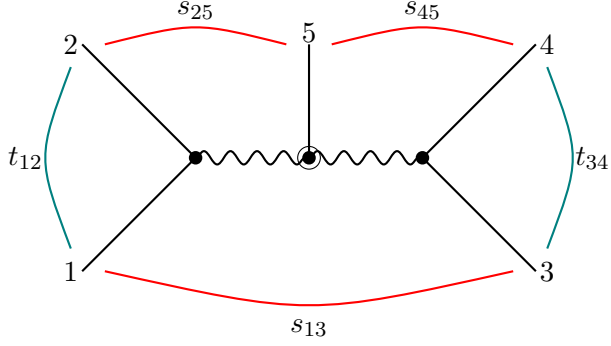


FIGURE 3.10: Regge kinematics for scattering amplitudes can be defined as $s_{13}, s_{25}, s_{45} \rightarrow \frac{1}{x^2}, x \rightarrow 0$ while keeping t_{12} and t_{34} fixed. As can be seen in Mellin space the dominant contribution to the kinematics described in figure 3.8 is the same.

One of the reasons to use Mellin amplitudes is their simple analytic structure. They are meromorphic functions of the Mellin variables δ_{ij} with just simple poles. This property follows, in a loose sense, from the structure of the OPE [144]. The exchange of primary operator with dimension Δ and spin J (and its conformal family) implies that the Mellin amplitude has a infinite set of poles whose residues are given by a dynamical part (related to OPE data) and a kinematical one, *i.e.* determined by symmetry²⁰

$$\mathcal{M}(\delta_{ij}) \approx \mathcal{M}_\Delta \equiv \frac{R_m(\delta_{ij})}{\delta_{LR} - (\Delta - J + 2m)}, \quad m = 0, 1, \dots, \quad (3.96)$$

where

$$\delta_{LR} = \sum_{a=1}^k \sum_{i=k+1}^n \delta_{ai}, \quad (3.97)$$

m labels subleading twists and R_m is related with lower-point Mellin amplitudes whose precise form has been studied in [144]. This property is analogous to the factorization in flat space scattering amplitudes.

The residue itself, depending on the number of points, can have poles. To see this, take as an example the Mellin amplitude of a five-point correlator and look, without loss of generality, to poles in δ_{12} (this corresponds to setting $k = 2$ and $n = 5$ in (3.97)). The residue $R_m(\delta_{ij})$, as mentioned before, depends on a kinematical part and on the four-point Mellin amplitude $\mathcal{M}_{\mathcal{O}345}$, where \mathcal{O} is the operator being exchanged. A four-point Mellin amplitude can also have poles for the very same argument.

²⁰This formula should be valid for any CFT. The fact that we decided to extract Γ functions in the definition of Mellin amplitudes does not imply that we are assuming the existence of double trace like operators. If they do not exist in the spectrum then the Mellin amplitude should have zeros that cancel the poles of these Γ functions.

In this language, the exchange of operators of dimension Δ_1 and Δ_2 in the channels (12) and (34) is respectively encoded by the presence of poles in the Mellin amplitude $\mathcal{M}_5(s_{ij}, t_{ij})$ at $t_{12} = (\Delta_1 - J_1 + 2m_1)$ and $t_{34} = (\Delta_2 - J_2 + 2m_2)$,

$$\mathcal{M}_5(s_{ij}, t_{ij}) \approx \sum_{m_i} \frac{Q_{m_1, m_2}(s_{25}, s_{45}, s_{13})}{(t_{12} - (\tau_1 + 2m_1))(t_{34} - (\tau_2 + 2m_2))} + \dots, \quad (3.98)$$

where the \dots represent regular terms (or poles at other locations). Notice that the poles with $m_1 = m_2 = 0$ are associated with the position space lightcone blocks 3.75 and $m_i > 0$ correspond to corrections around the lightcone. The residue for these sequential poles is related to three-point functions involving the operators that are exchanged.

Now it remains to analyze the large s_{ij} limit of the Mellin amplitude $\mathcal{M}(t_{ij}, s_{ij})$. As for the four-point case, the Casimir differential equations can be translated into Mellin space, where it transforms to a recurrence relation that we defer to (3.130) in appendix 3.A. For the $m_i = 0$ sector, the difference equation simplifies considerably. Moreover, for each pair of spins (J_1, J_2) , there are $1 + \min(J_1, J_2)$ polynomial solutions which can be labeled by an integer ℓ and have the leading large s_{ij} behavior

$$Q_{m_1, m_2}(s_{25}, s_{45}, s_{13}) = c_{\ell, m_1, m_2} s_{25}^{J_1 - \ell} s_{45}^{J_2 - \ell} s_{13}^{\ell} + \dots, \quad (3.99)$$

where \dots represent lower degree terms in the Regge limit. Note that the ℓ denotes a different basis of tensor structure compared to the position space. We have Mellin transformed the lightcone blocks (3.75) and verified the behavior (3.99) in terms of scaling.

The recurrence relation (3.130) can be used to derive relations between c_{ℓ, m_1, m_2} with different values of m_i

$$2m_1 c_{\ell, m_1, m_2} (d - 2(J_1 + m_1 + \tau_1)) - c_{\ell, m_1 - 1, m_2} (\Delta_\phi + 2J_2 - 2m_{12} - \tau_{12} - 2\ell) \\ \times (2m_1 + \tau_1 - 2\Delta_\phi) + c_{\ell, m_1 - 1, m_2 - 1} (2m_1 + \tau_1 - 2\Delta_\phi) (2m_2 + \tau_2 - 2\Delta_\phi) = 0, \quad (3.100)$$

for the (12) channel where $m_{ij} = m_i - m_j$. This particular limit is important in the Regge kinematics. It gives two recurrence relations for the coefficients c_{ℓ, m_1, m_2} that allow to fix them all in terms of the seed $c_{\ell, 0, 0}$. As mentioned before, the label m_i in the poles are related to corrections around the lightcone blocks. Fortunately, we have worked out all these corrections for scalar operators in position space in (3.128) and it is a simple exercise to translate the result into Mellin space, written in (3.129). In particular, this solution is consistent with (3.100).

It is possible to construct another solution to the scalar Casimir equation, written in Mellin space, by studying conformal partial waves (or alternatively, exchanged Witten diagrams using the split representation [183]). The idea behind this approach is simple, however the computation involves several steps and for this reason is given in the appendix [3.B](#). The five-point scalar partial wave can be defined by

$$\mathcal{M}_{\nu_1, \nu_2, 0, 0, 0}(\delta_{ij}) = \frac{\pi^{2h} \left[\prod_{i=1}^2 \Gamma\left(\frac{\Delta_{2i-1} + \Delta_{2i} - t_{2i-1, 2i}}{2}\right) \left(\prod_{\sigma=\pm} \Gamma\left(\frac{h+\sigma(\Delta_{2i-1} - \Delta_{2i}) + i\nu_i}{2}\right) \right) \right]^{-1}}{\Gamma(\Delta_5) \Gamma\left(\frac{\Delta_5 - i\nu_1 + i\nu_2}{2}\right) \Gamma\left(\frac{t_{12} - t_{34} + \Delta_5}{2}\right) \Gamma\left(\frac{2h - \Delta_5 - i\nu_1 - i\nu_2}{2}\right) \Gamma\left(\frac{h - t_{12} + \Delta_5 - i\nu_2}{2}\right)} \quad (3.101)$$

$$\left[\left(\prod_{\sigma=\pm} \Gamma\left(\frac{h - t_{12} + \sigma\Delta_5 - i\nu_2}{2}\right) \Gamma\left(\frac{\Delta_5 + \sigma i\nu_1 + i\nu_2}{2}\right) \right) \Gamma\left(\frac{h - t_{34} + i\nu_2}{2}\right) \Gamma\left(\frac{t_{12} - t_{34} + \Delta_5}{2}\right) \right.$$

$${}_3F_2\left(\frac{\frac{t_{12} - t_{34} + \Delta_5}{2}, \frac{\Delta_5 - i\nu_1 + i\nu_2}{2}, \frac{\Delta_5 + i\nu_1 + i\nu_2}{2}}{\Delta_5, \frac{2 - h + t_{12} + \Delta_5 + i\nu_2}{2}}; 1\right) + \Gamma(\Delta_5) \Gamma\left(\frac{t_{12} - h + \Delta_5 + i\nu_2}{2}\right)$$

$$\left. \left(\prod_{\sigma=\pm} \prod_{i=1}^2 \Gamma\left(\frac{h - t_{2i-1, 2i} + \sigma i\nu_i}{2}\right) \right) {}_3F_2\left(\frac{\frac{h - t_{12} - i\nu_1}{2}, \frac{h - t_{12} + i\nu_1}{2}, \frac{h - t_{34} - i\nu_2}{2}}{\frac{2 + h - t_{12} - \Delta_5 - i\nu_2}{2}, \frac{h - t_{12} + \Delta_5 - i\nu_2}{2}}; 1\right) \right],$$

where we use the notation $\delta_{ij} = (\Delta_i + \Delta_j - t_{ij})/2$. Obviously, the Mellin amplitude of the scalar conformal partial wave only depends on the variables t_{12} and t_{34} and it is symmetric under $\nu \rightarrow -\nu$. More importantly, it gives a solution valid at finite t_{ij} and reduces to the solution (3.129) when t_{ij} are at the poles. This leads us to study the casimir equation away from the poles. For this purpose let us write the Mellin amplitude as

$$\mathcal{M}_{J_1, J_2}(s_{ij}, t_{ij}) = s_{25}^{J_1 - \ell} s_{45}^{J_2 - \ell} s_{13}^\ell f(t_{12}, t_{34}), \quad (3.102)$$

and plug it in the the recurrence relation (3.130). In turn, this leads difference equation for t_{12} and t_{34} that reads

$$f_{00}(t_{12} - \tau_1)(d - t_{12} - \tau_1 - 2J_1) + f_{-20}(2\Delta_\phi - t_{12})(t_{34} - t_{12} + \Delta_\phi + 2J_2 - 2\ell) + f_{-2-2}(2\Delta_\phi - t_{12})(2\Delta_\phi - t_{34}) = 0, \quad (3.103)$$

where the subindices denote $f_{a_1 a_2} \equiv f(t_{12} + a_1, t_{34} + a_2)$. This difference equation can be further simplified by redefining $f(t_{12}, t_{34})$

$$\tilde{f}_{00}(\tau_1 - t_{12})(d - 2J_1 - \tau_1 - t_{12}) + 2\tilde{f}_{-20}(t_{12} - t_{34} - \Delta_\phi - 2J_2 + 2\ell) - 4\tilde{f}_{-2-2} = 0 \quad (3.104)$$

where \tilde{f} is given by

$$f(t_{12}, t_{34}) = \frac{\tilde{f}(t_{12}, t_{34})}{\Gamma(\frac{2\Delta_\phi - t_{12}}{2}) \Gamma(\frac{2\Delta_\phi - t_{34}}{2})}. \quad (3.105)$$

Note that this prefactor is precisely the same as the one that comes from the Gamma functions in the definition of Mellin amplitudes (3.90). It is now simple to see that the equation for $J_1 = J_2$ and generic ℓ can be obtained from the scalar difference equation by doing the following shifts

$$\Delta_\phi \rightarrow \Delta_\phi + 2(J_1 - \ell), \quad d \rightarrow d - 2J_1. \quad (3.106)$$

This suggests that the Mellin partial wave for equal spin $J_1 = J_2$ and generic ℓ can be obtained from (3.101) by doing these replacements. One way to check this statement is to build solutions with the recursion relations in spin derived in [62] (we have rederived parts of these relations in the appendix 3.A using lightcone blocks) and verify that it agrees with the solution that we proposed above.

These solutions for Mellin amplitudes can then be inserted in (3.95) to obtain the conformal block in the Regge limit, that is

$$G_{J_1, J_2, \ell, \nu_1, \nu_2}^\circlearrowleft(\sigma_i, \rho_i) = \sigma_1^{1-J_1} \sigma_2^{1-J_2} \bar{\mathcal{H}}_{\nu_1 \nu_2}(\xi_1, \xi_2, \xi_3), \quad (3.107)$$

with

$$\begin{aligned} \bar{\mathcal{H}}_{\nu_1 \nu_2}(\xi_1, \xi_2, \xi_3) &= \int dt_{12} dt_{34} \Gamma\left(\frac{2\Delta_\phi - t_{12}}{2}\right) \Gamma\left(\frac{2\Delta_\phi - t_{34}}{2}\right) \Gamma\left(\frac{2\ell - \Delta_\phi + t_{12} + t_{34} - 2}{2}\right) \\ &\quad \Gamma\left(\frac{2J_1 - 2\ell + \Delta_\phi + t_{12} - t_{34}}{2}\right) \Gamma\left(\frac{2J_2 - 2\ell + \Delta_\phi - t_{12} + t_{34}}{2}\right) \mathcal{M}_{\nu_1, \nu_2}(t_{12}, t_{34}) \\ &\quad \xi_1^{\frac{t_{34} - t_{12} - \Delta_\phi - 2J_1 + 2\ell}{2}} \xi_2^{\frac{t_{12} - t_{34} - \Delta_\phi - 2J_2 + 2\ell}{2}} \xi_3^{\frac{2 - t_{12} - t_{34} + \Delta_\phi - 2\ell}{2}}, \end{aligned} \quad (3.108)$$

where $\mathcal{M}_{\nu_1, \nu_2}(t_{12}, t_{34})$ is the conformal partial wave in Mellin space in the Regge limit. This expression highlights two properties of the Regge limit, firstly the limit is dominated by operators of high spin and, secondly, it depends on three fixed cross ratios that can be thought of as angles, which is similar to what happens in the Euclidean OPE limit as we mentioned before. In fact $\bar{\mathcal{H}}_{\nu_1 \nu_2}$ solves the Casimir differential equation in the Euclidean region (3.57) but with a different eigenvalue C . Let us point out that the integral (3.108) can be done by picking up poles.

It follows from what was said above that $\bar{\mathcal{H}}_{\nu_1 \nu_2}(\xi_1, \xi_2, \xi_3)$ must have the same form as (3.60), as it solves the same conformal Casimir equation.

3.4.3 Comment on position space

The analysis of the Regge limit in Mellin space of the previous section exposed the similarities to flat space scattering amplitudes but it does not emphasize enough the role of analytic continuation in the cross ratios in changing the behavior of the conformal block. This aspect is clearer in position space, in particular, in the lightcone expressions introduced in subsection 3.3.2. The kinematics of the Regge limit (where some pair of points are timelike while others are spacelike) can be reached from the Euclidean configuration after doing analytic continuations in u_2, u_4 and u_5 around 0 as explained in section 3.4.1.

The analysis is simpler for the discontinuities around $u_4, u_5 = 0$ in the lightcone blocks (3.75) and contains most of the physics we want to highlight in this subsection. These discontinuities come from the first two terms in the denominator of (3.75), provided that $u_2 > 0$. The origin of branch point at, say $u_5 = 0$, comes from the region $t_1 \approx 1/(1 - u_5)$ where the denominator $(1 - (1 - u_5)t_1)$ changes sign. To deal with this it is convenient to divide the integration region in two parts,

$$\int_0^1 dt_1 \mathcal{I} \rightarrow \int_0^{\frac{1}{1-u_5}} dt_1 \mathcal{I} + (-1)^{(h_1 - \tau_2 - 2\ell + \Delta_\phi)} \int_{\frac{1}{1-u_5}}^1 dt_1 \mathcal{I}, \quad (3.109)$$

where the phase comes from the change of sign in the factor $(1 - (1 - u_5)t_1)$. The first term drops out when taking the discontinuity and so we obtain

$$\text{Disc}_{u_5=0} \int_0^1 dt_1 \mathcal{I} = (1 - (-1)^{(h_1 - \tau_2 - 2\ell + \Delta_\phi)}) \frac{u_5}{u_5 - 1} \int_0^1 d\tau_1 \mathcal{I}, \quad (3.110)$$

where we have changed variables to $t_1 = (u_5\tau_1 - 1)/(u_5 - 1)$ in order to have the integration running from 0 to 1 again. It is possible to repeat the same steps to take the discontinuity of u_4 .

Recall that the cross ratios u_4, u_5 and u_2 approach 1 with $\frac{(1-u_2)}{(1-u_4)(1-u_5)} = \frac{1+\zeta}{2}$ fixed in the Regge limit. The discontinuity in u_4 and u_5 of the lightcone block after the Regge limit is given by

$$\lim_{\substack{u_4, u_5 \rightarrow 1 \\ \zeta \text{ fixed}}} \text{Disc}_{u_5, u_4=0} \mathcal{G} = \frac{u_1^{\frac{1-J_1}{2}} u_3^{\frac{1-J_2}{2}} (1 + \zeta)^\ell}{\xi_2^{\Delta_2 - 1} \xi_1^{\Delta_1 - 1} 2^\ell} \sum_{m=0}^{\infty} \frac{\binom{\frac{\Delta_\phi - \tau_1 - \tau_2 - 2J_1 - 2J_2}{2}}{m}}{\Gamma\left(\frac{2J_1 + \Delta_\phi - 2\ell + \tau_{12}}{2}\right) \Gamma\left(\frac{2J_2 + \Delta_\phi - 2\ell + \tau_{21}}{2}\right)} \left(-\frac{1+\zeta}{2}\right)^m F_1 F_2, \quad (3.111)$$

where we have used $\tau_{ij} = \tau_i - \tau_j$, the cross ratios (3.53) and

$$F_i = \frac{\pi \Gamma^2(\frac{\tau_i+2J_i}{2}) \Gamma(\tau_i + 2J_i) \Gamma(\tau_i + 2J_i + m - 1)}{2^{J_i - \frac{1}{2}} \Gamma\left(\frac{\tau_1 + \tau_2 + 2J_i + 2m + 2\ell - \Delta_\phi}{2}\right)} {}_2F_1\left(\frac{\ell - J_i, \tau_{i+1} + 2J_{i+1} + m - 1}{\frac{2J_{i+1} + 2m + 2\ell + \tau_1 + \tau_2 - \Delta_\phi}{2}}, \frac{\zeta + 1}{2}\right).$$

The discontinuities in u_4 and u_5 are enough to reveal that the discontinuities of conformal block behave with $\sigma_1^{1-J_1} \sigma_2^{1-J_2}$ in the Regge limit, which compares with $\sigma_1^{\Delta_1} \sigma_2^{\Delta_2}$ of the Euclidean block²¹. It can also be shown from the previous formula that three sequential discontinuities, $\text{Disc}_{u_2, u_4, u_5}$, evaluate to zero. Recall that four-point conformal blocks have vanishing double discontinuity. We believe that conformal blocks have this property away from the lightcone limit.

3.4.4 Conformal Regge theory for five points

Let us consider the representation of the five-point correlation function in terms of conformal partial waves, and its implications for the Regge limit. This basis is complete and orthogonal. Since we have more control over the analytic properties of the partial waves in Mellin space, we consider the expansion

$$\mathcal{M}(s_{ij}, t_{ij}) = \sum_{J_1, J_2=0}^{\infty} \sum_{\ell=0}^{\min(J_1, J_2)} \int \frac{d\nu_1}{2\pi i} \frac{d\nu_2}{2\pi i} b_{J_1, J_2, \ell}(\nu_1, \nu_2) \mathcal{M}_{J_1, J_2, \ell}(s_{ij}, t_{ij}). \quad (3.112)$$

We suppress the dependence of the Mellin partial wave $\mathcal{M}_{J_1, J_2, \ell}$ on the scaling dimensions, as the nontrivial analytic continuation occurs in other quantum numbers. We have introduced poles in the variables ν_1 and ν_2 with residues corresponding to the OPE coefficients, using

$$b_{J_1, J_2, \ell}(\nu_1, \nu_2) \approx \frac{P_{\nu_1, \nu_2, J_1, J_2}^{\ell}}{(\nu_1^2 + (\Delta_1 - h)^2)(\nu_2^2 + (\Delta_2 - h)^2)}, \quad (3.113)$$

where $\Delta_i = \Delta_i(J_i)$ is the dimension of the i -th exchanged operator of spin J_i . We remark that the product of the OPE coefficients $P_{\nu_1, \nu_2, J_1, J_2}^{\ell}$ in (3.113) is a linear combination of those in (3.49) that appear in the conformal block expansion.

²¹We also need to consider the monodromy of the lightcone block around the branch point at $u_2 = 0$. It is possible to do a Mellin transform of the lightcone block and apply the method of the previous subsection to derive all discontinuities. In the appendix, we provide several checks that the discontinuity of the block in u_2 has the same behavior.

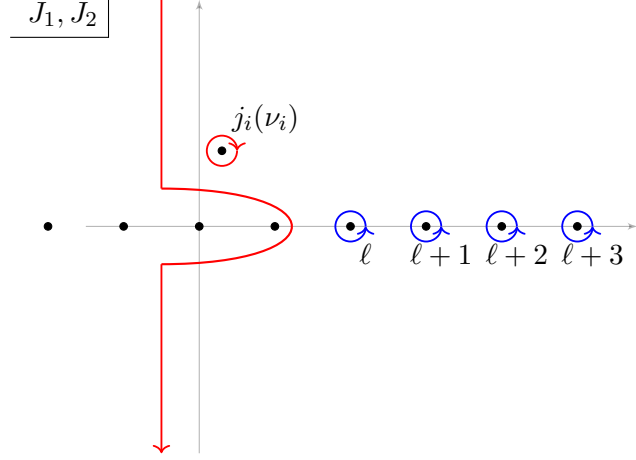


FIGURE 3.11: Integration contour in spins J_1, J_2 . The blue contour can be deformed to the red contour. We assume the leading Regge pole in the J_i -plane is located at $j_i(\nu)$ and we don't draw any further dynamical singularities that might exist to the left. Red contour is understood to be deformed to the right of the other infinite series of poles depending on ℓ lying on the left in the J_i -plane.

We would like to provide a Sommerfeld-Watson representation of (3.112). First, we swap the range of summations as

$$\mathcal{M}(s_{ij}, t_{ij}) = \sum_{\ell=0}^{\infty} \sum_{J_1, J_2=\ell}^{\infty} \int \frac{d\nu_1}{2\pi i} \frac{d\nu_2}{2\pi i} b_{J_1, J_2, \ell}(\nu_1, \nu_2) \mathcal{M}_{J_1, J_2, \ell}(s_{ij}, t_{ij}). \quad (3.114)$$

Next, we analytically continue in the spin quantum numbers. However, the $b_{J_1, J_2, \ell}$ are not expected to have a unique analytic continuation in the quantum numbers. For that reason we need to consider their *signatured* counterparts.

Let us remind the reader the analogous construction [86] for the four-point correlator $\mathcal{A}(u, v)$ in terms of the cross ratios

$$u = \frac{x_{12}^2 x_{34}^2}{x_{13}^2 x_{24}^2}, \quad v = \frac{x_{14}^2 x_{23}^2}{x_{13}^2 x_{24}^2}. \quad (3.115)$$

After expanding in Euclidean partial waves, we can write the correlation function as

$$\mathcal{A}(u, v) = \sum_{J=0}^{\infty} \int_{\frac{d}{2} + i\mathbb{R}} \frac{d\Delta}{2\pi i} c_{\Delta, J} F_{\Delta, J}(u, v), \quad (3.116)$$

where $c_{\Delta, J}$ denotes the OPE function and $F_{\Delta, J}$ is the Euclidean partial wave. It can be transformed to Mellin space as

$$\mathcal{M}(s, t) = \sum_{J=0}^{\infty} \int_{\frac{d}{2} + i\mathbb{R}} \frac{d\Delta}{2\pi i} c_{\Delta, J} \mathcal{M}_{\Delta, J}(s, t). \quad (3.117)$$

Again, the OPE function $c_{\Delta,J}$ is not uniquely defined in the complex J plane. Thus, we define the signatured OPE function $c_{\Delta,J}^\theta$ by

$$\mathcal{M}_\theta(s, t) = \sum_{J=0}^{\infty} \int_{\frac{d}{2}+i\mathbb{R}} \frac{d\Delta}{2\pi i} c_{\Delta,J}^\theta \mathcal{M}_{\Delta,J}^\theta(s, t), \quad (3.118)$$

where the signatured Mellin partial waves are given by

$$\mathcal{M}_{\Delta,J}^\theta(s, t) = \frac{1}{2} [\mathcal{M}_{\Delta,J}(s, t) + \theta \mathcal{M}_{\Delta,J}(-s, t)], \quad (3.119)$$

with $\theta = \pm$. The signatured Mellin amplitude allows for a unique analytic continuation of the signatured OPE function $c_{\Delta,J}^\theta$ [79]. The problem of the non-signatured OPE function can be traced back the factor of $(-1)^J$ that appears in the transformation $s \rightarrow -s$, which follows from the large s behavior $\mathcal{M}_{\Delta,J}(s, t) \approx s^J$.

A similar construction can be done for five-point functions. We split the full correlator into eight parts depending on the *signature* denoted by $\theta = (\theta_1, \theta_2, \theta_{12})$ where each component can be \pm . We define the *signatured* amplitudes as

$$\begin{aligned} \mathcal{M}_\theta(s_{25}, s_{45}, s_{13}) = & \frac{1}{8} [\mathcal{M}(s_{25}, s_{45}, s_{13}) + \theta_1 \mathcal{M}(-s_{25}, s_{45}, s_{13}) + \theta_2 \mathcal{M}(s_{25}, -s_{45}, s_{13}) \\ & + \theta_1 \theta_2 \mathcal{M}(-s_{25}, -s_{45}, s_{13}) + \theta_{12} \mathcal{M}(-s_{25}, -s_{45}, -s_{13}) + \theta_1 \theta_{12} \mathcal{M}(s_{25}, -s_{45}, -s_{13}) \\ & + \theta_{12} \theta_2 \mathcal{M}(-s_{25}, s_{45}, -s_{13}) + \theta_1 \theta_{12} \theta_2 \mathcal{M}(s_{25}, s_{45}, -s_{13})]. \end{aligned} \quad (3.120)$$

This equation is suitable only for $s_{ij} \gg 1$. We also suppress the dependence on t_{ij} for brevity. We justify it by using the properties of the Mellin partial wave (3.102) which, in terms of $J'_i = J_i - \ell$, behaves in the Regge limit as

$$\mathcal{M}_{J'_1, J'_2, \ell}(s_{ij}, t_{ij}) = s_{25}^{J'_1} s_{45}^{J'_2} s_{13}^\ell f(t_{12}, t_{34}). \quad (3.121)$$

By analogy with the four-point case, we expect that OPE functions associated with the expansion of the signatured amplitudes in (3.120) have a unique analytic continuation in all quantum numbers J'_1, J'_2, ℓ . It would be interesting to put this on a firm footing by deriving dispersion relations along the lines of [79]. The full Mellin amplitude can then be written in terms of the signatured Mellin amplitude as

$$\mathcal{M}(s_{25}, s_{45}, s_{13}) = \sum_{\theta \in \{-1, 1\}^3} \mathcal{M}_\theta(s_{25}, s_{45}, s_{13}). \quad (3.122)$$

In terms of the signatured analogue of partial waves defined through (3.120), we write

$$\mathcal{M}_\theta(s_{ij}, t_{ij}) = \sum_{\ell=0}^{\infty} \sum_{J'_1, J'_2=0}^{\infty} \int \frac{d\nu_1}{2\pi i} \frac{d\nu_2}{2\pi i} b_{J'_1, J'_2, \ell}^\theta(\nu_1, \nu_2) \mathcal{M}_{J'_1, J'_2, \ell}^\theta(s_{ij}, t_{ij}). \quad (3.123)$$

Next we perform a Sommerfeld-Watson transform on the ℓ contour

$$\mathcal{M}_\theta(s_{ij}, t_{ij}) = \int_{\mathbf{C}} \frac{d\ell}{2\pi i} \frac{1}{\sin(\pi\ell)} \sum_{J'_1, J'_2=0}^{\infty} \int \frac{d\nu_1}{2\pi i} \frac{d\nu_2}{2\pi i} b_{J'_1, J'_2, \ell}^\theta(\nu_1, \nu_2) \mathcal{M}_{J'_1, J'_2, \ell}^\theta(s_{ij}, t_{ij}). \quad (3.124)$$

where \mathbf{C} is the contour that encircles the poles at non-negative integers in ℓ complex plane counterclockwise.

Next we analytically continue in J'_1 and J'_2 by means of two Sommerfeld-Watson transforms. The analytic structure in these variables is analogous to the case of four-point correlation functions. Figure 3.11 shows the analytic structure of the integrand. In particular, there is a leading Regge pole in the J_i plane at $J_i = j_i(\nu_i)$ given by

$$\left[\Delta_i(j_i(\nu_i)) - h \right]^2 + \nu_i^2 = 0. \quad (3.125)$$

Picking the poles in the complex spin planes at $J'_1 = j_1(\nu_1) - \ell$ and $J'_2 = j_2(\nu_2) - \ell$, we obtain the following expression for the signatured correlators

$$\mathcal{M}_\theta = \int \frac{d\nu_1}{2\pi i} \frac{d\nu_2}{2\pi i} s_{25}^{j_1(\nu_1)} s_{45}^{j_2(\nu_2)} \int_{\mathbf{C}} \frac{d\ell}{2\pi i} \frac{b_{j_1(\nu_1), j_2(\nu_2), \ell}^\theta(\nu_1, \nu_2) f_{\nu_1, \nu_2, \ell}^\theta(t_{ij}) \eta^\ell}{\sin(\pi\ell) \sin(\pi(j_1(\nu_1) - \ell)) \sin(\pi(j_2(\nu_2) - \ell))}, \quad (3.126)$$

where $f_{\nu_1, \nu_2, \ell}^\theta$ is defined as the signatured analogue of f in (3.105).

The integral over ℓ remains to be performed as we did not consider any particular limit in η . One should however comment on the anticipated singularities in this complex plane. Indeed, we expect no dynamical poles in ℓ , *i.e.* $b_{j_1(\nu_1), j_2(\nu_2), \ell}^\theta(\nu_1, \nu_2)$ should not have poles in ℓ and therefore all the singularities to be considered are determined by the explicit sine functions in the integrand. This assumption is inspired by an analogous procedure for the five-particle S-matrix. Indeed, the quantum number ℓ here labels a choice of tensor basis for three-point functions but it also seems to control the scaling and the asymptotic behaviour of the amplitude in multi-Regge limit. It seems unreasonable that the asymptotic scaling can be basis dependent and therefore we expect the singularities in ℓ to be fully determined by the singularities in spin. This is just like the discussion for the helicity quantum number in flat space following [166].

In the Regge limit the full correlator takes the form

$$\mathcal{M} = \int \frac{d\nu_1}{2\pi i} \frac{d\nu_2}{2\pi i} s_{25}^{j_1(\nu_1)} s_{45}^{j_2(\nu_2)} \int_{\mathbf{C}} \frac{d\ell}{2\pi i} \eta^\ell g_{\nu_1, \nu_2, \ell}(t_{ij}), \quad (3.127)$$

where the function $g_{\nu_1, \nu_2, \ell}(t_{ij})$ is defined from replacing (3.126) in (3.122). This allows us to represent the Reggeized Mellin amplitude in terms of the operator content of the leading Regge trajectories and their couplings to the external states.

3.5 Discussion

In this chapter, we discussed and analyzed the generalization of Regge limit to five-point correlation functions in conformal field theories. The kinematics of this limit is similar to the one of the four-point case [86] with one crucial difference, the insertion of one extra point. In particular, the fifth point is essential to have different rapidities between the first set of four operators. The location of the fifth point is also important for the interpretation of the five-point Regge limit as an OPE limit in the second sheet. In particular, the dimension and spin of the exchanged operators in this second sheet OPE are transformed from the usual (Δ, J) to $(1 - J, 1 - \Delta)$, which can be interpreted in terms of light-ray operators [99].

Our proposal for the five-point Regge limit is also confirmed by the exploration of this kinematics in Mellin space. More concretely, we verified that the Regge limit is dominated by a region in Mellin space characterized by some large Mellin variables in close analogy to the Regge limit of scattering amplitudes in flat space. This similarity leads us to focus more on Mellin amplitudes to study the Regge limit. In particular, we analyzed the generalization of Mack polynomials for Mellin amplitudes and discussed some of its properties. We derived the conformal partial waves in Mellin space in the Regge limit for when the two exchanged operators have the same spin and studied, in position space, the behaviour of the conformal block in this limit, using recent results on lightcone blocks for higher-point functions.

Equipped with a new formula for the conformal partial waves in the Regge limit in Mellin space, we extended conformal Regge theory to five-point correlation functions by borrowing methods used in flat-space multi-point amplitudes. Our final result for the five-point correlator in the Regge limit corresponds to the exchange of two Reggeon operators.

In the process, we discussed a novel basis of three-point functions of operators with spin $(J_1, J_2, 0)$, respectively. In this basis and in the Euclidean OPE limit the five-point conformal block factorizes into products of Gegenbauer polynomials. These expressions

appear to be a natural generalization of the Wigner d -functions used in the partial-wave decomposition of five-particle amplitudes. This suggests that the typical basis used in the literature for three-point functions of operators with spin (J_1, J_2, J_3) might not be the most natural one for the study of Euclidean conformal blocks. Given the importance of conformal blocks in bootstrap, it would be interesting to study the properties of this basis in more detail. The case of (J_1, J_2, J_3) three-point function is accessible in the Euclidean OPE limit of six-point function in the snowflake channel.

While the study of the analytic structure of higher-point functions is still in its infancy, we expect that it admits some sort of simplification in the multi-Regge limit. It would be interesting and relevant, nonetheless, to investigate if possible "anomalous" branch-cuts can affect the Regge limit both in flat space and in CFTs.

A more ambitious goal would be the derivation of a Lorentzian inversion formula for higher-point functions. This would clarify many of the questions we raised here, namely if there is or not some sort of analyticity in the label of tensor structures of three-point functions with spin. We expect that an important ingredient towards that goal is the multivariable generalization of the Cauchy formula, called the Bargman-Weil formula.

It would be interesting to generalize the Regge limit considered in this chapter to higher-point functions. The generalization of the partial-wave expansion in S-matrix literature is done in [163] for four dimensional quantum field theories. An analogous generalization of the partial-wave expansion is expected to be within reach for three-dimensional CFTs for n -point functions, where we would benefit from the fact that there are no representations of the rotation subgroup of the conformal group in three dimensions with more than one row in the Young tableaux. However, for higher dimensions, there will be proliferation of indices labelling the internal vertices and no such simplification can be considered.

Finally, in flat-space literature, a crucial ingredient for the absence of singularities in ℓ was the use of Steinmann relations. It would be interesting to explore the analogue of Steinmann relations in CFTs, with or without large central charge limit.

Appendices for chapter 3

3.A Lightcone blocks

The scalar five-point conformal blocks, mentioned in the main text, can be expressed in terms of an expansion around the lightcone (3.77) by acting with (3.74) on a three-point function. In (3.77) we have written it in terms of a function $\tilde{\mathcal{I}}_{n_1, n_2}$ given by

$$\begin{aligned} \tilde{\mathcal{I}}_{n_1, n_2} = & \frac{\left(\frac{a-\Delta_5}{2}\right)_{n_1} \left(\frac{2n_1-\Delta_5+a}{2}\right)_{n_2} \left(\frac{a+4-\Delta_5-d}{2}\right)_{n_1} \left(\frac{2n_1-\Delta_5+a+4-d}{2}\right)_{n_2}}{\left(t_1^2 u_1 u_4 - t_1 (t_2 (1-u_5) + t_2 u_4 (u_2 u_5 - 1) + u_1 u_4 + u_5 - 1) + u_5 (t_2^2 u_3 - t_2 (u_3 - u_2 u_4 + 1) + 1)\right)^{\frac{a+2n_1+2n_2-\Delta_5}{2}}} \\ & \prod_{i=1}^2 \frac{(-1)^{n_i} \Gamma(2n_i + \Delta_{k_i}) \left(\frac{\Delta_{k_i}}{2}\right)_{n_i}^2 (t_i(1-t_i))^{\frac{\Delta_{k_i}+2n_i}{2}-1}}{n_i! (\Delta_{k_i})_{2n_i} \left(\frac{2\Delta_{k_i}+4-d}{2}\right)_{n_i} \Gamma^2\left(\frac{2n_i+\Delta_{k_i}}{2}\right)} \end{aligned} \quad (3.128)$$

where $a = \Delta_{k_1} + \Delta_{k_2}$. One nice feature of this result is that it allows to do analytic continuations in u_2, u_4, u_5 at all orders in u_1 and u_3 , this is specially useful to verify that the analytic continuation of the conformal block has a distinct behavior in the Regge limit. With this expression in our hands we can also do a Mellin transform and obtain the Mellin amplitude associated with the scalar conformal block. For instance the function Q_{m_1, m_2} in (3.98) is given in this case by

$$\begin{aligned} Q_{m_1, m_2} = & \sum_{n_i=0} \prod_{i=1}^2 \frac{2(-1)^{m_i} \Gamma(\Delta_{k_i})}{(m_i - n_i)! \Gamma^2\left(\frac{\Delta_{k_i}}{2}\right) \Gamma\left(\Delta_\phi - m_i - \frac{\Delta_{k_i}}{2}\right) \left(1 - \frac{d}{2} + \Delta_{k_i}\right)_{m_i - n_i}} \frac{\left(\frac{\bar{\Delta} - \Delta_\phi}{2}\right)_{m_1 - n_1} \left(n_1 + n_2 + \frac{\Delta_\phi}{2} - m_1 - m_2 - \frac{\bar{\Delta}}{2}\right)}{\Gamma\left(\frac{\Delta_\phi + 2m_1 - 2m_2 + \Delta_{k_1} - \Delta_{k_2}}{2}\right)} \\ & \times \frac{\left(\frac{\bar{\Delta} + 2 - d - \Delta_\phi}{2}\right)_{m_1 - n_1} \left(\frac{2m_1 + \bar{\Delta} - 2n_1 - \Delta_\phi}{2}\right)_{m_2 - n_2} \left(\frac{2m_1 + \bar{\Delta} + 2 - d - 2n_1 - \Delta_\phi}{2}\right)_{m_2 - n_2} \left(\frac{2n_2 + \Delta_\phi - 2m_1 - 2m_2 - \bar{\Delta}}{2}\right)}{\Gamma\left(\frac{\Delta_\phi - 2m_1 + 2m_2 - \Delta_{k_1} + \Delta_{k_2}}{2}\right) \Gamma\left(\frac{2m_1 + 2m_2 + \bar{\Delta} - \Delta_\phi}{2}\right)} \end{aligned} \quad (3.129)$$

where $\bar{\Delta} = \Delta_{k_1} + \Delta_{k_2}$. Note that it does not depend on the variables s_{ij} as expected since the exchanged operators are scalars. The apparent asymmetry in the channels (12) and (34) is related with the choice of which differential operator F_k we decide to act first on

a three-point function. Another advantage of having the Mellin amplitude for the scalar conformal block is that it can be used to generate some solutions for spinning blocks as we have shown in section 3.4.2.

We have checked that the solution (3.129) satisfies the Casimir recurrence equation, in the channel (12), given by

$$\begin{aligned}
& [\mathbf{d}_{00000}(2c_{\Delta_1 J_1} - a_1^2 + a_1(2a_4 + a_5 - a_3 - 2d + 3\Delta_\phi) - 2a_2(a_3 + a_4) + 2a_3^2 - 2a_3a_4 - 2a_3a_5 \\
& + \Delta_\phi(5a_3 - 4a_4 - 2a_5 + 4d) + 2a_4^2 + a_4a_5 - 2\Delta_\phi^2) \\
& + \mathbf{d}_{00-200}(a_1 - a_3 + a_4 - 2\Delta_\phi)(a_3 - 2a_2 - a_5 + 2\Delta_\phi) \\
& - \mathbf{d}_{000-20}(a_1 - 2a_2 + a_4 - \Delta_\phi)(a_1 - a_3 + a_4 - 2\Delta_\phi) - a_3\mathbf{d}_{002-20}(a_1 - 2a_2 + a_4 - \Delta_\phi) \\
& + a_1\mathbf{d}_{-2000-2}(a_1 - 2a_2 - a_5 + \Delta_\phi) + a_1\mathbf{d}_{-2002-2}(a_1 - 2a_2 - a_5 + \Delta_\phi) + 2a_1a_2\mathbf{d}_{-2-2-200} \\
& + 2a_1a_2\mathbf{d}_{-2-2000} + a_1a_5\mathbf{d}_{-20-220} + a_1a_5\mathbf{d}_{-20000} + a_4\mathbf{d}_{00-220}(2a_2 - a_3 + a_5 - 2\Delta_\phi) \\
& + a_4\mathbf{d}_{00020}(a_3 - a_4 - a_5 + \Delta_\phi) + a_3\mathbf{d}_{00200}(a_4 + a_5 - a_3 - \Delta_\phi)]f(t_{ij}, s_{ij}) = 0
\end{aligned} \tag{3.130}$$

where $\mathbf{d}_{i_1 i_2 i_3 i_4 i_5}$ is defined by $\mathbf{d}_{i_1 i_2 i_3 i_4 i_5}f(t_{12}, t_{34}, s_{13}, s_{25}, s_{45}) = f(t_{12} + i_1, \dots, s_{45} + i_5)$ and the coefficients a_i are given by

$$\begin{aligned}
a_1 &= 2\Delta_\phi - t_{12}, \quad a_2 = \frac{2\Delta_\phi - t_{34}}{2}, \quad a_3 = \Delta_\phi - s_{13}, \\
a_4 &= s_{25} + t_{12} - t_{34} + \Delta_\phi, \quad a_5 = s_{45} - t_{12} + t_{34} + \Delta_\phi.
\end{aligned} \tag{3.131}$$

This recurrence relation is also valid for spinning conformal blocks.

3.A.1 Spinning recursion relations

In [62] the authors have derived identities that blocks with different values of spin satisfy. It is possible to verify part of these relations using lightcone blocks for unequal external dimensions introduced in the previous subsection. Using (3.72) we can verify that the lightcone blocks satisfy

$$\begin{aligned}
& (2J_1 + 2\ell + \tau_1 + \tau_2 - 2 - \Delta_5)G_{\tau_1, J_1, \tau_2, J_2, \ell}^{\Delta_1, \Delta_5, \Delta_3} + 2(J_2 - \ell)G_{\tau_1, J_1, \tau_2, J_2, \ell+1}^{\Delta_1, \Delta_5, \Delta_3} \\
& + \frac{4(2J_1 + \tau_1 - 2)(2J_1 + \tau_1 - 1)}{(2J_1 + \tau_1 - \Delta_{12} - 2)} \left[\frac{\sqrt{u_5}G_{\tau_1+1, J_1-1, \tau_2, J_2, \ell}^{\Delta_1+1, \Delta_5+1, \Delta_3}}{\sqrt{u_1}} - G_{\tau_1, J_1-1, \tau_2, J_2, \ell}^{\Delta_1, \Delta_5, \Delta_3} \right] = 0
\end{aligned} \tag{3.132}$$

where $G_{\tau_1, J_1, \tau_2, J_2, \ell}^{\Delta_1, \Delta_5, \Delta_3}$ represents the lightcone conformal block for the exchange of a twist τ_i and spin J_i in the channels (12) and (34) for external with dimension Δ_i ,

$$G_{\tau_1, J_1, \tau_2, J_2, \ell}^{\Delta_1, \Delta_5, \Delta_3} = u_1^{\frac{\tau_1}{2}} u_3^{\frac{\tau_2}{2}} u_5^{\frac{\Delta_5}{2}} (1 - u_2)^\ell \int [dt_1 dt_2] (1 - u_2 u_5 + t_2(u_2 - 1)u_5)^{J_1 - \ell} \frac{(1 - u_2 u_4 + t_1(u_2 - 1)u_4)^{J_2 - \ell}}{(1 + t_1(u_5 - 1))^{\frac{\Delta_5 + 2J_1 + \tau_1 - \tau_2 - 2\ell}{2}} (1 + t_2(u_4 - 1))^{\frac{\Delta_5 + 2J_2 - \tau_1 + \tau_2 - 2\ell}{2}} (1 + (1 - t_1)(1 - t_2)(u_2 - 1))^{\frac{2J_1 + 2J_2 + \tau_1 + \tau_2 - \Delta_5}{2}}} \quad (3.133)$$

where $[dt_1 dt_2] = \prod_{i=1}^2 \frac{dt_i \Gamma(2J_i + \tau_i)t^{\frac{\tau_i + 2J_i + a_i}{2} - 1}(1 - t_i)^{\frac{\tau_i + 2J_i - a_i}{2} - 1}}{\Gamma(\frac{\tau_i + 2J_i + a_i}{2}) \Gamma(\frac{\tau_i + 2J_i - a_i}{2})}$ with $a_1 = \Delta_{12}, a_2 = \Delta_{34}$. As before, the index ℓ labels a particular structure in the three-point function (3.47)

By considering the Mellin transform of $G_{\tau_1, J_1, \tau_2, J_2, \ell}^{\Delta_1, \Delta_5, \Delta_3}$ we can phrase the recurrence relation in spin (3.132) in terms of a Mellin amplitudes

$$\begin{aligned} & \frac{2(2J_1 + \tau_1 - 2)(2J_1 + \tau_1 - 1)((\Delta_5 - 2\delta_{25} + \tau_{12})\mathcal{M}_{\tau_1+1, J_1-1, \tau_2, J_2, l}^{\Delta_1+1, \Delta_5+1, \Delta_3} - \mathcal{M}_{\tau_1, J_1-1, \tau_2, J_2, l}^{\Delta_1, \Delta_5, \Delta_3})}{(2J_1 + \tau_1 - \Delta_{12} - 2)} \\ & + (2J_1 + 2\ell + \tau_1 + \tau_2 - \Delta_5 - 2)\mathcal{M}_{\tau_1, J_1, \tau_2, J_2, \ell}^{\Delta_1, \Delta_5, \Delta_3} + 2(J_2 - \ell)\mathcal{M}_{\tau_1, J_1, \tau_2, J_2, \ell+1}^{\Delta_1, \Delta_5, \Delta_3} = 0 \end{aligned} \quad (3.134)$$

with

$$G_{\tau_1, J_1, \tau_2, J_2, \ell}^{\Delta_1, \Delta_5, \Delta_3} = u_1^{\frac{\tau_1}{2}} u_3^{\frac{\tau_2}{2}} \int [d\delta_{ij}] \mathcal{M}_{\tau_1, J_1, \tau_2, J_2, \ell}^{\Delta_1, \Delta_5, \Delta_3}(\delta_{ij}) u_4^{-\delta_{45}} u_5^{\delta_{25} + \frac{\tau_2 - \tau_1}{2}} u_2^{\delta_{13} - \delta_{45} + \frac{\Delta_5 - a_2 - \tau_1}{2}} \prod_{i < j} \Gamma(\delta_{ij}) \quad (3.135)$$

where we have used the constraints to eliminate the some of the δ_{ij} and δ_{12} and δ_{34} are set to $\frac{\Delta_1 + \Delta_2 - \tau_1}{2}$ and $\frac{\Delta_3 + \Delta_4 - \tau_2}{2}$ respectively. We have suppressed the dependence on Mellin variables in (3.134) since there are no shifts in them.

There is an extra identity that is needed to turn (3.132) into a self-consistent recurrence relation

$$\begin{aligned} & \frac{4(\tau_1 + 2\ell - 1)(\tau_2 + 2\ell - 1)(\tau_1 + \tau_2 + 4\ell - \Delta_5 - 4)}{(\tau_1 + 2\ell - \Delta_{12} - 2)(\Delta_{34} + \tau_2 + 2\ell - 2)} \left[\frac{G_{\tau_1+1, \ell-1, \tau_2+1, \ell-1, \ell-1}^{\Delta_1+1, \Delta_5, \Delta_3-1}}{\sqrt{u_1} \sqrt{u_3}} - G_{\tau_1, \ell-1, \tau_2, \ell-1, \ell-1}^{\Delta_1, \Delta_5, \Delta_3} \right] \\ & + \frac{(\Delta_5 - \tau_{12})(\tau_1 + 2\ell - 1)}{(\tau_2 + 2\ell - 2)(\tau_1 + 2\ell - \Delta_{12} - 2)} \left[\frac{\sqrt{u_5}(\Delta_5 + \tau_{12})G_{\tau_1+1, \ell-1, \tau_2, \ell, \ell-1}^{\Delta_1+1, \Delta_5+1, \Delta_3}}{\sqrt{u_1}} - 2G_{\tau_1, \ell-1, \tau_2, \ell, \ell-1}^{\Delta_1, \Delta_5, \Delta_3} \right] \\ & - \frac{(\Delta_5 + \tau_{12})(\tau_2 + 2\ell - 1)(\tau_1 + \tau_2 + 4\ell - \Delta_5 - 4)G_{\tau_1, \ell, \tau_2, \ell-1, \ell-1}^{\Delta_1, \Delta_5, \Delta_3}}{(\tau_1 + 2\ell - 2)(\Delta_{34} + \tau_2 + 2\ell - 2)} \\ & + (\tau_1 + \tau_2 + 4\ell - \Delta_5 - 2)G_{\tau_1, \ell, \tau_2, \ell, \ell}^{\Delta_1, \Delta_5, \Delta_3} = 0. \end{aligned} \quad (3.136)$$

3.B Scalar Mellin partial-wave

In this appendix, we derive the Mellin partial-wave for scalar exchange within a five-point function. We start from partial-wave definition in position space

$$F_{\nu_1, \nu_2, 0, 0, 0}(x_i) = \int dx_6 dx_7 \langle \phi_1 \phi_2 \phi(x_6) \rangle \langle \tilde{\phi}(x_6) \phi_5 \tilde{\phi}(x_7) \rangle \langle \phi_3 \phi_4 \phi(x_7) \rangle \quad (3.137)$$

where the subscripts 0 in $F_{\nu_1, \nu_2, 0, 0, 0}$ denote the scalar exchanges and ν_1, ν_2 refer to principal series representations of the exchanged operators. The notation $\langle \phi_i \phi_j \phi_k \rangle$ denotes kinematical structure of three-point functions

$$\langle \phi_1 \phi_2 \phi_3 \rangle = \frac{1}{(-2P_1 \cdot P_2)^{\frac{1}{2}(\Delta_1 + \Delta_2 - \Delta_3)} (-2P_1 \cdot P_3)^{\frac{1}{2}(\Delta_1 + \Delta_3 - \Delta_2)} (-2P_2 \cdot P_3)^{\frac{1}{2}(\Delta_2 + \Delta_2 - \Delta_1)}}, \quad (3.138)$$

where we use embedding space where $-2P_i \cdot P_j = x_{ij}^2$. Note that as we only consider scalar exchanges there is no sum over different possible tensor structures. In general, we consider unequal scalar fields labelled by their scaling dimensions Δ_i . For operators of fixed position we do the abuse of notation $\phi_i \equiv \phi(x_i)$ but we retain the dependence on integrated variables using $\phi(x_i)$. The latter notation corresponds to scalar operators of scaling dimension $h + i\nu_i$ with $h = d/2$. Moreover, shadow operators of scaling dimension $h - i\nu_i$ are denoted with an extra tilde.

In order to integrate over x_6 and x_7 we use the Schwinger parametrization

$$\frac{1}{(-2P_i \cdot P_j)^a} = \frac{1}{\Gamma(m + a)} \int_0^\infty \frac{dt_{ij}}{t_{ij}} t_{ij}^{m+a} (-\partial_{t_{ij}})^m e^{2t_{ij} P_i \cdot P_j}. \quad (3.139)$$

for any power a , $(-P_i \cdot P_j) > 0$ and some integer m such that $\text{Re}(m + a) > 0$. For our purposes here, it is enough to take $m = 0$. It will also be useful to consider the following change of variables

$$\begin{aligned} t_{12} &= 2t_1 t_2, & t_{16} &= 2t_1 t, & t_{26} &= 2t_2 t, & t_{34} &= 2t_3 t_4, & t_{37} &= 2t_3 s, \\ t_{47} &= 2t_4 s, & t_{56} &= 2t_5 \bar{t}, & t_{57} &= 2t_5 \bar{s}, & t_{67} &= 2\bar{t} \bar{s}, \end{aligned} \quad (3.140)$$

which is introduced to reproduce the form of integral one finds from considering a tree-level Witten diagram with two scalar exchanges using the notation of [143]. Here t_i 's are related with bulk-to-boundary propagators of the external scalars whereas t, \bar{t}, s, \bar{s} refer to split representations of the bulk-to-bulk propagators.

The integrals over x_6 and x_7 are easy to compute successively by noting [143]

$$\int_0^\infty \frac{dt d\bar{t}}{t\bar{t}} t^{\Delta_t} \bar{t}^{\Delta_{\bar{t}}} \int dP e^{2P \cdot (tX + \bar{t}Y)} = 2\pi^h \int_0^\infty \frac{dt d\bar{t}}{t\bar{t}} t^{\Delta_t} \bar{t}^{\Delta_{\bar{t}}} e^{(tX + \bar{t}Y)^2} \quad (3.141)$$

where $\Delta_t + \Delta_{\bar{t}} = 2h$ with X and Y two timelike vectors. We then find (dropping constants)

$$\begin{aligned} F_{\nu_1, \nu_2, 0, 0, 0}(x_i) \sim & \int \frac{dt d\bar{t} ds d\bar{s}}{t\bar{t} s\bar{s}} t^{h+i\nu_1} \bar{t}^{h-i\nu_1} s^{h+i\nu_2} \bar{s}^{h-i\nu_2} \left(\prod_{i=1}^5 \int \frac{dt_i}{t_i} t_i^{\Delta_i} \right) \exp \left[-t_1 t_2 x_{12}^2 \left(t^2 (\bar{s}^2 \bar{t}^2 + 1) + 1 \right) \right. \\ & -t_1 t_3 x_{13}^2 t\bar{t} s\bar{s} - t_1 t_4 x_{14}^2 t\bar{t} s\bar{s} - t_1 t_5 x_{15}^2 t\bar{t} \left(\bar{s}^2 (\bar{t}^2 + 1) + 1 \right) - t_2 t_3 x_{23}^2 t\bar{t} s\bar{s} - t_2 t_4 x_{24}^2 t\bar{t} s\bar{s} \\ & \left. -t_2 t_5 x_{25}^2 t\bar{t} \left(\bar{s}^2 (\bar{t}^2 + 1) + 1 \right) - t_3 t_4 x_{34}^2 (s^2 + 1) - t_3 t_5 x_{35}^2 s\bar{s} (\bar{t}^2 + 1) - t_4 t_5 x_{45}^2 s\bar{s} (\bar{t}^2 + 1) \right] \end{aligned} \quad (3.142)$$

which is of the form of Symanzik's formula [184]

$$2 \int_0^\infty \prod_{i=1}^n \frac{dt_i}{t_i} t_i^{\Delta_i} e^{-\sum_{i < j} t_i t_j Q_{ij}} = \frac{1}{(2\pi i)^{(n(n-3))/2}} \int d\delta_{ij} \prod_{i < j}^n \Gamma(\delta_{ij}) Q_{ij}^{-\delta_{ij}}, \quad (3.143)$$

with $Q_{ij} > 0$. The Mellin variables δ_{ij} are integrated along a contour parallel to the imaginary axis with $\text{Re}(\delta_{ij}) > 0$ and obey the constraints

$$\sum_{j \neq i} \delta_{ij} = \Delta_i. \quad (3.144)$$

This allows us to find the inverse Mellin transform of the position-space partial-wave and the Mellin partial-wave

$$F_{\nu_1, \nu_2, 0, 0, 0}(x_i) = \frac{1}{(2\pi i)^5} \int d\delta_{ij} \mathcal{M}_{\nu_1, \nu_2, 0, 0, 0}(\delta_{ij}) \prod_{i < j}^n \Gamma(\delta_{ij}) x_{ij}^{-2\delta_{ij}} \quad (3.145)$$

The remaining integrations in t, \bar{t}, s and \bar{s} are straightforward to do. We then find

$$\begin{aligned} \mathcal{M}_{\nu_1, \nu_2, 0, 0, 0}(\delta_{ij}) = & \frac{\pi^{2h} \left(\left(\prod_{i=1}^2 \Gamma \left(\frac{\Delta_{2i-1} + \Delta_{2i} - t_{2i-1} t_{2i}}{2} \right) \left(\prod_{\sigma=\pm} \Gamma \left(\frac{h+\sigma(\Delta_{2i-1} - \Delta_{2i}) + i\nu_i}{2} \right) \right) \right)^{-1} } }{ \Gamma(\Delta_5) \Gamma \left(\frac{\Delta_5 - i\nu_1 + i\nu_2}{2} \right) \Gamma \left(\frac{t_{12} - t_{34} + \Delta_5}{2} \right) \Gamma \left(\frac{2h - \Delta_5 - i\nu_1 - i\nu_2}{2} \right) \Gamma \left(\frac{h - t_{12} + \Delta_5 - i\nu_2}{2} \right) } \\ & \left[\left(\prod_{\sigma=\pm} \Gamma \left(\frac{h - t_{12} + \sigma \Delta_5 - i\nu_2}{2} \right) \Gamma \left(\frac{\Delta_5 + \sigma i\nu_1 + i\nu_2}{2} \right) \right) \Gamma \left(\frac{h - t_{34} + i\nu_2}{2} \right) \Gamma \left(\frac{t_{12} - t_{34} + \Delta_5}{2} \right) \right. \\ & 3F_2 \left(\frac{t_{12} - t_{34} + \Delta_5}{2}, \frac{\Delta_5 - i\nu_1 + i\nu_2}{2}, \frac{\Delta_5 + i\nu_1 + i\nu_2}{2}; 1 \right) + \Gamma(\Delta_5) \Gamma \left(\frac{t_{12} - h + \Delta_5 + i\nu_2}{2} \right) \\ & \left. \left(\prod_{\sigma=\pm} \prod_{i=1}^2 \Gamma \left(\frac{h - t_{2i-1} t_{2i} + \sigma i\nu_i}{2} \right) \right) 3F_2 \left(\frac{h - t_{12} - i\nu_1}{2}, \frac{h - t_{12} + i\nu_1}{2}, \frac{h - t_{34} - i\nu_2}{2}; 1 \right) \right] \end{aligned} \quad (3.146)$$

where we use the notation $\delta_{ij} = \frac{\Delta_i + \Delta_j - t_{ij}}{2}$.

Let us finish this appendix by noting that a similar computation can be performed for spinning exchanges using Schwinger parametrization (3.139). To do so, at each moment, we multinomially expand the integrand decomposing it into sums over integrands of similar form to the ones encountered for scalar exchanges. In the end, one finds a spinning Mellin partial wave written as several sums over scalar-type Mellin partial waves. In particular the sums are bounded by the values of spin of the exchanged operators. This is no-good for an analytic continuation in spin that we want to consider here. For that reason and due to its length we do not write that result here.

3.C Explicit examples in position space

In this appendix, we single-out a conformal block contribution in position space and compute its Regge-limit behavior.

We start with five-point conformal block lightcone limit in its integral representation

$$G_{k_1 k_2 \ell}(u_i) = u_1^{\frac{\tau_1}{2}} u_3^{\frac{\tau_2}{2}} (1 - u_2)^\ell u_5^{\frac{\Delta_\phi}{2}} \int_0^1 [dt_1][dt_2] \frac{(1 - t_1(1 - u_2)u_4 - u_2u_4)^{J_2 - \ell} (1 - t_2(1 - u_2)u_5 - u_2u_5)^{J_1 - \ell}}{(1 - (1 - u_4)t_2)^{\frac{h_2 - \tau_1 - 2\ell + \Delta_\phi}{2}} (1 - (1 - u_5)t_1)^{\frac{h_1 - \tau_2 - 2\ell + \Delta_\phi}{2}} (1 - (1 - t_1)(1 - t_2)(1 - u_2))^{\frac{h_1 + h_2 - \Delta_\phi}{2}}}, \quad (3.147)$$

where $\tau_i = \Delta_i - J_i$ is the twist and $h_i = \Delta_i + J_i$ the conformal spin of the i -th exchanged operator. The measure is given by $[dt] = \frac{\Gamma(\Delta_i + J_i)}{\Gamma^2(\frac{\Delta_i + J_i}{2})} (t(1 - t))^{\frac{\Delta_i + J_i}{2} - 1}$.

Generically, we do not know how to evaluate these integrals in terms of known analytic functions. However, when the exponents in the denominator of the integrand are integers, this is no longer the case.²² As a matter of example we consider the simple case of $\Delta_i = \Delta_\phi = 2$ and $J_1 = J_2 = \ell = 0$. Note that this is just a choice and spinning cases would also have a similar discussion but with longer explicit expressions. In this case, equation (3.147) can be integrated and yields (apart from an overall constant)

$$\begin{aligned} & \frac{u_1 u_3 u_5}{1 - u_5 + u_4 (u_2 u_5 - 1)} [\text{Li}_2(u_2 u_4) - \text{Li}_2(u_4) + \text{Li}_2(u_2 u_5) - \text{Li}_2(u_5) - \text{Li}_2(u_2) \\ & - \log(1 - u_2) \log(u_2) - \log(1 - u_4) \log(u_4) - \log(1 - u_5) \log(u_5) \\ & + \log(u_4) \log(u_5) + \log(u_2 u_5) \log(1 - u_2 u_5) + \log(u_2 u_4) \log(1 - u_2 u_4) + \zeta(2)] . \end{aligned} \quad (3.148)$$

²²The package HyperInt [146] is particularly useful to evaluate these integrals.

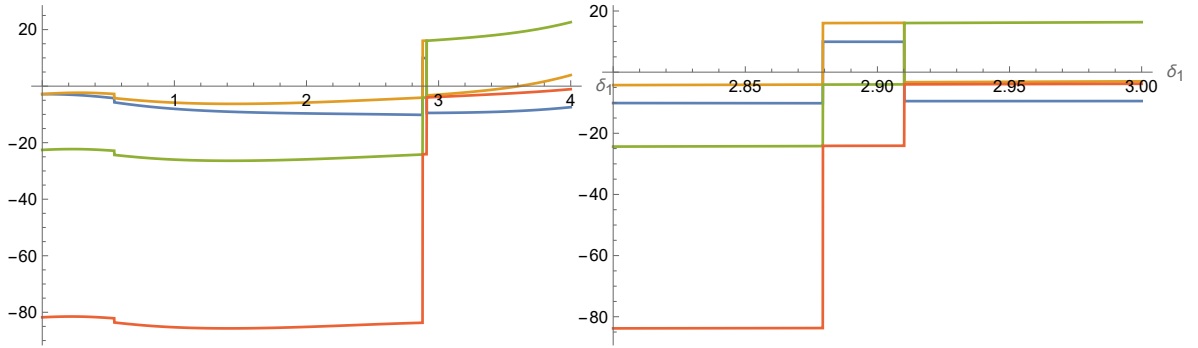


FIGURE 3.12: Discontinuities of lightcone block under analytic continuation (3.78). In blue, the real part of the stripped-off lightcone block. In orange, the real part of the block with $\log(u_2) \rightarrow \log(u_2) + 2\pi i$. In green, the previous with $\log(u_4) \rightarrow \log(u_4) - 2\pi i$ and in red, the latter with $\log(u_5) \rightarrow \log(u_5) - 2\pi i$. On the right, a zoomed-in version of the same plot. The plots are obtained with $\delta_2 = 0.73\delta_1$.

As we perform the analytic continuation from an Euclidean to double-Reggeon exchange kinematics that we presented in (3.78), we cross block branch-cuts and it mixes with other solutions of the Casimir equations. In particular, the discontinuities of the block contain the leading contributions in the Regge limit. Having an explicit expression to work with we can tell the full story.

As we perform the analytic continuation and as the lightcones are crossed, pairs of operators become timelike separated and cross-ratios u_2, u_4 and u_5 go around 0. Note then that we are indeed crossing branch-cuts of the expression (3.148). In particular, we observe that only log terms in (3.148) can contribute to the discontinuity as u_i goes around 0 with $\log(x) \rightarrow \log(x) \pm 2\pi i$. The actual sign one picks is determined by how one moves around branch-cuts. As we reviewed in the main text, this depends on the ordering of operators of the Wightman function we consider. As before, here we take an ordering compatible with the time-ordering of Regge kinematics, i.e. $\langle \phi_4 \phi_1 \phi_2 \phi_5 \phi_3 \rangle$. Taking this ordering and the associated $i\epsilon$ -prescription, we can perform the path continuation to Regge kinematics in our explicit-lightcone-block contribution and observe its discontinuities concretely. This is plotted in figure 3.12.²³ As we move according to the chosen path for analytic continuation, we observe that the lightcone block (blue) has discontinuities. The first one can be removed if one replaces $\log(u_2) \rightarrow \log(u_2) + 2\pi i$ as shown by the orange line. Clearly, this shows that the discontinuity of the lightcone block is due to a logarithmic discontinuity in u_2 . Similarly, when the orange line has a discontinuity, there is a continuation provided by the green line. The latter is defined from the former with the replacement $\log(u_4) \rightarrow \log(u_4) - 2\pi i$. We

²³In this plot we only considered the terms within the brackets in (3.148). Note that only this part is relevant for the discontinuities we want to study.

conclude that a discontinuity in u_4 has taken place. The same is true for the red line which provides the continuation of the green line once we take $\log(u_5) \rightarrow \log(u_5) - 2\pi i$ and once again a discontinuity, this time in u_5 , has to be considered. This simple example shows in practice what we had already guessed: the lightcone block has discontinuities associated with u_2, u_4 and u_5 going around 0 and all of them are important. Let us then study the discontinuities of (3.148) on these variables.

It is possible to use the integral representation of the lightcone block to argue that there are no sequential discontinuities involving u_2 , i.e.

$$\text{Disc}_{u_2} \text{Disc}_{u_4 \text{ or } u_5} G_{k_1, k_2, \ell} = \text{Disc}_{u_4 \text{ or } u_5} \text{Disc}_{u_2} G_{k_1, k_2, \ell} = 0. \quad (3.149)$$

In the expression (3.148) this is straightforward to see as there are no products of the type $\log(u_2) \log(u_4)$ or $\log(u_2) \log(u_5)$. As it was stated in the main text and as we will see below, it is actually the sum $\text{Disc}_{u_2} G_{k_1, k_2, \ell} + \text{Disc}_{u_5} \text{Disc}_{u_4} G_{k_1, k_2, \ell}$ that dominates the Regge behavior of the correlation function.

The discontinuity of expression (3.148) as u_2 goes around 0 with fixed $u_4, u_5 > 0$ is given by

$$\pm 2\pi i \frac{u_1 u_3 u_5}{1 - u_5 + u_4(u_2 u_5 - 1)} \log \left(\frac{1 - u_2}{(1 - u_2 u_4)(1 - u_2 u_5)} \right), \quad (3.150)$$

which in the limit $u_4, u_5 \rightarrow 1$ with $\chi_2 = \frac{1 - u_2}{(1 - u_4)(1 - u_5)}$ fixed simplifies to

$$\pm 2\pi i \frac{\sqrt{u_1} \sqrt{u_3}}{(\chi_2 - 1) \chi_4 \chi_5} \log(\chi_2), \quad (3.151)$$

where we also use $\chi_4 = \frac{1 - u_4}{\sqrt{u_3}}$ and $\chi_5 = \frac{1 - u_5}{\sqrt{u_1}}$ which approach infinity due to the order of limits considered. This order of limits does not correspond to the actual Regge limit: indeed, we will call this ordered limit a boundary condition for Regge limit. The name simply follows from the fact that we use it below as a boundary condition for a set of recursion relations where we compute the Regge limit of a conformal block starting from the lightcone. Note, moreover, that the scaling in both u_1 and u_3 in the expression above agrees with the expected $u_i^{(1-J_i)/2}$ of Regge limit. As stated above we are indeed describing a double Reggeon exchange. This clearly contrasts with the Euclidean OPE scaling, $u_i^{\Delta_i/2}$, manifesting the difference between Regge and Euclidean kinematics. Perhaps a more striking example would follow from considering a spinning case from the beginning. The story is no different in those cases but the expressions grow considerably in size. We also note the existence of a log term in the case at hand. We point out that some other examples where the lightcone block can be integrated do not have these contributions in the above limit.

Its existence in this case suggests however that a generic function for the discontinuity of the lightcone block as u_2 goes around 0 must contain log terms when the representation labels of the external and exchanged operators conspire in a certain way.

We now consider the discontinuity in u_4 with fixed and positive u_2, u_5 . This gives

$$\pm 2\pi i \frac{u_1 u_3 u_5}{1 - u_5 + u_4(u_2 u_5 - 1)} \log \left(\frac{1 - u_4}{(1 - u_2 u_4) u_5} \right), \quad (3.152)$$

which yields a boundary condition for Regge limit

$$\pm 2\pi i \frac{u_1 \sqrt{u_3}}{\chi_4}. \quad (3.153)$$

From the symmetry of (3.148) between u_4 and u_5 we immediately see that a similar result follows for the discontinuity in u_5 . Note that these terms are subdominant in the limit $u_1, u_3 \rightarrow 0$ when compared to (3.151). In particular, in expression (3.153) u_1 scales as $u_1^{\Delta_1/2}$ whereas u_3 scales as $u_3^{(1-J_2)/2}$. The converse happens in the discontinuity in u_5 complex plane. This behavior should correspond to single Reggeon exchanges. Notably, the sequential discontinuity in u_4 and u_5 produces a dominant contribution for the double Reggeon kinematics. To see this, consider (3.152) and take the sequential discontinuity in u_5 . This gives

$$\pm 4\pi^2 \frac{u_1 u_3 u_5}{1 - u_5 + u_4(u_2 u_5 - 1)}, \quad (3.154)$$

which fixes the boundary condition for Regge limit

$$4\pi^2 \frac{\sqrt{u_1} \sqrt{u_3}}{(\chi_2 - 1) \chi_4 \chi_5}, \quad (3.155)$$

that is as dominant as (3.151). We conclude in this simple example, the generic statement we have made in the main text that $\text{Disc}_{u_2} G_{k_1, k_2, \ell} + \text{Disc}_{u_5} \text{Disc}_{u_4} G_{k_1, k_2, \ell}$ provide the dominant contributions of the correlation function in Regge limit.

Even though the existence of log terms in the boundary condition for the Regge limit is not generic, we should however show how to deal with them when we compute the conformal blocks at Regge limit. If there are no log terms in your case of interest, simply set those terms to zero in the procedure below. We consider the Casimir equations in the limit of $u_1, u_3 \rightarrow 0$ with a block that scales as

$$\mathcal{G}_{k'_1 k'_2 \ell}(x_i) \propto u_1^{\frac{1-J_1}{2}} u_3^{\frac{1-J_2}{2}} \mathcal{H}(\chi_2, \chi_4, \chi_5). \quad (3.156)$$

In this limit, the Casimir equations for \mathcal{H} simplify and read

$$\left[\chi_4^2 \left(4(2\chi_2 - 1)(\partial_{\chi_2} - \chi_5 \partial_{\chi_2} \partial_{\chi_5}) - (d-1)\chi_5^3 \partial_{\chi_5} - (\chi_5^2 - 4)\chi_5^2 \partial_{\chi_5}^2 \right) + 4 \left((\chi_2 - 1)\chi_2 \chi_4^2 + 1 \right) \partial_{\chi_2}^2 + (\Delta_1 - 1)(\Delta_1 - d + 1)\chi_4^2 \chi_5^2 \right] \mathcal{H}(\chi_2, \chi_4, \chi_5) = 0 \quad (3.157)$$

with an entirely similar second equation obtained from the above by replacing Δ_1 by Δ_2 and permuting the roles of χ_4 and χ_5 . In our particular case of study, in the limit of $u_1, u_3 \rightarrow 0$, large χ_4, χ_5 and fixed χ_2 , the leading Regge contribution of the block behaves as

$$\frac{\sqrt{u_1} \sqrt{u_3}}{(\chi_2 - 1)\chi_4 \chi_5} (a + b \log(\chi_2)) \quad (3.158)$$

where a and b are constants. We can thus further impose in (3.157)

$$\mathcal{H}(\chi_2, \chi_4, \chi_5) = \frac{\mathbb{H}(\chi_2, \chi_4, \chi_5)}{\chi_4 \chi_5}. \quad (3.159)$$

According to (3.158) and considering a small- χ_2 limit, we can look for solutions of the Casimir equations of the form

$$\mathbb{H}(\chi_2, \chi_4, \chi_5) = \sum_{n_1, n_2, n_3} a_{n_1, n_2, n_3} \chi_2^{n_1} \chi_4^{-n_2} \chi_5^{-n_3} + b_{n_1, n_2, n_3} \log(\chi_2) \chi_2^{n_1} \chi_4^{-n_2} \chi_5^{-n_3} \quad (3.160)$$

where the coefficients a_{n_1, n_2, n_3} and b_{n_1, n_2, n_3} reduce to a and b , respectively, when all n_i are 0. The remaining expansion coefficients a_{n_1, n_2, n_3} and b_{n_1, n_2, n_3} are fixed by the Casimir equations. It is easy to see that this ansatz gives rise to terms in the Casimir equations of the form

$$\chi_2^{c_1+n_1} \chi_4^{c_2-n_2} \chi_5^{c_3-n_3} \times \begin{cases} a_{n_1, n_2, n_3} \\ b_{n_1, n_2, n_3} \\ b_{n_1, n_2, n_3} \log(\chi_2) \end{cases}. \quad (3.161)$$

Clearly, the terms that depend on \log should cancel among each other in order to satisfy the Casimir equation. This leads to two constraints per Casimir equation, one for the \log -dependent terms and one for the remaining. For the isolated \log terms, we find recursion relations for the coefficients by removing the χ -dependence from the equations. To do so, we shift each term accordingly, i.e. $n_1 \rightarrow n_1 - c_1$, $n_2 \rightarrow n_2 + c_2$ and $n_3 \rightarrow n_3 + c_3$. This

leads to the following recursion relations

$$b_{n_1, n_2, n_3} = \frac{1}{n_3(d - n_3 - 4)} \left[4(n_1 + 1) \left((n_1 + n_3)b_{n_1+1, n_2, n_3-2} - (n_1 + 2)b_{n_1+2, n_2-2, n_3-2} \right) - 4(n_1 + n_3 - 1)(n_1 + n_3)b_{n_1, n_2, n_3-2} \right] \quad (3.162)$$

with a similar one where we exchange the roles of n_3 and n_2 . Clearly, the above recursion relation cannot be used whenever $n_3 = 0$. In such case, the other recursion relation can be used instead (and vice-versa). An entirely similar argument follows for the non-log-dependent terms. We find the recursion relations

$$a_{n_1, n_2, n_3} = \frac{4}{n_2(4 - d + n_2)} \left[(n_1 + n_2 - 1)(n_1 + n_2)a_{n_1, n_2-2, n_3} - (n_1 + 1)(n_1 + n_2)a_{n_1+1, n_2-2, n_3} \right. \\ \left. + (n_1 + 1)(n_1 + 2)a_{n_1+2, n_2-2, n_3-2} + (2n_1 + 2n_2 - 1)b_{n_1, n_2-2, n_3} - (2n_1 + n_2 + 1)b_{n_1+1, n_2-2, n_3} \right. \\ \left. + (2n_1 + 3)b_{n_1+2, n_2-2, n_3-2} \right] \quad (3.163)$$

with another equivalent relation where the roles of n_2 and n_3 are swapped.

These recursion relations are only meaningful once one prescribes a boundary condition. We impose that

$$a_{n_1, n_2, n_3} = b_{n_1, n_2, n_3} = 0 \quad \text{if} \quad n_1 < 0 \vee n_2 < 0 \vee n_3 < 0, \\ a_{0,0,0} = a \quad \text{and} \quad b_{0,0,0} = b. \quad (3.164)$$

It is easy to check that these recursion relations fix the behavior of all the coefficients up to those of the form $a_{n_1, 0, 0}$ and $b_{n_1, 0, 0}$ but note that these can be read from (3.158) by expanding it on small χ_2 limit.

3.D Other Regge kinematics

In this short appendix, we detail other possible Regge kinematics that we did not explore in detail in this chapter but that might be worth studying in the future.

Single Reggeon exchange

Within a five-point function, one can consider a single Reggeon exchange. In terms of Mandelstam invariants s_{25} or s_{45} of figure 3.1 only one of the two becomes large. In the context of CFTs, this translates to having only two operators, one in the first and one in

the second Poincare patches, approaching each other in such a way that there is only one cross-ratio going to 0 rather than two.

One possible analytic continuation that describes single Reggeon exchange is given by

$$\begin{aligned} x_1 &= -r (\sinh(\delta_1), \cosh(\delta_1), \mathbf{0}_{d-2}) & x_3 &= (0, 1, \mathbf{0}_{d-2}) & x_5 &= (0, h_1, h_2, \mathbf{0}_{d-3}) \\ x_2 &= r (\sinh(\delta_2), \cosh(\delta_2), \mathbf{0}_{d-2}) & x_4 &= (0, -1, \mathbf{0}_{d-2}) . \end{aligned} \quad (3.165)$$

with positive rapidities δ_i and $\mathbf{0}_d$ denoting a d -dimensional vector of zeros. In the large-rapidities limit, one can check that $u_1 \rightarrow 0$ and $u_2, u_5 \rightarrow 1$ with unfixed u_3 and u_4 . This agrees with the Euclidean OPE limit in the (12) channel. Again, we emphasize that this limit is attained after branch-cuts are crossed and thus in an intrinsically Lorentzian Regge sheet.

Six-point snowflake

The six-point conformal block of external scalars is known in the lightcone limit in the snowflake topology [1]. Even though here we did not attempt to analyze the cut-structure of this block, we nonetheless write down an analytic continuation prescription to achieve a Regge limit configuration that is consistent at the level of the cross-ratios with the OPE on channels (12), (34) and (56).

We use the set of 9 cyclic cross-ratios

$$\begin{aligned} u_1 &= \frac{x_{12}^2 x_{35}^2}{x_{13}^2 x_{25}^2} \quad u_{i+1} = u_i|_{x_i \rightarrow x_{i+1}} \mod 6 \\ U_1 &= \frac{x_{13}^2 x_{46}^2}{x_{14}^2 x_{36}^2} \quad U_{i+1} = U_i|_{x_i \rightarrow x_{i+1}} \mod 3 . \end{aligned} \quad (3.166)$$

In the snowflake OPE limit $u_1, u_3, u_5 \rightarrow 0$ and the remaining all go to 1. In the Regge limit one should reobtain the same limiting values of the cross-ratios after some lightcones are crossed. We start with a totally spacelike configuration and perform the analytic continuation

$$\begin{aligned} x_1 &= -r_1 (\sinh(\delta_1), \cosh(\delta_1), \mathbf{0}_{d-2}) & x_4 &= (\sinh(\delta_1), -\cosh(\delta_1), \mathbf{0}_{d-2}) \\ x_2 &= r_1 (\sinh(\delta_2), \cosh(\delta_2), \mathbf{0}_{d-2}) & x_5 &= (r_2 \sinh(\delta_3), r_3, h, r_2 \cosh(\delta_3), \mathbf{0}_{d-4}) \\ x_3 &= (-\sinh(\delta_2), \cosh(\delta_2), \mathbf{0}_{d-2}) & x_6 &= (-r_2 \sinh(\delta_3), r_4, h, -r_2 \cosh(\delta_3), \mathbf{0}_{d-4}) . \end{aligned} \quad (3.167)$$

where one can see that we use 9 degrees of freedom. Note as well that for six-point functions one can at most use the conformal symmetry to state that any generic correlation function

is related to one that lives in some half-subspace in 4 dimensions [185]. Perhaps the most notorious difference in this case is the need to boost a pair of points along some different plane. It is easy to check however that this prescription indeed leads to the expected OPE behavior for a snowflake six-point function.

Chapter 4

Kaluza-Klein Five-Point Functions from $AdS_5 \times S^5$ Supergravity

4.1 Introduction

Recent years have seen significant progress in computing holographic correlators, which are key objects for exploring and exploiting the AdS/CFT correspondence. Traditionally, holographic correlators are computed by diagrammatic expansions in AdS. Such a method works in principle. However, in practice, it requires the precise knowledge of the exceedingly complicated effective Lagrangians and is extremely cumbersome to use. Therefore, for almost twenty years the diagrammatic approach led to only a handful of explicit results. The new developments, on the other hand, are based in a totally different strategy which relies on new principles. This is the bootstrap approach initiated in [128, 186], which eschews the explicit details of the effective Lagrangian altogether. The new approach works directly with the holographic correlators and uses superconformal symmetry and consistency conditions to fix these objects. The bootstrap strategy has produced an array of impressive results.¹ For example, at tree level general four-point functions for $\frac{1}{2}$ -BPS operators with arbitrary Kaluza-Klein (KK) levels have been computed in all maximally superconformal theories [128, 186, 188, 189], as well as in theories with half the amount of maximal superconformal symmetry [190–192]. Note that these general results are all in the realm of four-point functions. Higher-point functions still mostly remain *terra incognita*. In fact, only two five-point functions have been computed in the literature for IIB supergravity on $AdS_5 \times S^5$ [57] and SYM on $AdS_5 \times S^3$ [129] respectively, and both for the lowest KK

¹See [187] for a review.

modes only. For the latter case, recently in [130], the authors computed the six-point correlator of the lowest KK modes as well.

However, as stressed in this thesis, studying higher-point holographic correlator is of great importance. Firstly, higher-point correlators allow us to extract new CFT data which is not included in four-point functions. For example, the OPE coefficient of two double-trace operators and one single-trace operator can only be obtained from a five-point function. Moreover, via the AdS unitarity method [50] higher-point correlators are also necessary ingredients for constructing higher-loop correlators. Secondly, via the AdS/CFT correspondence holographic correlators correspond to on-shell scattering amplitudes in AdS. Recently, there has been a lot of progress in finding AdS generalizations of flat-space properties [129, 192–205]. As we know from flat space, many remarkable properties of amplitudes are only visible at higher multiplicities. To further explore the analogy between holographic correlators and scattering amplitudes it is necessary to go to higher points. Finally, it has been observed in [48] that a ten-dimensional hidden conformal symmetry is responsible for organizing all tree-level four-point functions for IIB supergravity on $AdS_5 \times S^5$. The nature of this hidden structure is still elusive. It is an interesting question whether the 10d hidden symmetry is just a curiosity for four points or it persists even at higher points.

For these reasons, in this chapter we continue to explore the bootstrap strategy for computing higher-point correlators. In particular, we will focus on computing the five-point functions of the form $\langle pp222 \rangle$ for IIB supergravity in $AdS_5 \times S^5$, where three of the operators have the lowest KK level but the other two have arbitrary KK level p . Our strategy will be similar to that of [57], which computed the $p = 2$ case, but with important differences. In [57], the starting point is an ansatz in position space which is a linear combination of all possible Witten diagrams with unfixed coefficients. To fix the coefficients, one imposes various constraints from superconformal symmetry and consistency conditions. These includes factorization in Mellin space [144], the chiral algebra constraint [206] and the Drukker-Plefka twist [207]. The first constraint is the consistency condition for decomposing the five-point function into four-point functions and three-point functions at its singularities. The second and the third conditions come from superconformal symmetry and are the statement that the appropriately twisted five-point function becomes topological. Although these conditions uniquely fix the $p = 2$ five-point function, the strategy of [144] suffers from a few drawbacks which make it difficult to apply efficiently

to correlators with higher KK levels. Firstly, computing the higher-point Witten diagrams in the ansatz is a nontrivial task. In particular, simplifications used in [144] for computing $p = 2$ diagrams no longer exist for $p > 2$ and the analysis is in general more complicated. Secondly, the three constraints were implemented in difference spaces, which makes the algorithm less efficient. Factorization is most convenient in Mellin space. However, the chiral algebra constraint and the Drukker-Plefka twist were implemented in the original position space. The position space implementation requires computing explicitly a set of five-point contact diagrams, *i.e.*, D -functions, to which the ansatz reduces. As was shown in [144], these D -functions can further be expressed in terms of one-loop box diagrams which can be written as Li_2 and logarithms. But the complexity of the expression for each D -function is determined by its total external conformal dimensions. For $\langle pp222 \rangle$ five-point functions, the sum of dimensions grows linearly with respect to p . Therefore, it soon becomes computationally very expensive for large enough p .

We overcome these difficulties by proposing a new algorithm. It relies on the key observation that a more careful analysis of the Mellin factorization condition together with the Drukker-Plefka twist allow us to completely fix the five-point correlators without using the chiral algebra constraint. Although computing Witten diagrams is difficult in position space, formulating the ansatz in Mellin space is straightforward thanks to their simplified analytic structure in Mellin space. This is further aided by a new pole truncation phenomenon which keeps the number of poles fixed irrespective of the KK levels. As a result, we can write down the ansatz for the Mellin amplitude for general p . Moreover, we find a way to implement the Drukker-Plefka twist directly in Mellin space. Therefore, we can perform the bootstrap entirely within Mellin space without ever taking the position space detour. This allows us to compute the five-point $\langle pp222 \rangle$ Mellin amplitudes for arbitrary p in a closed form. Although here we focused on this particular family of correlators, the strategy applies straightforwardly to more general five-point functions.

The rest of the chapter is organized as follows. In Sec. 4.2 we discuss the superconformal kinematics of the five-point functions. In particular, we will introduce the Drukker-Plefka twist. In Sec. 4.3 we review the Mellin space formalism and the factorization of Mellin amplitudes. We also explain how to implement the Drukker-Pleka twist in Mellin space. We bootstrap the five-point functions in Sec. 4.4 and give the general formula for the $\langle pp222 \rangle$ Mellin amplitudes. In Sec. 4.4.5 we also comment on how to perform the bootstrap in position space. We conclude in Sec. 4.5 with an outlook for future directions. Technical

details are contained in the two appendices. In Appendix 4.A we explain how to compute spinning four-point functions which are needed for factorizing the five-point functions. In Appendix 4.A.4 we discuss how to glue together the R-symmetry dependence when performing factorization.

4.2 Superconformal kinematics of five-point functions

We consider the correlation functions of the super primaries of the $\frac{1}{2}$ -BPS multiplets. These are scalar operators $\mathcal{O}_k^{I_1 \dots I_k}$ with $I = 1, \dots, 6$, $k = 2, 3, \dots$, transforming in the rank k symmetric traceless representation of the $SO(6)$ R-symmetry group. Their conformal dimensions are protected by supersymmetry and are determined by the R-symmetry representation $\Delta = k$. Via the AdS/CFT correspondence, they are dual to scalar fields in AdS with KK level k and are usually referred to as the super gravitons. A convenient way to keep track of the R-symmetry information is to contract the indices with null polarization vectors

$$\mathcal{O}_k(x; t) = \mathcal{O}_k^{I_1 \dots I_k} t_{I_1} \dots t_{I_k}, \quad t \cdot t = 0. \quad (4.1)$$

Our main target in this chapter is the following five-point correlator

$$G_p(x_i; t_i) = \langle \mathcal{O}_p(x_1; t_1) \mathcal{O}_p(x_2; t_2) \mathcal{O}_2(x_3; t_3) \mathcal{O}_2(x_4; t_4) \mathcal{O}_2(x_5; t_5) \rangle. \quad (4.2)$$

More precisely, we will compute the leading connected contribution which is of order $1/N^3$ and corresponds to tree-level scattering in AdS. The disconnected piece factorize into a three-point function and a two-point function, and is protected because the lower-point functions are.

Symmetry imposes strong constraints on the form the correlator. For example, conformal symmetry allows us to write the five-point function as a function of five conformal cross ratios after extracting an overall kinematic factor²

$$u_1 = \frac{x_{12}^2 x_{35}^2}{x_{13}^2 x_{25}^2}, \quad u_2 = \frac{x_{14}^2 x_{23}^2}{x_{13}^2 x_{24}^2}, \quad u_3 = \frac{x_{25}^2 x_{34}^2}{x_{24}^2 x_{35}^2}, \quad u_4 = \frac{x_{13}^2 x_{45}^2}{x_{14}^2 x_{35}^2}, \quad u_5 = \frac{x_{15}^2 x_{24}^2}{x_{14}^2 x_{25}^2} \quad (4.3)$$

where we have defined $x_{ij} = x_i - x_j$. Similarly, extracting a kinematic factor also allows us to express the R-symmetry dependence as a function of the following five R-symmetry

²We are using a different, but equivalent, set of cross ratios here compared to [57]. These new cross ratios have appeared before in [64]. One reason why these variables are nice is that it is possible to associate some x_{ij}^2 to u_k , for example x_{12} only appears in u_1 . Another interesting property is that they are cyclically related to each other.

cross ratios

$$\sigma_1 = \frac{t_{12}t_{35}}{t_{13}t_{25}}, \quad \sigma_2 = \frac{t_{14}t_{23}}{t_{13}t_{24}}, \quad \sigma_3 = \frac{t_{25}t_{34}}{t_{24}t_{35}}, \quad \sigma_4 = \frac{t_{13}t_{45}}{t_{14}t_{35}}, \quad \sigma_5 = \frac{t_{15}t_{24}}{t_{14}t_{25}} \quad (4.4)$$

where we have introduced the shorthand notation $t_{ij} = t_i \cdot t_j$. However, there is more we can say about the R-symmetry dependence. Since the polarization vectors t_i are just multiplied to saturate the R-symmetry indices, they must appear in G_p with positive powers. Therefore, G_p must be a collection of monomials of the form $\prod_{i < j} t_{ij}^{a_{ij}}$, with the conditions

$$a_{ij} = a_{ji} \geq 0, \quad \sum_{j \neq i} a_{ij} = k_i, \quad (4.5)$$

where $k_1 = k_2 = p$, $k_3 = k_4 = k_5 = 2$ are the weights of the external operators. Note the number of these monomials is finite and we will refer to them as different R-symmetry structures. In Section 4.2.1, we will explicitly write down these structures.

The considerations so far have only used the bosonic symmetries in the full superconformal group. The dependence on the spacetime variables x_{ij}^2 and on the R-symmetry variables t_{ij} are not related. However, the fermionic generators in the superconformal group will impose further constraints which correlate the x_{ij}^2 and t_{ij} dependence. For five-point functions, a thorough analysis the full consequence of the fermionic symmetries has not been performed in the literature. However, two classes of such constraints are known. The first is the chiral algebra construction [206] which constrain the five-point function when all the operators are inserted on a two dimensional plane. The other is the Drukker-Plefka twist [207] which imposes constraints on the correlator with generic insertion positions. In this chapter, we will only need the latter. We will review these conditions in Section 4.2.2.

4.2.1 R-symmetry

A systematic way to enumerate the R-symmetry structures of the $\langle pp222 \rangle$ five-point function is to consider the Wick contractions. Different Wick contractions are illustrated in

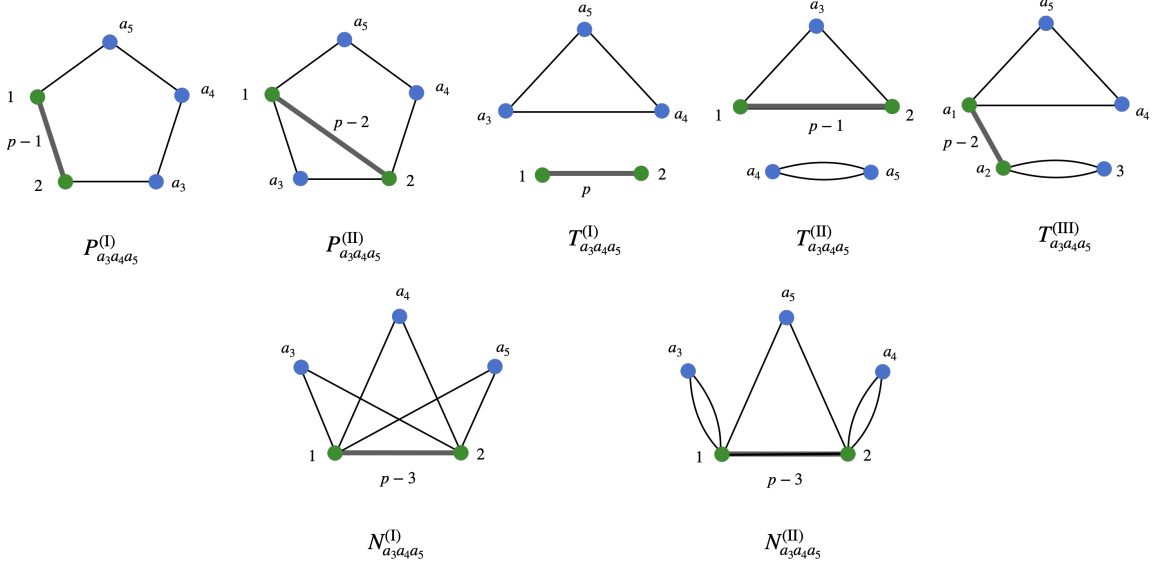


FIGURE 4.1: Inequivalent R-symmetry structures in the $\langle pp222 \rangle$ five-point function. Here (a_1, a_2) is $(1, 2)$ or $(2, 1)$ and (a_3, a_4, a_5) can be any permutation of $(3, 4, 5)$. Each thin line represents a single contraction. The thick line represents the multi-contraction t_{12}^a with the power a given by the number next to the line. The R-symmetry structures in the first row have counterparts in the $\langle 22222 \rangle$ five-point correlator. For $\langle pp222 \rangle$ they are simply obtained by multiplying the $p = 2$ structures with t_{12}^{p-2} . The R-symmetry structures in the second row are new and do not appear in $\langle 22222 \rangle$.

Fig. 4.1 and the corresponding R-symmetry structures are explicitly given by

$$\begin{aligned}
 P_{a_3 a_4 a_5}^{(I)} &= t_{12}^{p-1} t_{2a_3} t_{a_3 a_4} t_{a_4 a_5} t_{1a_5} , \\
 P_{a_3 a_4 a_5}^{(II)} &= t_{12}^{p-2} t_{1a_3} t_{2a_3} t_{2a_4} t_{a_4 a_5} t_{1a_5} , \\
 T_{a_3 a_4 a_5}^{(I)} &= t_{12}^p t_{a_3 a_4} t_{a_4 a_5} t_{a_3 a_5} , \\
 T_{a_3 a_4 a_5}^{(II)} &= t_{12}^{p-1} t_{2a_3} t_{1a_3} t_{a_4 a_5}^2 , \\
 T_{a_1 a_2 a_3 a_4 a_5}^{(III)} &= t_{a_1 a_2}^{p-2} t_{a_1 a_4} t_{a_4 a_5} t_{1a_5} t_{a_2 a_3}^2 , \\
 N_{a_3 a_4 a_5}^{(I)} &= t_{12}^{p-3} t_{1a_3} t_{1a_5} t_{2a_3} t_{2a_5} t_{1a_4} t_{2a_4} , \\
 N_{a_3 a_4 a_5}^{(II)} &= t_{12}^{p-3} t_{1a_3}^2 t_{2a_4}^2 t_{1a_5} t_{2a_5} .
 \end{aligned} \tag{4.6}$$

Here (a_1, a_2) is $(1, 2)$ or $(2, 1)$ and (a_3, a_4, a_5) can be any permutation of $(3, 4, 5)$. The Wick contractions in the first row of Fig. 4.1 exist for all $p \geq 2$ while the second row are only possible when $p \geq 3$. This is a new phenomena that arises at the level of five-point functions and should be contrasted with the four-point function case. In the four-point function $\langle pp22 \rangle$, the number of Wick contractions is the same irrespective of the Kaluza-Klein weight p .³

³In fact, this is true even in the more general case $\langle pqrs \rangle$ as long as the extremality E of the correlator remains the same. Here extremality is defined as $E = s - p - q - r$ and we have assumed that s is the largest weight of them.

For $p = 2$, all the five points are on the same footing and there is no distinction between $P_{a_3 a_4 a_5}^{(I)}$, $P_{a_3 a_4 a_5}^{(II)}$ and among $T_{a_3 a_4 a_5}^{(I)}$, $T_{a_3 a_4 a_5}^{(II)}$, $T_{a_1 a_2 a_3 a_4 a_5}^{(III)}$. Multiplying them by t_{12}^{p-2} gives the corresponding structures when $p > 2$. Note that even when $p \geq 3$, some of these R-symmetry structures in Fig. 4.1 still have residual symmetries and are invariant under certain permutations of $\{a_3, a_4, a_5\}$. For example, $T_{a_3 a_4 a_5}^{(I)} = T_{a_4 a_3 a_5}^{(I)} = T_{a_3 a_5 a_4}^{(I)}$ and $T_{a_3 a_4 a_5}^{(II)} = T_{a_3 a_5 a_4}^{(II)}$. We choose the independent R-symmetry structures to be

$$\begin{aligned}
P_{a_3 a_4 a_5}^{(I,II)} : \quad & (a_3, a_4, a_5) \in \{(3, 4, 5), (3, 5, 4), (4, 3, 5), (4, 5, 3), (5, 3, 4), (5, 4, 3)\} , \\
T_{a_3 a_4 a_5}^{(I)} : \quad & (a_3, a_4, a_5) \in \{(3, 4, 5)\} , \\
T_{a_3 a_4 a_5}^{(II)} : \quad & (a_3, a_4, a_5) \in \{(3, 4, 5), (4, 3, 5), (5, 3, 4)\} , \\
T_{a_1 a_2 a_3 a_4 a_5}^{(III)} : \quad & (a_1, a_2, a_3, a_4, a_5) \in \{(1, 2, 3, 4, 5), (1, 2, 4, 3, 5), (1, 2, 5, 3, 4), (2, 1, 3, 4, 5), \\
& (2, 1, 4, 3, 5), (2, 1, 5, 3, 4)\} , \\
N_{a_3 a_4 a_5}^{(I)} : \quad & (a_3, a_4, a_5) \in \{(3, 4, 5)\} , \\
N_{a_3 a_4 a_5}^{(II)} : \quad & (a_3, a_4, a_5) \in \{(3, 4, 5), (3, 5, 4), (4, 3, 5), (4, 5, 3), (5, 3, 4), (5, 4, 3)\} .
\end{aligned} \tag{4.7}$$

This gives in total 29 independent R-symmetry structures. When $p = 2$, $N_{a_3 a_4 a_5}^{(I)}$ and $N_{a_3 a_4 a_5}^{(II)}$ do not exist and we have 22 structures.

4.2.2 Drukker-Plefka twist and chiral algebra

A highly nontrivial constraint from superconformal symmetry is given by the topological twist discovered in [207], which we will refer to as the Drukker-Plefka twist. In [207], it was found that when the operators have the following position-dependent polarization vectors (commonly referred to as a twist)

$$\bar{t}_i = (ix_i^1, ix_i^2, ix_i^3, ix_i^4, \frac{i}{2}(1 - (x^\mu)^2), \frac{1}{2}(1 + (x^\mu)^2)) , \tag{4.8}$$

the twisted correlator preserves certain nilpotent supercharge. The twisted operators are in its cohomology. More importantly, the translations of operators while keeping the polarizations twisted are exact. It then follows that the twisted correlators are topological, *i.e.*, independent of the insertion locations

$$G_p(x_i; \bar{t}_i) = \text{constant} . \tag{4.9}$$

Note that in terms of the variables x_{ij}^2 and t_{ij} , the twist condition can also be written as $t_{ij} = x_{ij}^2$.

Let us also mention another twist for contrast, namely the chiral algebra [206]. However, we will not exploit this twist here. The chiral algebra twist requires that all the operators are inserted on a two dimensional plane. The coordinates therefore can be parameterized by the complex coordinates z, \bar{z} . Furthermore, the polarization vectors need to be restricted to be four dimensional

$$t_i = (t_i^\mu, 0, 0) , \quad \mu = 1, 2, 3, 4 , \quad (4.10)$$

where t^μ can be written in terms of two-component spinors

$$t_i^\mu = \sigma_{\alpha\dot{\alpha}}^\mu v^\alpha \bar{v}^{\dot{\alpha}} . \quad (4.11)$$

Using the rescaling freedom of the polarization vector, we can write v and \bar{v} as

$$v_i = (1, w_i) , \quad \bar{v} = (1, \bar{w}_i) . \quad (4.12)$$

When we twist the operators by setting $\bar{w}_i = \bar{z}_i$, the correlator also preserves certain nilpotent supercharge. The twisted operators are in its cohomology while the antiholomorphic twisted translations are exact. Therefore, the twisted correlator are meromorphic functions of z_i only.

4.3 Mellin representation

It has been commonly advertised that Mellin space [142, 143] is a natural language for discussing holographic correlators. In this formalism, the connected correlators are expressed as a multi-dimensional inverse Mellin transformation

$$\langle \mathcal{O}(x_1) \dots \mathcal{O}(x_5) \rangle_{\text{conn}} = \int [d\delta] \mathcal{M}(\delta_{ij}) \prod_{1 \leq i < j \leq 5} \Gamma(\delta_{ij}) (x_{ij}^2)^{-\delta_{ij}} , \quad (4.13)$$

where the Mellin-Mandelstam variables satisfy

$$\delta_{ij} = \delta_{ji} , \quad \delta_{ii} = -\Delta_i , \quad \sum_j \delta_{ij} = 0 . \quad (4.14)$$

The function $\mathcal{M}(\delta_{ij})$ encodes the dynamical information and is referred to as the Mellin amplitude. Note that this definition is a bit schematic. To be precise, both the correlator and the Mellin amplitude also depend on R-symmetry structures. However, for the moment we will suppress this dependence to emphasize the analytic structure related to spacetime.

One of the reasons that Mellin amplitudes is convenient for describing scattering in AdS is they are meromorphic functions of the Mellin-Mandelstam variables. This follows directly from the existence of the OPE in CFT. Moreover, in the supergravity limit, the poles are associated with the exchanged single-trace particles in AdS. This makes the Mellin amplitudes have similar analytic structure as tree-level scattering amplitudes in flat space and allows us to apply flat-space intuitions in AdS.

More precisely, the exchange of a conformal primary operator with spin J and dimension $\Delta = \tau + J$ in a channel is represented by a series of poles in the Mellin amplitude, labelled by $m = 0, 1, 2, \dots$, starting from the conformal twist τ

$$\mathcal{M} \approx \frac{\mathcal{Q}_m(\delta_{ij})}{\delta_{LR} - (\tau + 2m)}, \quad \delta_{LR} = \sum_{a=1}^q \sum_{b=q+1}^n \delta_{ab}. \quad (4.15)$$

Here, the exchange channel divides the external particles into two sets which we refer to as L and R. We label the particles in L from 1 to q and the ones in R from $q + 1$ to n . δ_{LR} is the Mandelstam variable in this channel. The residues $\mathcal{Q}_m(\delta_{ij})$ have nontrivial structures. They are related to the lower-point Mellin amplitudes \mathcal{M}_L and \mathcal{M}_R for the $(q + 1)$ - and $(n - q + 1)$ -point functions involving particles in L and R respectively (Figure 4.2). The extra external state in each lower-point amplitude is the exchanged particle which has now been put on-shell. This is the basic idea of Mellin factorization [144, 208]. In fact, it is very similar to the factorization of amplitudes in flat space which has been studied for a long time. However, there are also important differences. In flat space, the poles are located at the squared masses of the exchanged particles. In Mellin space, as already pointed out, the squared mass is replaced by the conformal twist and there is in general a series of poles for each particle which are labelled by m in (4.15). These are related to the conformal descendants. However, in theories with special spectra such as $AdS_5 \times S^5$ IIB supergravity, the series usually truncates. For example, for $p = 2$ the series truncates at $m = 0$ and contains just one term. Moreover, compared to flat-space amplitudes, the lower-point Mellin amplitudes also appear in the residue \mathcal{Q}_m in a more complicated way. The precise expression for the residues depends on the spin of the operator that is exchanged. The goal of the following subsection is to explain all the details of this formula. In particular, we will present the explicit residue formulas for exchanged fields with spins up to 2. We should emphasize that the structure of factorization for the general $\langle pp222 \rangle$ five-point functions will turn out to be far richer than for the simple case of $p = 2$ which was analyzed in [57]. In particular, we will see poles with $m \geq 1$.

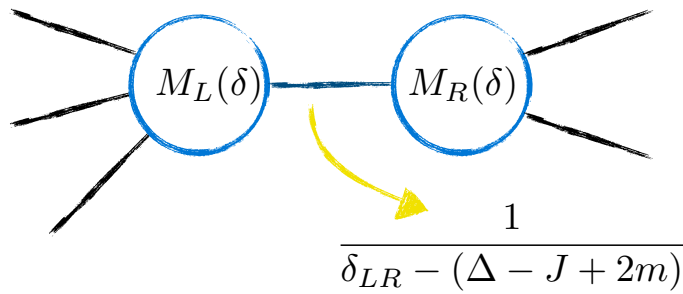


FIGURE 4.2: Mellin amplitudes have poles corresponding to the exchange of single-trace operators. The residues at the poles are associated with lower-point Mellin amplitudes. In the channel depicted in the figure, we have $n = 5$ and $q = 3$. The Mellin amplitude on the left has four points while the one on the right has only three.

Note that for the five-point function G_p with $p > 2$ there are three non-equivalent factorization channels which we choose to be

$$\begin{aligned} (12) : \quad & \langle pp\star \rangle \langle \star 222 \rangle , \\ (45) : \quad & \langle 22\star \rangle \langle \star pp2 \rangle , \\ (13) : \quad & \langle 2p\star \rangle \langle \star p22 \rangle , \end{aligned} \tag{4.16}$$

In each of them there are exchanged primary operators with spins ranging from 0 to 2 as will be discussed in the following subsection.

4.3.1 Mellin factorization

To discuss Mellin factorization, we need to be more explicit about what fields can be exchanged as they give rise to different lower-point functions. The problem of enumerating exchanged fields reduces to finding all the possible cubic vertices $s_{k_1}s_{k_2}X$ where s_k is the scalar field dual to the superconformal primary \mathcal{O}_k and X is a field to be determined. This problem already appears in the case of four-point functions and therefore the answer is also the same. The possible cubic vertices are determined by two conditions. The first is the R-symmetry selection rule. The second is the condition that the cubic vertices cannot be extremal⁴. These determine the possible exchange fields to be [128, 186]

$$\begin{aligned} \{k_1, k_2\} = \{p, p\} : \quad & X = s_2, A_{2,\mu}, \varphi_{2,\mu\nu} . \\ \{k_1, k_2\} = \{2, 2\} : \quad & X = s_2, A_{2,\mu}, \varphi_{2,\mu\nu} , \\ \{k_1, k_2\} = \{2, p\} : \quad & X = s_p, A_{p,\mu}, \varphi_{p,\mu\nu} . \end{aligned} \tag{4.17}$$

⁴It also follows that four-point functions cannot be extremal or next-to-extremal. In particular, we do not have the four-point functions $\langle 4222 \rangle$ and $\langle 6222 \rangle$.

Here s_k is a scalar field and is dual to the superconformal primary \mathcal{O}_k which has dimension $\Delta = k$ and transform in the $[0, k, 0]$ representation of $SU(4)$. $A_{k,\mu}$ is a vector field and is dual to a spin-1 operator $\mathcal{J}_{k,\mu}$ which has dimension $\Delta = k + 1$ and transforms in the $[1, k - 2, 1]$ representation. $\varphi_{k,\mu\nu}$ is a spin-2 tensor field and is dual to a spin-2 operator $\mathcal{T}_{k,\mu\nu}$ which has dimension $\Delta = k + 2$ and representation $[0, k - 2, 0]$. When $k = 2$, $A_{2,\mu}$ is the graviphoton and $\varphi_{2,\mu\nu}$ is the graviton. Their dual operators are correspondingly the R-symmetry current and the stress energy tensor.

Let us emphasize again that in this subsection we will only focus on the Mellin-Mandelstam variable dependence. Both \mathcal{M}_L and \mathcal{M}_R in fact also depend on R-symmetry variables. Therefore in the residues \mathcal{Q}_m there is also a gluing of the lower-point R-symmetry structures. However, this gluing is purely group theoretic. To avoid distracting the reader from the discussion of the dynamics, we will leave the details of R-symmetry gluing to Appendix 4.A.4. Alternatively, we can view the discussion in this subsection as the Mellin factorization for each R-symmetry structure.

4.3.1.1 Exchange of scalars

The simplest example of factorization is the exchange of a scalar operator with dimension Δ . The resulting \mathcal{M}_L and \mathcal{M}_R are again scalar Mellin amplitudes. Nevertheless, this example contains most of the features we shall need. In particular, the m dependence will be shared in the spinning cases. Therefore, we will first analyze this case in detail. The residue \mathcal{Q}_m introduced in (4.15) is given in [144]

$$\mathcal{Q}_m = \frac{-2\Gamma(\Delta)m!}{\left(1 + \Delta - \frac{d}{2}\right)_m} L_m R_m, \quad (4.18)$$

where L_m is related to \mathcal{M}_L by⁵

$$L_m = \sum_{\substack{n_{ab} \geq 0 \\ \sum n_{ab} = m}} \mathcal{M}_L(\delta_{ab} + n_{ab}) \prod_{1 \leq a < b \leq q} \frac{(\delta_{ab})_{n_{ab}}}{n_{ab}!} \quad (4.19)$$

and similarly for R_m . Notice that here and in the following we will often leave the spacetime dimension d unspecified, but it should always be set to 4. This equation has several interesting consequences, which will become more evident after analyzing a few examples. Let us start with a three-point Mellin amplitude for \mathcal{M}_L , which is just a constant c . In

⁵Notice that $\mathcal{M}_L(\delta_{ab} + n_{ab})$ is well defined when the Mellin-Mandelstam variables satisfy the pole condition (4.15), in addition to their constraints (4.14). The parallel with scattering amplitudes makes this point clear.

this case, recalling that $\delta_{12} = \frac{1}{2}(\Delta_1 + \Delta_2 - \delta_{LR})$ and δ_{LR} is set to $\Delta + 2m$ by the pole condition (4.15), equation (4.18) with $q = 2$ immediately gives

$$\mathcal{M}_L^{\text{3-pt}} = c \implies L_m = c \frac{(\bar{\delta}_{LR})_m}{m!}, \quad \bar{\delta}_{LR} := \frac{1}{2}(\Delta_1 + \Delta_2 - \Delta) - m. \quad (4.20)$$

Factorizing a five-point function leads to a three-point function and a four-point function. For $\langle pp222 \rangle$, there are three inequivalent factorization channels, which can be chosen to be (12), (45) and (13). From (4.17), we know that the exchanged scalar operators in these three channels have twists 2, 2 and p respectively. Thus, $\bar{\delta}_{LR}$ in each case is given by

$$\begin{aligned} (12) : \quad & \bar{\delta}_{LR} = p - 1 - m, \\ (45) : \quad & \bar{\delta}_{LR} = 1 - m, \\ (13) : \quad & \bar{\delta}_{LR} = 1 - m, \end{aligned} \quad (4.21)$$

and the corresponding values of δ_{LR} are $2 + m, 2 + m, p + m$. After plugging these values in (4.20), it is straightforward to see that the residue vanishes for $m > 0$ in the channels (13) and (45), and for $m \geq p - 1$ in the channel (12)⁶. Naively, one would conclude that in the (12) channel the number of poles increases with p . However, this is too fast since the other part R_m can give more constraints. To see this explicitly, let us look at a four-point Mellin amplitude which has the following generic form

$$\begin{aligned} \mathcal{M}_R^{\text{4pt}} = & \frac{c_1 \delta_{45}^2 + c_2 \delta_{45} + c_3}{\delta_{34} - 1} + c_4 + c_5 \delta_{34} + c_6 \delta_{45} \implies R_m = \frac{1}{m!} \left[\frac{c_1 m \delta_{45} (\delta_{45} + 1) (3 - m)_{m-1}}{\delta_{34} - 1} \right. \\ & \left. + \left(\frac{c_1 \delta_{45}^2 + c_2 \delta_{45} + c_3}{\delta_{34} - 1} + c_4 \right) (2 - m)_m + \frac{c_3 (1 - m)_m}{\delta_{34} - 1} + (c_5 \delta_{34} + c_6 \delta_{45}) (3 - m)_m \right]. \end{aligned} \quad (4.22)$$

Here we have evaluated the expression at the pole $\delta_{LR} = \tau + 2m$. It follows that R_m vanishes for this four-point Mellin \mathcal{M}_R for $m \geq 3$ and therefore the number of poles does not increase for arbitrary value of p . Let us also emphasize that all four-point Mellin amplitudes that appear in the OPE of the correlator $\langle pp222 \rangle$ have this structure as can be checked in Appendix 4.A.

Let us note that the absence of poles for $m \geq p - 1$ can also be understood from the pole structure of the Mellin integrand. The Gamma functions in the definition of Mellin amplitude already have poles in this location and a pole in the Mellin amplitude at $m \geq p - 1$ would give rise to a double pole. Such double poles are associated with the appearance of

⁶The zeros in these pochhammer symbols are exactly at a position to avoid a double pole, formed by one coming from the explicit Gamma functions in the definition and the other from the factorization formula (4.15).

anomalous dimension [128, 143, 186], which we do not expect at this order. On the other hand, at the moment we do not have a direct physical argument for the truncation of poles at $m \geq 3$. Finally, this truncation continues to hold for the factorization formulas when the exchanged operators have spins. This will be analyzed in the following subsubsection.

4.3.1.2 Exchange of operators with spins 1 and 2

In this subsection we will be interested in studying the contribution of operators with spins. As it turns out, the analysis of the scalar case straightforwardly generalizes to the spinning case. It is convenient to get rid of the Lorentz indices of these operators by contracting them with null polarization vectors

$$\mathcal{O}(x, z) = \mathcal{O}^{a_1 \dots a_J}(x) z^{a_1} \dots z^{a_J}, \quad (4.23)$$

where $z^2 = 0$ ensures the operator is traceless (we refer the reader to Section 3 of [144] for a more detailed review). The definition of Mellin amplitudes of one spinning operator and n scalar operators is given by [144]

$$\langle \mathcal{O}(x_0, z_0) \dots \mathcal{O}_n \rangle = \sum_{a_1, \dots, a_J=1}^n \prod_{i=1}^J (z_0 \cdot x_{a_i 0}) \int [d\delta] \mathcal{M}^{\{a\}}(\delta_{ij}) \prod_{i=1}^n \frac{\Gamma(\delta_i + \{a\}_i)}{(x_{i0}^2)^{\delta_i + \{a\}_i}} \prod_{1 \leq i < j \leq n} \frac{\Gamma(\delta_{ij})}{(x_{ij}^2)^{\delta_{ij}}}, \quad (4.24)$$

where

$$\{a\}_i = \delta_i^{a_1} + \dots + \delta_i^{a_J}, \quad \delta_i = - \sum_{j=1}^n \delta_{ij}, \quad \sum_{i,j=1}^n \delta_{ij} = J - \Delta_0. \quad (4.25)$$

We have used δ to denote the Kronecker delta so that it can be distinguished from the Mellin-Mandelstam variables δ . The Mellin amplitudes $\mathcal{M}^{\{a\}}$ satisfy certain linear relations that follows from the conformal invariance of the correlator, see equation (46) in [144]. Let us first focus on the spinning generalization of (4.18) for the conserved currents which reside in the $k = 2$ supermultiplet. For exchanging the graviphoton, the residues are given by⁷

$$\mathcal{Q}_m = \frac{(d-1)\Gamma(d-2)m!}{\left(\frac{d}{2}\right)_m} \sum_{a=1}^q \sum_{b=q+1}^n \delta_{ab} L_m^a R_m^b, \quad (4.26)$$

For exchanging the graviton, the residues are

$$\mathcal{Q}_m = \frac{-(d+1)\Gamma(d-1)m!}{2\left(\frac{d}{2}+1\right)_m} \left[\mathcal{Q}_m^{(1)} - \left(\frac{1}{2m} + \frac{1}{d} \right) \tilde{L}_m \tilde{R}_m \right], \quad (4.27)$$

⁷As above we write d to denote the dimension of space-time and we will always set $d = 4$.

where

$$\begin{aligned} \mathcal{Q}_m^{(1)} &= \sum_{a,b=1}^q \sum_{i,j=q+1}^n \delta_{ai}(\delta_{bj} + \delta_b^a \delta_j^i) L_m^{ab} R_m^{ij}, \\ \tilde{L}_m &= \sum_{a,b=1}^q \delta_{ab} [L_{m-1}^{ab}]^{ab}, \quad \tilde{R}_m = \sum_{a,b=1}^q \delta_{ab} [R_{m-1}^{ab}]^{ab}. \end{aligned} \quad (4.28)$$

Here we used the notation $[f(\delta_{ij})]^{ab} = f(\delta_{ij} + \delta_i^a \delta_j^b + \delta_j^a \delta_i^b)$. The functions L_m^a and L_m^{ab} (and analogously R_m^a , R_m^{ab}) are defined in the same way as in (4.19). Let us also add that for $m = 0$ the second term in Q_m for spin 2 is zero since both \tilde{L}_0 and \tilde{R}_0 vanish from the definition. Therefore, the appearance of the pole in m does not lead to a divergence.

These residue formulas for spinning operators clearly are not the full story as there are also non-conserved currents in the multiplets with $k > 2$. However, from (4.17) we can see that such non-conserved currents only appear in the channel with s_2 and s_p . Similar to the scalar case (4.21), the analysis of the three-point functions requires the truncation at $m = 0$. The residues are

$$Q_0 = -\Delta\Gamma(\Delta - 1) \sum_{a=1}^q \sum_{b=q+1}^n \delta_{ab} L_0^a R_0^b, \quad \text{for spin 1 ,} \quad (4.29)$$

$$Q_0 = -\frac{(\Delta + 1)\Gamma(\Delta - 1)}{2} \sum_{a,b=1}^q \sum_{i,j=q+1}^n \delta_{ai}(\delta_{bj} + \delta_b^a \delta_j^i) L_0^{ab} R_0^{ij} \quad \text{for spin 2 .} \quad (4.30)$$

The most general expressions for factorization with arbitrary external and internal dimensions and m can be found in [144]. But they are not needed in this chapter.

As in the scalar case, the truncation of poles also relies on the form of the spinning four-point amplitudes. They are given in Appendix 4.B (see (4.154) and (4.159) for explicit expressions). In particular, they have the same analytic structure as the scalar four-point amplitude (4.22) except that now they carry additional indices. As a result, the truncation of poles also holds for the exchange of spinning operators. More precisely, we have the same pole locations as in (4.21) where the allowed values for m are $m = 0, 1, 2$ for (12) and $m = 0$ for (45), (13).

To summarize, the Mellin factorization formulas allow us to reconstruct all the polar part of the amplitude from the lower-point Mellin amplitudes. Furthermore, the spectrum of the theory gives rise to a further simplification where the poles truncate to a finite range independent of p .

4.3.2 Drukker-Plefka twist in Mellin space

As we reviewed in the introduction, the two superconformal constraints, namely the chiral algebra and the Drukker-Plefka twist, were both formulated and implemented in position space [57]. To have a more streamlined algorithm, we would like to perform the bootstrap entirely within Mellin space and therefore need to translate such position space constraints into Mellin space. Let us first define the Mellin amplitude more precisely by restoring the R-symmetry dependence suppressed in the definition (4.13). For the $\langle pp22 \rangle$ correlator, we have

$$G_p(x_i, t_i) = \int [d\delta] \mathcal{M}(\delta_{ij}, t_{ij}) \prod_{1 \leq i < j \leq 5} \Gamma(\delta_{ij})(x_{ij}^2)^{-\delta_{ij}}, \quad (4.31)$$

where $\mathcal{M}(\delta_{ij}, t_{ij})$ is a linear combination of the 29 R-symmetry structures listed in (4.7). Usually the implementation of the twists in Mellin space is achieved by using the observation that x_{ij}^2 monomials multiplying the Mellin transform (4.31) can be absorbed into the definition by shifting the Mellin-Mandelstam variables. This gives rise to difference equations in Mellin space. This strategy has been used, for example, in [209, 210] to rewrite the superconformal Ward identities in Mellin space for four-point functions. In our case, there are extra complexities.

The issue is that the chiral algebra constraint requires all the operators to be on a two dimensional plane. When the number of operators $n > 4$, this cannot be achieved by a conformal transformation and there are relations among the cross ratios.⁸ The meromorphy of the correlator after the chiral algebra twist depends crucially on these relations. On the other hand, these relations do not hold in the definition of the Mellin amplitude where the locations of the operators are assumed to be general. Therefore, the position space chiral algebra condition cannot be translated into Mellin space using the same strategy.

By contrast, the Drukker-Plefka twist only imposes conditions on the R-symmetry polarizations and has no restriction on the operator insertions. Therefore, we can use the same trick to implement the Drukker-Plefka twist in Mellin space. More precisely, we can extract a kinematic factor and rewrite (4.31) in terms of cross ratios (4.3), (4.4)

$$G_p(x_i, t_i) = K_p \int d\delta_{ij} \mathcal{M}(\delta_{ij}, \sigma_i) \Gamma_{pp222} u_1^{p-\delta_{12}} u_2^{-\delta_{23}} u_3^{2-\delta_{34}} u_4^{-\delta_{45}} u_5^{1-\delta_{15}}. \quad (4.32)$$

⁸In two dimensions, the number of independent cross ratios is $2n - 6$ for $n \geq 2$. However, in high enough spacetime dimensions, the number of independent cross ratios is $\frac{n(n-3)}{2}$. The relation for the cross ratios can be written in form of $\det M = 0$ where the matrix M has elements $M_{ij} = x_{ij}^2$.

Here K_p is a kinematic factor

$$K_p = \frac{x_{13}^2 t_{12}^p t_{34}^2 t_{15} t_{35}}{(x_{12}^2)^p (x_{34}^2)^2 (x_{15}^2 x_{35}^2) t_{13}} , \quad (4.33)$$

and

$$\begin{aligned} \Gamma_{\text{pp222}} = & \Gamma(\delta_{12}) \Gamma(\delta_{15}) \Gamma(\delta_{23}) \Gamma(\delta_{15} - \delta_{23} - \delta_{34} + 1) \Gamma(\delta_{34}) \Gamma(\delta_{23} + 1 - \delta_{15} - \delta_{45}) \Gamma(\delta_{45}) \\ & \Gamma(p - \delta_{12} - \delta_{15} + \gamma_{34} - 1) \Gamma(\delta_{12} - p - \delta_{34} - \delta_{45} + 3) \Gamma(p - \delta_{12} - \delta_{23} + \delta_{45} - 1) . \end{aligned} \quad (4.34)$$

Moreover, we have chosen $\delta_{12}, \delta_{23}, \delta_{34}, \delta_{45}$ and δ_{15} as the independent Mellin variables. Performing the Drukker–Plefka twist amounts to setting $t_{ij} \rightarrow x_{ij}^2$, or equivalently $\sigma \rightarrow u$ for the cross ratios. To implement this in practice, we notice that doing the twist reduces to multiplying the Mellin representation of different terms of the correlator $K_p^{-1} G_p(x_i, t_i)$ by monomials $u_1^{n_1} u_2^{n_2} u_3^{n_3} u_4^{n_4} u_5^{n_5}$

$$\mathcal{M}(\delta_{ij}, \sigma_i) = \sum_{\{n_i\}} \sigma_1^{n_1} \sigma_2^{n_2} \sigma_3^{n_3} \sigma_4^{n_4} \sigma_5^{n_5} \mathcal{M}_{\{n_i\}}(\delta_{ij}) \rightarrow \sum_{\{n_i\}} u_1^{n_1} u_2^{n_2} u_3^{n_3} u_4^{n_4} u_5^{n_5} \mathcal{M}_{\{n_i\}}(\delta_{ij}) . \quad (4.35)$$

We can absorb them by shifting δ_{ij} and this has the effect on the Mellin amplitudes by acting with a difference operator

$$u_1^{n_1} u_2^{n_2} u_3^{n_3} u_4^{n_4} u_5^{n_5} \mathcal{M}_{\{n_i\}}(\delta_{ij}) \rightarrow \mathbb{D}_{n_1, \dots, n_5} \circ \mathcal{M}_{\{n_i\}}(\delta_{ij}) , \quad (4.36)$$

where the explicit action of $\mathbb{D}_{n_1, \dots, n_5}$ reads

$$\begin{aligned} \mathbb{D}_{n_1, \dots, n_5} \circ \mathcal{M}_{\{n_i\}}(\delta_{ij}) = & \mathcal{M}_{\{n_i\}}(\delta_{12} + n_1, \delta_{23} + n_2, \dots) \times (\delta_{12})_{n_1} (\delta_{15})_{n_5} (\delta_{23})_{n_2} (\delta_{34})_{n_3} (\delta_{45})_{n_4} \\ & (\delta_{15} - \delta_{23} - \delta_{34} + 1)_{n_5 - n_2 - n_3} (\delta_{23} - \delta_{15} - \delta_{45} + 1)_{n_2 - n_4 - n_5} (p - \delta_{12} - \delta_{15} + \delta_{34} - 1)_{n_3 - n_1 - n_5} \\ & (\delta_{12} - p - \delta_{34} - \delta_{45} + 3)_{n_1 - n_3 - n_4} (p - \delta_{12} - \delta_{23} + \delta_{45} - 1)_{n_4 - n_1 - n_2} . \end{aligned} \quad (4.37)$$

The various Pochhammer symbols come from comparing the shifted Gamma factor with the one in the Mellin representation definition. The full difference operator from the Drukker–Plefka twist, denoted as \mathbb{D}_{DP} , is then a sum of such operators acting on different R-symmetry structures. As we explained in Sec. 4.2.2, the twisted correlator is just a constant in position space. Following [128, 186], we should interpret its Mellin amplitude as zero. Therefore, the Drukker–Plefka twist condition becomes in Mellin space

$$\mathbb{D}_{\text{DP}} \circ \mathcal{M}(\delta_{ij}, \sigma_i) = 0 , \quad (4.38)$$

which explicitly reads

$$\sum_{\{n_i\}} \mathbb{D}_{n_1, \dots, n_5} \circ \mathcal{M}_{\{n_i\}}(\delta_{ij}) = 0. \quad (4.39)$$

The implications of this equation are discussed in the following section.

4.4 Bootstrapping five-point Mellin amplitudes

4.4.1 Strategy and ansatz

After introducing all the necessary ingredients, we are now ready to state our strategy. Our strategy is comprised of three steps. First, we start by formulating an ansatz in Mellin space which is based on our analysis of the analytic structure of the Mellin amplitudes. Second, we impose the Mellin factorization condition which is the statement that the pole residues should be correctly reproduced by the lower-point amplitudes. Finally, we implement the Drukker-Plefka twist in Mellin space and completely fix the ansatz. In the following, we explain the details of each step.

Step 1: Ansatz

As we emphasized in the previous section, Mellin amplitudes are meromorphic functions with simple poles corresponding to exchanging single-trace operators and residues related to lower-point amplitudes via factorization. Based on this, we have the following ansatz for the $\langle pp222 \rangle$ Mellin amplitude

$$\begin{aligned} \mathcal{M}(\delta_{ij}, t_{ij}) = & \sum_{m=0}^2 \frac{A_m(\delta_{ij}, t_{ij})}{(\delta_{12} + 1 + m - p)} + \sum_{\bar{a}=1,2, a=3,4,5} \frac{B_{\bar{a}a}(\delta_{ij}, t_{ij})}{\delta_{\bar{a}a} - 1} + \sum_{3 \leq a < b \leq 5} \frac{C_{ab}(\delta_{ij}, t_{ij})}{\delta_{ab} - 1} \\ & + D(\delta_{ij}, t_{ij}). \end{aligned} \quad (4.40)$$

Here $A_m(\delta_{ij}, t_{ij})$ is a rational function with possible poles in $\delta_{34}, \delta_{35}, \delta_{45}$. In particular, it includes simultaneous poles which correspond to double exchange processes in the (12), (34) channels *etc.* Similarly, $B_{\bar{a}a}(\delta_{ij}, t_{ij})$ is a rational function with possible poles in δ_{kl} at $\delta_{kl} = 1$. The labels k, l need to satisfy $k, l \neq \bar{a}, a$ but can be both from the set $\{3, 4, 5\}$, or belong to different sets $\{1, 2\}$ and $\{3, 4, 5\}$, see equation (4.44). To avoid double counting, $C_{jk}(\delta_{ij}, t_{ij})$ and $D(\delta_{ij}, t_{ij})$ do not have poles and they are polynomial functions of the Mellin-Mandelstam variables. Note that here we have also used our Mellin factorization analysis for the subleading poles from Section 4.3.1. We imposed that the poles in the (12) channel truncate to $m = 0, 1, 2$.

More concretely, the function $A_m(\delta_{ij}, t_{ij})$ in the ansatz has the following form

$$A_m(\delta_{ij}, t_{ij}) = \frac{A_{34,m}(\delta_{ij}, t_{ij})}{\delta_{34} - 1} + \frac{A_{35,m}(\delta_{ij}, t_{ij})}{\delta_{35} - 1} + \frac{A_{45,m}(\delta_{ij}, t_{ij})}{\delta_{45} - 1} + A_{\emptyset,m}(\delta_{ij}, t_{ij}), \quad (4.41)$$

where $A_{34,m}$, $A_{35,m}$ and $A_{45,m}$ are polynomials of degree 2 and $A_{\emptyset,m}$ is a polynomial of degree 1. Written explicitly, $A_{34,m}$ reads

$$A_{34,m}(\delta_{ij}, t_{ij}) = \sum_{\alpha_i}^{\alpha_1 + \alpha_2 + \alpha_3 \leq 2} \sum_{I=1}^{29} a_{34,m,\{\alpha_i\}}^I \delta_{23}^{\alpha_1} \delta_{25}^{\alpha_2} \delta_{45}^{\alpha_3} \mathcal{T}_I, \quad (4.42)$$

where $\{\delta_{23}, \delta_{25}, \delta_{45}\}$ are chosen to be the independent Mellin-Mandelstam variables in addition to δ_{12} and δ_{34} which already appear in the poles. We have also used $\{\mathcal{T}_I\}$ to denote collectively the 29 independent R-symmetry structures in (4.7). The expressions for $A_{35,m}$, $A_{45,m}$ are similar. The polynomial $A_{\emptyset,m}$ is given by

$$A_{\emptyset,m} = \sum_{\alpha_i}^{\alpha_1 + \alpha_2 + \alpha_3 + \alpha_4 \leq 1} \sum_{I=1}^{29} a_{\emptyset,m,\{\alpha_i\}}^I \delta_{23}^{\alpha_1} \delta_{25}^{\alpha_2} \delta_{45}^{\alpha_3} \delta_{34}^{\alpha_4} \mathcal{T}_I. \quad (4.43)$$

The other terms in the ansatz are similar and are given by

$$\begin{aligned} B_{13} &= \sum_{I=1}^{29} \left(\sum_{\alpha_i}^{\alpha_1 + \dots + \alpha_3 \leq 2} \left[\frac{b_{13,24,\{\alpha_i\}}^I \delta_{15}^{\alpha_1} \delta_{23}^{\alpha_2} \delta_{45}^{\alpha_3}}{\delta_{24} - 1} + \frac{b_{13,45,\{\alpha_i\}}^I \delta_{15}^{\alpha_1} \delta_{23}^{\alpha_2} \delta_{34}^{\alpha_3}}{\delta_{45} - 1} + \frac{b_{13,25,\{\alpha_i\}}^I \delta_{23}^{\alpha_1} \delta_{34}^{\alpha_2} \delta_{45}^{\alpha_3}}{\delta_{25} - 1} \right] \right. \\ &\quad \left. + \sum_{\alpha_i}^{\alpha_1 + \dots + \alpha_4 \leq 1} b_{13,\emptyset,\{\alpha_i\}}^I \delta_{23}^{\alpha_1} \delta_{34}^{\alpha_2} \delta_{45}^{\alpha_3} \delta_{15}^{\alpha_4} \right) \mathcal{T}_I, \\ C_{34} &= \sum_{\alpha_i}^{\alpha_1 + \dots + \alpha_3 \leq 1} \sum_{I=1}^{29} c_{34,\{\alpha_i\}}^I \delta_{12}^{\alpha_1} \delta_{23}^{\alpha_2} \delta_{45}^{\alpha_3} \delta_{15}^{\alpha_4} \mathcal{T}_I, \\ D &= \sum_{I=1}^{29} d^I \mathcal{T}_I. \end{aligned} \quad (4.44)$$

In making the ansatz we have assumed that the degrees of various polynomials are the same as in the $p = 2$ correlator. This is expected from the flat-space limit which is related to the high energy limit of the Mellin amplitude [143]. This can also be confirmed by Mellin factorization, which will be used in greater detail in the next step.⁹

Step 2: Mellin factorization

⁹For example, it is straightforward to see that these are the correct degrees when exchanging scalar operators. Exchanging vector or tensor fields is a bit more nontrivial but it is possible to check that the degrees are correct. The only subtle point which avoids the factorization argument is the degree of the regular piece. However, it is natural to assume that the degree is the same as the $p = 2$ case so that it has the same high energy growth as the other terms.

The second step of our strategy is to impose Mellin factorization. As explained in the previous section, all the polar terms of the Mellin amplitude can be completely fixed in terms of the lower-point Mellin amplitudes. For the $\langle pp222 \rangle$ five-point function, all these lower-point amplitudes are known and are given in Appendix 4.B. These lower point functions depend on R -symmetry polarization vectors. One important detail which we did not discuss is how to glue together the R -symmetry structures in the lower-point functions using the representation of the exchanged fields. This step is explained in detail in Appendix 4.A.4. Thus all terms in the ansatz (4.40), except for the regular term D , can be fixed by using this factorization procedure. Note that the number of coefficients that remain unfixed in the ansatz is quite low as D is just a constant with respect to the Mellin-Mandelstam variables. It can depend only on the linear combination coefficients of the 29 R -symmetry structures.

Step 3: Drukker-Plefka twist

The final step is to impose the Drukker-Plefka twist. As explained in Section 4.3.2 this twist can be phrased in terms of a difference operator \mathbb{D}_{DP} acting on the Mellin amplitude, see (4.38). This relates the regular part with the singular part already fixed by factorization and completely fixes the remaining coefficients¹⁰.

Using this strategy, we obtain the $\langle pp222 \rangle$ Mellin amplitudes in a closed form for arbitrary p . The final result for the Mellin amplitudes will be presented in the next section¹¹.

4.4.2 Mellin amplitude for $p = 2$

Due to the many R-symmetry structures involved, the expression for the full Mellin amplitude appears to be quite complicated at first sight. Therefore, before we present the Mellin amplitude for general p , let us first revisit the $p = 2$ result of [57] and present it in a simpler way.

When $p = 2$, the amplitude is symmetric under permutations of all the five external points. The 22 R-symmetry structures also split into two classes and within each class the

¹⁰At the same time the Drukker-Plefka twist provides a very non trivial consistency check for the procedure of extracting correlation functions of super-descendants and gluing of R-symmetry structures described in Appendix.

¹¹It would also be interesting to extend this analysis to the first correction in α' . One promising candidate is the $p = 2$ case since it is more symmetric and we can also use the known results for the four-point function as an input [211].

structures are related by permutations. The first class is the pentagon contraction

$$P_a = \{t_{12}t_{23}t_{34}t_{45}t_{15}, \dots\}, \quad a = 1, 2, \dots, 12, \quad (4.45)$$

which includes $P_{a_3a_4a_5}^{(\text{I,II})}$ in (4.7). The second class is the contraction of three points times the contraction of the remaining two points

$$T_a = \{t_{12}t_{23}t_{13}t_{45}^2, \dots\}, \quad a = 1, 2, \dots, 10, \quad (4.46)$$

which includes $T_{a_3a_4a_5}^{(\text{I,II,III})}$ in (4.7). The full amplitude can be written as

$$\mathcal{M}_{p=2} = \sum_{a=1}^{12} \mathcal{M}_a^P P_a + \sum_{a=1}^{10} \mathcal{M}_a^T T_a. \quad (4.47)$$

It is sufficient to determine the coefficient amplitudes \mathcal{M}_1^P and \mathcal{M}_1^T as the rest can be obtained by permutations. We find

$$\begin{aligned} \mathcal{M}_1^P = 4\sqrt{2} & \left\{ \frac{(\delta_{14} + \delta_{24})(\delta_{13} + \delta_{14})}{(\delta_{12} - 1)(\delta_{34} - 1)} + \frac{(\delta_{14} + \delta_{24})(\delta_{24} + \delta_{25})}{(\delta_{12} - 1)(\delta_{45} - 1)} + \frac{(\delta_{25} + \delta_{35})(\delta_{24} + \delta_{25})}{(\delta_{23} - 1)(\delta_{45} - 1)} \right. \\ & + \frac{(\delta_{25} + \delta_{35})(\delta_{13} + \delta_{35})}{(\delta_{23} - 1)(\delta_{15} - 1)} + \frac{(\delta_{13} + \delta_{35})(\delta_{13} + \delta_{14})}{(\delta_{15} - 1)(\delta_{34} - 1)} + \frac{1}{2} \left(\frac{\delta_{35}}{\delta_{12} - 1} + \frac{\delta_{14}}{\delta_{23} - 1} \right. \\ & \left. \left. + \frac{\delta_{25}}{\delta_{34} - 1} + \frac{\delta_{13}}{\delta_{45} - 1} + \frac{\delta_{24}}{\delta_{15} - 1} \right) - 2 \right\}, \end{aligned} \quad (4.48)$$

$$\mathcal{M}_1^T = -2\sqrt{2} \left(\frac{(\delta_{13} + \delta_{14})(\delta_{23} + \delta_{24})}{(\delta_{12} - 1)(\delta_{34} - 1)} + \frac{(\delta_{13} + \delta_{15})(\delta_{23} + \delta_{25})}{(\delta_{12} - 1)(\delta_{35} - 1)} + \frac{(\delta_{14} + \delta_{15})(\delta_{24} + \delta_{25})}{(\delta_{12} - 1)(\delta_{45} - 1)} \right).$$

It is clear that terms of the same structure are related by the permutations preserved by the R-symmetry structure. We will see that the Mellin amplitude for general p also has similar structures.

4.4.3 Mellin amplitudes for general p

For $p > 2$, we no longer have the full permutation symmetry and there are seven types of R-symmetry structures as we discussed in Section 4.2.1. The Mellin amplitude can be written as a sum over all the inequivalent R-symmetry structures

$$\begin{aligned} \mathcal{M}_p = & \sum_{\mathcal{I}_1} \mathcal{M}_{a_3a_4a_5}^{P,(\text{I})} P_{a_3a_4a_5}^{(\text{I})} + \sum_{\mathcal{I}_1} \mathcal{M}_{a_3a_4a_5}^{P,(\text{II})} P_{a_3a_4a_5}^{(\text{II})} + \mathcal{M}_{345}^{T,(\text{I})} T_{345}^{(\text{I})} + \sum_{\mathcal{I}_2} \mathcal{M}_{a_3a_4a_5}^{T,(\text{II})} T_{a_3a_4a_5}^{(\text{II})} \\ & + \sum_{\mathcal{I}_3} \mathcal{M}_{a_1a_2a_3a_4a_5}^{T,(\text{III})} T_{a_1a_2a_3a_4a_5}^{(\text{III})} + \mathcal{M}_{345}^{N,(\text{I})} N_{345}^{(\text{I})} + \sum_{\mathcal{I}_1} \mathcal{M}_{a_3a_4a_5}^{N,(\text{II})} N_{a_3a_4a_5}^{(\text{II})}, \end{aligned} \quad (4.49)$$

where the sets $\mathcal{I}_{1,2,3}$ contain the following permutations

$$\begin{aligned}\mathcal{I}_1 &= \{(3, 4, 5), (3, 5, 4), (4, 3, 5), (4, 5, 3), (5, 3, 4), (5, 4, 3)\}, \\ \mathcal{I}_2 &= \{(3, 4, 5), (4, 3, 5), (5, 3, 4)\}, \\ \mathcal{I}_3 &= \{(1, 2, 3, 4, 5), (1, 2, 4, 3, 5), (1, 2, 5, 3, 4), (2, 1, 3, 4, 5), (2, 1, 4, 3, 5), (2, 1, 5, 3, 4)\}\end{aligned}\tag{4.50}$$

The coefficient Mellin amplitudes are given as follows. For the structures of $P_{a_3 a_4 a_5}^{(I)}$, $P_{a_3 a_4 a_5}^{(II)}$, the coefficients are

$$\begin{aligned}\mathcal{M}_{a_3 a_4 a_5}^{P,(I)} &= 2\sqrt{2}p \left\{ \frac{2}{p} \frac{\delta_{1a_4} + \delta_{2a_4}}{\delta_{12} - p + 1} \left(\frac{\delta_{1a_3} + \delta_{1a_4}}{\delta_{a_3 a_4} - 1} + \frac{\delta_{2a_4} + \delta_{2a_5}}{\delta_{a_4 a_5} - 1} \right) + \frac{1}{p} \frac{\delta_{a_3 a_5}}{\delta_{12} - p + 1} \right. \\ &\quad + \frac{p-2}{p} \frac{\delta_{1a_4} + \delta_{2a_4} - 1}{\delta_{12} - p + 2} \left(\frac{\delta_{1a_3} + \delta_{1a_4}}{\delta_{a_3 a_4} - 1} + \frac{\delta_{2a_4} + \delta_{2a_5}}{\delta_{a_4 a_5} - 1} - 1 \right) \\ &\quad - \frac{(p-2)(p-3)}{2p} \frac{\delta_{a_3 a_5}}{\delta_{12} - p + 3} + \frac{(\delta_{2a_5} + \delta_{a_3 a_5})(\delta_{2a_4} + \delta_{2a_5})}{(\delta_{2a_3} - 1)(\delta_{a_4 a_5} - 1)} + \frac{(\delta_{1a_3} + \delta_{a_3 a_5})(\delta_{1a_3} + \delta_{1a_4})}{(\delta_{1a_5} - 1)(\delta_{a_3 a_4} - 1)} \\ &\quad + \frac{p}{2} \frac{(\delta_{1a_3} + \delta_{a_3 a_5})(\delta_{2a_5} + \delta_{a_3 a_5})}{(\delta_{1a_5} - 1)(\delta_{2a_3} - 1)} + \frac{1}{2} \left(\frac{\delta_{2a_4}}{\delta_{1a_5} - 1} + \frac{\delta_{1a_4}}{\delta_{2a_3} - 1} \right) \\ &\quad \left. + \frac{p-1}{p} \left(\frac{\delta_{2a_5}}{\delta_{a_3 a_4} - 1} + \frac{\delta_{1a_3}}{\delta_{a_4 a_5} - 1} \right) + \frac{6-7p}{2p} \right\},\end{aligned}\tag{4.51}$$

$$\begin{aligned}\mathcal{M}_{a_3 a_4 a_5}^{P,(II)} &= \sqrt{2}p^2 \left\{ \frac{(\delta_{12} + \delta_{2a_5})(\delta_{2a_5} + \delta_{a_3 a_5})}{(\delta_{1a_5} - 1)(\delta_{2a_3} - 1)} + \frac{(\delta_{12} + \delta_{1a_4})(\delta_{1a_4} + \delta_{a_3 a_4})}{(\delta_{2a_4} - 1)(\delta_{1a_3} - 1)} \right. \\ &\quad + \frac{(\delta_{12} + \delta_{2a_5})(\delta_{12} + \delta_{1a_4})}{(\delta_{1a_5} - 1)(\delta_{2a_4} - 1)} - \frac{(p-2)\delta_{12}}{(\delta_{1a_5} - 1)(\delta_{2a_4} - 1)} + \frac{2\delta_{12}}{p(\delta_{a_4 a_5} - 1)} \left(\frac{\delta_{1a_4}}{\delta_{2a_3} - 1} + \frac{\delta_{2a_5}}{\delta_{1a_3} - 1} \right) \\ &\quad - \frac{2(p+1)\delta_{12}}{p^2(\delta_{a_4 a_5} - 1)} + \frac{(p-2)(\delta_{12} + 1) + \delta_{a_3 a_4}}{p(\delta_{1a_5} - 1)} + \frac{(p-2)(\delta_{12} + 1) + \delta_{a_3 a_5}}{p(\delta_{2a_4} - 1)} \\ &\quad \left. + \frac{1-p}{p} \left(\frac{\delta_{1a_4}}{\delta_{2a_3} - 1} + \frac{\delta_{2a_5}}{\delta_{1a_3} - 1} \right) + \frac{p-2}{p} \right\}.\end{aligned}\tag{4.52}$$

Upon setting $p = 2$, the two coefficient amplitudes become degenerate up to permutations and reproduce \mathcal{M}_1^P in (4.48). The coefficient Mellin amplitudes of $T_{345}^{(I)}$, $T_{a_3 a_4 a_5}^{(II)}$ and $T_{a_1 a_2 a_3 a_4 a_5}^{(III)}$ are given by

$$\begin{aligned}\mathcal{M}_{345}^{T,(I)} &= -2\sqrt{2} \left\{ \frac{1}{\delta_{12} - p + 1} \left(\frac{(\delta_{1a_3} + \delta_{1a_4})(\delta_{2a_3} + \delta_{2a_4})}{\delta_{a_3 a_4} - 1} + \frac{(\delta_{1a_3} + \delta_{1a_5})(\delta_{2a_3} + \delta_{2a_5})}{\delta_{a_3 a_5} - 1} \right. \right. \\ &\quad \left. \left. + \frac{(\delta_{1a_4} + \delta_{1a_5})(\delta_{2a_4} + \delta_{2a_5})}{\delta_{a_4 a_5} - 1} \right) + \frac{(p-2)(\delta_{12} - p)}{\delta_{12} - p + 2} \right\},\end{aligned}\tag{4.53}$$

$$\begin{aligned} \mathcal{M}_{a_3 a_4 a_5}^{T,(\text{II})} = & -\frac{\sqrt{2}p(p-1)}{\delta_{a_4 a_5} - 1} \left\{ \frac{(\delta_{2a_4} + \delta_{3a_4})(\delta_{2a_5} + \delta_{3a_5})}{\delta_{2a_3} - 1} + \frac{(\delta_{1a_4} + \delta_{3a_4})(\delta_{1a_5} + \delta_{3a_5})}{\delta_{1a_3} - 1} \right. \\ & + \frac{2}{p(p-1)} \frac{(\delta_{1a_4} + \delta_{2a_4})(\delta_{1a_5} + \delta_{2a_5})}{\delta_{12} - p + 1} + \frac{4(p-2)}{p(p-1)} \left(\frac{(\delta_{1a_4} + \delta_{2a_4} - 1)(\delta_{1a_5} + \delta_{2a_5} - 1)}{\delta_{12} - p + 2} \right. \\ & \left. \left. + \frac{p-3}{4} \frac{(\delta_{1a_4} + \delta_{2a_4} - 2)(\delta_{1a_5} + \delta_{2a_5} - 2)}{\delta_{12} - p + 3} - \frac{1}{2}(p\delta_{a_4 a_5} - p - 1) \right) \right\}, \end{aligned} \quad (4.54)$$

$$\begin{aligned} \mathcal{M}_{a_1 a_2 a_3 a_4 a_5}^{T,(\text{III})} = & -\frac{\sqrt{2}p(p-1)}{\delta_{a_2 a_3} - 1} \left\{ \frac{(\delta_{a_1 a_2} + \delta_{a_2 a_5})(\delta_{a_1 a_3} + \delta_{a_3 a_5})}{\delta_{a_1 a_5} - 1} + \frac{(\delta_{a_1 a_2} + \delta_{a_2 a_4})(\delta_{a_1 a_3} + \delta_{a_3 a_4})}{\delta_{a_1 a_4} - 1} \right. \\ & + \frac{2}{p(p-1)} \frac{(\delta_{a_2 a_4} + \delta_{a_2 a_5})(\delta_{a_3 a_4} + \delta_{a_3 a_5} + p - 2)}{\delta_{a_4 a_5} - 1} - \frac{p-2}{p-1} \left(\frac{\delta_{a_1 a_2} \delta_{a_2 a_4}}{\delta_{a_1 a_5} - 1} + \frac{\delta_{a_1 a_2} \delta_{a_2 a_5}}{\delta_{a_1 a_4} - 1} \right. \\ & \left. \left. - \frac{1+2p}{p} \delta_{a_1 a_2} - \frac{\delta_{a_2 a_3}}{p} + 1 \right) \right\}. \end{aligned} \quad (4.55)$$

They become \mathcal{M}_1^T in (4.49) when $p = 2$. Finally, the coefficients of the two new structures $N_{345}^{(\text{I})}$, $N_{a_3 a_4 a_5}^{(\text{II})}$ are

$$\begin{aligned} \mathcal{M}_{345}^{N,(\text{I})} = & \sqrt{2}p^2(p-2)\delta_{12} \left\{ \frac{1}{(\delta_{15} - 1)(\delta_{23} - 1)} + \frac{1}{(\delta_{15} - 1)(\delta_{24} - 1)} + \frac{1}{(\delta_{13} - 1)(\delta_{24} - 1)} \right. \\ & + \frac{1}{(\delta_{13} - 1)(\delta_{25} - 1)} + \frac{1}{(\delta_{14} - 1)(\delta_{23} - 1)} + \frac{1}{(\delta_{14} - 1)(\delta_{25} - 1)} \\ & \left. - \frac{2}{p} \left(\frac{1}{\delta_{15} - 1} + \frac{1}{\delta_{25} - 1} + \frac{1}{\delta_{13} - 1} + \frac{1}{\delta_{23} - 1} + \frac{1}{\delta_{14} - 1} + \frac{1}{\delta_{24} - 1} \right) \right\}, \end{aligned} \quad (4.56)$$

$$\begin{aligned} \mathcal{M}_{a_3 a_4 a_5}^{N,(\text{II})} = & -\sqrt{2}p(p-2)\delta_{12} \left\{ \frac{\delta_{2a_3}}{(\delta_{1a_5} - 1)(\delta_{2a_4} - 1)} + \frac{\delta_{1a_4}}{(\delta_{2a_5} - 1)(\delta_{1a_3} - 1)} \right. \\ & \left. + \frac{1 + \delta_{12} - p(\delta_{1a_3} + \delta_{2a_4} + \delta_{a_3 a_4})}{p(\delta_{2a_4} - 1)(\delta_{1a_3} - 1)} \right\}. \end{aligned} \quad (4.57)$$

Note that they are proportional to $p - 2$ and therefore vanish for $p = 2$.

Let us also make a comment regarding the seemingly confusing behavior at the flat-space limit. The flat-space amplitude which one obtains from holographic correlators corresponds to that of gravitons. In general, one expects that the dependence on the KK levels should factorize as different KK modes all correspond to the same particle in flat space. However, this is not the case if we naively take the high energy limit of the Mellin amplitudes. Clearly, the p -dependence is not factored out as the component amplitudes of the new R-symmetry structures for $p > 2$ have the same high energy scaling behavior as the other component amplitudes. To understand this, it is important to note that the flat-space amplitude from AdS is in a special kinematic configuration where the polarizations of the gravitons are perpendicular to all the momenta [192]. However, such an amplitude for five points is zero

in flat space.¹² Therefore, the high energy limit of the Mellin amplitudes is not the flat-space amplitude as one might have naively expected. In fact, in applying the prescription of [143], there is an additional power of the inverse AdS radius $1/R$ which renders the flat-space limit zero. In other words, the high energy limit of the Mellin amplitudes computes only the $1/R$ corrections. We expect these corrections to have the same power counting for different KK modes. However, we do not expect their explicit expressions to be universal.

4.4.4 A comment on consistency

Let us make a comment regarding the consistency of our result. In Section 4.3 we proved the truncation of the poles in δ_{12} by using factorization in the (12) channel which only exploits the general analytic structure of the resulting four-point amplitude. Here we point out that the truncation can also be seen from a different point of view when it involves simultaneous poles with another channel. For concreteness, let us focus on the residue of the amplitude at the pole $\delta_{45} = 1$. The residue is, via the factorization in the (45) channel, related to a four-point function $\langle pp2X \rangle$ where the first three operators are 1, 2, 3 respectively. As we know from (4.17), the operator X belongs to the $k = 2$ multiplet and can be the superprimary \mathcal{O}_2 , the R-symmetry current \mathcal{J}_μ or the stress tensor $\mathcal{T}_{\mu\nu}$. The Mellin amplitude of $\langle pp2X \rangle$ contains poles in δ_{12} due to the operator exchanges in the (12) channel. These four-point Mellin amplitudes are given explicitly in Appendix 4.B and we observe a truncation of the subleading poles in δ_{12} for $m \geq 3$. This gives another derivation of the structure of the simultaneous poles in δ_{12} and δ_{45} .

Similar consistency checks have also been performed in other channels (*e.g.*, in the (13) and (45) channel), as well as for the R-symmetry gluing (see Appendix 4.A.4 for details).

4.4.5 Comments on position space

Up to this point, all of our discussions are exclusively in Mellin space. This is mainly because of the simplified analytic structure of Mellin amplitudes, as can be seen from our main result (4.49). However, it is also sometimes convenient to have position space expressions as some information is difficult to extract from the Mellin space representation. This has to do with the fact that certain nonzero expressions in position space may naively vanish in Mellin space. More precisely, different inverse Mellin transformations can only

¹²This is easiest to see using double copy. The gluon five-point amplitude with orthogonal polarizations vanishes because it is impossible to contract five polarization vectors among themselves. By double copy, the graviton five-point amplitude also vanishes.

be added up if their contours can be smoothly deformed from one to another. Usually the contour part is ignored for simplicity and one just adds up the Mellin amplitudes. This causes some information to be lost in the process. In fact, we have already encountered such an example in this chapter: The Drukker-Plefka twisted correlator is a constant in position space but has zero Mellin amplitude.¹³ The existence of the ambiguities makes a direct translation of Mellin space results into position space difficult.

One could also try to directly extend the position space algorithm of [57] to the $\langle pp222 \rangle$ correlators. However, as explained in the introduction, this is technically difficult. Here we propose a hybrid approach. As explained in [57, 129], all five-point Witten diagrams can be expressed as a linear combinations of five-point D -functions by using integrated vertex identities¹⁴. It is then natural to construct an ansatz in position space directly in terms of the D -functions. This will avoid directly computing the Witten diagrams which is a nontrivial task. More concretely, we propose that the ansatz for G_p in position space should have the following form

$$A_{\Delta_1 \dots \Delta_5}(x_i) = \sum_{\{\beta\}} c_{\{\beta\}}(t_{ij})(x_{ij}^2)^{-\beta_{ij}} D_{\tilde{\Delta}_1 \dots \tilde{\Delta}_5}(x_i), \quad (4.58)$$

where the coefficients $c_{\{\beta\}}(t_{ij})$ are linear combinations of all possible R-symmetry structures. The summation over β_{ij} are subjected to the constraints

$$\tilde{\Delta}_i + \sum_j \beta_{ij} = \Delta_i, \quad (4.59)$$

$$\sum_i \tilde{\Delta}_i \leq 2 + \sum_i \Delta_i, \quad (4.60)$$

$$\beta_{ij} > 0, \quad \beta_{kl} > 0, \quad \text{only if } \{i, j\} \neq \{k, l\} \quad (4.61)$$

$$\beta_{ij} \geq -2, \quad (4.62)$$

$$\beta_{12} \leq p - 1, \quad \beta_{ij} \leq 1 \quad (i, j \neq 1, 2). \quad (4.63)$$

Let us now unpack these constraints a little. The first condition (4.59) ensures that the external operators have the correct weights under conformal transformations. The constraint (4.60) imposes a bound on the sum of weights in each D -functions.¹⁵ This is expected

¹³See also [128] for more examples in four-point functions.

¹⁴It is known for some time [121] that four point exchange Witten diagrams can be express in terms D -functions when certain conditions on the dimension of the operators are met, which is what often happens in $\mathcal{N} = 4$ SYM.

¹⁵One can see explicitly that it is the case for the $p = 2$ five-point function. Moreover, the same bound also holds for four-point functions of higher KK modes.

if we use the integrated vertex identities¹⁶ to reduce the exchange Witten diagrams to contact Witten diagrams. Exchanging single-trace operators leads to singularities in position space. The condition (4.61) is the statement that particle exchanges have to be in the compatible channels. The constraint (4.62) arises because the exchanged single-trace operator operators have maximal spin 2. To understand this more precisely, let us notice the following translation between position and Mellin space

$$\prod_{1 \leq i < j \leq 5} (x_{ij}^2)^{-\alpha_{ij}} D_{\tilde{\Delta}_1 \dots \tilde{\Delta}_5} \rightarrow \mathcal{M}^{\alpha_{ij}}(\delta) = \frac{\pi^{\frac{d}{2}} \Gamma\left(\frac{\sum_i \tilde{\Delta}_i - d}{2}\right)}{\prod_i \Gamma(\tilde{\Delta}_i)} \prod_{i < j} \frac{\Gamma(\delta_{ij} - \alpha_{ij})}{\Gamma(\delta_{ij})}. \quad (4.64)$$

The condition (4.62) ensures in Mellin space that the numerator associated with an exchange pole is at most quadratic. Finally, the constraint (4.63) controls the twists of the exchanged single-trace operators. Let us emphasize that this position ansatz, as it stands, does not manifest the truncation of poles seen in (4.40). Nevertheless, this truncation can still be imposed in position space, though in a more intricate manner (this is in stark contrast with Mellin space). We notice that a given negative power $(x_{12}^2)^{-\alpha}$ will lead to poles in Mellin space at all the locations $\delta_{12} = 1, 2, \dots, \alpha$. Therefore, even though the δ_{12} poles in Mellin space truncate according to (4.40), in position space the result will necessarily involve all negative powers of $(x_{12}^2)^{-\alpha}$ with $\alpha = 1, 2, \dots, p-1$. Truncation only implies that the negative powers are related but cannot just simply eliminate a subset of them. This is another instance where we can see explicitly that Mellin space is simpler.

To fix the coefficients in the ansatz, one can translate the ansatz back into Mellin space and compare with the Mellin amplitude (4.49). This can be achieved by using the rule (4.64). However, as explained above, only some of the coefficients can be fixed due to the ambiguities of the translation. One may wonder if implementing the Drukker-Plefka twist and the chiral algebra condition in position space¹⁷ will give rise to additional constraints. But unfortunately we find that this is not the case. There still remains the possibility that one can fix the remaining coefficients using the recently derived higher-point lightcone conformal blocks [133] to impose factorization in position space. But we have not found a very efficient way to implement this. Therefore, we will postpone the task of finding the expressions in position space and leave it to future work.

¹⁶These will generalize the ones presented in Appendix A of [57] for $p = 2$.

¹⁷See Appendix D of [57] for more details on how to obtain explicit expressions for D -functions.

4.5 Discussion

In this chapter we continued the journey of exploring the structure of five-point functions of $\frac{1}{2}$ -BPS operators of 4d $\mathcal{N} = 4$ SYM in the strongly coupled regime which is dual to $AdS_5 \times S^5$ IIB supergravity. We improved the bootstrap approach of [57] which relies only on superconformal symmetry and consistency with factorization. The important difference compared to the old approach is that both constraints are now implemented in Mellin space. Moreover, in the new method we only need to use the Drukker-Plefka twist and the chiral algebra condition is not needed. Using this approach, we obtained in a closed form the Mellin amplitudes for the infinite family of correlators of the form $\langle pp222 \rangle$.

Compared to the simplest $\langle 22222 \rangle$ case studied in [57], the pole structure of the Mellin amplitudes of operators with higher KK levels is in general more complicated. However, an important simplifying feature we observed here is a new type of pole truncation phenomenon. We find that the residues of certain poles associated with conformal descendants vanish. Moreover, in the $\langle pp222 \rangle$ case the number of poles does not grow with respect to p when p is large enough. Consequently, the pole structure of the Mellin amplitudes is much simpler than what is naively expected. This property played an important role in obtaining the $\langle pp222 \rangle$ amplitudes and also gives us hope to bootstrap in closed forms more general families of five-point functions with different KK levels.

Note that in deriving the pole truncation conditions, we have only used general properties of Mellin factorization. The same argument holds in many other theories and we expect similar simplifications in the pole structure. This leads to a number of possible extensions of our results in different setups. A prime example to consider is the gluon sector of certain 4d $\mathcal{N} = 2$ SCFTs which is dual to SYM in $AdS_5 \times S^3$. The first five-point function for the lowest KK level has been computed in [129]. To make further progress in computing amplitudes of higher KK levels, one can adapt the strategy used here. One important ingredient which still needs to be worked out is the relations between different component correlators of the super four-point functions (see [202] for progress in this direction). This would be the input for exploiting the full power of the Mellin factorization. However, this will be a direct generalization to what we have done in Appendix 4.A. Another interesting application is the 6d $\mathcal{N} = (2, 0)$ theory which is dual to eleven dimensional supergravity in $AdS_7 \times S^4$.

Going beyond five-point functions, an exciting future direction is to compute the super graviton six-point function of $AdS_5 \times S^5$ IIB supergravity. This will provide a new

benchmark for the program of holographic correlators at higher points. The results in this chapter can already help us gain a nontrivial amount of knowledge of the structure of this new correlator. Moreover, much of the technology developed here, in particular the Mellin Drukker-Plefka twist, can also be straightforwardly applied to that problem. It appears to be a feasible target and we hope to report progress in this direction in the near future.

Finally, let us mention that the $\langle pp222 \rangle$ five-point functions we computed in this chapter contain a wealth of new data of 4d $\mathcal{N} = 4$ SYM. Through OPE, we can extract various non-protected three- and four-point functions. In [57] the authors constructed five-point conformal blocks (see [1, 60, 61, 64, 212] for progress in higher-point conformal blocks) and explained how to use them to extract data from the $p = 2$ five-point correlator. It would be interesting to perform a similar analysis here for the $\langle pp222 \rangle$ correlators. The expression we have for general p will be helpful for solving the mixing problem for the CFT data which is similar to the one appearing in four-point functions. It would also be interesting to extract the chiral algebra correlator from our supergravity result and compare with the field theory calculation. The four-point function case has been analyzed in [213, 214].

Appendices for chapter 4

4.A Higher R-charge super multiplet

A key element of the bootstrap analysis undertaken in the main text is the factorization of Mellin amplitudes into lower-point correlators. As explained in Section 4.3.1 we do need as an input the explicit expression for the Mellin amplitudes associated with the four-point functions

$$\langle \mathcal{O}_2 \mathcal{O}_2 \mathcal{O}_2 \mathcal{O}_2 \rangle \quad \langle \mathcal{J}_2 \mathcal{O}_2 \mathcal{O}_2 \mathcal{O}_2 \rangle \quad \langle \mathcal{T}_2 \mathcal{O}_2 \mathcal{O}_2 \mathcal{O}_2 \rangle \quad (4.65)$$

$$\langle \mathcal{O}_2 \mathcal{O}_p \mathcal{O}_p \mathcal{O}_2 \rangle \quad \langle \mathcal{J}_2 \mathcal{O}_p \mathcal{O}_p \mathcal{O}_2 \rangle \quad \langle \mathcal{T}_2 \mathcal{O}_p \mathcal{O}_p \mathcal{O}_2 \rangle \quad (4.66)$$

$$\langle \mathcal{O}_p \mathcal{O}_p \mathcal{O}_2 \mathcal{O}_2 \rangle \quad \langle \mathcal{J}_p \mathcal{O}_p \mathcal{O}_2 \mathcal{O}_2 \rangle \quad \langle \mathcal{T}_p \mathcal{O}_p \mathcal{O}_2 \mathcal{O}_2 \rangle \quad (4.67)$$

where \mathcal{O}_p , \mathcal{J}_p and \mathcal{T}_p denotes the following components of the half-BPS supermultiplet \mathbb{O}_p

$$\mathcal{O}_p : \quad \Delta = p, \quad \mathcal{R} = [0, p, 0], \quad \text{spin 0}, \quad (4.68)$$

$$\mathcal{J}_p : \quad \Delta = p + 1, \quad \mathcal{R} = [1, p - 2, 1], \quad \text{spin 1}, \quad (4.69)$$

$$\mathcal{T}_p : \quad \Delta = p + 2, \quad \mathcal{R} = [0, p - 2, 0], \quad \text{spin 2}. \quad (4.70)$$

In the special case $p = 2$ they correspond respectively to the $\mathfrak{su}(4)$ current and stress tensor, hence their names. The first goal of this appendix is to explain how the correlators above can be extracted from the $\langle \mathcal{O}_p \mathcal{O}_p \mathcal{O}_2 \mathcal{O}_2 \rangle$ component. This is a generalization of what has been done in [215] for the case $p = 2$. The second goal of this appendix is to explain how the factorization in Mellin space is implemented in the presence of some global symmetry. This is done in Appendix 4.A.4. A final warning about notation is necessary. In the main text we use the six component null vectors on which the R-symmetry act linearly. Here, as it is natural from the super-space prospective will use four component R-symmetry variables y . The basic two-point invariants are identified as

$$t_{ij} = y_{ij}^2. \quad (4.71)$$

4.A.1 Conventions

In the following we will list all the conventions for raising and lowering indices

$$y^{a\dot{a}} = \epsilon^{ab} y_{b\dot{b}} \epsilon^{\dot{b}\dot{a}}, \quad (4.72)$$

where the ϵ tensor is defined with

$$\epsilon^{12} = \epsilon_{12} = 1. \quad (4.73)$$

It follows that

$$(y_{1i})_{\dot{a}a} (y_{1j})^{a\dot{a}} = y_{1i}^2 + y_{1j}^2 - y_{ij}^2, \quad (4.74)$$

which, in a particular case becomes

$$\det y_{ij} = \frac{1}{2} (y_{ij})_{\dot{a}a} (y_{ij})^{a\dot{a}} = y_{ij}^2. \quad (4.75)$$

The Schouten identity can be used to show that

$$\epsilon^{\dot{a}\dot{b}} \epsilon^{ba} y_{ij}^2 = y_{ij}^{a\dot{a}} y_{ij}^{b\dot{b}} - y_{ij}^{b\dot{a}} y_{ij}^{a\dot{b}}. \quad (4.76)$$

Finally, the inverse can easily be seen to be

$$y_{\dot{a}a}^{-1} = \frac{y_{\dot{a}a}}{y^2}, \quad (4.77)$$

and, with these conventions we also have

$$\frac{\partial}{\partial y^{a\dot{a}}} y^2 = y_{\dot{a}a}. \quad (4.78)$$

4.A.2 Differential Operators

In order to consider different components of the $\frac{1}{2}$ -BPS supermultiplets we will work in analytic superspace. The eight bosonic and eight fermionic coordinates of this superspace are packaged in a supermatrix

$$X^{\mathbb{A}\dot{\mathbb{A}}} = \begin{pmatrix} x^{\alpha\dot{\alpha}} & \rho^{\alpha\dot{a}} \\ \bar{\rho}^{a\dot{\alpha}} & y^{a\dot{a}} \end{pmatrix}, \quad (4.79)$$

whose superdeterminant is

$$\text{sdet} X = \frac{\det (x^{\alpha\dot{\alpha}} - \rho^{\alpha\dot{a}} y_{\dot{a}a}^{-1} \bar{\rho}^{a\dot{\alpha}})}{\det y^{a\dot{a}}}. \quad (4.80)$$

The supersymmetrization of the propagator $d_{ij} = y_{ij}^2/x_{ij}^2$ is given by

$$\hat{d}_{ij} = \frac{1}{\text{sdet}(X_{ij})} = \frac{y_{ij}^2}{\hat{x}_{ij}^2}, \quad (4.81)$$

where we introduce the short-hand notation

$$\hat{x}^{\alpha\dot{\alpha}} = x^{\alpha\dot{\alpha}} - \rho^{\alpha\dot{a}} y_{\dot{a}a}^{-1} \bar{\rho}^{a\dot{\alpha}}. \quad (4.82)$$

The two-point function of half-BPS superfields \mathbb{O}_p is then simply

$$\langle \mathbb{O}_p(X_i) \mathbb{O}_p(X_j) \rangle = (\hat{d}_{ij})^p. \quad (4.83)$$

The relevant superdescendants are obtained extracting the appropriate component by acting with certain differential operators:

$$\begin{aligned} \mathcal{J}_p &= \frac{1}{2} \mathcal{D}^{(J)} \mathbb{O}_p(X) \Big|_{\rho=\bar{\rho}=0}, \\ \mathcal{T}_p &= \frac{1}{4} \mathcal{D}^{(T)} \mathbb{O}_p(X) \Big|_{\rho=\bar{\rho}=0}. \end{aligned} \quad (4.84)$$

Given the charges and symmetries of those operators the ansatz for the differential operators needs to be¹⁸

$$\mathcal{D}^{(J)} = \lambda^\alpha \bar{\lambda}^{\dot{\alpha}} v^a \bar{v}^{\dot{a}} \left(\frac{\partial}{\partial \bar{\rho}^{a\dot{\alpha}}} \frac{\partial}{\partial \rho^{\alpha\dot{a}}} + \mu \frac{\partial}{\partial y^{a\dot{a}}} \frac{\partial}{\partial x^{\alpha\dot{\alpha}}} \right), \quad (4.85)$$

and

$$\begin{aligned} \mathcal{D}^{(T)} = & \lambda^{\alpha_1} \lambda^{\alpha_2} \bar{\lambda}^{\dot{\alpha}_1} \bar{\lambda}^{\dot{\alpha}_2} \epsilon^{\dot{a}_1 \dot{a}_2} \epsilon^{a_1 a_2} \times \left(\frac{\partial}{\partial \bar{\rho}^{a_1 \dot{\alpha}_1}} \frac{\partial}{\partial \bar{\rho}^{a_2 \dot{\alpha}_2}} \frac{\partial}{\partial \rho^{\alpha_1 \dot{a}_1}} \frac{\partial}{\partial \rho^{\alpha_2 \dot{a}_2}} + \right. \\ & \left. + \nu_1 \frac{\partial}{\partial \bar{\rho}^{a_1 \dot{\alpha}_1}} \frac{\partial}{\partial \rho^{\alpha_1 \dot{a}_1}} \frac{\partial}{\partial y^{a_2 \dot{a}_2}} \frac{\partial}{\partial x^{\alpha_2 \dot{\alpha}_2}} + \nu_2 \frac{\partial}{\partial y^{a_1 \dot{a}_1}} \frac{\partial}{\partial y^{a_2 \dot{a}_2}} \frac{\partial}{\partial x^{\alpha_1 \dot{a}_1}} \frac{\partial}{\partial x^{\alpha_2 \dot{a}_2}} \right), \end{aligned} \quad (4.86)$$

Before fixing the coefficients let us quote two simple identities which are very useful in the following¹⁹

$$\frac{\partial}{\partial X^{\mathbb{A}\dot{\mathbb{A}}}} \frac{1}{\text{sdet}(X)} = -(-1)^{|\mathbb{A}|} \frac{X_{\dot{\mathbb{A}}\mathbb{A}}^{-1}}{\text{sdet}(X)}, \quad (4.88)$$

$$\frac{\partial}{\partial X^{\mathbb{A}\dot{\mathbb{A}}}} X_{\dot{\mathbb{B}}\mathbb{B}}^{-1} = -(-1)^{(|\mathbb{A}|+|\dot{\mathbb{A}}|)(|\mathbb{B}|+|\dot{\mathbb{B}}|)} X_{\dot{\mathbb{B}}\mathbb{A}}^{-1} X_{\dot{\mathbb{A}}\mathbb{B}}^{-1}, \quad (4.89)$$

¹⁸These differential operators depend on p through the coefficients μ, ν_1, ν_2 . This dependence is not explicit in the notation.

¹⁹The second identity is obtained as follows

$$0 = \frac{\partial}{\partial X^{\mathbb{A}\dot{\mathbb{A}}}} \delta_{\mathbb{B}}^{\mathbb{C}} = \frac{\partial}{\partial X^{\mathbb{A}\dot{\mathbb{A}}}} X^{\mathbb{C}\dot{\mathbb{B}}} X_{\dot{\mathbb{B}}\mathbb{B}}^{-1} = \delta_{\mathbb{A}}^{\mathbb{C}} \delta_{\mathbb{A}}^{\dot{\mathbb{B}}} X_{\dot{\mathbb{B}}\mathbb{B}}^{-1} + (-1)^{(|\mathbb{A}|+|\dot{\mathbb{A}}|)(|\mathbb{C}|+|\dot{\mathbb{B}}|)} X^{\mathbb{C}\dot{\mathbb{B}}} \frac{\partial}{\partial X^{\mathbb{A}\dot{\mathbb{A}}}} X_{\dot{\mathbb{B}}\mathbb{B}}^{-1}. \quad (4.87)$$

Multiplying this equation by $(-1)^{(|\mathbb{A}|+|\dot{\mathbb{A}}|)(|\mathbb{C}|+|\dot{\mathbb{B}}|)}$ and $X_{\dot{\mathbb{C}}\mathbb{C}}^{-1}$ from the left (with summation over \mathbb{C}) we obtain (4.89).

where $|\alpha| = |\dot{\alpha}| = 0$, $|a| = |\dot{a}| = 1$. In order to fix the coefficients in the ansatz (4.85), (4.86) it suffices to impose that two-point functions do not have off-diagonal components between different superdescendants. So we impose

$$\langle \mathcal{J}_p(1) \mathcal{O}_p(2) \rangle = \mathcal{D}_1^{(J)} \langle \mathbb{O}_p(X_1) \mathbb{O}_p(X_2) \rangle \Big|_{\rho, \bar{\rho}=0} \stackrel{!}{=} 0, \quad (4.90)$$

which fixes the unknown coefficient in $\mathcal{D}^{(J)}$ to be

$$\mu = \frac{1}{p}. \quad (4.91)$$

The action of the resulting operator on the two-point function is given by²⁰

$$\mathcal{D}_1^{(J)} (\hat{d}_{12})^p = (1 - p^2) \lambda_1^\alpha \bar{\lambda}_1^{\dot{\alpha}} v_1^a \bar{v}_1^{\dot{a}} X_{\dot{\alpha}a}^{-1} X_{\dot{a}\alpha}^{-1} (\hat{d}_{12})^p, \quad (4.92)$$

where $X = X_{12}$, from which one derives the two-point function of the descendant \mathcal{J} using the formula

$$\mathcal{D}_1^{(J)} \mathcal{D}_2^{(J)} (\hat{d}_{12})^p \Big|_{\rho, \bar{\rho}=0} = (1 - p^2) \left(\bar{\lambda}_1 x_{12}^{-1} \lambda_2 \right) \left(\bar{\lambda}_2 x_{12}^{-1} \lambda_1 \right) \left(\bar{v}_1 y_{12}^{-1} v_2 \right) \left(\bar{v}_2 y_{12}^{-1} v_1 \right) (d_{12})^p. \quad (4.93)$$

From this equation we can extract the normalization of \mathcal{J}_p . For the spin 2 operator we need to consider

$$\begin{aligned} \langle \mathcal{T}_p(1) \mathcal{O}_p(2) \rangle &= \mathcal{D}_1^{(T)} \langle \mathbb{O}_p(X_1) \mathbb{O}_p(X_2) \rangle \Big|_{\rho, \bar{\rho}=0} \stackrel{!}{=} 0, \\ \langle \mathcal{T}_p(1) \mathcal{J}_p(2) \rangle &= \mathcal{D}_1^{(T)} \mathcal{D}_2^{(J)} \langle \mathbb{O}_p(X_1) \mathbb{O}_p(X_2) \rangle \Big|_{\rho, \bar{\rho}=0} \stackrel{!}{=} 0, \end{aligned} \quad (4.94)$$

which in turn fixes the coefficients ν_i to be

$$\nu_1 = -\frac{4}{2+p}, \quad \nu_2 = -\frac{2}{(1+p)(2+p)}. \quad (4.95)$$

In the case of the stress tensor multiplet, when $p = 2$, these coefficients agree with those found in [215]. The action of the resulting operator on the two-point function is given by

$$\mathcal{D}_1^{(T)} (\hat{d}_{12})^p = 2p^2(p-1)(p+3) \lambda_1^{\alpha_1} \bar{\lambda}_1^{\dot{\alpha}_1} \bar{\lambda}_1^{\dot{\alpha}_2} \epsilon^{\dot{\alpha}_1 \dot{\alpha}_2} \epsilon^{a_1 a_2} \epsilon^{a_1 a_2} X_{\dot{\alpha}_1 a_1}^{-1} X_{\dot{\alpha}_2 a_2}^{-1} X_{\dot{a}_1 \alpha_1}^{-1} X_{\dot{a}_2 \alpha_2}^{-1} (\hat{d}_{12})^p, \quad (4.96)$$

²⁰The fact that it vanishes when $p = 1$ is consistent with the fact that in this case the (field strength) supermultiplet is ultrashort and does not possess a \mathcal{J} component.

where $X = X_{12}$, from which one derives the two-point function of the descendant \mathcal{T} using the formula

$$\mathcal{D}_1^{(T)} \mathcal{D}_2^{(T)} (\widehat{d}_{12})^p \Big|_{\rho, \bar{\rho}=0} = 16p^2(p-1)(p+3) \left(\bar{\lambda}_1 x_{12}^{-1} \lambda_2 \right)^2 \left(\bar{\lambda}_2 x_{12}^{-1} \lambda_1 \right)^2 \frac{(y_{12}^2)^{p-2}}{(x_{12}^2)^{p+2}}. \quad (4.97)$$

Three-point function with one descendant operator can be obtained using the formulae

$$\mathcal{D}_1^{(J)} (\widehat{d}_{12})^a (\widehat{d}_{13})^{p-a} \Big|_{\rho, \bar{\rho}=0} = A \Lambda_{1,23} V_{1,23} (d_{12})^a (d_{13})^{p-a}, \quad (4.98)$$

$$\mathcal{D}_1^{(T)} (\widehat{d}_{12})^p (\widehat{d}_{13})^{p-a} \Big|_{\rho, \bar{\rho}=0} = B (\Lambda_{1,23})^2 \det(y_{12}^{-1} - y_{13}^{-1}) (d_{12})^a (d_{13})^{p-a}, \quad (4.99)$$

where

$$\Lambda_{1,23} := \bar{\lambda}_1 (x_{12}^{-1} - x_{13}^{-1}) \lambda_1, \quad V_{1,23} := \bar{v}_1 (y_{12}^{-1} - y_{13}^{-1}) v_1. \quad (4.100)$$

and

$$A = -\frac{a(p-a)}{p}, \quad B = -\frac{8a(a+1)(p-a)(p-a+1)}{(p+1)(p+2)}. \quad (4.101)$$

4.A.3 Four-point functions

The two- and three-point functions of \mathbb{O}_p operators are related in a simple way to the ones of their superprimaries \mathcal{O}_p : they are obtained by replacing the propagators d_{ij} with the super-propagators \widehat{d}_{ij} . For four-point functions the situation is more involved due to the presence of cross ratios, but it is still true that the correlators of \mathbb{O}_p is uniquely fixed by the one of \mathcal{O}_p . This is achieved by replacing the familiar space-time and R-symmetry cross ratios

$$\begin{aligned} u &= \frac{x_{12}^2 x_{34}^2}{x_{13}^2 x_{24}^2} = z\bar{z}, & v &= \frac{x_{14}^2 x_{23}^2}{x_{13}^2 x_{24}^2} = (1-z)(1-\bar{z}), \\ \sigma &= \frac{y_{12}^2 y_{34}^2}{y_{13}^2 y_{24}^2} = \alpha\bar{\alpha}, & \tau &= \frac{y_{14}^2 y_{23}^2}{y_{13}^2 y_{24}^2} = (1-\alpha)(1-\bar{\alpha}). \end{aligned} \quad (4.102)$$

with their super-symmetrizations, namely the four eigenvalues of the supermatrix

$$Z = X_{12} X_{13}^{-1} X_{34} X_{24}^{-1}. \quad (4.103)$$

More explicitly, we can extract the independent superconformal invariants by taking four independent supertraces

$$\widehat{t}_k = \text{Str}(Z^k) = \widehat{z}^k + \widehat{\bar{z}}^k - \widehat{\alpha}^k - \widehat{\bar{\alpha}}^k, \quad k = 1, 2, 3, 4. \quad (4.104)$$

When all fermionic variables are set to zero the matrix above reduces to

$$Z|_{\rho, \bar{\rho}=0} = \begin{pmatrix} x_{12}x_{13}^{-1}x_{34}x_{24}^{-1} & 0 \\ 0 & y_{12}y_{13}^{-1}y_{34}y_{24}^{-1} \end{pmatrix}. \quad (4.105)$$

and upon taking the supertrace gives

$$t_k := \widehat{t}_k|_{\rho, \bar{\rho}=0} = z^k + \bar{z}^k - \alpha^k - \bar{\alpha}^k, \quad (4.106)$$

which establishes the relation between the quantities t_k and the cross ratios introduced above. In terms of the cross-ratios the four point function reads

$$\langle \mathcal{O}_{p_1}(X_1)\mathcal{O}_{p_1}(X_2)\mathcal{O}_{p_2}(X_3)\mathcal{O}_{p_2}(X_4) \rangle = (\widehat{d}_{12})^{p_1} (\widehat{d}_{34})^{p_2} \mathcal{G}(\widehat{z}, \widehat{\bar{z}}; \widehat{\alpha}, \widehat{\bar{\alpha}}). \quad (4.107)$$

The function \mathcal{G} satisfies the super-conformal Ward Identities and have a specific polynomial dependence on the R-symmetry cross ratios. We will come back to these constraints momentarily. To extract the relevant components from (4.107) we need to act with the differential operators $\mathcal{D}^{(J)}$ and $\mathcal{D}^{(T)}$ given in (4.85), (4.86).

Action of $\mathcal{D}^{(J)}$, $\mathcal{D}^{(T)}$ on four-point functions. The spinning four-point functions are extracted by the action of the differential operators from (4.85) and (4.86)

$$\begin{aligned} \langle \mathcal{J}_{p_1}(1)\mathcal{O}_{p_1}(2)\mathcal{O}_{p_2}(3)\mathcal{O}_{p_2}(4) \rangle &= \tfrac{1}{2}\mathcal{D}_1^{(J)}\langle \mathcal{O}(X_1)\mathcal{O}_{p_1}(X_2)\mathcal{O}_{p_2}(X_3)\mathcal{O}_{p_2}(X_4) \rangle|_{\rho, \bar{\rho}=0}, \\ \langle \mathcal{T}_{p_1}(1)\mathcal{O}_{p_1}(2)\mathcal{O}_{p_2}(3)\mathcal{O}_{p_2}(4) \rangle &= \tfrac{1}{4}\mathcal{D}_1^{(T)}\langle \mathcal{O}(X_1)\mathcal{O}_{p_1}(X_2)\mathcal{O}_{p_2}(X_3)\mathcal{O}_{p_2}(X_4) \rangle|_{\rho, \bar{\rho}=0}, \end{aligned} \quad (4.108)$$

with coefficients determined in (4.91) and (4.95) above. In what follows we will always apply the differential operator at point 1, so we will need to consider two particular cases of the four-point function, either $p_1 = 2$ and $p_2 = p$, or the opposite. The action of derivatives on the superpropagators are discussed in the previous section. The action of derivatives on the \mathcal{G} factor is done in two steps. First we relate the derivatives with respect to the eigenvalues of the Z matrix

$$z_1 = \widehat{z}, \quad z_2 = \widehat{\bar{z}}, \quad z_3 = \widehat{\alpha}, \quad z_4 = \widehat{\bar{\alpha}}. \quad (4.109)$$

to derivatives with respect to the supertraces (4.104). This is done by using the chain rule

$$\frac{\partial \mathcal{G}}{\partial \widehat{t}_j} = \sum_{i=1}^4 \frac{\partial z_i}{\partial \widehat{t}_j} \frac{\partial \mathcal{G}}{\partial z_i}. \quad (4.110)$$

The Jacobian matrix can be derived easily since the variables are related according to (4.106), and is given by

$$\frac{\partial z_i}{\partial t_j} = \frac{(-1)^{j+F_i}}{j} \frac{Q_{4-j}^{(i)}}{\prod_{k \neq i} (z_i - z_k)}, \quad (4.111)$$

where $Q_{4-j}^{(i)}$ are symmetric polynomials formed with the three variables $z_{k \neq i}$ (here written for $i = 4$)

$$\begin{aligned} Q_0^{(4)} &= 1, & Q_1^{(4)} &= z_1 + z_2 + z_3, \\ Q_2^{(4)} &= z_1 z_2 + z_1 z_3 + z_2 z_3, & Q_3^{(4)} &= z_1 z_2 z_3, \end{aligned} \quad (4.112)$$

and $F_1 = F_2 = 0$ and $F_3 = F_4 = 1$. The second step is to take derivatives of \hat{t}_k with respect to the supercoordinates $X_1^{\mathbf{A}\dot{\mathbf{A}}}$ using, for example

$$\frac{\partial}{\partial Z_{\mathbf{B}}^{\mathbf{A}}} \hat{t}_k = k (-1)^{|\mathbf{A}|} (Z^{k-1})_{\mathbf{A}}^{\mathbf{B}}, \quad (4.113)$$

$$\frac{\partial}{\partial X_1^{\mathbf{A}\dot{\mathbf{A}}}} \hat{t}_k = k (-1)^{|\mathbf{A}|} (X_{12}^{-1} Z^k X_{12})_{\dot{\mathbf{A}}}^{\dot{\mathbf{B}}} (X_{12}^{-1} - X_{13}^{-1})_{\dot{\mathbf{B}}\mathbf{A}}, \quad (4.114)$$

and similarly for higher derivatives. This procedure is straightforward but tedious, the result takes the schematic form given in (4.126).

General structure of the correlator. Superconformal Ward identities and polynomiality in the R-symmetry variables imply that

$$\langle \mathcal{O}_p(1) \mathcal{O}_p(2) \mathcal{O}_2(3) \mathcal{O}_2(4) \rangle = G^{\text{free}} + d_{12}^{p-2} R H_p(u, v), \quad (4.115)$$

where R is the well-known function

$$\begin{aligned} R = v d_{12}^2 d_{34}^2 + \frac{v}{u} d_{13}^2 d_{24}^2 + \frac{v^2}{u} d_{14}^2 d_{23}^2 + \frac{v}{u} (v - u - 1) d_{12} d_{13} d_{24} d_{34} \\ + \frac{v}{u} (1 - u - v) d_{12} d_{14} d_{23} d_{34} + \frac{v}{u} (u - 1 - v) d_{13} d_{14} d_{23} d_{24}. \end{aligned} \quad (4.116)$$

The free piece of the correlator can be supersymmetrized as shown in the next paragraph, while the supersymmetrization of the anomalous component is achieved with the method described above, where we supersymmetrize the cross ratios. The spinning anomalous functions will then be expressed in terms of derivatives of the dynamical function $H_p(u, v)$.

The free theory check. As a check of the formulae derived in the previous section, will now consider the case of correlators in the free field theory. In the $SU(N)$ gauge theory, and for the particular configuration we are interested in, the tree-level four-point functions

at any value of N are

$$\begin{aligned} \langle \mathcal{O}_p(1)\mathcal{O}_p(2)\mathcal{O}_2(3)\mathcal{O}_2(4) \rangle^{\text{free}} &= d_{12}^p d_{34}^2 + \delta_{2p} \left(d_{14}^2 d_{23}^2 + d_{13}^2 d_{24}^2 \right) + \frac{2p(p-1)}{N^2-1} d_{12}^{p-2} d_{14} d_{23} d_{13} d_{24} \\ &+ \frac{2p}{N^2-1} d_{12}^{p-1} d_{34} (d_{14} d_{23} + d_{13} d_{24}). \end{aligned} \quad (4.117)$$

The four-point function $\langle \mathbb{O}_p \mathbb{O}_p \mathbb{O}_2 \mathbb{O}_2 \rangle$ is obtained from the above by simply replacing the propagator d_{ij} with its supersymmetrized version \hat{d}_{ij} introduced in (4.81). We can rewrite this expression in terms of cross ratios as

$$G_{pp22} = 1 + \delta_{2p} \left(\frac{v^2 \sigma^2}{u^2 \tau^2} + \frac{\sigma^2}{u^2} \right) + \frac{2p}{N^2-1} \left((p-1) \frac{u^2 \tau}{v \sigma^2} + \frac{u \tau}{v \sigma} + \frac{u}{\sigma} \right). \quad (4.118)$$

In this case, the correlation function of superdescendants can be obtained either applying the general procedure discussed in the previous paragraph or by replacing the propagator d_{ij} with \hat{d}_{ij} in (4.117) and then applying the differential operators $\mathcal{D}^{(J)}$, $\mathcal{D}^{(T)}$. Both procedures give the same result, as they should, providing a check of the general procedure.

Frame simplifications. The computation we described can be simplified by choosing a frame. First, we wish only to apply the differential operator on the point 1 of the four-point function, so we can set to zero the fermionic variables associated to the remaining points from the beginning. Second, the matrix Z is superconformally invariant, so we can take advantage of conformal and R -symmetry transformations to send both x_2 and y_2 to 0, while sending x_3 and y_3 to infinity. Effectively the computation simplifies significantly to the evaluation of

$$\hat{t}_k = \text{Str} \left((X_1 X_4^{-1})^k \right) \Big|_{\rho_{i>1}, \bar{\rho}_{i>1}=0}, \quad (4.119)$$

where the matrix Z becomes

$$\left(X_1 X_4^{-1} \right)_{\mathbf{B}}^{\mathbf{A}} \Big|_{\rho_4, \bar{\rho}_4=0} = \begin{pmatrix} (x_1 x_4^{-1})_{\beta}^{\alpha} & (\rho_1 y_4^{-1})_{\beta}^{\alpha} \\ (\bar{\rho}_1 x_4^{-1})_{\beta}^a & (y_1 y_4^{-1})_{\beta}^a \end{pmatrix}, \quad (4.120)$$

and the cross ratios in this frame are given by

$$\begin{aligned} \frac{x_1^2}{x_4^2} &= z\bar{z}, & \frac{x_{14}^2}{x_4^2} &= (1-z)(1-\bar{z}), \\ \frac{y_1^2}{y_4^2} &= \alpha\bar{\alpha}, & \frac{y_{14}^2}{y_4^2} &= (1-\alpha)(1-\bar{\alpha}). \end{aligned} \quad (4.121)$$

With a simple calculation we obtain (in this frame)

$$\hat{t}_1 = t_1 = \text{Tr}(x_1 x_4^{-1}) - \text{Tr}(y_1 y_4^{-1}) = z + \bar{z} - \alpha - \bar{\alpha} \quad (4.122)$$

$$\begin{aligned} \hat{t}_2 &= t_2 - 2 \text{Tr} \left(\bar{\rho} x_4^{-1} \rho y_4^{-1} \right), \\ \hat{t}_3 &= t_3 - 3 \text{Tr} \left(\bar{\rho} x_4^{-1} x_1 x_4^{-1} \rho y_4^{-1} \right) - 3 \text{Tr} \left(\bar{\rho} x_4^{-1} \rho y_4^{-1} y_1 y_4^{-1} \right), \\ \hat{t}_4 &= t_4 - 4 \text{Tr} \left(\bar{\rho} x_4^{-1} (x_1 x_4^{-1})^2 \rho y_4^{-1} \right) - 4 \text{Tr} \left(\bar{\rho} x_4^{-1} \rho y_4^{-1} (y_1 y_4^{-1})^2 \right) \\ &\quad - 4 \text{Tr} \left(\bar{\rho} x_4^{-1} x_1 x_4^{-1} \rho y_4^{-1} y_1 y_4^{-1} \right) - 2 \text{Tr} \left(\bar{\rho} x_4^{-1} \rho y_4^{-1} \bar{\rho} x_4^{-1} \rho y_4^{-1} \right), \end{aligned} \quad (4.123)$$

where $\rho = \rho_1$, $\bar{\rho} = \bar{\rho}_1$.

Summary. The final expression for the spinning correlators in (4.108) involves the structures $\Lambda_{1,ij}$ and $V_{1,ij}$ introduced in (4.100). These quantities are not independent but satisfy the relation

$$\Lambda_{1,24} = \Lambda_{1,23} + \Lambda_{1,34}, \quad (4.124)$$

and similarly for $V_{1,ij}$. In particular the correlator involving \mathcal{J}_p is linear in $\Lambda_{1,ij}$ and $V_{1,ij}$, while the one involving \mathcal{T}_p is quadratic in $\Lambda_{1,ij}$ and independent of $V_{1,ij}$. Once the general expression for the correlator is obtained in terms of $\Lambda_{1,ij}$, one can decompose into

$$\bar{\lambda}_1 x_{1k}^{-1} \lambda_1 = \frac{z \cdot x_{1k}}{x_{1k}^2}, \quad z^\mu = \sigma_{\alpha\dot{\alpha}}^\mu \lambda_1^\alpha \bar{\lambda}_1^{\dot{\alpha}} \quad (4.125)$$

elements, which will have a natural counterpart in the Mellin approach of the next section (compare to (4.24))

$$\begin{aligned} \langle \mathcal{J}_{p_1}(1) \mathcal{O}_{p_1}(2) \mathcal{O}_{p_2}(3) \mathcal{O}_{p_2}(4) \rangle &= \frac{1}{x_{12}^{2p_1} x_{34}^{2p_2}} \sum_{k=2}^4 \alpha_{p_1, p_2}^{(k)}(u, v; y_{ij}, Y_{1,ij}) \frac{z \cdot x_{1k}}{x_{1k}^2}, \\ \langle \mathcal{T}_{p_1}(1) \mathcal{O}_{p_1}(2) \mathcal{O}_{p_2}(3) \mathcal{O}_{p_2}(4) \rangle &= \frac{1}{x_{12}^{2p_1} x_{34}^{2p_2}} \sum_{k,l=2}^4 \beta_{p_1, p_2}^{(k,l)}(u, v; y_{ij}) \frac{z \cdot x_{1k}}{x_{1k}^2} \frac{z \cdot x_{1l}}{x_{1l}^2}, \end{aligned} \quad (4.126)$$

where

$$Y_{1,ij} = y_{1i}^2 y_{1j}^2 V_{1,ij}. \quad (4.127)$$

4.A.4 R- Symmetry gluing

Realization of $\mathfrak{su}(4)$ R-symmetry in the space of polynomials. It is convenient to use an index free notation to implement finite dimensional representations of $\mathfrak{su}(4)$. The components of a given representation are packaged in a polynomial $\mathcal{O}_{\mathcal{R}}(y, v, \bar{v})$ in the variables $y^{a\dot{a}}, v^a, \bar{v}^{\dot{a}}$ (here $a \in \{1, 2\}$, $\dot{a} \in \{\dot{1}, \dot{2}\}$) subject to certain constraints that depend on the

$\mathfrak{su}(4)$ Dynkin labels $\mathcal{R} = [q, p, r]$. The first constraint states that $O_{\mathcal{R}}(y, v, \bar{v})$ is homogeneous in v and \bar{v} of degree q and r respectively. The second constraint is slightly more involved. In the case $\mathcal{R} = [0, p, 0]$, so that $O_{\mathcal{R}}$ is independent of v, \bar{v} it reads

$$\left(w^a \bar{w}^{\dot{a}} \frac{\partial}{\partial y^{a\dot{a}}} \right)^{p+1} O_{\mathcal{R}}(y) = 0, \quad \forall w, \bar{w}. \quad (4.128)$$

The case $\mathcal{R} = [1, p-2, 1]$ is more involved. Since we will not use it in this work we will not present the identification of $\mathcal{R} = [1, p-2, 1]$ as the kernel of differential operators. Two-point functions take the form

$$G_{[q,p,r]}(1, 2) = (y_{12}^2)^p (v_1 y_{12} \bar{v}_2)^q (v_2 y_{12} \bar{v}_1)^r. \quad (4.129)$$

Projections and gluing. To implement factorization in Mellin space in the presence of some global symmetry (in our case the $\mathfrak{su}(4)$ R-symmetry) it is necessary to take into account this extra structure. To do so, we introduce a projector that singles out the contribution of a given operator²¹ O which we denote by

$$|O| = \frac{1}{\mathcal{N}_O} \mathcal{D}_{\mathcal{R}[O]}^{(\ell,r)} |O(\ell)\rangle \langle O^*(r)| \Big|_{\ell=r}, \quad (4.130)$$

where \mathcal{D} is a differential operator which is fixed (up to a normalization that will be explained momentarily) by the requirement that (4.130) is invariant under $\mathfrak{su}(4)$. The notation $*$ denotes conjugation which acts on representations as $[q, p, r]^* = [r, p, q]$. When we insert the quantity $|O|$ in an n-point correlation function it is understood that we first place $|O(\ell)\rangle \langle O^*(r)|$, next act with the differential operator \mathcal{D} on the coordinates ℓ and r and finally set the coordinates ℓ and r to be equal. To fix the normalization of \mathcal{D} we insert $|O|$ in the two-point function

$$\langle O^*(1) O(2) \rangle = \mathcal{N}_O G_{\mathcal{R}[O]}(1, 2), \quad (4.131)$$

where $G_{\mathcal{R}}$ is given in (4.129) and obtain the condition

$$\mathcal{D}_{\mathcal{R}}^{(\ell,r)} G_{\mathcal{R}}(1, \ell) G_{\mathcal{R}}(r, 2) \Big|_{\ell=r} = G_{\mathcal{R}}(1, 2). \quad (4.132)$$

The explicit form of $\mathcal{D}_{\mathcal{R}}$ is slightly complicated. The simplest one is given by

$$\mathcal{D}_{[0,p,0]}^{(\ell,r)} = \sum_{n=0}^p \frac{(-\partial_{\ell} \cdot \partial_r)^{p-n}}{\Gamma(p+1) \Gamma(p+2)} \sum_{k=0}^n (-1)^{n-M(k,n-k)} \frac{(p-n+1)_{m(k,n-k)+1}}{\Gamma(m(k, n-k) + 1)} (\square_{\ell})^k (\square_r)^{n-k}, \quad (4.133)$$

²¹Here we use the notation O instead of \mathcal{O} since we are ignoring the space-time part.

where $(a)_n$ denotes the Pochhammer symbol, $M(a, b) = \max(a, b)$, $m(a, b) = \min(a, b)$ and

$$\partial_i \cdot \partial_j := \epsilon^{a_1 a_2} \epsilon^{\dot{a}_1 \dot{a}_2} \frac{\partial}{\partial y_i^{a_1 \dot{a}_1}} \frac{\partial}{\partial y_j^{a_2 \dot{a}_2}}, \quad \square_i = \frac{1}{2} \partial_i \cdot \partial_i. \quad (4.134)$$

The general expression for the differential operator $\mathcal{D}_{[1,p-2,1]}$ is more complicated, but it is easy to obtain for fixed p using the defining relation (4.132). Let us report the simplest member of this family as an example

$$\mathcal{D}_{[1,0,1]}^{(\ell,r)} = (\partial_{v_\ell} \partial_{v_r}) (\partial_{\bar{v}_\ell} \partial_{\bar{v}_r}) \left(\frac{1}{2} \partial_\ell \cdot \partial_r - \square_\ell - \square_r \right) - \frac{3}{16} (\partial_{v_\ell} \partial_{y_\ell} \partial_{\bar{v}_\ell}) (\partial_{v_r} \partial_{y_r} \partial_{\bar{v}_r}), \quad (4.135)$$

where the contraction of indices is understood using the ϵ tensor.

Application to five-point functions. When we insert the projector (4.130) in a 5-point function we will produce a product of a 3-point and a 4-point function on which the differential operator \mathcal{D} acts. In the following we denote by \rightarrow the combination of acting with $\mathcal{D}^{(\ell,r)}$ and setting the coordinates $\ell = r$. The case that is relevant for the exchange of \mathcal{O}_p which transform in a $[0, p, 0]$ representation is

$$[(y_{1\ell}^2) (y_{2\ell}^2)^{p-1}] [(y_{ri}^2)^{p-2} (y_{rj}^2) (y_{rk}^2)] \rightarrow \quad (4.136)$$

$$\frac{1}{p} (y_{2i}^2)^{p-3} \left(y_{2i}^2 (y_{2j}^2 y_{1k}^2 + y_{1j}^2 y_{2k}^2) + (p-2) y_{1i}^2 y_{2j}^2 y_{2k}^2 - \frac{p-2}{p+1} y_{12}^2 (y_{2k}^2 y_{ij}^2 + y_{2j}^2 y_{ik}^2) - \frac{1}{p+1} y_{12}^2 y_{2i}^2 y_{jk}^2 \right) \quad (4.137)$$

Similarly, using the definitions above, gluing the 3 and 5 point functions corresponding to the exchange of \mathcal{J}_p (which transforms in the representation $[1, p-2, 1]$) is achieved by the substitution

$$[(y_{2\ell}^2)^{p-2} Y_{\ell,12}] \left[(y_{ri}^2)^{p-3} (y_{rj}^2) Y_{r,kl} \right] \rightarrow \quad (4.138)$$

$$(y_{2i}^2)^{p-4} \left(y_{2i}^2 y_{2j}^2 (y_{1k}^2 y_{2l}^2 - y_{1l}^2 y_{2k}^2) + y_{12}^2 \left(\frac{p-3}{p+2} y_{2j}^2 (y_{il}^2 y_{2k}^2 - y_{2l}^2 y_{ik}^2) + \frac{1}{p+2} y_{2i}^2 (y_{jl}^2 y_{2k}^2 - y_{2l}^2 y_{jk}^2) \right) \right) \quad (4.139)$$

For the exchange of \mathcal{T}_p we use the same rules as (4.136) with p replaced by $p-2$.

4.B Strong coupling correlators

We can define the inverse Mellin transform of the scalar correlator as

$$\langle \mathcal{O}_{p_1}(1) \mathcal{O}_{p_1}(2) \mathcal{O}_{p_2}(3) \mathcal{O}_{p_2}(4) \rangle = d_{12}^{p_1} d_{34}^{p_2} G(z_k) = \int d\delta_{ij} \mathcal{M}(\delta_{ij}, y_{ij}) \prod_{i < j} \frac{\Gamma(\delta_{ij})}{x_{ij}^{2\delta_{ij}}}. \quad (4.140)$$

Conformal symmetry requires the Mellin variables δ_{ij} to obey the following equations

$$\sum_{j \neq i} \delta_{ij} = \Delta_i, \quad (4.141)$$

effectively leaving only two degrees of freedom for four-point functions. It is useful to consider the following parametrization

$$\delta_{ij} = \frac{\Delta_i + \Delta_j - s_{ij}}{2}, \quad (4.142)$$

so that the solution is given simply as

$$s_{12} = s_{34} = s, \quad s_{14} = s_{23} = t, \quad s_{13} = s_{24} = 2(p_1 + p_2) - s - t. \quad (4.143)$$

For the configuration we are interested in we can then write the inverse Mellin transform as

$$G(u, v; \sigma, \tau) = \int \frac{ds dt}{4} u^{\frac{s}{2}} v^{\frac{t-p_1-p_2}{2}} \mathcal{M}(s, t; \sigma, \tau) \prod_{i < j} \Gamma(\delta_{ij}(s, t)). \quad (4.144)$$

Equivalently, the Mellin transform of the spacetime correlator is

$$\mathcal{M}(s, t; \sigma, \tau) \prod_{i < j} \Gamma(\delta_{ij}(s, t)) = \int_0^\infty du \int_0^\infty dv u^{-\frac{s}{2}-1} v^{\frac{p_1+p_2-t}{2}-1} G(u, v; \sigma, \tau). \quad (4.145)$$

When the correlator has a factorized form as in (4.115), then it is convenient to introduce the Mellin transform of the dynamical function $\mathcal{H}_p(u, v)$

$$\widetilde{\mathcal{M}}_p(s, t) \prod_{i < j} \Gamma(\tilde{\delta}_{ij}(s, t)) = \int_0^\infty du \int_0^\infty dv u^{-\frac{s}{2}-1} v^{\frac{p-t}{2}-1} H_p(u, v), \quad (4.146)$$

where the shifted variables are defined as

$$\begin{aligned} \tilde{\delta}_{13} &= \delta_{13} + 2, & \tilde{\delta}_{24} &= \delta_{24} + 2, \\ \delta_{ij} &= \tilde{\delta}_{ij} \quad \text{otherwise,} \end{aligned} \quad (4.147)$$

and make crossing properties of the Mellin amplitude simpler. At strong coupling the Mellin space version of the correlator was found to have a particularly simple structure [128, 186], and in the case under consideration it reduces to

$$\widetilde{\mathcal{M}}_p(s, t) = \frac{32}{(s-2)(t-p)(p-s-t)}. \quad (4.148)$$

For the spinning correlators we can also write inverse Mellin transforms as follows

$$\begin{aligned} \langle \mathcal{J}_{p_1}(1) \mathcal{O}_{p_1}(2) \mathcal{O}_{p_2}(3) \mathcal{O}_{p_2}(4) \rangle &= \sum_{k=2}^4 \frac{z \cdot x_{1k}}{x_{1k}^2} \int [d\delta] \mathcal{M}_{p_1, p_2}^k \prod_{i=2}^4 \frac{\Gamma(\delta_i + \delta_i^k)}{x_{1i}^{2\delta_i}} \prod_{i < j} \frac{\Gamma(\delta_{ij})}{x_{ij}^{2\delta_{ij}}}, \\ \langle \mathcal{T}_{p_1}(1) \mathcal{O}_{p_1}(2) \mathcal{O}_{p_2}(3) \mathcal{O}_{p_2}(4) \rangle &= \sum_{k, l=2}^4 \frac{z \cdot x_{1k}}{x_{1k}^2} \frac{z \cdot x_{1l}}{x_{1l}^2} \int [d\delta] \mathcal{M}_{p_1, p_2}^{kl} \prod_{i=2}^4 \frac{\Gamma(\delta_i + \delta_i^k + \delta_i^l)}{x_{1i}^{2\delta_i}} \prod_{i < j} \frac{\Gamma(\delta_{ij})}{x_{ij}^{2\delta_{ij}}}, \end{aligned} \quad (4.149)$$

with δ_i^k the Kronecker-delta, and the Mellin variables are constrained by

$$\delta_i = - \sum_{j=2}^4 \delta_{ij}, \quad \delta_{ii} = -\Delta_i, \quad \sum_{i, j=2}^4 \delta_{ij} = S - \Delta_1. \quad (4.150)$$

In the two cases of interest we have $S - \Delta_1 = p_1$, so the δ_{ij} variables have the same solution as in the scalar case, see (4.142) and (4.143). Comparing with the form of the correlators obtained in the previous section, we can see that the inverse Mellin trasform of the functions introduced in (4.126) are exactly the \mathcal{M}^k and \mathcal{M}^{kl} above

$$\begin{aligned} \alpha_{p_1, p_2}^{(k)}(u, v; y_{ij}, Y_{1,ij}) &= \int \frac{ds dt}{4} u^{\frac{s}{2}} v^{\frac{t-p_1-p_2}{2}} \mathcal{M}_{p_1, p_2}^k(s, t; y_{ij}, Y_{1,ij}) \prod_{i=2}^4 \Gamma(\delta_i + \delta_i^k) \prod_{i < j} \Gamma(\delta_{ij}), \\ \beta_{p_1, p_2}^{(k,l)}(u, v; y_{ij}) &= \int \frac{ds dt}{4} u^{\frac{s}{2}} v^{\frac{t-p_1-p_2}{2}} \mathcal{M}_{p_1, p_2}^{kl}(s, t; y_{ij}) \prod_{i=2}^4 \Gamma(\delta_i + \delta_i^k + \delta_i^l) \prod_{i < j} \Gamma(\delta_{ij}). \end{aligned} \quad (4.151)$$

Inversing the logic we then have

$$\begin{aligned} \mathcal{M}_{p_1, p_2}^k(s, t; y_{ij}, Y_{1,ij}) \prod_{i=2}^4 \Gamma(\delta_i + \delta_i^k) \prod_{i < j} \Gamma(\delta_{ij}) &= \int_0^\infty du dv u^{-\frac{s}{2}-1} v^{\frac{p_1+p_2-t}{2}-1} \alpha_{p_1, p_2}^{(k)}(u, v; y_{ij}, Y_{1,ij}), \\ \mathcal{M}_{p_1, p_2}^{kl}(s, t; y_{ij}) \prod_{i=2}^4 \Gamma(\delta_i + \delta_i^k + \delta_i^l) \prod_{i < j} \Gamma(\delta_{ij}) &= \int_0^\infty du dv u^{-\frac{s}{2}-1} v^{\frac{p_1+p_2-t}{2}-1} \beta_{p_1, p_2}^{(k,l)}(u, v; y_{ij}). \end{aligned} \quad (4.152)$$

As explained in the previous section, the functions $\alpha_{p_1, p_2}^{(k)}$ and $\beta_{p_1, p_2}^{(k,l)}$ are given in terms of derivatives of the dynamical function from the scalar correlator. When $p_1 = 2$ and $p_2 = p$, or $p_1 = p$ and $p_2 = 2$, we are then relating with H_p from (4.115), and so we should use

$$\begin{aligned} &\int_0^\infty du \int_0^\infty dv u^{-\frac{s}{2}-1} v^{\frac{p+2-t}{2}-1} u^m v^n \frac{\partial^a}{\partial u^a} \frac{\partial^b}{\partial v^b} H_p(u, v) = \widetilde{\mathcal{M}}_p(s-2m+2a, t-2n+2b) \\ &\times (-1)^{a+b} \left(m - a - \frac{s}{2} \right)_a \left(n - b + \frac{p+2-t}{2} \right)_b \prod_{i < j} \Gamma(\tilde{\delta}_{ij}(s-2m-2a, t-2n-2b)), \end{aligned} \quad (4.153)$$

which allows us to write \mathcal{M}_{p_1,p_2}^k and $\mathcal{M}_{p_1,p_2}^{kl}$ for those two configurations in terms of the scalar Mellin amplitude $\widetilde{\mathcal{M}}_p(s,t)$. At the end of the day, the Mellin amplitudes for $\langle \mathcal{J}_2 \mathcal{O}_2 \mathcal{O}_p \mathcal{O}_p \rangle$ are

$$\begin{aligned} \mathcal{M}_{2,p}^2 &= -2(t-p-2) \left(\frac{2(p-2)}{s-4} + \frac{2}{s-2} + \frac{p}{4+p-s-t} \right) y_{24}^2 y_{34}^{2(p-1)} Y_{1,23} \\ &\quad - 2(2+p-s-t) \left(\frac{2(p-2)}{s-4} + \frac{2}{s-2} + \frac{p}{t-p} \right) y_{23}^2 y_{34}^{2(p-1)} Y_{1,24} \\ &\quad - 2p(s-2p) \left(\frac{1}{t-p} - \frac{1}{4+p-s-t} \right) y_{23}^2 y_{24}^2 y_{34}^{2(p-2)} Y_{1,34}, \\ \mathcal{M}_{2,p}^3 &= 2(t-p-2) \left(\frac{2}{s-2} + \frac{p}{4+p-s-t} \right) y_{24}^2 y_{34}^{2(p-1)} Y_{1,23} \\ &\quad + 2(2+p-s-t) \left(\frac{2}{s-2} - \frac{p}{t-p} \right) y_{23}^2 y_{34}^{2(p-1)} Y_{1,24} \\ &\quad - 2p(s-2p) \left(\frac{1}{t-p} + \frac{1}{4+p-s-t} \right) y_{23}^2 y_{24}^2 y_{34}^{2(p-2)} Y_{1,34}. \end{aligned} \quad (4.154)$$

Note that in general we expected poles at $s-2$, $t-p$ and $p+4-s-t$. However, in the $\mathcal{M}_{2,p}^2$ component we see also the presence of a pole at $s-4$. While this might appear unexpected at first, it is in fact due to the shift in the Gamma functions of spinning correlators. When $p_1 = 2$ and $p_2 = p$ the relevant factors are

$$\Gamma(\delta_2 + 1)\Gamma(\delta_{34}) = \Gamma\left(3 - \frac{s}{2}\right)\Gamma\left(p - \frac{s}{2}\right). \quad (4.155)$$

It is then evident that the Gamma functions do not prohibit the satellite pole at $s-4$ (unless $p=2$, in which case the residue vanishes). Meanwhile for $\langle \mathcal{J}_p \mathcal{O}_2 \mathcal{O}_2 \mathcal{O}_2 \rangle$ we have

$$\begin{aligned} \mathcal{M}_{p,2}^2 &= \frac{2(p-2)s}{p} \left[\frac{t-p-2}{4+p-s-t} y_{12}^{2(p-3)} y_{13}^2 y_{24}^4 Y_{1,23} + \frac{2+p-s-t}{t-p} y_{12}^{2(p-3)} y_{14}^2 y_{23}^4 Y_{1,24} \right. \\ &\quad \left. + 2 \left(1 + \frac{p}{t-p} + \frac{p}{4+p-s-t} \right) y_{12}^{2(p-3)} y_{14}^2 y_{23}^2 y_{24}^2 Y_{1,23} \right] \\ &\quad + \frac{2(t-p-2)}{p} \left(p-2 - \frac{4}{s-2} - \frac{2p}{4+p-s-t} \right) y_{12}^{2(p-2)} y_{24}^2 y_{34}^2 Y_{1,23} \\ &\quad + \frac{2(2+p-s-t)}{p} \left(p-2 - \frac{4}{s-2} - \frac{2p}{t-p} \right) y_{12}^{2(p-2)} y_{23}^2 y_{34}^2 Y_{1,24} \\ &\quad + \frac{2}{p} \left(s(p-2) - \frac{2p(s-2p)}{t-p} + \frac{2p(s(p-1)-2p)}{4+p-s-t} \right) y_{12}^{2(p-2)} y_{23}^2 y_{24}^2 Y_{1,34}, \end{aligned}$$

$$\begin{aligned}
\mathcal{M}_{p,2}^3 = & \frac{2(p-2)(s-2p)}{p} \left[\frac{t-p-2}{4+p-s-t} y_{12}^{2(p-3)} y_{13}^2 y_{24}^4 Y_{1,23} + \frac{2+p-s-t}{t-p} y_{12}^{2(p-3)} y_{14}^2 y_{23}^4 Y_{1,24} \right. \\
& + 2 \left(1 + \frac{p}{t-p} + \frac{p}{4+p-s-t} \right) y_{12}^{2(p-3)} y_{14}^2 y_{23}^2 y_{24}^2 Y_{1,23} \left. \right] \\
& + \frac{2(t-p-2)}{p} \left(p-2 + \frac{4(p-1)}{s-2} + \frac{2p(p-1)}{4+p-s-t} \right) y_{12}^{2(p-2)} y_{24}^2 y_{34}^2 Y_{1,23} \\
& + \frac{2(2+p-s-t)}{p} \left(p-2 + \frac{4(p-1)}{s-2} - \frac{2p}{t-p} \right) y_{12}^{2(p-2)} y_{23}^2 y_{34}^2 Y_{1,24} \\
& + \frac{2(s-2p)}{p} \left(p-2 - \frac{2p}{t-p} - \frac{2p}{4+p-s-t} \right) y_{12}^{2(p-2)} y_{23}^2 y_{24}^2 Y_{1,34}. \tag{4.156}
\end{aligned}$$

In this case the Gamma factors for $\mathcal{M}_{p,2}^2$ are

$$\Gamma(\delta_2 + 1)\Gamma(\delta_{34}) = \Gamma\left(p + 1 - \frac{s}{2}\right)\Gamma\left(2 - \frac{s}{2}\right), \tag{4.157}$$

and that is why the shift does not lead to any unexpected pole. For the other Mellin components \mathcal{M}_{p_1,p_2}^3 and \mathcal{M}_{p_1,p_2}^4 we have

$$\begin{aligned}
\Gamma(\delta_3 + 1)\Gamma(\delta_{24}) &= \Gamma\left(\frac{s+t-p}{2}\right)\Gamma\left(\frac{s+t-p-2}{2}\right), \\
\Gamma(\delta_4 + 1)\Gamma(\delta_{23}) &= \Gamma\left(\frac{4+p-t}{2}\right)\Gamma\left(\frac{2+p-t}{2}\right), \tag{4.158}
\end{aligned}$$

which explains why there cannot be any new poles in these channels for any of the two configurations considered.

Moving on to the spin 2 case, the Mellin amplitudes for the $\langle \mathcal{T}_2 \mathcal{O}_2 \mathcal{O}_p \mathcal{O}_p \rangle$ correlator are

$$\begin{aligned}
\mathcal{M}_{2,p}^{2,2} &= \frac{16}{3} \left(1 - p + 6(p-2) \left(\frac{p-3}{s-6} + \frac{2}{s-4} \right) + \frac{2}{s-2} + \frac{p(p-1)}{t-p} + \frac{p(p-1)}{4+p-s-t} \right) y_{23}^2 y_{24}^2 y_{34}^{2(p-1)}, \\
\mathcal{M}_{2,p}^{2,3} &= \frac{16}{3} \left(1 - p - \frac{6(p-2)}{s-4} - \frac{4}{s-2} + \frac{p(p-1)}{t-p} - \frac{2p(p-1)}{4+p-s-t} \right) y_{23}^2 y_{24}^2 y_{34}^{2(p-1)}, \\
\mathcal{M}_{2,p}^{3,3} &= \frac{16}{3} \left(1 - p + \frac{2}{s-2} + \frac{p(p-1)}{t-p} + \frac{p(p-1)}{4+p-s-t} \right) y_{23}^2 y_{24}^2 y_{34}^{2(p-1)}. \tag{4.159}
\end{aligned}$$

There are once again some satellite poles, but the explanation follows exactly the same reasoning as before. The relevant Gamma factors in $\mathcal{M}_{2,p}^{2,2}$ are in this case

$$\Gamma(\delta_2 + 2)\Gamma(\delta_{34}) = \Gamma\left(4 - \frac{s}{2}\right)\Gamma\left(p - \frac{s}{2}\right), \tag{4.160}$$

thus allowing poles both at $s - 4$ and $s - 6$ (except if $p = 2, 3$). Meanwhile, for $\mathcal{M}^{2,3}$ (and also $\mathcal{M}^{2,4}$) the relevant Gammas are

$$\Gamma(\delta_2 + \delta_2^2)\Gamma(\delta_{34}) = \Gamma\left(3 - \frac{s}{2}\right)\Gamma\left(p - \frac{s}{2}\right), \quad (4.161)$$

and so the only satellite pole in those Mellin components is at $s - 4$. At last, for the correlator $\langle \mathcal{T}_p \mathcal{O}_p \mathcal{O}_2 \mathcal{O}_2 \rangle$ we have

$$\begin{aligned} \mathcal{M}_{p,2}^{2,2} &= \frac{8(p-2)(s+2)}{(p+1)(p+2)} \left[\left(\frac{s(p-1)-2p}{t-p} + \frac{2p}{4+p-s-t} \right) y_{12}^{2(p-3)} y_{14}^2 y_{23}^4 y_{24}^2 \right. \\ &\quad \left. + \left(\frac{2p}{t-p} + \frac{s(p-1)-2p}{4+p-s-t} \right) y_{12}^{2(p-3)} y_{13}^2 y_{23}^2 y_{24}^4 \right] \\ &\quad + \frac{8 y_{12}^{2(p-2)} y_{23}^2 y_{24}^2 y_{34}^2}{(p+1)(p+2)} \left((p-1)(p-2)s - 4(p^2-2) + \frac{16}{s-2} \right. \\ &\quad \left. - \frac{2p(s(p-2)-2p)}{t-p} - \frac{2p(s(p-2)-2p)}{4+p-s-t} \right), \\ \mathcal{M}_{p,2}^{2,3} &= \frac{8(p-2)}{(p+1)(p+2)} \left[\left(\frac{s^2(p-1)-2p^2s-2(p+2)(p-1)}{t-p} - \frac{p(s(p-1)+6p+2)}{4+p-s-t} \right) y_{12}^{2(p-3)} y_{14}^2 y_{23}^4 y_{24}^2 \right. \\ &\quad \left. + \left(\frac{2p(s-p+1)}{t-p} + \frac{s^2(p-1)-sp(p-1)+2(p^2+p+2)}{4+p-s-t} \right) y_{12}^{2(p-3)} y_{13}^2 y_{23}^2 y_{24}^4 \right] \\ &\quad + \frac{8 y_{12}^{2(p-2)} y_{23}^2 y_{24}^2 y_{34}^2}{(p+1)(p+2)} \left((p-1)(p-2)s - 2(p+2)(p-1) - \frac{16p}{s-2} \right. \\ &\quad \left. - \frac{2p(s(p-2)-(p-1)(p+2))}{t-p} + \frac{p(s(p-1)(p-2)-2(p^2+p+2))}{4+p-s-t} \right), \\ \mathcal{M}_{p,2}^{3,3} &= \frac{8(p-2)(s-2p)}{(p+1)(p+2)} \left[\left(\frac{2p^2-(s-2)(p-1)}{t-p} - \frac{2p^2}{4+p-s-t} \right) y_{12}^{2(p-3)} y_{14}^2 y_{23}^4 y_{24}^2 \right. \\ &\quad \left. + \left(\frac{2p}{t-p} + \frac{s(p-1)+2}{4+p-s-t} \right) y_{12}^{2(p-3)} y_{13}^2 y_{23}^2 y_{24}^4 \right] \\ &\quad + \frac{8 y_{12}^{2(p-2)} y_{23}^2 y_{24}^2 y_{34}^2}{(p+1)(p+2)} \left((p-1)(p-2)s - 4p + \frac{8p(p-1)}{s-2} \right. \\ &\quad \left. + \frac{2p(2(p^2-2)-s(p-2))}{t-p} + \frac{2p^2(s(p-2)+2)}{4+p-s-t} \right). \end{aligned} \quad (4.162)$$

Note that in the final expressions above we omit the \mathcal{M}_{p_1,p_2}^4 and $\mathcal{M}_{p_1,p_2}^{k,4}$ cases, but they can be easily obtained from the equations relating different Mellin components

$$\begin{aligned} \sum_k \delta_k \mathcal{M}^k &= 0, \\ \sum_k (\delta_k + \delta_k^l) \mathcal{M}^{kl} &= 0, \end{aligned} \tag{4.163}$$

which play a similar role to the equation (4.124) relating the tensor structures in position space. Finally, note that for the particular case of $p_1 = p_2 = 2$ the expressions above simplify and agree with those found in our earlier work [57].

4.B.1 Example of factorization

The goal of this subsection is to show explicitly how to use factorization, lower-point Mellin amplitudes and the R -symmetry gluing rules from Appendix 4.A.4 to recover part of the five-point function. To simplify the presentation we will focus on the factorization of the scalar **20'** operator exchanged in the channel (45).

The building blocks for the factorization are the Mellin amplitude of the four-point function $\langle \mathcal{O}_p \mathcal{O}_p \mathcal{O}_2 \mathcal{O}_2 \rangle$ and the three-point function $\langle \mathcal{O}_2 \mathcal{O}_2 \mathcal{O}_2 \rangle$

$$\begin{aligned} \mathcal{M}_{pp22} &= \frac{4t_{01}t_{23}t_{12}^{p-2} \left(\delta_{12} (p(t_{02}t_{13} - t_{03}t_{12}) - (p-1)t_{01}t_{23}) + (p-1)pt_{03}t_{12} + \delta_{12}^2 t_{01}t_{23} \right)}{\delta_{23} - 1} + \dots \\ \mathcal{M}_{222} &= C_{OOO} t_{45}t_{40}t_{50} \end{aligned} \tag{4.164}$$

where we decided to write explicitly only part of the four point function to simplify even further the analysis. The label 0 in the formula is associated to the operator that is being exchanged in the factorization channel.

Now we can borrow the formula from (4.15,4.18) to obtain

$$\mathcal{M}_{pp222} = 2\Gamma(2) \frac{\mathcal{M}_{pp22} \mathcal{M}_{222}}{(2\delta_{45} - 2)} + \dots \tag{4.165}$$

where the \dots stand for other poles and contributions of other operators. The gluing in R -symmetry space gives, implementing²² (4.136) for $p = 2$,

$$t_{\ell 4} t_{\ell 5} t_{ri_1} t_{ri_2} \rightarrow \frac{1}{2} \left((t_{4i_1} t_{5i_2} + t_{4i_2} t_{5i_1}) - \frac{t_{45} t_{i_1 i_2}}{3} \right), \tag{4.166}$$

$$t_{\ell 4} t_{\ell 5} t_{ri_1}^2 \rightarrow t_{4i_1} t_{5i_1}. \tag{4.167}$$

²²Recall that $t_{ij} = y_{ij}^2$.

Thus we obtain

$$\begin{aligned} \mathcal{M}_{pp222} = & \frac{2C_{OOO}t_{23}t_{45}t_{12}^{p-2}}{3(\delta_{23}-1)(\delta_{45}-1)} \left[\left(3\delta_{12} \left(p t_{15} (t_{13}t_{24} - t_{12}t_{34}) + t_{14} (p(t_{13}t_{25} - t_{12}t_{35}) \right. \right. \right. \\ & \left. \left. \left. - 2(p-1)t_{15}t_{23} \right) \right) + (p-1)pt_{12} (3t_{15}t_{34} + 3t_{14}t_{35} - t_{13}t_{45}) + 6\delta_{12}^2 t_{14}t_{15}t_{23} \right) \right] + \dots \end{aligned} \quad (4.168)$$

where, again, the dots stand for other poles and contributions of other operators. In particular this formula can be compared with our previous result for five point function of **20'** operators.

Chapter 5

Conclusion and open directions

In this last chapter, we summarize the contributions of this thesis and comment on possible open avenues extending this work. We hold ourselves from repeating the discussions in the end of each chapter, but for convenience we stress the main conclusions and targets for future research.

Motivated by the potential game-changer and revolution that higher-point functions can be in the bootstrap program discussed in chapter 1, we made significant contributions to make these observables more amenable to analytic studies in various regimes.

In chapter 2, we introduced an analytic lightcone bootstrap for five and six-point correlators in a snowflake topology. In doing so, we found the form of the large spin behaviour of new OPE coefficients. For the five-point case, this includes the OPE coefficients of two double-twist-like operators and the external scalar. For the six-point correlators, we went one step further. Besides finding the large-spin behaviour of OPE coefficients with three spinning operators of the leading double-twist family $[\phi\phi]_{0,J}$, we considered subleading corrections in the direct channel. These are reproduced in the cross channel by considering anomalous dimensions and corrections to the OPE coefficients of these operators. There are some clear open directions stemming from this work that one may want to pursue. As mentioned above, this program was carried out in a snowflake decomposition of the correlators. The extension of these ideas to the comb-channel decomposition of six-point correlators would provide access to large-spin behaviour of triple-twist operators. The first steps towards this goal were done in the recent work [66]. It would be interesting to push further their ideas by analysing more possible contributions in the direct channel. Still in the snowflake channel, there is more to be done. Similarly to the four-point follow-ups of the original works [44, 45], one can consider subleading contributions in conformal spin for

both anomalous dimensions and OPE corrections as done in [75, 76]. This can in principle be done by using only the lightcone blocks that are available in this chapter, but it is not clear yet what role will be played by the label for different tensor structures of three-point functions in this generalization. On the other hand, by computing subleading corrections to the lightcone blocks, one expects to be able to bootstrap subleading families of double-twist operators. These are directions we intend to study in the near future.

An important question raised by our lightcone bootstrap for higher-point functions is the possible existence of analyticity of OPE coefficients not only in spin but also in the label of different three-point functions involving spinning operators. This question was also naturally found in chapter 3. In this chapter, we discussed the generalization of Regge limit and Regge theory for five-point correlation functions of primary operators in CFT. We proposed Regge limit's corresponding kinematics and stressed the relevance of the position of the new fifth operator. In particular, we showed that this kinematics leads to a similar cross-ratio behaviour to that of Euclidean OPE limit but only after crossing branch-cuts of the conformal block. Also, in Mellin space, we noted that the proposed kinematics is translated to the dominance of a region of large Mellin variables in close analogy with the Regge limit of scattering amplitudes in flat space. After reviewing flat-space literature for multi-Regge theory, we extended conformal Regge theory to higher-point functions. In this process, we found the need to appeal for analyticity of CFT data in spin and in the basis of tensor structures of three-point functions with spins in (at least) 8 different signatures. However, this label is basis dependent and does not identify the operators of the theory, therefore we expect no dynamical poles in it.

Finding a Lorentzian inversion formula for higher-point correlators would answer the question about the existence of analyticity in this label or not. Note, however, that as there is a basis choice to make, it is not clear if the analyticity can only be made manifest in a given basis and, if so, what basis that is.

For the derivation of a Lorentzian inversion formula for higher-point functions, we expect Regge boundedness to be an important ingredient. Even though we expect this boundedness to be true for our choice of kinematics, we have not provided a proof of that fact. The general proof for four-point correlators uses a positive-definite Rindler inner product and explores the fact that the Regge limit is given by a Rindler-symmetric configuration. This is not the case of the five-point Regge limit we presented. It would be interesting to establish Regge boundedness by other means. For example, by exploring

a different OPE channel where no cuts are crossed and OPE convergence is guaranteed. Alternatively, by finding some conformal mapping between this kinematics and other that can be bounded by the Euclidean correlator. This calls for a more systematic understanding of singularities in higher-point functions. Proving Regge boundedness is important per se but would, most likely, also invite the explorations of conformal dispersion relations for higher-point functions.

As a byproduct of our studies in chapter 3, we also introduced a new basis for three-point functions with spins, that allowed us to completely factorize the conformal block in the Euclidean limit. The full implications and simplifications that this basis can bring to the efficient computation of higher-point conformal blocks are yet to be discovered, but we hope to report on that soon.

In chapter 4, we continued exploring the structure of five-point functions of half-BPS operators in $\mathcal{N} = 4$ SYM in the strongly coupled regime, dual to IIB supergravity in $\text{AdS}_5 \times S^5$. We presented an algorithmic bootstrap approach and found the closed-form expression in Mellin space for the infinite number of correlators $\langle pp222 \rangle$, extending previous results for $p = 2$ [57]. Our method is entirely done in Mellin space and relies only on Mellin factorization and a superconformal twist. A key and essential simplification allowing us to study generic p contributions was the discovered pole truncation mechanism in Mellin space that allows us to have an ansatz with a pole structure much simpler than one could have previously anticipated. This property gives us hope that it is possible to bootstrap the form of more generic five-point functions with different Kaluza Klein modes. This is an avenue that we wish to pursue. Moreover, we believe the algorithm, with slight modifications, can be applied in a broad spectrum of problems such as five-point correlation functions in different superconformal theories and six-point functions in $\text{AdS}_5 \times S^5$. Furthermore, it would be interesting to use the factorization properties of Mellin amplitudes to compute stringy corrections to our result. This is another open direction in which we hope to report news in the near future.

Let us conclude this thesis by making some final remarks about other potential applications of higher-point functions that would be very interesting to explore. As stressed throughout the thesis, scalar higher-point functions probe infinitely many OPE coefficients between generic spinning operators in a very natural way. This opens the door to extract CFT data that is unreachable by current methods. It would be interesting to further develop numerical bootstrap methods for higher-point functions. First steps towards this

goal were done in [58, 59, 68]. In Lorentzian kinematics, causality imposes nontrivial constraints on CFT data. In this regard, extending causality constraints to higher-point functions may then help us find new bounds for OPE coefficients of generic spin operators and, for instance, further constrain the effective action of dual gravity theories in AdS.

Bibliography

- [1] António Antunes et al. “Lightcone bootstrap at higher points”. In: *JHEP* 03 (2022), p. 139. DOI: [10.1007/JHEP03\(2022\)139](https://doi.org/10.1007/JHEP03(2022)139). arXiv: [2111.05453 \[hep-th\]](https://arxiv.org/abs/2111.05453).
- [2] Miguel S. Costa et al. “Conformal multi-Regge theory”. In: *JHEP* 09 (2023), p. 155. DOI: [10.1007/JHEP09\(2023\)155](https://doi.org/10.1007/JHEP09(2023)155). arXiv: [2305.10394 \[hep-th\]](https://arxiv.org/abs/2305.10394).
- [3] Vasco Gonçalves et al. “Kaluza-Klein five-point functions from $\text{AdS}_5 \times S^5$ supergravity”. In: *JHEP* 08 (2023), p. 067. DOI: [10.1007/JHEP08\(2023\)067](https://doi.org/10.1007/JHEP08(2023)067). arXiv: [2302.01896 \[hep-th\]](https://arxiv.org/abs/2302.01896).
- [4] Joseph Polchinski. “Scale and Conformal Invariance in Quantum Field Theory”. In: *Nucl. Phys. B* 303 (1988), pp. 226–236. DOI: [10.1016/0550-3213\(88\)90179-4](https://doi.org/10.1016/0550-3213(88)90179-4).
- [5] Markus A. Luty, Joseph Polchinski, and Riccardo Rattazzi. “The a -theorem and the Asymptotics of 4D Quantum Field Theory”. In: *JHEP* 01 (2013), p. 152. DOI: [10.1007/JHEP01\(2013\)152](https://doi.org/10.1007/JHEP01(2013)152). arXiv: [1204.5221 \[hep-th\]](https://arxiv.org/abs/1204.5221).
- [6] Anatoly Dymarsky et al. “On Scale and Conformal Invariance in Four Dimensions”. In: *JHEP* 10 (2015), p. 171. DOI: [10.1007/JHEP10\(2015\)171](https://doi.org/10.1007/JHEP10(2015)171). arXiv: [1309.2921 \[hep-th\]](https://arxiv.org/abs/1309.2921).
- [7] Slava Rychkov. *EPFL Lectures on Conformal Field Theory in $D \geq 3$ Dimensions*. SpringerBriefs in Physics. Jan. 2016. ISBN: 978-3-319-43625-8, 978-3-319-43626-5. DOI: [10.1007/978-3-319-43626-5](https://doi.org/10.1007/978-3-319-43626-5). arXiv: [1601.05000 \[hep-th\]](https://arxiv.org/abs/1601.05000).
- [8] Aleix Gimenez-Grau, Yu Nakayama, and Slava Rychkov. “Scale without Conformal Invariance in Dipolar Ferromagnets”. In: (Sept. 2023). arXiv: [2309.02514 \[hep-th\]](https://arxiv.org/abs/2309.02514).
- [9] David Simmons-Duffin. “The Conformal Bootstrap”. In: *Theoretical Advanced Study Institute in Elementary Particle Physics: New Frontiers in Fields and Strings*. 2017, pp. 1–74. DOI: [10.1142/9789813149441_0001](https://doi.org/10.1142/9789813149441_0001). arXiv: [1602.07982 \[hep-th\]](https://arxiv.org/abs/1602.07982).

- [10] David Poland and David Simmons-Duffin. “The conformal bootstrap”. In: *Nature Phys.* 12.6 (2016), pp. 535–539. DOI: [10.1038/nphys3761](https://doi.org/10.1038/nphys3761).
- [11] David Poland, Slava Rychkov, and Alessandro Vichi. “The Conformal Bootstrap: Theory, Numerical Techniques, and Applications”. In: *Rev. Mod. Phys.* 91 (2019), p. 015002. DOI: [10.1103/RevModPhys.91.015002](https://doi.org/10.1103/RevModPhys.91.015002). arXiv: [1805.04405 \[hep-th\]](https://arxiv.org/abs/1805.04405).
- [12] Shai M. Chester. “Weizmann lectures on the numerical conformal bootstrap”. In: *Phys. Rept.* 1045 (2023), pp. 1–44. DOI: [10.1016/j.physrep.2023.10.008](https://doi.org/10.1016/j.physrep.2023.10.008). arXiv: [1907.05147 \[hep-th\]](https://arxiv.org/abs/1907.05147).
- [13] David Poland and David Simmons-Duffin. “Snowmass White Paper: The Numerical Conformal Bootstrap”. In: *Snowmass 2021*. Mar. 2022. arXiv: [2203.08117 \[hep-th\]](https://arxiv.org/abs/2203.08117).
- [14] Slava Rychkov and Ning Su. “New Developments in the Numerical Conformal Bootstrap”. In: (Nov. 2023). arXiv: [2311.15844 \[hep-th\]](https://arxiv.org/abs/2311.15844).
- [15] Miguel F. Paulos et al. “The S-matrix bootstrap II: two dimensional amplitudes”. In: *JHEP* 11 (2017), p. 143. DOI: [10.1007/JHEP11\(2017\)143](https://doi.org/10.1007/JHEP11(2017)143). arXiv: [1607.06110 \[hep-th\]](https://arxiv.org/abs/1607.06110).
- [16] Miguel F. Paulos et al. “The S-matrix bootstrap. Part I: QFT in AdS”. In: *JHEP* 11 (2017), p. 133. DOI: [10.1007/JHEP11\(2017\)133](https://doi.org/10.1007/JHEP11(2017)133). arXiv: [1607.06109 \[hep-th\]](https://arxiv.org/abs/1607.06109).
- [17] Miguel F. Paulos et al. “The S-matrix bootstrap. Part III: higher dimensional amplitudes”. In: *JHEP* 12 (2019), p. 040. DOI: [10.1007/JHEP12\(2019\)040](https://doi.org/10.1007/JHEP12(2019)040). arXiv: [1708.06765 \[hep-th\]](https://arxiv.org/abs/1708.06765).
- [18] Alexandre Homrich et al. “The S-matrix Bootstrap IV: Multiple Amplitudes”. In: *JHEP* 11 (2019), p. 076. DOI: [10.1007/JHEP11\(2019\)076](https://doi.org/10.1007/JHEP11(2019)076). arXiv: [1905.06905 \[hep-th\]](https://arxiv.org/abs/1905.06905).
- [19] Xizhi Han, Sean A. Hartnoll, and Jorrit Kruthoff. “Bootstrapping Matrix Quantum Mechanics”. In: *Phys. Rev. Lett.* 125.4 (2020), p. 041601. DOI: [10.1103/PhysRevLett.125.041601](https://doi.org/10.1103/PhysRevLett.125.041601). arXiv: [2004.10212 \[hep-th\]](https://arxiv.org/abs/2004.10212).
- [20] David Berenstein and George Hulsey. “Bootstrapping Simple QM Systems”. In: (Aug. 2021). arXiv: [2108.08757 \[hep-th\]](https://arxiv.org/abs/2108.08757).

[21] David Berenstein and George Hulsey. “Bootstrapping more QM systems”. In: *J. Phys. A* 55.27 (2022), p. 275304. DOI: [10.1088/1751-8121/ac7118](https://doi.org/10.1088/1751-8121/ac7118). arXiv: [2109.06251 \[hep-th\]](https://arxiv.org/abs/2109.06251).

[22] David Berenstein and George Hulsey. “Semidefinite programming algorithm for the quantum mechanical bootstrap”. In: *Phys. Rev. E* 107.5 (2023), p. L053301. DOI: [10.1103/PhysRevE.107.L053301](https://doi.org/10.1103/PhysRevE.107.L053301). arXiv: [2209.14332 \[hep-th\]](https://arxiv.org/abs/2209.14332).

[23] David Berenstein and George Hulsey. “One-dimensional reflection in the quantum mechanical bootstrap”. In: *Phys. Rev. D* 109.2 (2024), p. 025013. DOI: [10.1103/PhysRevD.109.025013](https://doi.org/10.1103/PhysRevD.109.025013). arXiv: [2307.11724 \[hep-th\]](https://arxiv.org/abs/2307.11724).

[24] Henry W. Lin. “Bootstrap bounds on D0-brane quantum mechanics”. In: *JHEP* 06 (2023), p. 038. DOI: [10.1007/JHEP06\(2023\)038](https://doi.org/10.1007/JHEP06(2023)038). arXiv: [2302.04416 \[hep-th\]](https://arxiv.org/abs/2302.04416).

[25] Filip Kos et al. “Precision Islands in the Ising and $O(N)$ Models”. In: *JHEP* 08 (2016), p. 036. DOI: [10.1007/JHEP08\(2016\)036](https://doi.org/10.1007/JHEP08(2016)036). arXiv: [1603.04436 \[hep-th\]](https://arxiv.org/abs/1603.04436).

[26] Juan Martin Maldacena. “The Large N limit of superconformal field theories and supergravity”. In: *Adv. Theor. Math. Phys.* 2 (1998), pp. 231–252. DOI: [10.4310/ATMP.1998.v2.n2.a1](https://doi.org/10.4310/ATMP.1998.v2.n2.a1). arXiv: [hep-th/9711200](https://arxiv.org/abs/hep-th/9711200).

[27] S. S. Gubser, Igor R. Klebanov, and Alexander M. Polyakov. “Gauge theory correlators from noncritical string theory”. In: *Phys. Lett. B* 428 (1998), pp. 105–114. DOI: [10.1016/S0370-2693\(98\)00377-3](https://doi.org/10.1016/S0370-2693(98)00377-3). arXiv: [hep-th/9802109](https://arxiv.org/abs/hep-th/9802109).

[28] Edward Witten. “Anti-de Sitter space and holography”. In: *Adv. Theor. Math. Phys.* 2 (1998), pp. 253–291. DOI: [10.4310/ATMP.1998.v2.n2.a2](https://doi.org/10.4310/ATMP.1998.v2.n2.a2). arXiv: [hep-th/9802150](https://arxiv.org/abs/hep-th/9802150).

[29] Martin Ammon and Johanna Erdmenger. *Gauge/gravity duality: Foundations and applications*. Cambridge: Cambridge University Press, Apr. 2015. ISBN: 978-1-107-01034-5, 978-1-316-23594-2. DOI: [10.1017/CBO9780511846373](https://doi.org/10.1017/CBO9780511846373).

[30] Simão Meneses et al. “A structural test for the conformal invariance of the critical 3d Ising model”. In: *JHEP* 04 (2019), p. 115. DOI: [10.1007/JHEP04\(2019\)115](https://doi.org/10.1007/JHEP04(2019)115). arXiv: [1802.02319 \[hep-th\]](https://arxiv.org/abs/1802.02319).

[31] Davide Gaiotto et al. “Generalized Global Symmetries”. In: *JHEP* 02 (2015), p. 172. DOI: [10.1007/JHEP02\(2015\)172](https://doi.org/10.1007/JHEP02(2015)172). arXiv: [1412.5148 \[hep-th\]](https://arxiv.org/abs/1412.5148).

[32] Miguel S. Costa et al. “Spinning Conformal Correlators”. In: *JHEP* 11 (2011), p. 071. DOI: [10.1007/JHEP11\(2011\)071](https://doi.org/10.1007/JHEP11(2011)071). arXiv: [1107.3554 \[hep-th\]](https://arxiv.org/abs/1107.3554).

[33] Miguel S. Costa and Tobias Hansen. “Conformal correlators of mixed-symmetry tensors”. In: *JHEP* 02 (2015), p. 151. DOI: [10.1007/JHEP02\(2015\)151](https://doi.org/10.1007/JHEP02(2015)151). arXiv: [1411.7351 \[hep-th\]](https://arxiv.org/abs/1411.7351).

[34] Miguel S. Costa et al. “Projectors and seed conformal blocks for traceless mixed-symmetry tensors”. In: *JHEP* 07 (2016), p. 018. DOI: [10.1007/JHEP07\(2016\)018](https://doi.org/10.1007/JHEP07(2016)018). arXiv: [1603.05551 \[hep-th\]](https://arxiv.org/abs/1603.05551).

[35] H. Osborn and A. C. Petkou. “Implications of conformal invariance in field theories for general dimensions”. In: *Annals Phys.* 231 (1994), pp. 311–362. DOI: [10.1006/aphy.1994.1045](https://doi.org/10.1006/aphy.1994.1045). arXiv: [hep-th/9307010](https://arxiv.org/abs/hep-th/9307010).

[36] J. Polchinski. *String theory. Vol. 1: An introduction to the bosonic string*. Cambridge Monographs on Mathematical Physics. Cambridge University Press, Dec. 2007. ISBN: 978-0-511-25227-3, 978-0-521-67227-6, 978-0-521-63303-1. DOI: [10.1017/CBO9780511816079](https://doi.org/10.1017/CBO9780511816079).

[37] Duccio Pappadopulo et al. “OPE Convergence in Conformal Field Theory”. In: *Phys. Rev. D* 86 (2012), p. 105043. DOI: [10.1103/PhysRevD.86.105043](https://doi.org/10.1103/PhysRevD.86.105043). arXiv: [1208.6449 \[hep-th\]](https://arxiv.org/abs/1208.6449).

[38] F. A. Dolan and H. Osborn. “Conformal four point functions and the operator product expansion”. In: *Nucl. Phys. B* 599 (2001), pp. 459–496. DOI: [10.1016/S0550-3213\(01\)00013-X](https://doi.org/10.1016/S0550-3213(01)00013-X). arXiv: [hep-th/0011040](https://arxiv.org/abs/hep-th/0011040).

[39] F. A. Dolan and H. Osborn. “Conformal partial waves and the operator product expansion”. In: *Nucl. Phys. B* 678 (2004), pp. 491–507. DOI: [10.1016/j.nuclphysb.2003.11.016](https://doi.org/10.1016/j.nuclphysb.2003.11.016). arXiv: [hep-th/0309180](https://arxiv.org/abs/hep-th/0309180).

[40] F. A. Dolan and H. Osborn. “Conformal Partial Waves: Further Mathematical Results”. In: (Aug. 2011). arXiv: [1108.6194 \[hep-th\]](https://arxiv.org/abs/1108.6194).

[41] João Penedones, Emilio Trevisani, and Masahito Yamazaki. “Recursion Relations for Conformal Blocks”. In: *JHEP* 09 (2016), p. 070. DOI: [10.1007/JHEP09\(2016\)070](https://doi.org/10.1007/JHEP09(2016)070). arXiv: [1509.00428 \[hep-th\]](https://arxiv.org/abs/1509.00428).

[42] Matthijs Hogervorst and Slava Rychkov. “Radial Coordinates for Conformal Blocks”. In: *Phys. Rev. D* 87 (2013), p. 106004. DOI: [10.1103/PhysRevD.87.106004](https://doi.org/10.1103/PhysRevD.87.106004). arXiv: [1303.1111 \[hep-th\]](https://arxiv.org/abs/1303.1111).

- [43] Miguel S. Costa et al. “Radial expansion for spinning conformal blocks”. In: *JHEP* 07 (2016), p. 057. doi: [10.1007/JHEP07\(2016\)057](https://doi.org/10.1007/JHEP07(2016)057). arXiv: [1603.05552 \[hep-th\]](https://arxiv.org/abs/1603.05552).
- [44] A. Liam Fitzpatrick et al. “The Analytic Bootstrap and AdS Superhorizon Locality”. In: *JHEP* 12 (2013), p. 004. doi: [10.1007/JHEP12\(2013\)004](https://doi.org/10.1007/JHEP12(2013)004). arXiv: [1212.3616 \[hep-th\]](https://arxiv.org/abs/1212.3616).
- [45] Zohar Komargodski and Alexander Zhiboedov. “Convexity and Liberation at Large Spin”. In: *JHEP* 11 (2013), p. 140. doi: [10.1007/JHEP11\(2013\)140](https://doi.org/10.1007/JHEP11(2013)140). arXiv: [1212.4103 \[hep-th\]](https://arxiv.org/abs/1212.4103).
- [46] Miguel S. Costa et al. “Spinning Conformal Blocks”. In: *JHEP* 11 (2011), p. 154. doi: [10.1007/JHEP11\(2011\)154](https://doi.org/10.1007/JHEP11(2011)154). arXiv: [1109.6321 \[hep-th\]](https://arxiv.org/abs/1109.6321).
- [47] Denis Karateev, Petr Kravchuk, and David Simmons-Duffin. “Weight Shifting Operators and Conformal Blocks”. In: *JHEP* 02 (2018), p. 081. doi: [10.1007/JHEP02\(2018\)081](https://doi.org/10.1007/JHEP02(2018)081). arXiv: [1706.07813 \[hep-th\]](https://arxiv.org/abs/1706.07813).
- [48] Simon Caron-Huot and Anh-Khoi Trinh. “All tree-level correlators in $AdS_5 \times S_5$ supergravity: hidden ten-dimensional conformal symmetry”. In: *JHEP* 01 (2019), p. 196. doi: [10.1007/JHEP01\(2019\)196](https://doi.org/10.1007/JHEP01(2019)196). arXiv: [1809.09173 \[hep-th\]](https://arxiv.org/abs/1809.09173).
- [49] David Meltzer, Eric Perlmutter, and Allic Sivaramakrishnan. “Unitarity Methods in AdS/CFT”. In: *JHEP* 03 (2020), p. 061. doi: [10.1007/JHEP03\(2020\)061](https://doi.org/10.1007/JHEP03(2020)061). arXiv: [1912.09521 \[hep-th\]](https://arxiv.org/abs/1912.09521).
- [50] Ofer Aharony et al. “Loops in AdS from Conformal Field Theory”. In: *JHEP* 07 (2017), p. 036. doi: [10.1007/JHEP07\(2017\)036](https://doi.org/10.1007/JHEP07(2017)036). arXiv: [1612.03891 \[hep-th\]](https://arxiv.org/abs/1612.03891).
- [51] Vladimir Rosenhaus. “Multipoint Conformal Blocks in the Comb Channel”. In: *JHEP* 02 (2019), p. 142. doi: [10.1007/JHEP02\(2019\)142](https://doi.org/10.1007/JHEP02(2019)142). arXiv: [1810.03244 \[hep-th\]](https://arxiv.org/abs/1810.03244).
- [52] Jean-François Fortin, Wen-Jie Ma, and Witold Skiba. “All Global One- and Two-Dimensional Higher-Point Conformal Blocks”. In: (Sept. 2020). arXiv: [2009.07674 \[hep-th\]](https://arxiv.org/abs/2009.07674).
- [53] Jean-François Fortin, Wenjie Ma, and Witold Skiba. “Higher-Point Conformal Blocks in the Comb Channel”. In: *JHEP* 07 (2020), p. 213. doi: [10.1007/JHEP07\(2020\)213](https://doi.org/10.1007/JHEP07(2020)213). arXiv: [1911.11046 \[hep-th\]](https://arxiv.org/abs/1911.11046).

- [54] Sarthak Parikh. “A multipoint conformal block chain in d dimensions”. In: *JHEP* 05 (2020), p. 120. doi: [10.1007/JHEP05\(2020\)120](https://doi.org/10.1007/JHEP05(2020)120). arXiv: [1911.09190 \[hep-th\]](https://arxiv.org/abs/1911.09190).
- [55] Jean-François Fortin, Wen-Jie Ma, and Witold Skiba. “Six-point conformal blocks in the snowflake channel”. In: *JHEP* 11 (2020), p. 147. doi: [10.1007/JHEP11\(2020\)147](https://doi.org/10.1007/JHEP11(2020)147). arXiv: [2004.02824 \[hep-th\]](https://arxiv.org/abs/2004.02824).
- [56] Jean-François Fortin, Wen-Jie Ma, and Witold Skiba. “Seven-point conformal blocks in the extended snowflake channel and beyond”. In: *Phys. Rev. D* 102.12 (2020), p. 125007. doi: [10.1103/PhysRevD.102.125007](https://doi.org/10.1103/PhysRevD.102.125007). arXiv: [2006.13964 \[hep-th\]](https://arxiv.org/abs/2006.13964).
- [57] Vasco Gonçalves, Raul Pereira, and Xian Zhou. “20’ Five-Point Function from $AdS_5 \times S^5$ Supergravity”. In: *JHEP* 10 (2019), p. 247. doi: [10.1007/JHEP10\(2019\)247](https://doi.org/10.1007/JHEP10(2019)247). arXiv: [1906.05305 \[hep-th\]](https://arxiv.org/abs/1906.05305).
- [58] David Poland, Valentina Prilepsina, and Petar Tadić. “Improving the five-point bootstrap”. In: (Dec. 2023). arXiv: [2312.13344 \[hep-th\]](https://arxiv.org/abs/2312.13344).
- [59] David Poland, Valentina Prilepsina, and Petar Tadić. “The five-point bootstrap”. In: *JHEP* 10 (May 2023), p. 153. doi: [10.1007/JHEP10\(2023\)153](https://doi.org/10.1007/JHEP10(2023)153). arXiv: [2305.08914 \[hep-th\]](https://arxiv.org/abs/2305.08914).
- [60] Ilija Buric et al. “From Gaudin Integrable Models to d -dimensional Multipoint Conformal Blocks”. In: *Phys. Rev. Lett.* 126.2 (2021), p. 021602. doi: [10.1103/PhysRevLett.126.021602](https://doi.org/10.1103/PhysRevLett.126.021602). arXiv: [2009.11882 \[hep-th\]](https://arxiv.org/abs/2009.11882).
- [61] Ilija Buric et al. “Gaudin models and multipoint conformal blocks: general theory”. In: *JHEP* 10 (2021), p. 139. doi: [10.1007/JHEP10\(2021\)139](https://doi.org/10.1007/JHEP10(2021)139). arXiv: [2105.00021 \[hep-th\]](https://arxiv.org/abs/2105.00021).
- [62] David Poland and Valentina Prilepsina. “Recursion relations for 5-point conformal blocks”. In: *JHEP* 10 (2021), p. 160. doi: [10.1007/JHEP10\(2021\)160](https://doi.org/10.1007/JHEP10(2021)160). arXiv: [2103.12092 \[hep-th\]](https://arxiv.org/abs/2103.12092).
- [63] S. Ferrara et al. “Analyticity properties and asymptotic expansions of conformal covariant green’s functions”. In: *Nuovo Cim. A* 19 (1974), pp. 667–695. doi: [10.1007/BF02813413](https://doi.org/10.1007/BF02813413).
- [64] Carlos Bercini, Vasco Gonçalves, and Pedro Vieira. “Light-Cone Bootstrap of Higher Point Functions and Wilson Loop Duality”. In: *Phys. Rev. Lett.* 126.12 (2021), p. 121603. doi: [10.1103/PhysRevLett.126.121603](https://doi.org/10.1103/PhysRevLett.126.121603). arXiv: [2008.10407 \[hep-th\]](https://arxiv.org/abs/2008.10407).

[65] Apratim Kaviraj et al. “Multipoint lightcone bootstrap from differential equations”. In: *JHEP* 08 (2023), p. 011. doi: [10.1007/JHEP08\(2023\)011](https://doi.org/10.1007/JHEP08(2023)011). arXiv: [2212.10578](https://arxiv.org/abs/2212.10578) [hep-th].

[66] Sebastian Harris et al. “Comb Channel Lightcone Bootstrap II: Triple-Twist Anomalous Dimensions”. In: (Jan. 2024). arXiv: [2401.10986](https://arxiv.org/abs/2401.10986) [hep-th].

[67] Ferdinando Gliozzi. “More constraining conformal bootstrap”. In: *Phys. Rev. Lett.* 111 (2013), p. 161602. doi: [10.1103/PhysRevLett.111.161602](https://doi.org/10.1103/PhysRevLett.111.161602). arXiv: [1307.3111](https://arxiv.org/abs/1307.3111) [hep-th].

[68] António Antunes et al. “Lining up a Positive Semi-Definite Six-Point Bootstrap”. In: (Dec. 2023). arXiv: [2312.11660](https://arxiv.org/abs/2312.11660) [hep-th].

[69] Sridip Pal, Jiaxin Qiao, and Slava Rychkov. “Twist Accumulation in Conformal Field Theory: A Rigorous Approach to the Lightcone Bootstrap”. In: *Commun. Math. Phys.* 402.3 (2023), pp. 2169–2214. doi: [10.1007/s00220-023-04767-w](https://doi.org/10.1007/s00220-023-04767-w). arXiv: [2212.04893](https://arxiv.org/abs/2212.04893) [hep-th].

[70] Apratim Kaviraj, Kallol Sen, and Aninda Sinha. “Analytic bootstrap at large spin”. In: *JHEP* 11 (2015), p. 083. doi: [10.1007/JHEP11\(2015\)083](https://doi.org/10.1007/JHEP11(2015)083). arXiv: [1502.01437](https://arxiv.org/abs/1502.01437) [hep-th].

[71] Apratim Kaviraj, Kallol Sen, and Aninda Sinha. “Universal anomalous dimensions at large spin and large twist”. In: *JHEP* 07 (2015), p. 026. doi: [10.1007/JHEP07\(2015\)026](https://doi.org/10.1007/JHEP07(2015)026). arXiv: [1504.00772](https://arxiv.org/abs/1504.00772) [hep-th].

[72] Otto Nachtmann. “Positivity constraints for anomalous dimensions”. In: *Nucl. Phys. B* 63 (1973), pp. 237–247. doi: [10.1016/0550-3213\(73\)90144-2](https://doi.org/10.1016/0550-3213(73)90144-2).

[73] Sandipan Kundu. “A Generalized Nachtmann Theorem in CFT”. In: *JHEP* 11 (2020), p. 138. doi: [10.1007/JHEP11\(2020\)138](https://doi.org/10.1007/JHEP11(2020)138). arXiv: [2002.12390](https://arxiv.org/abs/2002.12390) [hep-th].

[74] Juan Maldacena and Alexander Zhiboedov. “Constraining Conformal Field Theories with A Higher Spin Symmetry”. In: *J. Phys. A* 46 (2013), p. 214011. doi: [10.1088/1751-8113/46/21/214011](https://doi.org/10.1088/1751-8113/46/21/214011). arXiv: [1112.1016](https://arxiv.org/abs/1112.1016) [hep-th].

[75] Luis F. Alday and Alexander Zhiboedov. “An Algebraic Approach to the Analytic Bootstrap”. In: *JHEP* 04 (2017), p. 157. doi: [10.1007/JHEP04\(2017\)157](https://doi.org/10.1007/JHEP04(2017)157). arXiv: [1510.08091](https://arxiv.org/abs/1510.08091) [hep-th].

[76] Luis F. Alday, Agnese Bissi, and Tomasz Lukowski. “Large spin systematics in CFT”. In: *JHEP* 11 (2015), p. 101. doi: [10.1007/JHEP11\(2015\)101](https://doi.org/10.1007/JHEP11(2015)101). arXiv: [1502.07707 \[hep-th\]](https://arxiv.org/abs/1502.07707).

[77] Luis F. Alday. “Large Spin Perturbation Theory for Conformal Field Theories”. In: *Phys. Rev. Lett.* 119.11 (2017), p. 111601. doi: [10.1103/PhysRevLett.119.111601](https://doi.org/10.1103/PhysRevLett.119.111601). arXiv: [1611.01500 \[hep-th\]](https://arxiv.org/abs/1611.01500).

[78] David Simmons-Duffin. “The Lightcone Bootstrap and the Spectrum of the 3d Ising CFT”. In: *JHEP* 03 (2017), p. 086. doi: [10.1007/JHEP03\(2017\)086](https://doi.org/10.1007/JHEP03(2017)086). arXiv: [1612.08471 \[hep-th\]](https://arxiv.org/abs/1612.08471).

[79] Simon Caron-Huot. “Analyticity in Spin in Conformal Theories”. In: *JHEP* 09 (2017), p. 078. doi: [10.1007/JHEP09\(2017\)078](https://doi.org/10.1007/JHEP09(2017)078). arXiv: [1703.00278 \[hep-th\]](https://arxiv.org/abs/1703.00278).

[80] S. Donnachie et al. *Pomeron physics and QCD*. Vol. 19. Cambridge University Press, Dec. 2004. ISBN: 978-0-511-06050-2, 978-0-521-78039-1, 978-0-521-67570-3.

[81] S. Mandelstam. “An extension of the Regge formula”. In: *Annals of Physics* 19.2 (Aug. 1962), pp. 254–261. doi: [10.1016/0003-4916\(62\)90218-X](https://doi.org/10.1016/0003-4916(62)90218-X).

[82] Lorenzo Cornalba et al. “Eikonal Approximation in AdS/CFT: From Shock Waves to Four-Point Functions”. In: *JHEP* 08 (2007), p. 019. doi: [10.1088/1126-6708/2007/08/019](https://doi.org/10.1088/1126-6708/2007/08/019). arXiv: [hep-th/0611122](https://arxiv.org/abs/hep-th/0611122).

[83] Lorenzo Cornalba et al. “Eikonal Approximation in AdS/CFT: Conformal Partial Waves and Finite N Four-Point Functions”. In: *Nucl. Phys. B* 767 (2007), pp. 327–351. doi: [10.1016/j.nuclphysb.2007.01.007](https://doi.org/10.1016/j.nuclphysb.2007.01.007). arXiv: [hep-th/0611123](https://arxiv.org/abs/hep-th/0611123).

[84] Lorenzo Cornalba, Miguel S. Costa, and Joao Penedones. “Eikonal approximation in AdS/CFT: Resumming the gravitational loop expansion”. In: *JHEP* 09 (2007), p. 037. doi: [10.1088/1126-6708/2007/09/037](https://doi.org/10.1088/1126-6708/2007/09/037). arXiv: [0707.0120 \[hep-th\]](https://arxiv.org/abs/0707.0120).

[85] Lorenzo Cornalba, Miguel S. Costa, and Joao Penedones. “Eikonal Methods in AdS/CFT: BFKL Pomeron at Weak Coupling”. In: *JHEP* 06 (2008), p. 048. doi: [10.1088/1126-6708/2008/06/048](https://doi.org/10.1088/1126-6708/2008/06/048). arXiv: [0801.3002 \[hep-th\]](https://arxiv.org/abs/0801.3002).

[86] Miguel S. Costa, Vasco Goncalves, and Joao Penedones. “Conformal Regge theory”. In: *JHEP* 12 (2012), p. 091. doi: [10.1007/JHEP12\(2012\)091](https://doi.org/10.1007/JHEP12(2012)091). arXiv: [1209.4355 \[hep-th\]](https://arxiv.org/abs/1209.4355).

[87] Thomas Hartman, Sachin Jain, and Sandipan Kundu. “Causality Constraints in Conformal Field Theory”. In: *JHEP* 05 (2016), p. 099. DOI: [10.1007/JHEP05\(2016\)099](https://doi.org/10.1007/JHEP05(2016)099). arXiv: [1509.00014 \[hep-th\]](https://arxiv.org/abs/1509.00014).

[88] Thomas Hartman, Sachin Jain, and Sandipan Kundu. “A New Spin on Causality Constraints”. In: *JHEP* 10 (2016), p. 141. DOI: [10.1007/JHEP10\(2016\)141](https://doi.org/10.1007/JHEP10(2016)141). arXiv: [1601.07904 \[hep-th\]](https://arxiv.org/abs/1601.07904).

[89] Thomas Hartman, Sandipan Kundu, and Amirhossein Tajdini. “Averaged Null Energy Condition from Causality”. In: *JHEP* 07 (2017), p. 066. DOI: [10.1007/JHEP07\(2017\)066](https://doi.org/10.1007/JHEP07(2017)066). arXiv: [1610.05308 \[hep-th\]](https://arxiv.org/abs/1610.05308).

[90] Diego M. Hofman and Juan Maldacena. “Conformal collider physics: Energy and charge correlations”. In: *JHEP* 05 (2008), p. 012. DOI: [10.1088/1126-6708/2008/05/012](https://doi.org/10.1088/1126-6708/2008/05/012). arXiv: [0803.1467 \[hep-th\]](https://arxiv.org/abs/0803.1467).

[91] Diego M. Hofman et al. “A Proof of the Conformal Collider Bounds”. In: *JHEP* 06 (2016), p. 111. DOI: [10.1007/JHEP06\(2016\)111](https://doi.org/10.1007/JHEP06(2016)111). arXiv: [1603.03771 \[hep-th\]](https://arxiv.org/abs/1603.03771).

[92] Nima Afkhami-Jeddi et al. “Einstein gravity 3-point functions from conformal field theory”. In: *JHEP* 12 (2017), p. 049. DOI: [10.1007/JHEP12\(2017\)049](https://doi.org/10.1007/JHEP12(2017)049). arXiv: [1610.09378 \[hep-th\]](https://arxiv.org/abs/1610.09378).

[93] Daliang Li, David Meltzer, and David Poland. “Conformal Bootstrap in the Regge Limit”. In: *JHEP* 12 (2017), p. 013. DOI: [10.1007/JHEP12\(2017\)013](https://doi.org/10.1007/JHEP12(2017)013). arXiv: [1705.03453 \[hep-th\]](https://arxiv.org/abs/1705.03453).

[94] Manuela Kulaxizi, Andrei Parnachev, and Alexander Zhiboedov. “Bulk Phase Shift, CFT Regge Limit and Einstein Gravity”. In: *JHEP* 06 (2018), p. 121. DOI: [10.1007/JHEP06\(2018\)121](https://doi.org/10.1007/JHEP06(2018)121). arXiv: [1705.02934 \[hep-th\]](https://arxiv.org/abs/1705.02934).

[95] Luis F. Alday, Agnese Bissi, and Eric Perlmutter. “Holographic Reconstruction of AdS Exchanges from Crossing Symmetry”. In: *JHEP* 08 (2017), p. 147. DOI: [10.1007/JHEP08\(2017\)147](https://doi.org/10.1007/JHEP08(2017)147). arXiv: [1705.02318 \[hep-th\]](https://arxiv.org/abs/1705.02318).

[96] Miguel S. Costa, Tobias Hansen, and João Penedones. “Bounds for OPE coefficients on the Regge trajectory”. In: *JHEP* 10 (2017), p. 197. DOI: [10.1007/JHEP10\(2017\)197](https://doi.org/10.1007/JHEP10(2017)197). arXiv: [1707.07689 \[hep-th\]](https://arxiv.org/abs/1707.07689).

[97] Petr Kravchuk, Jiaxin Qiao, and Slava Rychkov. “Distributions in CFT. Part II. Minkowski space”. In: *JHEP* 08 (2021), p. 094. DOI: [10.1007/JHEP08\(2021\)094](https://doi.org/10.1007/JHEP08(2021)094). arXiv: [2104.02090 \[hep-th\]](https://arxiv.org/abs/2104.02090).

- [98] Slava Rychkov. “Lorentzian methods in Conformal Field Theory”. Notes from IPhT course in 2019.
- [99] Petr Kravchuk and David Simmons-Duffin. “Light-ray operators in conformal field theory”. In: *JHEP* 11 (2018), p. 102. DOI: [10.1007/JHEP11\(2018\)102](https://doi.org/10.1007/JHEP11(2018)102). arXiv: [1805.00098 \[hep-th\]](https://arxiv.org/abs/1805.00098).
- [100] David Simmons-Duffin. “TASI Lectures on Conformal Field Theory in Lorentzian Signature”. Notes from TASI 2019.
- [101] David Simmons-Duffin, Douglas Stanford, and Edward Witten. “A spacetime derivation of the Lorentzian OPE inversion formula”. In: *JHEP* 07 (2018), p. 085. DOI: [10.1007/JHEP07\(2018\)085](https://doi.org/10.1007/JHEP07(2018)085). arXiv: [1711.03816 \[hep-th\]](https://arxiv.org/abs/1711.03816).
- [102] J. A. Minahan and K. Zarembo. “The Bethe ansatz for N=4 superYang-Mills”. In: *JHEP* 03 (2003), p. 013. DOI: [10.1088/1126-6708/2003/03/013](https://doi.org/10.1088/1126-6708/2003/03/013). arXiv: [hep-th/0212208](https://arxiv.org/abs/hep-th/0212208).
- [103] Niklas Beisert et al. “Review of AdS/CFT Integrability: An Overview”. In: *Lett. Math. Phys.* 99 (2012), pp. 3–32. DOI: [10.1007/s11005-011-0529-2](https://doi.org/10.1007/s11005-011-0529-2). arXiv: [1012.3982 \[hep-th\]](https://arxiv.org/abs/1012.3982).
- [104] F. A. Dolan and H. Osborn. “On short and semi-short representations for four-dimensional superconformal symmetry”. In: *Annals Phys.* 307 (2003), pp. 41–89. DOI: [10.1016/S0003-4916\(03\)00074-5](https://doi.org/10.1016/S0003-4916(03)00074-5). arXiv: [hep-th/0209056](https://arxiv.org/abs/hep-th/0209056).
- [105] Francesco Aprile et al. “Double-trace spectrum of $N = 4$ supersymmetric Yang-Mills theory at strong coupling”. In: *Phys. Rev. D* 98.12 (2018), p. 126008. DOI: [10.1103/PhysRevD.98.126008](https://doi.org/10.1103/PhysRevD.98.126008). arXiv: [1802.06889 \[hep-th\]](https://arxiv.org/abs/1802.06889).
- [106] Daniel Z. Freedman et al. “Correlation functions in the CFT(d) / AdS(d+1) correspondence”. In: *Nucl. Phys. B* 546 (1999), pp. 96–118. DOI: [10.1016/S0550-3213\(99\)00053-X](https://doi.org/10.1016/S0550-3213(99)00053-X). arXiv: [hep-th/9804058](https://arxiv.org/abs/hep-th/9804058).
- [107] Sangmin Lee et al. “Three point functions of chiral operators in $D = 4$, $N=4$ SYM at large N ”. In: *Adv. Theor. Math. Phys.* 2 (1998), pp. 697–718. DOI: [10.4310/ATMP.1998.v2.n4.a1](https://doi.org/10.4310/ATMP.1998.v2.n4.a1). arXiv: [hep-th/9806074](https://arxiv.org/abs/hep-th/9806074).
- [108] Kenneth A. Intriligator. “Bonus symmetries of $N=4$ superYang-Mills correlation functions via AdS duality”. In: *Nucl. Phys. B* 551 (1999), pp. 575–600. DOI: [10.1016/S0550-3213\(99\)00242-4](https://doi.org/10.1016/S0550-3213(99)00242-4). arXiv: [hep-th/9811047](https://arxiv.org/abs/hep-th/9811047).

[109] Kenneth A. Intriligator and Witold Skiba. “Bonus symmetry and the operator product expansion of N=4 SuperYang-Mills”. In: *Nucl. Phys. B* 559 (1999), pp. 165–183. DOI: [10.1016/S0550-3213\(99\)00430-7](https://doi.org/10.1016/S0550-3213(99)00430-7). arXiv: [hep-th/9905020](https://arxiv.org/abs/hep-th/9905020).

[110] B. Eden, Paul S. Howe, and Peter C. West. “Nilpotent invariants in N=4 SYM”. In: *Phys. Lett. B* 463 (1999), pp. 19–26. DOI: [10.1016/S0370-2693\(99\)00705-4](https://doi.org/10.1016/S0370-2693(99)00705-4). arXiv: [hep-th/9905085](https://arxiv.org/abs/hep-th/9905085).

[111] Anastasios Petkou and Kostas Skenderis. “A Nonrenormalization theorem for conformal anomalies”. In: *Nucl. Phys. B* 561 (1999), pp. 100–116. DOI: [10.1016/S0550-3213\(99\)00514-3](https://doi.org/10.1016/S0550-3213(99)00514-3). arXiv: [hep-th/9906030](https://arxiv.org/abs/hep-th/9906030).

[112] Paul S. Howe et al. “Explicit construction of nilpotent covariants in N=4 SYM”. In: *Nucl. Phys. B* 571 (2000), pp. 71–90. DOI: [10.1016/S0550-3213\(99\)00768-3](https://doi.org/10.1016/S0550-3213(99)00768-3). arXiv: [hep-th/9910011](https://arxiv.org/abs/hep-th/9910011).

[113] P. J. Heslop and Paul S. Howe. “OPEs and three-point correlators of protected operators in N=4 SYM”. In: *Nucl. Phys. B* 626 (2002), pp. 265–286. DOI: [10.1016/S0550-3213\(02\)00023-8](https://doi.org/10.1016/S0550-3213(02)00023-8). arXiv: [hep-th/0107212](https://arxiv.org/abs/hep-th/0107212).

[114] Marco Baggio, Jan de Boer, and Kyriakos Papadodimas. “A non-renormalization theorem for chiral primary 3-point functions”. In: *JHEP* 07 (2012), p. 137. DOI: [10.1007/JHEP07\(2012\)137](https://doi.org/10.1007/JHEP07(2012)137). arXiv: [1203.1036 \[hep-th\]](https://arxiv.org/abs/1203.1036).

[115] Eric D’Hoker et al. “Extremal correlators in the AdS / CFT correspondence”. In: (Aug. 1999). Ed. by Mikhail A. Shifman, pp. 332–360. DOI: [10.1142/9789812793850_0020](https://doi.org/10.1142/9789812793850_0020). arXiv: [hep-th/9908160](https://arxiv.org/abs/hep-th/9908160).

[116] Massimo Bianchi and Stefano Kovacs. “Nonrenormalization of extremal correlators in N=4 SYM theory”. In: *Phys. Lett. B* 468 (1999), pp. 102–110. DOI: [10.1016/S0370-2693\(99\)01211-3](https://doi.org/10.1016/S0370-2693(99)01211-3). arXiv: [hep-th/9910016](https://arxiv.org/abs/hep-th/9910016).

[117] B. Eden et al. “Extremal correlators in four-dimensional SCFT”. In: *Phys. Lett. B* 472 (2000), pp. 323–331. DOI: [10.1016/S0370-2693\(99\)01442-2](https://doi.org/10.1016/S0370-2693(99)01442-2). arXiv: [hep-th/9910150](https://arxiv.org/abs/hep-th/9910150).

[118] J. Erdmenger and M. Perez-Victoria. “Nonrenormalization of next-to-extremal correlators in N=4 SYM and the AdS / CFT correspondence”. In: *Phys. Rev. D* 62 (2000), p. 045008. DOI: [10.1103/PhysRevD.62.045008](https://doi.org/10.1103/PhysRevD.62.045008). arXiv: [hep-th/9912250](https://arxiv.org/abs/hep-th/9912250).

- [119] B. U. Eden et al. “Extremal and next-to-extremal n point correlators in four-dimensional SCFT”. In: *Phys. Lett. B* 494 (2000), pp. 141–147. DOI: [10.1016/S0370-2693\(00\)01181-3](https://doi.org/10.1016/S0370-2693(00)01181-3). arXiv: [hep-th/0004102](https://arxiv.org/abs/hep-th/0004102).
- [120] G. Arutyunov and S. Frolov. “Scalar quartic couplings in type IIB supergravity on $AdS(5) \times S^{*5}$ ”. In: *Nucl. Phys. B* 579 (2000), pp. 117–176. DOI: [10.1016/S0550-3213\(00\)00210-8](https://doi.org/10.1016/S0550-3213(00)00210-8). arXiv: [hep-th/9912210](https://arxiv.org/abs/hep-th/9912210).
- [121] Eric D’Hoker, Daniel Z. Freedman, and Leonardo Rastelli. “AdS / CFT four point functions: How to succeed at z integrals without really trying”. In: *Nucl. Phys. B* 562 (1999), pp. 395–411. DOI: [10.1016/S0550-3213\(99\)00526-X](https://doi.org/10.1016/S0550-3213(99)00526-X). arXiv: [hep-th/9905049](https://arxiv.org/abs/hep-th/9905049) [hep-th].
- [122] G. Arutyunov and S. Frolov. “Four point functions of lowest weight CPOs in $N=4$ SYM(4) in supergravity approximation”. In: *Phys. Rev. D* 62 (2000), p. 064016. DOI: [10.1103/PhysRevD.62.064016](https://doi.org/10.1103/PhysRevD.62.064016). arXiv: [hep-th/0002170](https://arxiv.org/abs/hep-th/0002170).
- [123] G. Arutyunov et al. “Correlation functions and massive Kaluza-Klein modes in the AdS / CFT correspondence”. In: *Nucl. Phys. B* 665 (2003), pp. 273–324. DOI: [10.1016/S0550-3213\(03\)00448-6](https://doi.org/10.1016/S0550-3213(03)00448-6). arXiv: [hep-th/0212116](https://arxiv.org/abs/hep-th/0212116).
- [124] G. Arutyunov and Emery Sokatchev. “On a large N degeneracy in $N=4$ SYM and the AdS / CFT correspondence”. In: *Nucl. Phys. B* 663 (2003), pp. 163–196. DOI: [10.1016/S0550-3213\(03\)00353-5](https://doi.org/10.1016/S0550-3213(03)00353-5). arXiv: [hep-th/0301058](https://arxiv.org/abs/hep-th/0301058).
- [125] Leon Berdichevsky and Pieter Naaijkens. “Four-point functions of different-weight operators in the AdS/CFT correspondence”. In: *JHEP* 01 (2008), p. 071. DOI: [10.1088/1126-6708/2008/01/071](https://doi.org/10.1088/1126-6708/2008/01/071). arXiv: [0709.1365](https://arxiv.org/abs/0709.1365) [hep-th].
- [126] Linda I. Uruchurtu. “Four-point correlators with higher weight superconformal primaries in the AdS/CFT Correspondence”. In: *JHEP* 03 (2009), p. 133. DOI: [10.1088/1126-6708/2009/03/133](https://doi.org/10.1088/1126-6708/2009/03/133). arXiv: [0811.2320](https://arxiv.org/abs/0811.2320) [hep-th].
- [127] Linda I. Uruchurtu. “Next-next-to-extremal Four Point Functions of $N=4$ 1/2 BPS Operators in the AdS/CFT Correspondence”. In: *JHEP* 08 (2011), p. 133. DOI: [10.1007/JHEP08\(2011\)133](https://doi.org/10.1007/JHEP08(2011)133). arXiv: [1106.0630](https://arxiv.org/abs/1106.0630) [hep-th].
- [128] Leonardo Rastelli and Xian Zhou. “How to Succeed at Holographic Correlators Without Really Trying”. In: *JHEP* 04 (2018), p. 014. DOI: [10.1007/JHEP04\(2018\)014](https://doi.org/10.1007/JHEP04(2018)014). arXiv: [1710.05923](https://arxiv.org/abs/1710.05923) [hep-th].

[129] Luis F. Alday, Vasco Gonçalves, and Xinan Zhou. “Supersymmetric Five-Point Gluon Amplitudes in AdS Space”. In: *Phys. Rev. Lett.* 128.16 (2022), p. 161601. DOI: [10.1103/PhysRevLett.128.161601](https://doi.org/10.1103/PhysRevLett.128.161601). arXiv: [2201.04422 \[hep-th\]](https://arxiv.org/abs/2201.04422).

[130] Luis F. Alday et al. “Six-point AdS gluon amplitudes from flat space and factorization”. In: *Phys. Rev. Res.* 6.1 (2024), p. L012041. DOI: [10.1103/PhysRevResearch.6.L012041](https://doi.org/10.1103/PhysRevResearch.6.L012041). arXiv: [2307.06884 \[hep-th\]](https://arxiv.org/abs/2307.06884).

[131] David Meltzer and Eric Perlmutter. “Beyond $a = c$: gravitational couplings to matter and the stress tensor OPE”. In: *JHEP* 07 (2018), p. 157. DOI: [10.1007/JHEP07\(2018\)157](https://doi.org/10.1007/JHEP07(2018)157). arXiv: [1712.04861 \[hep-th\]](https://arxiv.org/abs/1712.04861).

[132] Xian O. Camanho et al. “Causality Constraints on Corrections to the Graviton Three-Point Coupling”. In: *JHEP* 02 (2016), p. 020. DOI: [10.1007/JHEP02\(2016\)020](https://doi.org/10.1007/JHEP02(2016)020). arXiv: [1407.5597 \[hep-th\]](https://arxiv.org/abs/1407.5597).

[133] Carlos Bercini et al. “The Wilson loop — large spin OPE dictionary”. In: *JHEP* 07 (2022), p. 079. DOI: [10.1007/JHEP07\(2022\)079](https://doi.org/10.1007/JHEP07(2022)079). arXiv: [2110.04364 \[hep-th\]](https://arxiv.org/abs/2110.04364).

[134] Simon Caron-Huot, Yan Gobeil, and Zahra Zahraee. “The leading trajectory in the 2+1D Ising CFT”. In: *JHEP* 02 (2023), p. 190. DOI: [10.1007/JHEP02\(2023\)190](https://doi.org/10.1007/JHEP02(2023)190). arXiv: [2007.11647 \[hep-th\]](https://arxiv.org/abs/2007.11647).

[135] Junyu Liu et al. “The Lorentzian inversion formula and the spectrum of the 3d $O(2)$ CFT”. In: *JHEP* 09 (2020). [Erratum: *JHEP* 01, 206 (2021)], p. 115. DOI: [10.1007/JHEP09\(2020\)115](https://doi.org/10.1007/JHEP09(2020)115). arXiv: [2007.07914 \[hep-th\]](https://arxiv.org/abs/2007.07914).

[136] V. K. Dobrev et al. “Dynamical Derivation of Vacuum Operator Product Expansion in Euclidean Conformal Quantum Field Theory”. In: *Phys. Rev. D* 13 (1976), p. 887. DOI: [10.1103/PhysRevD.13.887](https://doi.org/10.1103/PhysRevD.13.887).

[137] Luis F. Alday, Johan Henriksson, and Mark van Loon. “Taming the ϵ -expansion with large spin perturbation theory”. In: *JHEP* 07 (2018), p. 131. DOI: [10.1007/JHEP07\(2018\)131](https://doi.org/10.1007/JHEP07(2018)131). arXiv: [1712.02314 \[hep-th\]](https://arxiv.org/abs/1712.02314).

[138] Johan Henriksson and Mark Van Loon. “Critical $O(N)$ model to order ϵ^4 from analytic bootstrap”. In: *J. Phys. A* 52.2 (2019), p. 025401. DOI: [10.1088/1751-8121/aaf1e2](https://doi.org/10.1088/1751-8121/aaf1e2). arXiv: [1801.03512 \[hep-th\]](https://arxiv.org/abs/1801.03512).

[139] Luis F. Alday, Johan Henriksson, and Mark van Loon. “An alternative to diagrams for the critical $O(N)$ model: dimensions and structure constants to order $1/N^2$ ”. In: *JHEP* 01 (2020), p. 063. doi: [10.1007/JHEP01\(2020\)063](https://doi.org/10.1007/JHEP01(2020)063). arXiv: [1907.02445 \[hep-th\]](https://arxiv.org/abs/1907.02445).

[140] Vasco Goncalves. “Skeleton expansion and large spin bootstrap for ϕ^3 theory”. In: (Sept. 2018). arXiv: [1809.09572 \[hep-th\]](https://arxiv.org/abs/1809.09572).

[141] Ferdinando Gliozzi et al. “The analytic structure of conformal blocks and the generalized Wilson-Fisher fixed points”. In: *JHEP* 04 (2017), p. 056. doi: [10.1007/JHEP04\(2017\)056](https://doi.org/10.1007/JHEP04(2017)056). arXiv: [1702.03938 \[hep-th\]](https://arxiv.org/abs/1702.03938).

[142] Gerhard Mack. “D-independent representation of Conformal Field Theories in D dimensions via transformation to auxiliary Dual Resonance Models. Scalar amplitudes”. In: (July 2009). arXiv: [0907.2407 \[hep-th\]](https://arxiv.org/abs/0907.2407).

[143] Joao Penedones. “Writing CFT correlation functions as AdS scattering amplitudes”. In: *JHEP* 03 (2011), p. 025. doi: [10.1007/JHEP03\(2011\)025](https://doi.org/10.1007/JHEP03(2011)025). arXiv: [1011.1485 \[hep-th\]](https://arxiv.org/abs/1011.1485).

[144] Vasco Gonçalves, João Penedones, and Emilio Trevisani. “Factorization of Mellin amplitudes”. In: *JHEP* 10 (2015), p. 040. doi: [10.1007/JHEP10\(2015\)040](https://doi.org/10.1007/JHEP10(2015)040). arXiv: [1410.4185 \[hep-th\]](https://arxiv.org/abs/1410.4185).

[145] Ellis Ye Yuan. “Simplicity in AdS Perturbative Dynamics”. In: (Jan. 2018). arXiv: [1801.07283 \[hep-th\]](https://arxiv.org/abs/1801.07283).

[146] Erik Panzer. “Algorithms for the symbolic integration of hyperlogarithms with applications to Feynman integrals”. In: *Comput. Phys. Commun.* 188 (2015), pp. 148–166. doi: [10.1016/j.cpc.2014.10.019](https://doi.org/10.1016/j.cpc.2014.10.019). arXiv: [1403.3385 \[hep-th\]](https://arxiv.org/abs/1403.3385).

[147] Lance J. Dixon, James M. Drummond, and Johannes M. Henn. “Bootstrapping the three-loop hexagon”. In: *JHEP* 11 (2011), p. 023. doi: [10.1007/JHEP11\(2011\)023](https://doi.org/10.1007/JHEP11(2011)023). arXiv: [1108.4461 \[hep-th\]](https://arxiv.org/abs/1108.4461).

[148] Christian Baadsgaard Jepsen and Sarthak Parikh. “Propagator identities, holographic conformal blocks, and higher-point AdS diagrams”. In: *JHEP* 10 (2019), p. 268. doi: [10.1007/JHEP10\(2019\)268](https://doi.org/10.1007/JHEP10(2019)268). arXiv: [1906.08405 \[hep-th\]](https://arxiv.org/abs/1906.08405).

[149] Vittorio Del Duca et al. “The one-loop six-dimensional hexagon integral with three massive corners”. In: *Phys. Rev. D* 84 (2011), p. 045017. doi: [10.1103/PhysRevD.84.045017](https://doi.org/10.1103/PhysRevD.84.045017). arXiv: [1105.2011 \[hep-th\]](https://arxiv.org/abs/1105.2011).

[150] Denis Karateev, Petr Kravchuk, and David Simmons-Duffin. “Harmonic Analysis and Mean Field Theory”. In: *JHEP* 10 (2019), p. 217. DOI: [10.1007/JHEP10\(2019\)217](https://doi.org/10.1007/JHEP10(2019)217). arXiv: [1809.05111 \[hep-th\]](https://arxiv.org/abs/1809.05111).

[151] E. S. Fradkin and M. Ya. Palchik. “Recent Developments in Conformal Invariant Quantum Field Theory”. In: *Phys. Rept.* 44 (1978), pp. 249–349. DOI: [10.1016/0370-1573\(78\)90172-2](https://doi.org/10.1016/0370-1573(78)90172-2).

[152] Ilija Buric et al. “Gaudin models and multipoint conformal blocks III: comb channel coordinates and OPE factorisation”. In: *JHEP* 06 (2022), p. 144. DOI: [10.1007/JHEP06\(2022\)144](https://doi.org/10.1007/JHEP06(2022)144). arXiv: [2112.10827 \[hep-th\]](https://arxiv.org/abs/2112.10827).

[153] Ilija Buric et al. “Gaudin models and multipoint conformal blocks. Part II. Comb channel vertices in 3D and 4D”. In: *JHEP* 11 (2021), p. 182. DOI: [10.1007/JHEP11\(2021\)182](https://doi.org/10.1007/JHEP11(2021)182). arXiv: [2108.00023 \[hep-th\]](https://arxiv.org/abs/2108.00023).

[154] António Antunes et al. “The perturbative CFT optical theorem and high-energy string scattering in AdS at one loop”. In: *JHEP* 04 (2021), p. 088. DOI: [10.1007/JHEP04\(2021\)088](https://doi.org/10.1007/JHEP04(2021)088). arXiv: [2012.01515 \[hep-th\]](https://arxiv.org/abs/2012.01515).

[155] Simon Caron-Huot et al. “Detectors in weakly-coupled field theories”. In: *JHEP* 04 (2023), p. 014. DOI: [10.1007/JHEP04\(2023\)014](https://doi.org/10.1007/JHEP04(2023)014). arXiv: [2209.00008 \[hep-th\]](https://arxiv.org/abs/2209.00008).

[156] Simon Caron-Huot et al. “AdS bulk locality from sharp CFT bounds”. In: *JHEP* 11 (2021), p. 164. DOI: [10.1007/JHEP11\(2021\)164](https://doi.org/10.1007/JHEP11(2021)164). arXiv: [2106.10274 \[hep-th\]](https://arxiv.org/abs/2106.10274).

[157] Pulkit Agarwal et al. “Embedding Space Approach to Lorentzian CFT Amplitudes and Causal Spherical Functions”. In: (Feb. 2023). arXiv: [2302.06469 \[hep-th\]](https://arxiv.org/abs/2302.06469).

[158] T. Regge. “Introduction to complex orbital momenta”. In: *Nuovo Cim.* 14 (1959), p. 951. DOI: [10.1007/BF02728177](https://doi.org/10.1007/BF02728177).

[159] P. Goddard and A. R. White. “Complex helicity and the sommerfeld-watson transformation of group-theoretic expansions”. In: *Nuovo Cim. A* 1 (1971), pp. 645–679. DOI: [10.1007/bf02734390](https://doi.org/10.1007/bf02734390).

[160] A. R. White. “The signatured froissart-gribov continuation of multiparticle amplitudes to complex helicity and angular momentum”. In: *Nucl. Phys. B* 39 (1972), pp. 432–460. DOI: [10.1016/0550-3213\(72\)90381-1](https://doi.org/10.1016/0550-3213(72)90381-1).

[161] A. R. White. “The analytic continuation of multiparticle unitarity in the complex angular momentum plane”. In: *Nucl. Phys. B* 39 (1972), pp. 461–478. DOI: [10.1016/0550-3213\(72\)90382-3](https://doi.org/10.1016/0550-3213(72)90382-3).

[162] A. R. White. “Signature, factorization and unitarity in multi-regge theory - the five-point function”. In: *Nucl. Phys. B* 67 (1973), pp. 189–231. DOI: [10.1016/0550-3213\(73\)90325-8](https://doi.org/10.1016/0550-3213(73)90325-8).

[163] Alan R. White. “The Analytic Foundations of Regge Theory”. In: *Institute on Structural Analysis of Multiparticle Collision Amplitudes in Relativistic Quantum Theory*. Feb. 1976.

[164] R. C. Brower, Carleton E. DeTar, and J. H. Weis. “Regge Theory for Multiparticle Amplitudes”. In: *Phys. Rept.* 14 (1974), p. 257. DOI: [10.1016/0370-1573\(74\)90012-x](https://doi.org/10.1016/0370-1573(74)90012-x).

[165] J. H. Weis. “Singularities in complex angular momentum and helicity”. In: *Phys. Rev. D* 6 (1972), pp. 2823–2841. DOI: [10.1103/PhysRevD.6.2823](https://doi.org/10.1103/PhysRevD.6.2823).

[166] H. D. I. Abarbanel and A. Schwimmer. “Analytic structure of multiparticle amplitudes in complex helicity”. In: *Phys. Rev. D* 6 (1972), pp. 3018–3031. DOI: [10.1103/PhysRevD.6.3018](https://doi.org/10.1103/PhysRevD.6.3018).

[167] Henry P. Stapp and Alan R. White. “An Asymptotic Dispersion Relation for the Six Particle Amplitude”. In: *Phys. Rev. D* 26 (1982), p. 2145. DOI: [10.1103/PhysRevD.26.2145](https://doi.org/10.1103/PhysRevD.26.2145).

[168] I. T. Drummond. “Multi-Reggeon Behavior of Production Amplitudes”. In: *Phys. Rev.* 176 (5 Dec. 1968), pp. 2003–2013. DOI: [10.1103/PhysRev.176.2003](https://doi.org/10.1103/PhysRev.176.2003). URL: <https://link.aps.org/doi/10.1103/PhysRev.176.2003>.

[169] Alan White. *Analytic Multi-regge Theory And The Pomeron In Qcd - Part 1*. <https://www.osti.gov/servlets/purl/7002400>. [Online; accessed 15-November-2022].

[170] C. E. DeTar et al. “Helicity Poles, Triple-Regge Behavior, and Single-Particle Spectra in High-Energy Collisions”. In: *Phys. Rev. Lett.* 26 (11 Mar. 1971), pp. 675–676. DOI: [10.1103/PhysRevLett.26.675](https://doi.org/10.1103/PhysRevLett.26.675). URL: <https://link.aps.org/doi/10.1103/PhysRevLett.26.675>.

[171] Steinmann. *Ueber den Zusammenhang zwischen den Wightmanfunktionen und den retardierten Kommutatoren*. <https://www.research-collection.ethz.ch/handle/20.500.11850/135473>. [Online; accessed 15-November-2022].

[172] John H. Schwarz. “Dual resonance theory”. In: *Phys. Rept.* 8 (1973), pp. 269–335. DOI: [10.1016/0370-1573\(73\)90003-3](https://doi.org/10.1016/0370-1573(73)90003-3).

[173] K. Bardakci and H. Ruegg. “Meson resonance couplings in a five-point veneziano model”. In: *Phys. Lett. B* 28 (1969), pp. 671–675. DOI: [10.1016/0370-2693\(69\)90219-6](https://doi.org/10.1016/0370-2693(69)90219-6).

[174] Juan Maldacena, David Simmons-Duffin, and Alexander Zhiboedov. “Looking for a bulk point”. In: *JHEP* 01 (2017), p. 013. DOI: [10.1007/JHEP01\(2017\)013](https://doi.org/10.1007/JHEP01(2017)013). arXiv: [1509.03612 \[hep-th\]](https://arxiv.org/abs/1509.03612).

[175] Simon Caron-Huot and Joshua Sandor. “Conformal Regge Theory at Finite Boost”. In: *Jhep* 05 (2021), p. 059. DOI: [10.1007/jhep05\(2021\)059](https://doi.org/10.1007/jhep05(2021)059). arXiv: [2008.11759 \[hep-th\]](https://arxiv.org/abs/2008.11759).

[176] Petr Kravchuk, Jiaxin Qiao, and Slava Rychkov. “Distributions in CFT. Part I. Cross-ratio space”. In: *Jhep* 05 (2020), p. 137. DOI: [10.1007/jhep05\(2020\)137](https://doi.org/10.1007/jhep05(2020)137). arXiv: [2001.08778 \[hep-th\]](https://arxiv.org/abs/2001.08778).

[177] M. Lüscher and G. Mack. “Global Conformal Invariance in Quantum Field Theory”. In: *Commun. Math. Phys.* 41 (1975), pp. 203–234. DOI: [10.1007/bf01608988](https://doi.org/10.1007/bf01608988).

[178] G. Mack. “Convergence of Operator Product Expansions on the Vacuum in Conformal Invariant Quantum Field Theory”. In: *Commun. Math. Phys.* 53 (1977), p. 155. DOI: [10.1007/bf01609130](https://doi.org/10.1007/bf01609130).

[179] R. F. Streater and A. S. Wightman. *PCT, spin and statistics, and all that*. 1989. ISBN: 978-0-691-07062-9.

[180] H. Casini. “Wedge reflection positivity”. In: *J. Phys. A* 44 (2011), p. 435202. DOI: [10.1088/1751-8113/44/43/435202](https://doi.org/10.1088/1751-8113/44/43/435202). arXiv: [1009.3832 \[hep-th\]](https://arxiv.org/abs/1009.3832).

[181] Juan Maldacena, Stephen H. Shenker, and Douglas Stanford. “A bound on chaos”. In: *Jhep* 08 (2016), p. 106. DOI: [10.1007/jhep08\(2016\)106](https://doi.org/10.1007/jhep08(2016)106). arXiv: [1503.01409 \[hep-th\]](https://arxiv.org/abs/1503.01409).

[182] Murat Kologlu et al. “Shocks, Superconvergence, and a Stringy Equivalence Principle”. In: *Jhep* 11 (2020), p. 096. DOI: [10.1007/jhep11\(2020\)096](https://doi.org/10.1007/jhep11(2020)096). arXiv: [1904.05905 \[hep-th\]](https://arxiv.org/abs/1904.05905).

[183] Miguel S. Costa, Vasco Gonçalves, and João Penedones. “Spinning AdS Propagators”. In: *Jhep* 09 (2014), p. 064. DOI: [10.1007/jhep09\(2014\)064](https://doi.org/10.1007/jhep09(2014)064). arXiv: [1404.5625 \[hep-th\]](https://arxiv.org/abs/1404.5625).

[184] K. Symanzik. “On Calculations in conformal invariant field theories”. In: *Lett. Nuovo Cim.* 3 (1972), pp. 734–738. DOI: [10.1007/BF02824349](https://doi.org/10.1007/BF02824349).

[185] Petr Kravchuk and David Simmons-Duffin. “Counting Conformal Correlators”. In: *Jhep* 02 (2018), p. 096. DOI: [10.1007/jhep02\(2018\)096](https://doi.org/10.1007/jhep02(2018)096). arXiv: [1612.08987 \[hep-th\]](https://arxiv.org/abs/1612.08987).

[186] Leonardo Rastelli and Xinan Zhou. “Mellin amplitudes for $AdS_5 \times S^5$ ”. In: *Phys. Rev. Lett.* 118.9 (2017), p. 091602. DOI: [10.1103/PhysRevLett.118.091602](https://doi.org/10.1103/PhysRevLett.118.091602). arXiv: [1608.06624 \[hep-th\]](https://arxiv.org/abs/1608.06624).

[187] Agnese Bissi, Aninda Sinha, and Xinan Zhou. “Selected topics in analytic conformal bootstrap: A guided journey”. In: *Phys. Rept.* 991 (2022), pp. 1–89. DOI: [10.1016/j.physrep.2022.09.004](https://doi.org/10.1016/j.physrep.2022.09.004). arXiv: [2202.08475 \[hep-th\]](https://arxiv.org/abs/2202.08475).

[188] Luis F. Alday and Xinan Zhou. “All Tree-Level Correlators for M-theory on $AdS_7 \times S^4$ ”. In: *Phys. Rev. Lett.* 125.13 (2020), p. 131604. DOI: [10.1103/PhysRevLett.125.131604](https://doi.org/10.1103/PhysRevLett.125.131604). arXiv: [2006.06653 \[hep-th\]](https://arxiv.org/abs/2006.06653).

[189] Luis F. Alday and Xinan Zhou. “All Holographic Four-Point Functions in All Maximally Supersymmetric CFTs”. In: *Phys. Rev. X* 11.1 (2021), p. 011056. DOI: [10.1103/PhysRevX.11.011056](https://doi.org/10.1103/PhysRevX.11.011056). arXiv: [2006.12505 \[hep-th\]](https://arxiv.org/abs/2006.12505).

[190] Leonardo Rastelli, Konstantinos Roumpedakis, and Xinan Zhou. “**AdS₃ × S³** Tree-Level Correlators: Hidden Six-Dimensional Conformal Symmetry”. In: *JHEP* 10 (2019), p. 140. DOI: [10.1007/JHEP10\(2019\)140](https://doi.org/10.1007/JHEP10(2019)140). arXiv: [1905.11983 \[hep-th\]](https://arxiv.org/abs/1905.11983).

[191] Stefano Giusto et al. “The CFT₆ origin of all tree-level 4-point correlators in AdS₃ × S³”. In: *Eur. Phys. J. C* 80.8 (2020), p. 736. DOI: [10.1140/epjc/s10052-020-8300-4](https://doi.org/10.1140/epjc/s10052-020-8300-4). arXiv: [2005.08560 \[hep-th\]](https://arxiv.org/abs/2005.08560).

[192] Luis F. Alday et al. “Gluon Scattering in AdS from CFT”. In: *JHEP* 06 (2021), p. 020. DOI: [10.1007/JHEP06\(2021\)020](https://doi.org/10.1007/JHEP06(2021)020). arXiv: [2103.15830 \[hep-th\]](https://arxiv.org/abs/2103.15830).

[193] Joseph A. Farrow, Arthur E. Lipstein, and Paul McFadden. “Double copy structure of CFT correlators”. In: *JHEP* 02 (2019), p. 130. DOI: [10.1007/JHEP02\(2019\)130](https://doi.org/10.1007/JHEP02(2019)130). arXiv: [1812.11129 \[hep-th\]](https://arxiv.org/abs/1812.11129).

[194] Connor Armstrong, Arthur E. Lipstein, and Jiajie Mei. “Color/kinematics duality in AdS_4 ”. In: *JHEP* 02 (2021), p. 194. DOI: [10.1007/JHEP02\(2021\)194](https://doi.org/10.1007/JHEP02(2021)194). arXiv: [2012.02059 \[hep-th\]](https://arxiv.org/abs/2012.02059).

[195] Soner Albayrak, Savan Kharel, and David Meltzer. “On duality of color and kinematics in (A)dS momentum space”. In: *JHEP* 03 (2021), p. 249. DOI: [10.1007/JHEP03\(2021\)249](https://doi.org/10.1007/JHEP03(2021)249). arXiv: [2012.10460 \[hep-th\]](https://arxiv.org/abs/2012.10460).

[196] Sachin Jain et al. “Double copy structure of parity-violating CFT correlators”. In: *JHEP* 07 (2021), p. 033. DOI: [10.1007/JHEP07\(2021\)033](https://doi.org/10.1007/JHEP07(2021)033). arXiv: [2104.12803 \[hep-th\]](https://arxiv.org/abs/2104.12803).

[197] Xian Zhou. “Double Copy Relation in AdS Space”. In: *Phys. Rev. Lett.* 127.14 (2021), p. 141601. DOI: [10.1103/PhysRevLett.127.141601](https://doi.org/10.1103/PhysRevLett.127.141601). arXiv: [2106.07651 \[hep-th\]](https://arxiv.org/abs/2106.07651).

[198] Pranav Diwakar et al. “BCJ amplitude relations for Anti-de Sitter boundary correlators in embedding space”. In: *JHEP* 10 (2021), p. 141. DOI: [10.1007/JHEP10\(2021\)141](https://doi.org/10.1007/JHEP10(2021)141). arXiv: [2106.10822 \[hep-th\]](https://arxiv.org/abs/2106.10822).

[199] Clifford Cheung, Julio Parra-Martinez, and Allic Sivaramakrishnan. “On-shell correlators and color-kinematics duality in curved symmetric spacetimes”. In: *JHEP* 05 (2022), p. 027. DOI: [10.1007/JHEP05\(2022\)027](https://doi.org/10.1007/JHEP05(2022)027). arXiv: [2201.05147 \[hep-th\]](https://arxiv.org/abs/2201.05147).

[200] Aidan Herderschee, Radu Roiban, and Fei Teng. “On the differential representation and color-kinematics duality of AdS boundary correlators”. In: *JHEP* 05 (2022), p. 026. DOI: [10.1007/JHEP05\(2022\)026](https://doi.org/10.1007/JHEP05(2022)026). arXiv: [2201.05067 \[hep-th\]](https://arxiv.org/abs/2201.05067).

[201] J. M. Drummond, R. Glew, and M. Santagata. “BCJ relations in $AdS_5 \times S^3$ and the double-trace spectrum of super gluons”. In: (Feb. 2022). arXiv: [2202.09837 \[hep-th\]](https://arxiv.org/abs/2202.09837).

[202] Agnese Bissi et al. “Spinning correlators in $\mathcal{N} = 2$ SCFTs: Superspace and AdS amplitudes”. In: (Sept. 2022). arXiv: [2209.01204 \[hep-th\]](https://arxiv.org/abs/2209.01204).

[203] Connor Armstrong et al. “New recursions for tree-level correlators in (Anti) de Sitter space”. In: (Sept. 2022). arXiv: [2209.02709 \[hep-th\]](https://arxiv.org/abs/2209.02709).

[204] Hayden Lee and Xinkang Wang. “Cosmological Double-Copy Relations”. In: (Dec. 2022). arXiv: [2212.11282 \[hep-th\]](https://arxiv.org/abs/2212.11282).

[205] Yue-Zhou Li. “Flat-space structure of gluon and graviton in AdS”. In: (Dec. 2022). arXiv: [2212.13195 \[hep-th\]](https://arxiv.org/abs/2212.13195).

[206] Christopher Beem et al. “Infinite Chiral Symmetry in Four Dimensions”. In: *Commun. Math. Phys.* 336.3 (2015), pp. 1359–1433. DOI: [10.1007/s00220-014-2272-x](https://doi.org/10.1007/s00220-014-2272-x). arXiv: [1312.5344 \[hep-th\]](https://arxiv.org/abs/1312.5344).

[207] Nadav Drukker and Jan Plefka. “Superprotected n-point correlation functions of local operators in $N=4$ super Yang-Mills”. In: *JHEP* 04 (2009), p. 052. DOI: [10.1088/1126-6708/2009/04/052](https://doi.org/10.1088/1126-6708/2009/04/052). arXiv: [0901.3653 \[hep-th\]](https://arxiv.org/abs/0901.3653).

[208] A. Liam Fitzpatrick et al. “A Natural Language for AdS/CFT Correlators”. In: *JHEP* 11 (2011), p. 095. DOI: [10.1007/JHEP11\(2011\)095](https://doi.org/10.1007/JHEP11(2011)095). arXiv: [1107.1499 \[hep-th\]](https://arxiv.org/abs/1107.1499).

[209] Xinan Zhou. “On Superconformal Four-Point Mellin Amplitudes in Dimension $d > 2$ ”. In: *JHEP* 08 (2018), p. 187. DOI: [10.1007/JHEP08\(2018\)187](https://doi.org/10.1007/JHEP08(2018)187). arXiv: [1712.02800 \[hep-th\]](https://arxiv.org/abs/1712.02800).

[210] Xinan Zhou. “On Mellin Amplitudes in SCFTs with Eight Supercharges”. In: *JHEP* 07 (2018), p. 147. DOI: [10.1007/JHEP07\(2018\)147](https://doi.org/10.1007/JHEP07(2018)147). arXiv: [1804.02397 \[hep-th\]](https://arxiv.org/abs/1804.02397).

[211] Vasco Gonçalves. “Four point function of $\mathcal{N} = 4$ stress-tensor multiplet at strong coupling”. In: *JHEP* 04 (2015), p. 150. DOI: [10.1007/JHEP04\(2015\)150](https://doi.org/10.1007/JHEP04(2015)150). arXiv: [1411.1675 \[hep-th\]](https://arxiv.org/abs/1411.1675).

[212] Jean-François Fortin et al. “Feynman rules for scalar conformal blocks”. In: *JHEP* 10 (2022), p. 097. DOI: [10.1007/JHEP10\(2022\)097](https://doi.org/10.1007/JHEP10(2022)097). arXiv: [2204.08909 \[hep-th\]](https://arxiv.org/abs/2204.08909).

[213] Leonardo Rastelli and Xinan Zhou. “Holographic Four-Point Functions in the (2, 0) Theory”. In: *JHEP* 06 (2018), p. 087. DOI: [10.1007/JHEP06\(2018\)087](https://doi.org/10.1007/JHEP06(2018)087). arXiv: [1712.02788 \[hep-th\]](https://arxiv.org/abs/1712.02788).

[214] Connor Behan, Pietro Ferrero, and Xinan Zhou. “More on holographic correlators: Twisted and dimensionally reduced structures”. In: *JHEP* 04 (2021), p. 008. DOI: [10.1007/JHEP04\(2021\)008](https://doi.org/10.1007/JHEP04(2021)008). arXiv: [2101.04114 \[hep-th\]](https://arxiv.org/abs/2101.04114).

[215] A. V. Belitsky et al. “ $N=4$ superconformal Ward identities for correlation functions”. In: *Nucl. Phys. B* 904 (2016), pp. 176–215. DOI: [10.1016/j.nuclphysb.2016.01.008](https://doi.org/10.1016/j.nuclphysb.2016.01.008). arXiv: [1409.2502 \[hep-th\]](https://arxiv.org/abs/1409.2502).